

Université de Lille - Faculté de Sciences et Technologies
École Doctorale Biologie - Santé
Laboratoire de Physiologie Cellulaire – INSERM U1003

Thèse

Physiologie 66
Aspects moléculaires et cellulaires de la biologie

Role of Orai1 in prostate cancer proliferation and cancer stem cell quiescence/activation transition

Rôle d'Orai1 dans la prolifération des cellules cancéreuses
prostatiques et la transition quiescence/activation des cellules
souches cancéreuses

Thèse dirigée par Dr Loïc Lemonnier

Thèse préparée et soutenue publiquement par

Lucile Noyer

Le 23 juillet 2019

Pour obtenir le grade de Docteur

Membres du jury :

Dr Bruno Constantin, Université de Poitiers, CNRS (Poitiers, France)	Rapporteur
Dr Rainer Schindl, Medical University of Graz (Graz, Austria)	Rapporteur
Dr Dominique Collard, Université de Lille, CNRS (Lille, France)	Président du jury
Dr Julie Pannequin, Université de Montpellier, CNRS (Montpellier, France)	Examineur
Pr Natalia Prevarskaya, Université de Lille, INSERM (Lille, France)	Examineur
Dr Loïc Lemonnier, Université de Lille, INSERM (Lille, France)	Examineur

Abstract

Prostate cancer (PCa) is the most frequent and the third deadliest cancer in men in Europe. This pathology has the distinctive feature of being hormone-sensitive, and androgen-deprivation is often the first line of treatment for non-operable tumors. Although this therapy allows to significantly reduce PCa growth, it will inescapably lead to the development of an aggressive hormone-resistant cancer for which curative treatments are still lacking. There is thus a strong need to develop new markers and more efficient therapeutic strategies.

Cancer stem cells (CSC) represent a rare subset of cancer cells possessing stem-like properties. As a consequence, these cells are mostly quiescent, but highly tumorigenic when they activate. CSCs have thus been linked to tumor dormancy as well as relapse when they reactivate. The mechanisms regulating CSC dormancy/activation transition are therefore a critical question in cancer research.

Previous studies showed the importance of Orai proteins in PCa. Orai1 has first been implicated in apoptosis regulation through its involvement in store-operated calcium channels (SOC). In another study, Orai1 was shown to be involved in advanced prostate cancer cell proliferation via its association with Orai3 isoform to form arachidonic acid-regulated channels (ARC). However, the role of Orai1 remains to be studied in the context of proliferation of hormone-sensitive prostate cancer cells and PCa CSC physiology.

Moreover, in order to bypass current targeting limitations of Orai1, we aimed to identify a partner protein able to regulate Orai1 in PCa. Indeed, the importance of partner proteins in the regulation of ion channel activity has been well documented. For this purpose, we focused on the Sigma 1 receptor (S1R), a chaperone protein capable of ion channel regulation. Interestingly, S1R expression is increased in PCa and this protein can bind many different pharmacological compounds currently used in other clinical applications. This study thus aimed to first study the role of Orai1 in PCa and CSC physiology, and then characterize the role of S1R as a new regulator of Orai1 in PCa.

This work led to the identification of new roles for Orai1 in cancer. We first show that Orai1 is a key regulator of CSC transition between the quiescent state of dormancy and the active proliferative state via the NFAT pathway. The expression and activity of Orai1 are downregulated in CSCs as compared to their non-stem cancer cell counterpart, and this will push the cells towards dormancy at the expense of proliferation. These results thus suggest that Orai1 could represent a new interesting marker to determine PCa aggressiveness and identify the highly tumorigenic CSC population. Interestingly, we confirmed these results in melanoma CSCs, showing that Orai1 regulation of CSC quiescence/activation could be a trend not limited to prostate.

In this work, we also investigated new ways to target Orai1 through the S1R. We show here that the S1R directly interacts with Orai1 in plasma membrane, increasing its activity, and modulating PCa cell proliferation. Finally, we characterized the regulation of Orai1 and S1R expression by androgen, which dramatically affects their presence and role throughout PCa progression.

To summarize, our results led to the identification of a key regulator of PCa proliferation (Orai1) and propose an alternative method for its targeting through the identification of a new partner protein: the S1R. These results could therefore lead to the development of new markers and innovative therapeutic strategies by combining the clinically validated S1R modulators with ion channel pharmacology.

Résumé

Le cancer de la prostate (CaP) est le cancer le plus fréquent et le troisième plus mortel chez l'homme en Europe. Le CaP a la particularité d'être hormono-sensible ; ainsi la première ligne de traitement pour les tumeurs non opérables consiste en une privation d'androgènes. Malheureusement, ce traitement conduit inévitablement à un échappement thérapeutique et au développement d'un cancer hormono-résistant agressif pour lequel il n'existe pas de traitement curatif à l'heure actuelle. Il y a donc un réel besoin clinique d'identifier de nouveaux marqueurs et de proposer des stratégies thérapeutiques plus efficaces.

Les cellules souches cancéreuses (CSC) représentent une sous population de cellules cancéreuses présentant des propriétés de cellules souches. Les CSCs sont ainsi principalement quiescentes, mais elles sont hautement tumorigènes lors de leur activation. Les CSCs sont donc associées aux phénomènes de dormance tumorale, puis de rechute suite à leur réactivation. Les mécanismes régulant la transition dormance/prolifération constituent donc une question centrale, et leur identification permettrait de développer de nouvelles approches thérapeutiques.

L'importance des protéines Orai dans le CaP a déjà été montrée lors de précédentes études. Constituant majeur du SOC (store-operated calcium channel) dans les cellules cancéreuses prostatiques, Orai1 joue ainsi un rôle clé dans les mécanismes d'apoptose. Cette protéine canal a également été impliquée dans la prolifération des stades avancés du CaP par sa participation dans les canaux activés par l'acide arachidonique (ARC, arachidonic acid-regulated channels). Cependant, le rôle du canal Orai1 dans la prolifération pendant les stades précoces hormono-sensibles du CaP, ou son éventuelle implication dans le contrôle de la transition dormance/prolifération des CSC prostatiques, restaient inconnus.

Parallèlement, au vu du rôle clé d'Orai1 dans le CaP et pour répondre aux limitations de son ciblage direct, nous avons cherché à identifier ses éventuelles protéines partenaires. En effet, de plus en plus d'études montrent l'importance de ces protéines dans la régulation des canaux ioniques. Nous nous sommes ainsi intéressés au récepteur Sigma 1 (S1R), précédemment identifié comme un partenaire de plusieurs familles de canaux ioniques. De manière intéressante, il voit son expression augmenter dans le CaP, et il possède de nombreux modulateurs pharmacologiques utilisés en clinique. Ce travail avait donc un double objectif : étudier le rôle d'Orai1 dans le CaP et les CSC prostatiques, et caractériser fonctionnellement le rôle du S1R en tant que nouveau partenaire du canal Orai1.

Ces travaux ont ainsi permis d'identifier de nouveaux rôles du canal Orai1 dans le cancer. Nous avons tout d'abord mis en évidence l'importance d'Orai1 dans le contrôle de la transition entre l'état quiescent et l'état prolifératif des CSCs prostatiques grâce à la voie de signalisation NFAT. En effet, l'expression et l'activité d'Orai1 chutent dans les CSCs par rapport aux cellules

cancéreuses non souches, et cette diminution va orienter les CSCs vers la dormance aux dépens de la prolifération. Ces résultats suggèrent donc qu'Orai1 constituerait un nouveau marqueur permettant d'évaluer l'agressivité du PCa et d'identifier une sous-population de CSCs hautement tumorigènes. Le ciblage d'Orai1 pourrait également permettre le développement de thérapies spécifiques visant les CSCs. De plus, ces résultats ont été confirmés dans un autre modèle, les CSCs de mélanome, ce qui montrerait que le rôle d'Orai1 dans la transition entre quiescence et prolifération serait généralisable au-delà du modèle prostatique.

En parallèle, pour faciliter le ciblage d'Orai1, nous nous sommes intéressés au S1R dans le contexte du CaP. Nos travaux montrent que le S1R interagit directement avec Orai1 dans la membrane plasmique, et module positivement l'entrée capacitive de calcium (ECC) de canaux SOC, impactant ainsi la prolifération des cellules cancéreuses prostatiques. Nous avons également mis en évidence la régulation de l'expression de ces protéines par les androgènes, impactant dramatiquement leur présence et rôle dans l'évolution du CaP.

Nos résultats ont donc permis l'identification d'un acteur central du contrôle de la prolifération du CaP (Orai1), et la caractérisation d'une nouvelle protéine partenaire du canal Orai1 dans le CaP : le S1R. Ces résultats pourraient à terme permettre de développer des thérapies innovantes, notamment grâce à l'utilisation conjointe de modulateurs pharmacologiques du S1R cliniquement validés, et de modulateurs des canaux calciques.

Acknowledgement

I met many people during this journey and all of them, in some way, taught me something. I'd like to take some time to thank all of you: you helped me get where I am today.

First of all, I would like to thank the defense committee, **Dr Julie Pannequin** and **Dr Dominique Collard** for taking the time to evaluate my work, and especially **Dr Rainer Schindl** and **Dr Bruno Constantin**, who kindly accepted to be the referees for my defense.

I would like to thank **Natacha** for welcoming me in the lab. Thank you for your help and your feedback on my projects. And thank you for giving me great opportunities and helping me find a postdoc.

I would like to thank **Loïc**, my supervisor during this long journey. Thank you for everything you taught me, including patience with the exciting technique of patch-clamp and the never ending running jokes. Thanks for the opportunities you gave me and for trusting me with these projects. Again (this is your English version of "de nouveau", in case you did not notice), thank you.

To my fellow colleagues from the lab

I would like to thank **all the members of my lab** (past and present) for your welcome and your help.

A special thank you to the ***Bullshit team***: thank you for all the bullshit, the laughs, the coffee breaks, the protocols... It has been a pleasure to have you by my side during my PhD!

Grazie to my favorite pasta, ***Farfalle***! Thank you for your help, your advices and the laughs. I will send you a bill for the coffees!

I would like to thank **Guillaume**, it was a pleasure to share a desk and the ups and down of the PhD with you. And thank you for teaching me how to properly complain.

Pauline, thank you for the good times and your good spirit! I would also like to thank you for your great efficiency to make the lab work. I wish you the best and hope you'll get that dream job you deserve!

I would like to thank **Abigaël**, with whom I also shared the ups and down of the PhD. Thank you for your unbreakable good spirit, those long discussions and for being my fellow lab mate during the holidays when no one else was around! I wish you the best for what's next, you truly deserve it!

Thank you, **Aurélien**, and good luck for the end of your PhD. Maybe one day you'll share your secret to keep your cool at all times.

Thank you, **Alex**, for teaching me some techniques when I first arrived in the lab and thank you for your contribution to my project. I would like to thank **Oksana** as well. I wish your growing family the best!

I would like to thank **Myrto** for all your help, particularly in the molecular biology department, throughout my PhD.

Thank you, **Dima**, for your valuable input and great contributions to my project, cheers!

I would like to thank **Fabien**, for your support and your help making sure I survive this PhD. I would like to thank you as well for giving me the opportunity to participate in your work. I would also like to thank **Charlotte**, and wish your new team the best.

I would like to thank **Morad** and **Eric** for giving me the opportunity to contribute to your projects. And thank you, Morad, for the kind words of encouragement.

I would like to thank the super efficient and super nice duo, **Artem** and **Katya**, it was a pleasure having you as colleagues.

I would like to thank **Slava** for your help for the human sample study.

Thank you to **Manue**, **Ingrid** and **Pascal**, for the lively lunch debates.

Grazie to **Alessandra** and **Anna-Rita**.

To all the current students of the lab, **Mohamed**, **Aline**, **Antoine**, I wish you all good luck for what will be next for you. A special がんばって to Mohamed, thank you for your help.

Lina, I wish you the best for your PhD, with your dedication and your great supervisor I have no doubt it will be a very good one!

Merci à **Etienne** et **Christian**, pour tout ce que vous m'avez appris avec toutes ces « petites réponses » à mes « petites questions ».

Je souhaiterais remercier **Emilie**, pour les commandes, la gestion de la biocel qui ne doit pas toujours être facile. Merci aussi à ta main d'experte qui a sauvé mon orchidée !

Merci à également à **Nathalie**, pour la biologie moléculaire.

Merci à **Laurent** pour les midipreps et pour tout ce que tu fais pour la culture.

Enfin, merci à **Andrée** qui s'assure de la propreté du laboratoire.

To my fellow colleagues from the IRCL

I would like to thank my colleagues from the IRCL that welcome me regularly in their lab.

A big thank you to **Yasmine**. Thank you for everything you taught me and for your valuable help. It was a pleasure to work with you! I hope we will have the opportunity to work together again in the future!

I would also like to thank the flow cytometry experts, **Nathalie** and **Emilie**. Thank you for what you taught me, for your great efficiency and your help to tame the CyAn or Aria when they were not in the mood.

J'aimerais également remercier **Bernadette** et **Pascaline** pour votre gentillesse et votre aide technique.

To my fellow colleagues from the Sakai-lab, LIMMS, IIS

I met a lot of amazing people in Tokyo and would like to thank all the LIMMS, Sakai-lab and IIS members: thank you, *merci*, ありがとうございます for the very warm welcome!

酒井先生はありがとうございます。Thank you for inviting me, it was a pleasure to work in your lab.

I would like to thank **Eric** for welcoming me in your team, it was a pleasure working with you.

To **Mathieu**, thank you, *chef*, for the warm welcome and your help during those three months.

I would also like to thank our youngster, **Yannick**. Thank you for the welcome, it was a pleasure working with you! I'm looking forward to an herbal tea 飲み放題 the next I'm in Japan!

A special *danke* to my office neighbor, the oh so old **ベネちゃん**. Thank you for all the laughs, and your support. I hope you're taking good care of "Aby". Best of luck for your PhD, you're one of the hardest working student I've met, I hope you'll get all the "balloons" and the success you deserve! 先輩はありがとうございます。 Thank you for your help with the unpredictable confocal microscope. Thank you for all those meals and coffee breaks. Most of all, thank you for all those culinary, cultural, musical and many other discoveries. My time in Japan would not have been the same without you! I wish you the best for whatever you decide to do next.

Thank you, **Nicolas**, for those passionate discussions when we shared a coffee, a meal or a patisserie from *Le Ressort*. I hope you will always keep this insatiable curiosity and thirst for knowledge. I wish you good luck for your PhD, I have no doubt it will be brilliant if you manage to focus a little! And remember, you need to ask for permission before you dust your neighbor's futon.

I would also like to thank **Anthony, Yuki, Saeko, Shu, Meoul, Seogmin, Timothée, Vincent, Matthieu, Julie, Thalia, Kimura, Amal, Tokitou, Choi, Astia, Shinohara-san, Shimizu-san, Tobe-san** and **Hirano-san**.

To my other collaborators, valuable contributors to my project

I would like to thank **Olivier** from the university of Nice for your valuable input on the S1R, and for helping me to navigate through the tricky parts of the S1R such as pharmacology and immunostaining. I would also like to thank you for your participation in my PhD follow-up committee.

I would like to thank **Laurent** and **Alessandro**, from the PhLaM laboratory, for everything they taught me on imaging. Thank you for your help to decipher protein interactions. And thank you for making me discover the best workshop ever, MiFoBio!

To my family and friends

Finally, I would like to thank my friends and family for their support and love.

Ludo, thank you for supporting me during this long journey. Thank you for helping me, comforting me, encouraging me, making me laugh, lifting me... And thank you for following me across the Atlantic for our next chapter! Love you!

I would like to thank my parents and my grand-parents. **Ama**, merci pour *tout*. Je ne serais pas là sans toi et tout ce que tu as fait pour moi. **Aita**, merci pour ton soutien et pour toujours croire en moi.

Thank you to my best friend, **Naroa**. When we were young, everyone said we looked like sisters... But they were wrong, because we *are* sisters. We live far away from each other (and we will soon be further apart) and we work a lot, but we always will be there for each other. *Milesker. Maite zaitut.*

To my second family from the North, **Adrien, Julie, William** and **Raphaël**, thank you for all the good times in our second home in Lille!

After my *sister*, I have to thank my *big brother*. Thank you, **Ju**, for being there, you were my lifeline during some difficult moments. Thank you for your help and your support, and for making me smile during some of the hardest times.

I would also like to thank **Joëlle, Jean Louis** and all the **Leroux** for welcoming me into your family. To my second family from the South, **Maritxu & Tintin**, merci pour ces bons moments au pays! And, last but not least, thank you to **the girls** for taking time away from your business to make me feel better.

Financial support

This work was supported by a PhD grant cofounded by Région Hauts de France and INSERM, and followed by a grant founded ARTP.



and in the end,
we come back stronger,
different
and all that matters
is that we kept going.
r. m. drake

Table of contents

Abstract	3
Résumé	5
Acknowledgement	7
Financial support	11
Table of contents	15
List of figures and tables	21
List of abbreviations	25
Scientific contributions	33
Publications	33
First author publications	33
Co-author publications	33
Communications	35
Introduction	37
I. Prostate in health and disease	39
1. Prostate physiology	39
a. Anatomy and function	39
b. Histology	40
c. Regulation by androgens	40
2. Prostate cancer	41
a. Facts and figures	42
b. Development	42
c. Diagnostic and prognosis	42
d. Histological grading	44
e. Clinical staging	45
f. Treatment	46
g. Mechanisms of resistance	46
II. Cancer stem cells	48
III. Calcium channels	49
IV. Store-operated calcium channels	51
1. STIM1	51
2. Orai1	52
3. SOC activation mechanism	53
4. SOC inactivation mechanism	56
5. SOC modulation	57

6.	SOC pharmacology.....	57
a.	Lanthanides	57
b.	2-aminoethyldiphenyl borate (2-APB).....	57
c.	3,5-bis(trifluoromethyl)pyrazole (BTP2)	58
d.	Synta66.....	58
e.	GSK compounds.....	58
f.	RO2959.....	58
7.	Gene expression regulation via SOC channels	58
8.	SOC and cancer	60
V.	The sigma 1 receptor.....	63
1.	Identification and function	63
2.	S1R structure	63
3.	S1R and cancer	63
4.	S1R pharmacology	64
	Aims of the thesis	65
I.	Characterization of the calcium signature of stem-like cancer cells	68
II.	The S1R as a potential partner protein of calcium channels in PCa.....	68
1.	Study of the S1R expression in PCa	68
2.	Functional and physiological impacts of the S1R on SOC channels in PCa cells.....	68
3.	Regulation of other calcium channels by the S1R in PCa.....	69
	Material & Methods	71
I.	Biological materials	73
1.	Human samples	73
a.	Tissues.....	73
b.	cDNA.....	73
2.	Cell lines	74
a.	HEK-293 model cell line	74
b.	Prostate cancer cell lines.....	74
c.	Melanoma cell line.....	74
3.	Adherent culture conditions.....	74
4.	Sphere formation	75
5.	Identification of quiescent/slow cycling cells and FACS sorting	76
a.	Melanoma	76
b.	Prostate.....	77
II.	Transfection	78

1.	siRNA lipofection.....	78
2.	Plasmid transfection.....	79
	a. Plasmid lipofection	79
	b. Plasmid nucleofection	79
III.	Transcriptomics.....	81
1.	RNA extraction.....	81
2.	Reverse transcription.....	81
3.	Quantitative PCR	81
IV.	Proteomics	83
1.	Western blot and associated techniques.....	83
	a. Protein extraction	83
	b. Western Blot.....	83
	c. Coimmunoprecipitation.....	84
	d. Biotinylation.....	85
2.	Immunocytochemistry	85
	a. Standard protocol.....	86
	b. Specific protocol for S1R.....	86
V.	Functional studies	88
1.	Calcium signaling.....	88
	a. Patch-clamp	88
	b. Calcium imaging.....	90
2.	Confocal microscopy.....	91
	a. Dynamics (S1R/NFAT).....	91
	b. Time domain – fluorescence lifetime-imaging microscopy (TD-FLIM).....	91
3.	Cell viability and proliferation.....	93
4.	Cell cycle	93
	a. Propidium iodide	93
	b. PI-ki67 double staining.....	94
	c. EdU assay	94
5.	NFAT-Luciferase assay.....	94
6.	Apoptosis	95
7.	Cell migration.....	95
8.	In vivo studies	95
	a. Cancer stem cell validation.....	96
	b. S1R.....	96
	Results.....	97
	1. Orai1/NFAT pathway is a gatekeeper of cancer cell quiescence/activation transition ..	99

1.	Orai1 expression and function decrease in prostate cancer cells with stem-like properties	102
2.	Orai1 expression and function are also down-regulated in melanoma cells with stem-like properties	106
3.	Orai1 is involved in SOCE in both non-stem and stem-like subpopulations	109
4.	Orai1 inhibition increases a pool of cells with stem-like properties.....	111
5.	Orai1 regulates quiescence via calcineurin-NFAT modulation	113
6.	Chemotherapeutic stress induces quiescence and is associated with a decrease in Orai1 expression.....	115
2. The sigma 1 receptor, a new partner protein of store-operated channels in prostate cancer		117
1.	The S1R is overexpressed in PCa.....	120
2.	S1R expression is positively regulated by androgens in PCa	121
3.	Androgens regulate Orai1 expression, but not Orai3 and STIM1	123
4.	The S1R positively regulates SOC channels in PCa cells.....	125
5.	The S1R translocates to the plasma membrane (PM) upon SOCE activation...	130
6.	The S1R directly interacts with Orai1 to modulate SOCE	133
7.	The S1R increases PCa proliferation.....	135
8.	The S1R modulates PCa proliferation via SOC channels	137
9.	The S1R modulates NFATc3 nuclear translocation	139
10.	The S1R modulates prostate cancer cell quiescence via Orai1	142
11.	The S1R participates in apoptosis	143
12.	The S1R is also able to modulate the activity of TRPV6	144
13.	The S1R increases TRPM8 activity, enhancing its antimigratory effect in PCa.	145
Discussion.....		147
I.	Orai1/NFAT pathway is a key player of the proliferation/quiescence transition .	149
II.	The S1R, a new partner of SOC channels in PCa	151
1.	S1R expression is regulated by androgens in PCa cells	151
2.	Orai1 expression is regulated by androgens in PCa cells.....	152
3.	The S1R positively modulates SOC channels in PCa cells.....	153
4.	S1R modulates PCa proliferation via the SOC/NFAT pathway.....	155
5.	S1R modulates other calcium channels in PCa cells.....	157
6.	The S1R: a new pharmacological target for PCa treatment?.....	159
III.	General conclusion and perspectives	161
References.....		163
Annexes		181

1. Identification of the calcium signature during hiPS differentiation into mature functional hepatocytes	185
2. TRPM8 and prostate: a cold case?	193
3. TRPV1 variants impair intracellular Ca²⁺ signaling and may confer susceptibility to malignant hyperthermia.....	217
4. Activation of mutated TRPA1 ion channel by resveratrol in human prostate cancer associated fibroblasts (CAF).....	221
5. Functional and Modeling Studies of the Transmembrane Region of the TRPM8 Channel	225
Résumé substantiel	229
Introduction	231
I. Physiologie et pathologies de la prostate.....	231
1. Physiologie	231
a. Anatomie et fonction.....	231
b. Histologie	231
c. Régulation par les androgènes.....	231
2. Le cancer de la prostate.....	231
a. Chiffres.....	231
b. Développement.....	231
c. Diagnostic et pronostic	232
d. Grade histologique	232
e. Classification de la tumeur	232
f. Traitements	232
g. Mécanismes de résistance.....	233
II. Les cellules souches cancéreuses	233
III. Les canaux calciques	233
IV. Les canaux SOC (store-operated channels).....	234
V. Le récepteur Sigma 1 (S1R).....	235
Problématique et but du travail.....	236
Résultats.....	237
I. La voie Orai1/NFAT régule la transition quiescence/prolifération des cellules cancéreuses	237
1. L'expression et la fonction d'Orai1 sont diminués dans les CSC prostatiques	237
2. L'expression et la fonction d'Orai1 sont diminuées dans les CSC de mélanome	237

3.	L'inhibition d'Orai1 augmente la population de cellules cancéreuses avec des propriétés de cellules souches.....	238
4.	Orai1 régule la quiescence via la voie NFAT.....	238
5.	La quiescence induite par la chimiothérapie est associée à une chute d'expression d'Orai1.....	238
II.	Le S1R : protéine partenaire d'Orai1 dans le cancer de la prostate.....	239
1.	L'expression du S1R dans le cancer de la prostate.....	239
2.	L'expression d'Orai et STIM dans le cancer de la prostate.....	240
3.	Le S1R module positivement les canaux SOC dans le cancer de la prostate.....	240
4.	Le S1R se déplace vers la membrane plasmique lors de l'activation des SOC.....	240
5.	Le S1R interagit avec les canaux SOC.....	241
6.	L'inhibition du S1R ralentit la prolifération et la croissance tumorale.....	241
7.	Le S1R régule la prolifération via Orai1 et la voie NFAT.....	242
8.	Le S1R permet de réguler la quiescence des CSC prostatiques via Orai1.....	242
9.	Le S1R participe à l'apoptose.....	243
10.	Le S1R est capable de moduler l'activité de TRPV6.....	243
11.	Le S1R est également capable de moduler l'activité de TRPM8 et la migration.....	243
	Discussion.....	244
I.	La voie Orai1/NFAT joue un rôle clé dans la transition quiescence/prolifération des CSC.....	244
II.	Le S1R est un nouveau partenaire des canaux SOC dans le cancer de la prostate.....	245
1.	L'expression du S1R est régulée par les androgènes dans le CaP.....	245
2.	L'expression d'Orai1 est régulée par les androgènes dans le CaP.....	245
3.	Le S1R augmente l'activité des canaux SOC dans le CaP.....	246
4.	Le S1R augmente la prolifération des cellules du CaP via la voie SOC/NFAT.....	246
5.	Le S1R est capable de réguler d'autre canaux calciques dans le CaP..	247
6.	Le S1R : une nouvelle cible pharmacologique dans le traitement du CaP ?.....	248
III.	Conclusion générale et perspectives.....	249

List of figures and tables

INTRODUCTION

Figure 1: Zonal anatomy of the prostate.....	39
Figure 2: Cellular components of the prostate.....	41
Figure 3: Gleason histological patterns of PCa.....	44
Figure 4: Clinical staging of PCa.....	45
Figure 5: Simplified view of the calcium signaling.....	50
Figure 6: Molecular structure of STIM1.....	52
Figure 7: Molecular structure of Orai1.....	53
Figure 8: STIM1 activation sequence.....	54
Figure 9: STIM1 and Orai1 co-clustering.....	55
Figure 10: STIM1 and Orai1 binding models.....	56
Figure 11: NFAT structure and activation pathway.....	59
Figure 12: Calcium signaling and cancer.....	61

MATERIAL & METHODS

Figure 1: GFP dilution in HBL H2B-GFP cells.....	76
Figure 2: Dil dilution in PC3 cells.....	77
Figure 3: siS1R validation.....	78
Table 1: Name and sequence of siRNAs.....	78
Table 2: List and origin of the plasmids.....	80
Table 3: Name and sequence of primers.....	82
Table 4: List of antibodies used for western blot (WB), immunofluorescence (IF), immunohistochemistry (IHC) or flow cytometry (Flow Cy).....	87
Figure 4: Schematic representation of the four main patch-clamp configurations.....	89
Table 5: Composition of the intracellular solutions used during patch-clamp experiments.....	90
Table 6: Composition of the extracellular solutions used during patch-clamp experiments.....	90
Figure 5: CFP and YFP spectra.....	92

RESULTS

1. Orai1/NFAT pathway is a gatekeeper of cancer cell quiescence/activation transition

Figure 1: CD44-positive PC3 LRCs present stem-like properties.....	103
Figure 2: Orai1 expression is decreased in prostate cancer cells with stem-like properties.....	104
Figure 3: Orai1 function is decreased in prostate cancer cells with stem-like properties.....	105
Figure 4: HBL LRCs present stem-like properties.....	106
Figure 5: Orai1 expression is decreased in melanoma cells with stem-like properties.....	107

Figure 6: Orai1 function is decreased in melanoma cells with stem-like properties.....	108
Figure 7: Orai1 is a key actor in non-stem and stem-like PC3 cells SOCE.....	109
Figure 8: Orai1 is actor in HBL SOCE.....	110
Figure 9: Orai1 inhibition increases stemness in prostate cancer cells.....	111
Figure 10: Orai1 inhibition increases stemness in melanoma cells.....	112
Figure 11: Orai1 regulates quiescence via calcineurin-NFAT modulation.....	114
Figure 12: CBP is upregulated in LRCs and Orai1 inhibition-induced stemness.....	115
Figure 13: Chemotherapy treatment induces quiescence and is associated with a decrease in Orai1 expression.....	116

2. The sigma 1 receptor, a new partner of store-operated calcium channels in prostate cancer

Figure 1: S1R expression is increased in prostate cancer.....	120
Figure 2: S1R expression in prostate cancer cell lines.....	121
Figure 3: Androgens regulate S1R expression in PCa cells.....	122
Figure 4: Androgens regulate Orai1 but not Orai3 and STIM1 in PCa cells.....	124
Figure 5: Human S1R overexpression increases SOC channel activity in LNCaP cells.....	126
Figure 6: Endogenous S1R inhibition decreases SOC activity in LNCaP cells.....	127
Figure 7: Acute exposition with S1R agonists increases SOC activity.....	128
Figure 8: Chronic exposition with S1R agonists increases SOC activity.....	128
Figure 9: S1R is a positive modulator of SOCE in PC3 cells.....	129
Figure 10: S1R overexpression increases ER calcium content in PCa cells.....	129
Figure 11: S1R presence increases in the biotinylated fraction upon SOCE activation.....	130
Figure 12: Dynamic confocal studies show that S1R translocates to the PM during ER Ca ²⁺ store depletion.....	131
Figure 13: Endogenous S1R translocates to the PM during ER Ca ²⁺ store depletion.....	132
Figure 14: The S1R and Ora1 are found within the same protein complex.....	133
Figure 15: TD-FLIM experiments show that S1R interacts with STIM1 and Orai1.....	134
Figure 16: S1R inhibition decreases LNCaP cell proliferation and in vivo tumor growth.....	136
Figure 17: S1R inhibition decreases PC3 cell proliferation and in vivo tumor growth.....	137
Figure 18: Effect of combined inhibition of the S1R and Ora1s.....	138
Figure 19: S1R inhibition decreases NFATc3 nuclear translocation and activity.....	140
Figure 20: The S1R affects the dynamics of SOCE-induced nuclear translocation and retention of NFATc3 in LNCaP cells.....	141
Figure 21: S1R inhibition increases the quiescent Dil-positive subpopulation.....	142
Figure 22: S1R inhibition increases apoptosis resistance in LNCaP cells.....	143
Figure 23: The S1R decreases TRPV6 activity in HEK-293 cells.....	144
Figure 24: The S1R increases TRPM8 activity in HEK-293 cells.....	145

Figure 25: The S1R increases TRPM8-mediated inhibition of PCa cell migration.....146

DISCUSSION

Figure 1: Expression profile of our proteins of interest during PCa progression.....153

Figure 2: Activity profiles of SOC and ARC channels during PCa progression.....155

Figure 3: Physiological consequences of the SOC/ARC balance during PCa progression.....157

Figure 4: TRPV6 and TRPM8 expression profiles during PCa progression.....158

Figure 5: Potential roles of the S1R in PCa.....159

List of abbreviations

#

2-APB: 2-aminoethyldiphenyl borate

5-FU: 5-fluorouracil

A

ADP: adenosine diphosphate

ADT: androgen deprivation therapy

AKAP79: A-kinase anchor protein 79

AM: amplitude modulation

AM (Fura2-AM): acetoxymethyl ester

AMP: adenosine monophosphate

ANOVA: analysis of variance

AP1: activator protein 1

AR: androgen receptor

ARE: androgen response element

ATCC: American type culture collection

ATP: adenosine triphosphate

B

BAPTA: 1,2-bis(2-aminophenoxy)ethane-N,N,N',N'-tetraacetic acid

BCA: bicinchoninic acid assay

BCa: breast cancer

BPH: benign prostatic hyperplasia

BrdU: 5-bromo-2'-deoxyuridine

BSA: bovine serum albumin

BTP2: 3,5-bis(trifluoromethyl)pyrazole

C

CABIN1: calcineurin-binding protein 1

CAD: CRAC-activation domain

CaM: calmodulin

cAMP: cyclic AMP

CAR: calcium accumulating region

Cas9: CRISPR-associated protein 9

CBP: CREB-binding protein

CC: coiled-coil region
CCD: charge-coupled device
CCE: capacitative calcium entry
CD (CD44...): cluster of differentiation
CDI: calcium-dependent inactivation
CDK4: cyclin dependent kinase 4
cDNA: complementary deoxyribonucleic acid
CK1: casein kinase 1
CMD: CRAC modulatory domain
CMV: cytomegalovirus
CN: calcineurin
coIP: coimmunoprecipitation
CPA: cyclopiazonic acid
CRAC: calcium release-activated calcium channel
CRACR2A: CRAC regulatory protein 2A
CREB: cAMP response element-binding protein
CRISPR: clustered regularly interspaced short palindromic repeats
CRPC: castration-resistant prostate cancer
CsA: cyclosporine A
CSC: cancer stem cell
Ct: carboxy-terminus
Cy5: cyanine 5

D

DAG: diacylglycerol
DAPI: 4',6-diamidino-2-phénylindole
DHT: dihydrotestosterone
DiI: DiI18(3): 1,1'-Dioctadecyl-3,3,3',3'-tetramethylindocarbocyanine perchlorate
DMEM: Dulbecco/Vogt modified Eagle's minimal essential medium
DMT: N,N-dimethyltryptamine
DNA: deoxyribonucleic acid
dNTP: deoxyribose nucleoside triphosphate
DoceT: docetaxel
DPBS: Dulbecco's phosphate-buffered saline
DSCR: Down's syndrome critical region
DTT: dithiothreitol
DYRK: dual specificity tyrosine phosphorylation-regulated kinase

E

ECL: enhanced chemiluminescence

EDTA: ethylenediaminetetraacetic acid

EdU: 5-ethynyl-2'-deoxyuridine

EGF: epidermal growth factor

EGTA: ethylene glycol-bis(β -aminoethyl ether)-N,N,N',N'-tetraacetic acid

ER: endoplasmic reticulum

ETON: extended transmembrane Orai1 N-terminal domain

F

FACS: fluorescence-activated cell sorting

FBS: fetal bovine serum

FCCS: fluorescence cross-correlation spectroscopy

FCDI: fast CDI

FGF: fibroblast growth factor

FLIM: fluorescence-lifetime imaging microscopy

FM: frequency modulation

FP: fluorescent protein

FRET: Förster resonance energy transfer

G

G0 phase: gap 0 phase

G1 phase: gap 1 phase

G418: geneticin

GAPDH: glyceraldehyde 3-phosphate dehydrogenase

GF: growth factor

GFP: green fluorescent protein

GPCR: G protein-coupled receptor

GSK3: glycogen synthase kinase 3

GTP: guanosine triphosphate

H

H2B: histone 2B

HEK-293: human embryonic kidney 293

HEPES: 4-(2-hydroxyethyl)-1-piperazineethanesulfonic acid

hERG: human ether-à-go-go-related gene

hiPS: human induced pluripotent stem cells

HPRT: hypoxanthine-guanine phosphoribosyl transferase

HRP: horse radish peroxidase

hS1R: human S1R

HSA: human serum albumin

I

ICC: immunocytochemistry

ID: inhibitory domain

IF: immunofluorescence

IgG: immunoglobulin G

INMT: indolethylamine-N-methyltransferase

IP₃: inositol 1,4,5-trisphosphate

IP₃R: IP₃ receptor

IQGAP1: IQ motif-containing GTPase activating protein

K

K: lysine

KO: knock-out

L

LH: luteinizing hormone

LHRH: LH-releasing hormone

LNCaP: lymph node carcinoma of the prostate

LRC: label retaining cell

M

M phase: mitosis phase

MAM: mitochondria-associated membranes

MAPK: mitogen-activated protein kinase

MCU: mitochondrial calcium uniporter

MDM2: murine double minute 2

mRNA: messenger RNA

MTS: 3-(4,5-dimethylthiazol-2-yl)-5-(3-carboxymethoxyphenyl)-2-(4-sulfophenyl)-2H-tetrazolium

MuLV: murine leukemia virus

N

NA: numerical aperture

NFAT: nuclear factor of activated T cell

NFκB: nuclear factor kappa B

NHR: NFAT homology region

NLS: nuclear localization signal
NMRI: naval medical research institute
NOD: non-obese diabetic
NP-40: nonyl phenoxy polyethoxy ethanol-40
NRON: non-coding RNA repressor of NFAT
NSG: Nod SCID gamma
Nt: amino-terminus

O

OASF: Orai1-activating small fragment

P

PAGE: polyacrylamide gel electrophoresis
PARP: poly-ADP-ribose polymerase
PBS: phosphate-buffered saline
PC3: prostate cancer 3
PCa: prostate cancer
pcDNA4: plasmid circular DNA 4
PCNA: proliferating cell nuclear antigen
PCR: polymerase chain reaction
PDL: pulsed diode laser
pHEMA: poly(2-hydroxyethyl methacrylate)
PI: propidium iodide
PIN: prostatic intraepithelial neoplasia
PIP₂: phosphatidylinositol 4,5-bisphosphate
PKC: protein kinase C
PLC: phospholipase C
PM: plasma membrane
PMS: phenazine methosulfate
PNT1a: prostate non-tumor 1a
PS: proline/serine-rich domain
PSA: prostate-specific antigen
PVDF: polyvinylidene fluoride

Q

qPCR: quantitative PCR

R

RE: response element

RIPA: radioimmunoprecipitation assay
RHD: Rel-homology domain
rHu bFGF: recombinant human basic fibroblast growth factor
RNA: ribonucleic acid
RNase: ribonuclease
RPMI: Roswell Park memorial institute
rRNA: ribosomal RNA
rS1R: rat S1R
RT: reverse transcription

S

S phase: synthesis phase
S1R: sigma 1 receptor
SAM: sterile α -motif
SCDI: slow CDI
SCID: severe combined immunodeficiency
SCLC: small cell lung cancer
SDS: sodium dodecyl sulfate
SEM: standard error of the mean
SERCA: sarco/endoplasmic/reticulum Ca^{2+} -ATPase
SFU: sphere forming unit
SHGB: sex hormone binding globulin
shRNA: short hairpin RNA
siLuc: siRNA targeting Luciferase
siNeg: negative scramble siRNA
siRNA: small interfering RNA
SK3: small-conductance calcium-activated K^+ channel
SOAP: STIM1/Orai1 association pocket
SOAR: STIM-Orai activating region
SOC: store-operated channel
SOCE: store-operated calcium entry
SOX2: sex determining region Y-related high mobility group-box gene 2
SP: serine-proline-X-X repeat motif
SPAD: single photon avalanche photodiodes
SPCA2: secretory pathway Ca^{2+} -ATPase 2
SRR: serine-rich region
STIM: stromal interaction molecule
SYFP: super yellow fluorescent protein

T

TA: transient amplifying
TAD: transactivation domain
TBST: Tris-buffered saline with Tween 20
TCSPC: time-correlated single photon counting
TD-FLIM: time domain FLIM
TEA-Cl: tetraethylammonium chloride
TF: transcription factor
TKR: tyrosine-kinase receptor
TM: transmembrane
TMD: transmembrane domain
TME: tumor microenvironment
TNM: tumor, node, metastasis
TNT: Tris-NaCl-Tween buffer
Tris: tris(hydroxymethyl)aminomethane
TRIP: threonine-arginine-isoleucine-proline
TRP: transient receptor potential
TRPA: TRP ankyrin
TRPM: TRP melastatin
TRPV: TRP vanilloid

W

WB: western blot
WGA: wheat germ agglutinin

Scientific contributions

Publications

First author publications

1. **Noyer L**, Gordienko D, Furlan A, Bokhobza A, Touil Y, Borgese F, Gkika D, Mihalache A, Lehen'kyi S, Segard P, El-Kadiri M, Allart L, Ziental-Gelus N, Gosset P, Héliot L, Soriani O, Prevarskaya N, Lemonnier L. Identification of a new partner protein of Orai1 in prostate cancer. *In preparation*.
2. **Noyer L**, Flamenco P, Touil Y, Slomianny C, Ostyn C, Gkika D, Machhour RE, Vandomme J, Segard P, Abeele FV, Formstecher P, Polakowska R, Quesnel B, Prevarskaya N, Lemonnier L. Orai1/NFAT pathway is a gatekeeper of cancer stem cells quiescence/activation transition. *In preparation*.
3. **Noyer L**, Gkika D, Dannoy M, Bernier ML, Lemonnier L, Sakai Y, Leclerc E. Identification of the calcium signature in hepatocyte differentiation. *In preparation*.
4. **Noyer L**, Grolez GP, Prevarskaya N, Gkika D, Lemonnier L. TRPM8 and prostate: a cold case? *Pflugers Arch*. 2018 Jun 20. doi: 10.1007/s00424-018-2169-1. *Invited review*.

Co-author publications

1. Grolez GP, Hammadi M, **Noyer L**, Kondraskaya K, Bulk E, Genova T, Bollo A, Oullier T, Marionneau-Lambot S, Prevarskaya N, Fiorio Pla A, Gkika D. TRPM8 as an Anti-Tumoral Target in Prostate Cancer Growth and Metastasis Dissemination. *In preparation*.
2. Farfariello V, Gordienko D, Touil Y, Germain E, Fliniaux I, Desruelles E, Lemonnier L, Gkika D, Shapovalov G, Ritaine A, **Noyer L**, Lebas M, Allart L, Bernard D, Pluquet O, Quesnel B, Abbadie C, Parys JB, Putney JW, Prevarskaya N. Loss of ER-mitochondria Ca²⁺ transfer control unveils the pro-tumor behavior of senescent prostate stroma induced by chemotherapy. *In preparation*.
3. Vancauwenberghe E, Derouiche S, Mariot P, Lemonnier L, Gosset P, **Noyer L**, Warnier M, Bokhobza A, Slomianny C, Dewailly E, Delcourt P, Allart L, Desruelles E, Mauroy B, Bonnal JL, Prevarskaya N, Roudbaraki M. TRPA1 activation in prostate cancer-associated fibroblasts induces HGF secretion and chemotherapeutic resistance in prostate cancer cells. *Submitted*.

4. Dubois C, Bidaux G, Kondratskyi A, **Noyer L**, Vancauwenberghe E, Toillon RA, Mariot P, Roudbaraki M, Tierny D, Bonnal JL, Prevarskaya N, Abeelee FV. Apoptosis mediated by Mitochondrial Ca²⁺ Overload Requires Inhibition of Autophagy Revealing a Widespread Vulnerability of Cancer Cells. **Submitted**.
5. Abeelee FV, Lotteau S, Ducreux S, Dubois C, Monnier N, Hanna A, Gkika D, Romestaing C, **Noyer L**, Flourakis M, Tessier N, Al-Mawla R, Chouabe C, Lefai E, Lunardi J, Hamilton S, Fauré J, Van Coppenolle F, Prevarskaya N. TRPV1 variants impair intracellular Ca²⁺ signaling and may confer susceptibility to malignant hyperthermia. *Genet Med*. 2018 Jun 21. doi: 10.1038/s41436-018-0066-9.
6. Vancauwenberghe E, **Noyer L**, Derouiche S, Lemonnier L, Gosset P, Sadofsky LR, Mariot P, Warnier M, Bokhobza A, Slomianny C, Mauroy B, Bonnal JL, Dewailly E, Delcourt P, Allart L, Prevarskaya N, Roudbaraki M. Activation of mutated TRPA1 ion channel by resveratrol in human prostate cancer associated fibroblasts (CAF). *Mol carcinog*. 2017 Aug;56(8):1851-1867.
7. Bidaux G, Sgobba M, Lemonnier L, Borowiec AS, **Noyer L**, Jovanovic S, Zholos AV, Haider S. 2015. Functional and Modeling Studies of the Transmembrane Region of the TRPM8 Channel. *Biophys J*. 2015 Nov 3;109(9):1840-51.

Communications

1. AACR Annual Meeting 2019 – Atlanta, USA – March 29 - April 3rd 2019
Touil Y, Figeac M, Lemonnier L, Marot G, Segard P, Masselot B, **Noyer L**, Wisztorski M, Gimeno JP, Fournier I, Vincent A, Idziorek T, Quesnel B*. Omics unveils a specific signature of tumor dormancy in two murine models of leukemia and melanoma. **Oral presentation.**
2. COST meeting “What do we really know on Orai/Stim complex?” – Graz, AUSTRIA – February 11 - 14th 2019
Noyer L*, Touil Y, Flamenco P, Slomianny C, Ostyn C, Gkika D, Machhour RE, Vandomme J, Segard P, Formstecher P, Polakowska R, Quesnel B, Prevarskaya N, Lemonnier L. Orai1/NFAT pathway is a gatekeeper of cancer stem cells quiescence/activation transition. **Invited speaker.**
3. Feske laboratory – New York, USA – December 5th 2018
Noyer L*. **Invited seminar.**
4. 1st Ion Channels & Immunity symposium – New York, USA – December 3rd 2018
Noyer L*, Flamenco P, Touil Y, Polakowska R, Prevarskaya N, Lemonnier L. Orai1/NFAT pathway is a gatekeeper of cancer stem cell quiescence/activation transition. **Poster.**
5. 27th ARTP Annual Meeting – Paris, FRANCE – November 21th 2018
Noyer L*, Touil Y, Flamenco P, Slomianny C, Ostyn C, Gkika D, Machhour RE, Vandomme J, Segard P, Formstecher P, Polakowska R, Quesnel B, Prevarskaya N, Lemonnier L. Orai1/NFAT pathway is a gatekeeper of cancer stem cells quiescence/activation transition. **Invited speaker.**
6. LIMMS/CNRS-IIS (JAPAN) research activities: 2018 – 2019 booklet
Noyer L*. Characterization of the calcium signature during hepatocyte differentiation. **Poster.**
7. Functional Microscopy for Biology workshop – Seignosse, FRANCE – October 5 - 12th 2018
Noyer L*, Gordienko D, Furlan A, Héliot L, Y Touil, O Soriani, Prevarskaya N, Lemonnier L. Identification of a new partner of Orai1 in prostate cancer. **Poster.**
8. 29th Ion Channel Meeting – Sète, FRANCE – September 9 - 12th 2018
Noyer L*, Flamenco P, Touil Y, Polakowska R, Prevarskaya N, Lemonnier L. Orai1/NFAT pathway is a gatekeeper of cancer stem cell quiescence/activation transition. **Poster.**
Farfariello V*, Gordienko D, Touil Y, Germain E, Fliniaux I, Desruelles E, Lemonnier L, Gkika D, Shapovalov G, Ritaine A, **Noyer L**, Lebas M, Allart L, Bernard D, Pluquet O, Quesnel B, Abbadie C, Parys JB, Putney JW, Prevarskaya N. Loss of ER-mitochondria Ca²⁺ transfer control unveils the pro-tumor behavior of senescent prostate stroma induced by chemotherapy. **Poster.**

9. GDR 3697 Micronit – Marseille, FRANCE – January 30th - February 1st 2018
Touil Y, Figeac M, Lemonnier L, Marot G, Segard P, Masselot B, **Noyer L**, Wisztorski M, Gimeno JP, Fournier I, Vincent A, Idziorek T*, Quesnel B. Dorm-omics: Signature génétique, épigénétique et protéomique de deux modèles murins de dormance tumorale. **Oral presentation.**
10. 26th ARTP Annual Meeting – Paris, FRANCE – November 15th 2017
Noyer L*, Flamenco P, Touil Y, Polakowska R, Prevarskaya N, Lemonnier L. Orai1/NFAT pathway is a gatekeeper of cancer stem cell quiescence/activation transition. **Poster, best poster prize.**
11. 1st National Meeting on Ion Channels and Cancer – Amiens, FRANCE – November 14th 2017
Noyer L*, Flamenco P, Touil Y, Polakowska R, Prevarskaya N, Lemonnier L. Orai1/NFAT pathway is a gatekeeper of cancer stem cell quiescence/activation transition. **Poster, best poster prize.**
12. 28th Ion Channel Meeting, 6th SFICT Workshop – Paris, FRANCE – September 10 – 13th 2017
Haustrate A*, Kondratskyi A, **Noyer L**, Mihalache A, Prevarskaya N & Lehen'kyi V. TRPV6 calcium channel targeting by rabbit polyclonal antibodies raised against extracellular epitope induces apoptosis of the prostate cancer cell line LNCaP. **Poster.**
13. LIMMS – Femto-St meeting – Besançon, FRANCE – February 21 – 22nd 2017
Noyer L*, Touil Y, Gkika D, Gordienko D, Lehen'kyi V, Gosset P, Soriani O, Prevarskaya N, Lemonnier L. Identification of a new partner of SOC channels in prostate cancer. **Poster.**
14. 25th ARTP Annual Meeting – Paris, FRANCE – November 16th, 2016
Noyer L*, Touil Y, Gkika D, Gordienko D, Lehen'kyi V, Gosset P, Soriani O, Prevarskaya N, Lemonnier L. Identification of a new partner of SOC channels in prostate cancer. **Poster.**
15. Laboratory of Excellence, Ion Channel Science and Therapeutics, Young Researchers – Nice, FRANCE – October 6 - 7th, 2016
Noyer L*, Touil Y, Gkika D, Gordienko D, Lehen'kyi V, Gosset P, Soriani O, Prevarskaya N, Lemonnier L. Identification of a new partner of SOC channels in prostate cancer. **Poster.**
16. Workshop on BioMEMS and Cancer – Lille, FRANCE – December 17th, 2015
Noyer L*, Touil Y, Gkika D, Soriani O, Prevarskaya N, Lemonnier L. Identification of a new partner of SOC channels in prostate cancer. **Poster & talk.**
17. Laboratory of Excellence, Ion Channel Science and Therapeutics Meeting – Montpellier, FRANCE – November 30th - December 2nd, 2015
Noyer L*, Touil Y, Gkika D, Soriani O, Prevarskaya N, Lemonnier L. Identification of a new partner of SOC channels in prostate cancer. **Poster.**

Introduction

I. Prostate in health and disease

1. Prostate physiology

a. Anatomy and function

The prostate is a walnut sized muscular gland of the male reproductive system located directly below the bladder and above the pelvic floor muscles, behind the pubic symphysis and in front of the rectum.

The prostate anatomic model established by John McNeal (McNeal 1988) divides the gland in four anatomically and functionally distinct areas surrounded by a capsule (Figure 1):

- Central zone: representing approximately a quarter of the gland, this proximal area is located at the base of the prostate, surrounding the ejaculatory ducts.
- Peripheral zone: constituting 70% of the prostate gland, this large area posteriorly envelops the central zone, extends caudally to the apex of the prostate and wraps around the urethra below the seminal colliculus.
- Transitional zone: representing less than 5% of the total gland in healthy prostate, this region is constituted by two lobes wrapped around the urethra between the bladder and the seminal colliculus.
- Anterior fibromuscular stroma: small non-glandular zone constituting about 5% of the gland, located anteriorly to the urethra.

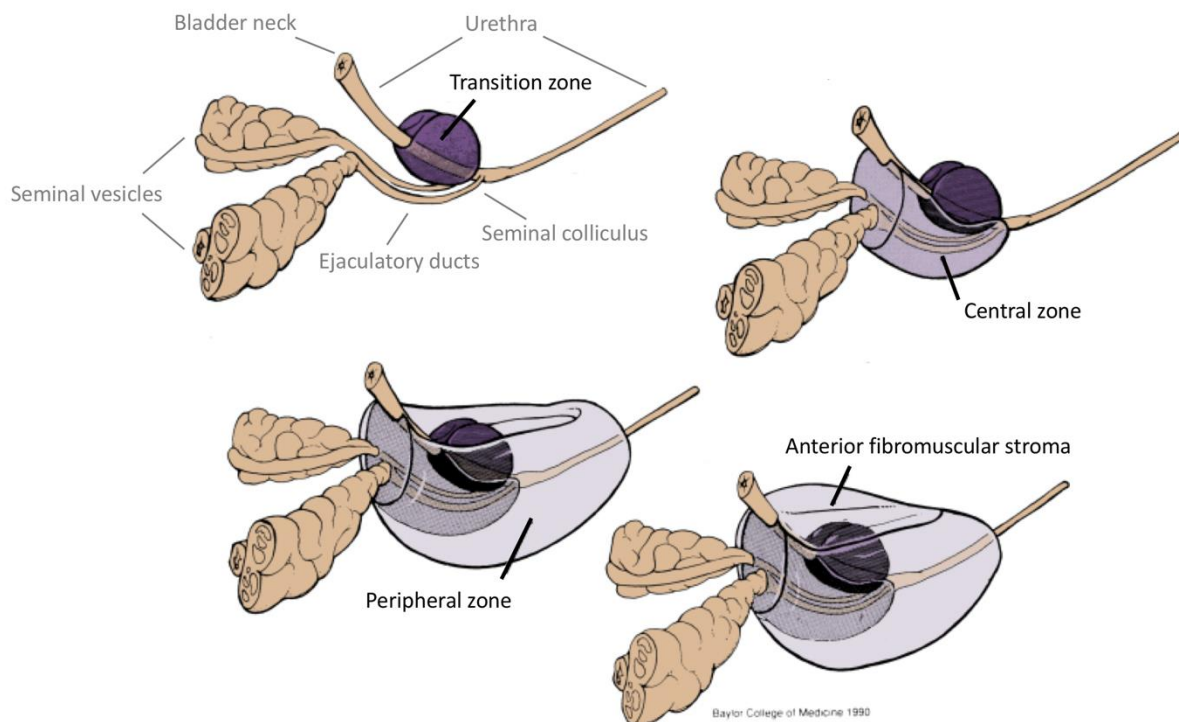


Figure 1: Zonal anatomy of the prostate

Adapted from Baylor College of Medicine 1990, based on McNeal 1988.

As pictured in [Figure 1](#), the prostate surrounds the proximal part of the urethra, called the prostatic urethra. This particular localization allows it to fulfill its dual role of prostate fluid secretion and fluid propelling during ejaculation and urination.

The main function of this gland is to produce the prostate fluid which makes up a third of the total semen volume. This liquid is composed of ions and enzymes such as the prostate specific antigen (PSA) which helps semen liquefaction. Prostate fluid helps the proper functioning of sperm cells and is therefore an important factor for men fertility.

The muscle component of the prostate helps ensure proper fluid excretion. First, during urination, prostate muscles contract in order to block ejaculatory ducts and help urine to go along the urethra from the bladder to the penile end. Prostate muscles also participate in the ejaculation process, with the help of bladder muscles, to block the upper part of the urethra leading to the bladder in order to avoid retrograde semen reflux to the bladder and ensure a proper propelling towards the external orifice at the penile end of the urethra.

b. Histology

The prostate tissue is composed of a fibromuscular stroma with glandular epithelia, both separated by a basal lamina.

The prostate epithelium is organized in glandular acini secreting the prostate fluid into the luminal space. Each acinus is composed by a luminal cubic layer of secretory epithelial cells followed by a layer of basal cells and neuroendocrine cells ([Figure 2](#); Barron and Rowley 2012). The basal cells constitute the unspecialized proliferating compartment of the acini; these cells will differentiate into secretory cells or, in rare case, undergo neuroendocrine differentiation.

The acini are surrounded by a fibromuscular stroma composed of a collagen-rich extracellular matrix containing fibroblasts, smooth muscle cells, blood vessels, autonomic nerves and immune cells.

c. Regulation by androgens

Through the androgen receptor (AR), androgens regulate key physiological processes in prostate epithelia such as proliferation, survival, differentiation and secretion (Dehm and Tindall 2006). Indeed, the suppression of the androgen stimuli leads to prostate atrophy due to a decreased epithelial cell proliferation and increased epithelial cell death (English et al. 1989; Wright et al. 1996). This shows the importance of androgens in the regulation of the life and death balance of prostate cells. Thus, the deregulation of this equilibrium can lead to pathological processes such as prostate cancer (see section I.2.).

Androgens are a type of steroid hormones mainly produced in the testes. This production is regulated by the hypothalamic luteinizing hormone (LH)-releasing hormone (LHRH) and downstream LH produced by the anterior pituitary. The main androgen is testosterone, produced by Leydig cells in testes (Miller and Auchus 2011). Testosterone reaches the bloodstream where it is transported bound to the liver-produced sex hormone binding globulin (SHGB) or human

serum albumin (HSA) (Zheng et al. 2015). When testosterone reaches prostate cells, it is transformed into dihydrotestosterone (DHT), a more potent AR activator (Askew et al. 2007), by the 5 α -reductase (Steers 2001).

The AR is a 110 kDa nuclear receptor that can act as a transcription factor upon ligand binding. Unbound AR is located in the cytoplasm, complexed to chaperone proteins. Upon androgen-binding, the receptor is translocated to the nucleus where it dimerizes and regulates specific genes expression by binding androgen response elements (ARE) (Heinlein and Chang 2004).

In addition to genomic regulation, the AR can also have rapid non-genomic effects including the modulation of signaling pathways within minutes of ligand binding (Foradori et al. 2008).

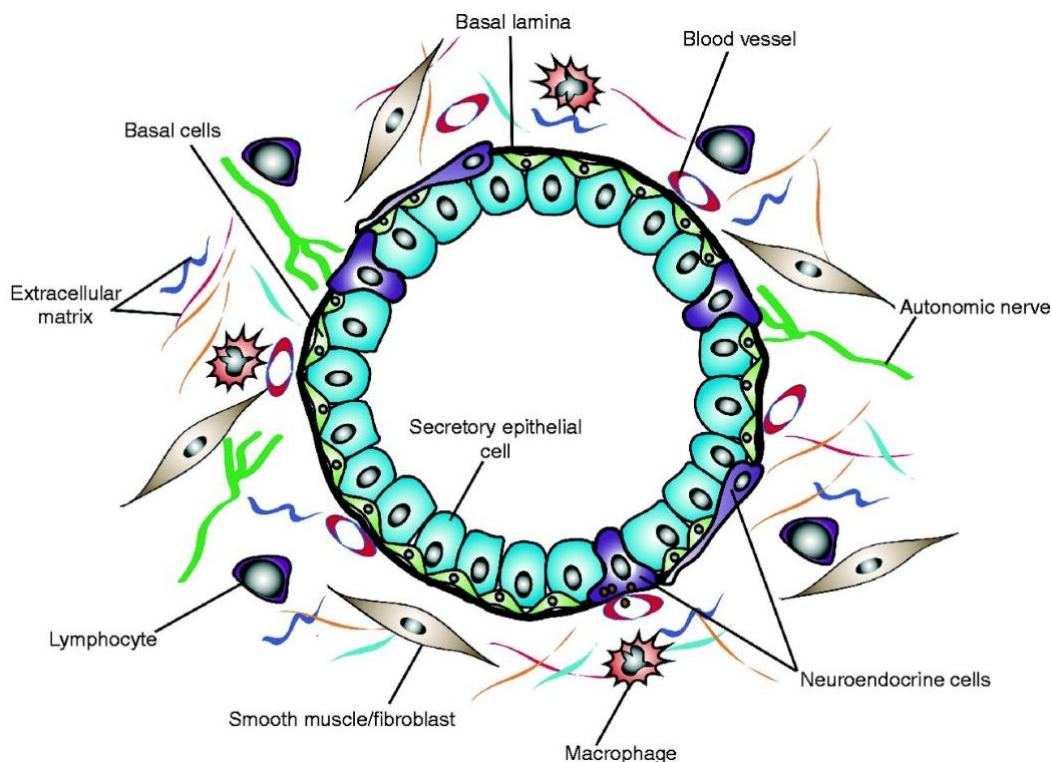


Figure 2: Cellular components of the prostate
Barron and Rowley 2012

2. Prostate cancer

The prostate can be affected by three main conditions:

- Prostatitis: a chronic or acute inflammation of the prostate, often, but not exclusively, due to bacterial infection.
- Benign prostatic hyperplasia (BPH): a nonmalignant growth of the prostate gland common in aging men. Indeed, most men present histologic features of BPH by 90 years. This hyperplasia takes place in the epithelia and stroma of the transition zone. This enlargement compresses the urethra causing lower urinary tract symptoms with obstruction and

increased frequency. BPH being mostly promoted by androgen stimuli, 5α -reductase inhibitors are used to alleviate the symptoms.

- Prostate cancer (PCa): an adenocarcinoma that develops preferentially, but not exclusively, in the peripheral zone of the prostate.

Here, we will focus on the PCa, that will be described below.

a. Facts and figures

With an estimated 1,276,106 new cases and 358,989 deaths in 2018, PCa is the second most frequent and fifth deadliest cancer worldwide (GLOBOCAN 2018, GCO, IARC). This pathology has more impact in developed countries, where it ranks as the most frequent and the third deadliest malignancy. This is due to the fact that this cancer has been linked with old age, and the ageing of the world's population will increase its prevalence in the coming years.

As indicated above, the main risk factor for PCa is age, it is the most diagnosed cancer in old men with an incidence rate of nearly 60% in men older than 65 years. Other risk factors include ethnicity, with the highest incidence in African-American men (SEER, NIH). Family history and dietary habits have also been linked to PCa development (Rawla 2019).

b. Development

PCa most probably arises from preneoplastic lesions called prostatic intraepithelial neoplasia (PIN) accompanied by genomic instability and key cellular events. This progression is characterized by a progressive loss of differentiation status, loss of basal lamina, accumulation of genetic alterations, development of neovascularization and increased proliferation. Although this affects epithelial cells, the stroma has been shown to be implicated as well during PIN formation. Indeed, the reactive stroma, i.e. the stroma adjacent to PINs and prostatic tumors, has been shown to play a crucial role in PCa development (Barron and Rowley 2012).

PCa develops progressively, first locally within the gland. The tumor will then spread across the capsule surrounding the prostate to spread to local structures such as seminal vesicles. The next step will be lymph node invasion. In the most advanced stages, PCa spreads via blood circulation to form metastasis in distant organs with a preference for liver, bones and lungs.

c. Diagnostic and prognosis

The most common symptoms of PCa are lower urinary tract symptoms such as blockages and increased frequency, but they do not manifest in every patient as PCa can be asymptomatic and indolent in its early stages.

However, PCa early diagnosis is important as it can impact patient survival. Numbers show a 100% 5-year survival rate in patients diagnosed with localized PCa, but survival is decreased to 30% in patients with metastatic PCa at diagnosis (SEER, NIH).

The first elements taken into account for PCa diagnosis are age and the symptoms briefly described above. Then, there are three steps for PCa diagnosis:

- Digital rectal exam: allows the detection of an abnormal growth of the posterior peripheral zone of the prostate that is near the rectal wall.
- PSA levels: as mentioned above, PSA is an androgen-dependent protein secreted by prostate glands (Kim and Coetzee 2004). This antigen can be found in high concentrations in blood during PCa, and was thus proposed as a PCa marker in the 1990s (Catalona et al. 1991). Since then, PSA has been the most used biomarker for this pathology. However, this is a controversial marker that can lead to false positives due to its variable expression. PSA have shown to be uncorrelated to PCa stages, and high PSA levels can be found in patients with BPH. Thus, PSA blood levels should be interpreted with caution. As a consequence, in some countries, recommendations have been made against routine PSA screening in elderly men. However, this marker is still widely used today to follow and help detect PCa. PSA can also be combined with the monitoring of other specific markers to increase its accuracy in PCa detection. Generally, patients with PSA levels > 4 ng/ml will be directed to the next step of PCa diagnosis.
- The final and essential step for PCa diagnosis is the biopsy to validate the diagnosis and grade the PCa.

Further imaging can be required to fully diagnose the pathology, such as bone scans to assess bone metastasis for example.

PCa advancement is then determined by clinical staging and histological grading. Those crucial steps will allow to evaluate the prognosis and define the optimal therapeutic strategies for the patient.

d. Histological grading

Histopathological grading is essential for staging. The recommended grading system is the Gleason score which evaluates the differentiation of the tissue (Gleason and Mellinger 1974). The tissue differentiation pattern is divided in five grades (Figure 3):



Figure 3: Gleason histological patterns of PCa
Gleason and Mellinger 1974

- Grade 1: small, defined, uniform, round acini with defined borders closely arranged together.
- Grade 2: the glands are well defined, but bigger and more spaced due to increased stroma.
- Grade 3: undefined glands of variable sizes, loss of margins and stroma invasion.
- Grade 4: most of the glands are fused, but some defined glands are still present.
- Grade 5: sheets of tumor cells, no apparent gland or any tissue structure.

The final Gleason grade is the sum of the two most prevalent grades in the sample, the primary followed by the secondary.

e. Clinical staging

The TNM (tumor, node, metastasis) classification method was first proposed in 1977 (Ammon et al. 1977) and revised in 2010 by the American Joint Committee on Cancer (Cheng et al. 2012). This staging initially relies on three criteria: primary tumor size and extent (T), local lymph node invasion (N) and distant metastasis development (M). The Gleason score (G) has later been added as a fourth component. This method defines four stages of PCa, from I to IV, with increasing aggressiveness (Figure 4):

- Stage I: small tumor, no lymph node invasion (N0), no metastasis (M0), Gleason 2-4.
- Stage IIA: the tumor is slightly bigger, N0, M0, Gleason 6-7 or lower.
- Stage IIB: the tumor is spread but localized within the prostate, N0, M0, any Gleason.
- Stage III: extracapsular tumor extension, N0, M0, any Gleason.
- Stage IV: the tumor invades structures other than seminal vesicles, possible lymph node invasion (N0-1), possible distant metastasis (M0-1), any Gleason.

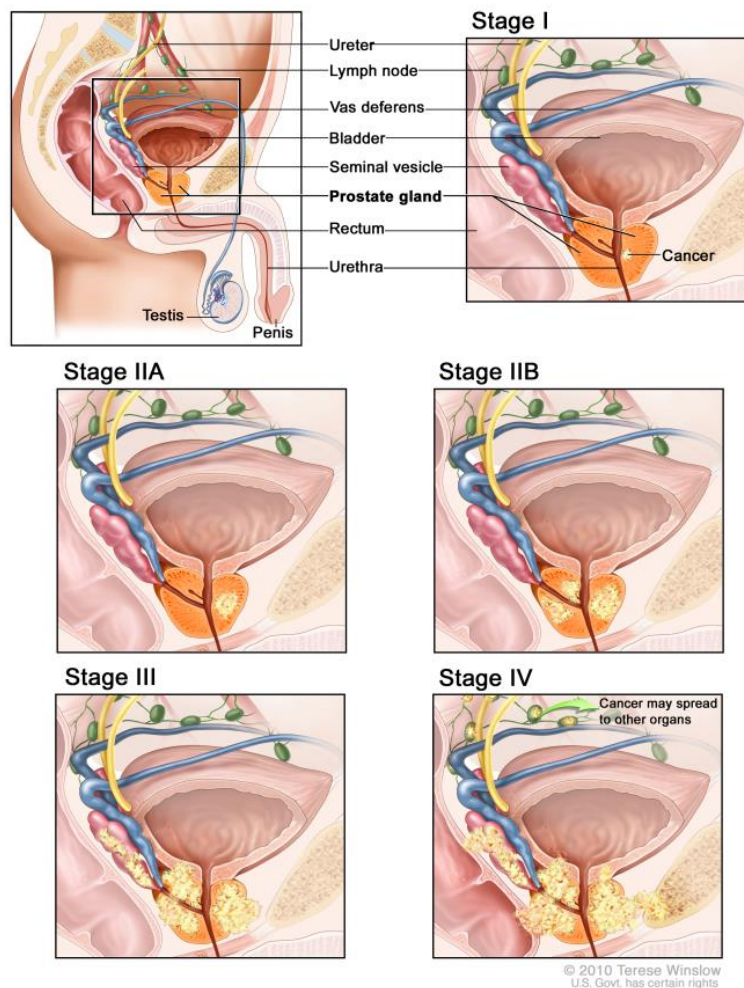


Figure 4: Clinical staging of PCa
PQD® Cancer Information Summaries, NIH

f. Treatment

Different therapeutic options are available depending on PCa staging.

As stated above, prostate cells proliferation/death balance is regulated by androgens, and PCa arises in part from the deregulation of this equilibrium. As a consequence, historically, androgen depletion was the first treatment developed for PCa (Denmeade and Isaacs 2002). The effect of androgen depletion therapy (ADT) on PCa was first showed in the 1940s by Charles Huggins (Huggins et al. 1941). Thus, throughout the decades, many different strategies have been developed to deprive prostate tumors of androgens. Currently, two main strategies of chemical castration are used to treat the patients: non-steroidal anti-androgens such as Bicalutamide (Casodex®) and LHRH agonists. However, studies showed that ADT is not able to cure PCa and has just palliative properties. Indeed, this treatment will inescapably lead to resistance and development of androgen-resistant aggressive tumors called castration resistant PCa (CRPC) for which there are no curative treatment available as of today (Feldman and Feldman 2001). But, recent studies showed that androgen deprivation can be useful when combined to other therapeutic strategies.

PCa can have a slow development, thus, for low grade localized tumors, the preferred option will be expectant management.

For a localized tumor of higher risk, the first line of treatment will be surgical removal by radical prostatectomy.

If the tumor is locally advanced, radiotherapy is the most used treatment. There are two main approaches: brachytherapy and external beam radiation. Brachytherapy, the implantation of small radioactive seeds directly in the prostate gland, has shown to be effective for PCa treatment (Ragde et al. 2000). External beamed radiation is a widely used technique today that has been highly improved by recent technological advances. It has been shown that combination with androgen deprivation increases its efficiency (Pilepich et al. 1995).

Finally, cytotoxic chemotherapy has been used to treat advanced metastatic PCa. Different combinations have been proposed with agents such as docetaxel and doxorubicin. Interestingly, studies showed that the monitoring of PSA levels during chemotherapies could help predict response to treatment.

g. Mechanisms of resistance

As indicated above, PCa can resist treatment and develop into CRPC. Several mechanisms have been proposed to explain this resistance on the basis of the selection of a clone with survival advantages. Indeed, the androgen deprivation will target androgen-sensitive PCa cells, but it will also select an androgen-independent subpopulation that has the ability to proliferate without androgen stimulus. These mechanisms can be categorized in two main subsets: androgen-dependent or androgen-independent mechanisms (reviewed in Crona and Whang 2017).

For the mechanisms involving the AR (reviewed in Waltering et al. 2012), there can be AR overexpression (Chen et al. 2004) or AR mutations affecting ligand affinity (Veldscholte et al. 1990) for example. It has also been shown that the AR could be activated by factors other than androgens (Culig et al. 1994). Constitutive AR splice variants have also been documented in CRPC (Kallio et al. 2018).

PCA cells can use other strategies to evade treatment, such as apoptosis inhibition and cell proliferation activation via androgen-independent pathways (reviewed in Crona and Whang 2017). Among them, one can find glucocorticoid receptor upregulation and the neuroendocrine differentiation.

Another hypothesis to explain PCa relapse is the existence of cancer cells with stem-like properties.

II. Cancer stem cells

Stem cells are undifferentiated, long-living cells that are unique in their ability to produce, by asymmetric division, a stem cell (SC) daughter in order to maintain the stem cell pool and a transient amplifying daughter that is destined to differentiate after several divisions. SC quiescence is crucial to protect their pool from exhaustion under conditions of diverse stresses and to ensure lifelong tissue preservation (Cheng et al. 2000; Cheung and Rando 2013). Increasing evidence supports the idea that cancer is driven by cancer stem cells (CSCs) (Nguyen et al. 2012; Reya et al. 2001). The CSC hypothesis states that not all tumor cells are equal in the sense that only a rare subset of cancer cells could be able to reconstitute a tumor mass: CSCs. According to this model, conventional therapies would only result in the elimination of dividing cancer cells with limited proliferative potential. These therapies would however spare the quiescent CSCs, which can be activated to proliferate and lead to metastatic tumor relapse after diverse periods of tumor dormancy (Coller et al. 2006). According to this model, the rare subset of CSCs would be responsible for tumor initiation, growth and relapse. CSCs have been identified for many cancer types, including PCa.

Although PCa cells derive from the luminal epithelial cell-type, studies showed that PCa initiating CSCs arise from basal cells (Goldstein et al. 2010). Basal cells are less differentiated cells that do not express the AR and the PSA. Through a combination of specific markers, prostate CSCs were isolated by different teams (Collins et al. 2005; Hurt et al. 2008; Patrawala et al. 2007). This rare subset representing less than 0.1% of the total cells showed increased invasive and self-renewal properties.

The proper characterization of prostate CSCs is still lacking, de facto preventing their targeting for therapeutic purposes.

III. Calcium channels

Calcium is the most tightly regulated ion within the cells and represents a highly versatile second messenger controlling key physiological processes. As a consequence, any disruption of calcium homeostasis via calcium channel expression and/or activity remodeling leads to abnormal processes. Calcium channels have thus been implicated in the hallmarks of cancer (Monteith et al. 2017; Prevarskaya et al. 2018).

Calcium signaling can have a plethora of consequences, depending on its specific spatial and temporal pattern (Berridge et al. 2003). The cytosolic calcium concentration is very low (around 100 nM free calcium), when in comparison, extracellular concentration is in the millimolar range (1-2 mM). Within the cell, calcium will be mainly stored in the endoplasmic reticulum (ER, 0.1-1 mM), and in other organelles to a lesser extent. The calcium signaling toolkit is also composed of highly sensitive calcium-binding effectors, allowing specific and effective signaling in response to calcium variations. As a consequence, calcium signaling events can have drastic and diversified effects within the cells.

The first component of calcium signaling is represented by calcium channels that are mainly present at the plasma membrane (PM). Among them one can find the TRP (transient receptor potential) family comprised of more than 30 members (Clapham et al. 2001). This highly diverse family contains members with variable calcium permeability, as well as activation properties. Other important PM calcium channels are the store-operated channels (SOC), also known as calcium release-activated calcium channels (CRAC). Constituted by Orai and STIM, these channels represent the major calcium entry pathway in non-excitable cells, called the store-operated calcium entry (SOCE) (reviewed in Derler et al. 2016; Prakriya and Lewis 2015) (Figure 5).

ER also plays a crucial role in calcium homeostasis. Among the calcium channels found in the ER, there is the IP₃R (inositol 1,4,5-trisphosphate receptor). This channel is activated by the IP₃ generated through the activation of a G-protein-coupled receptor (GPCR) or a tyrosine kinase receptor (TKR) at the plasma membrane, and associated phospholipase C (PLC). Its activation will lead to transient ER calcium store depletion into the cytoplasm. Cytosolic calcium can reenter the ER via the sarcoplasmic/endoplasmic reticulum calcium ATP-ases (SERCA).

Other organelles can also take part in calcium signaling. For example, in mitochondria, calcium uptake from the mitochondrial calcium uniporters (MCU) can regulate cell physiology and metabolism.

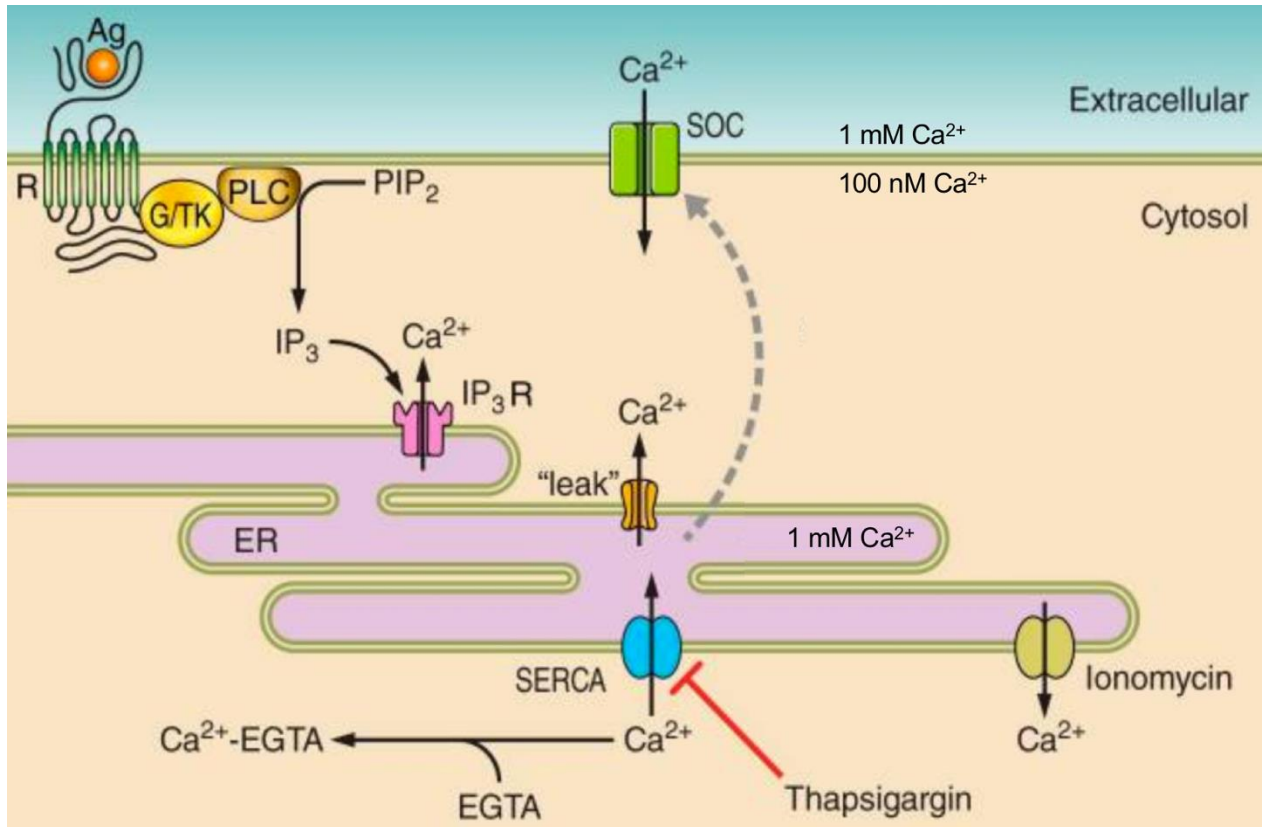


Figure 5: Simplified view of the calcium signaling

Prakryia and Lewis 2015

An agonist (Ag) binds to its receptor (R), either a G protein coupled receptor (GPCR) or a tyrosine-kinase receptor (TKR). The receptor will activate the phospholipase C (PLC) and produce IP_3 (inositol 1,4,5-trisphosphate) from PIP_2 (phosphatidylinositol 4,5-bisphosphate). The IP_3 binds and activates its receptor (IP_3R) at the ER, leading to a Ca^{2+} release from the ER to the cytoplasm, activating the SOC channels. Calcium leak channels are constitutively activated and leak calcium from the ER to the cytoplasm.

Also depicted on this diagram are the experimental procedures to activate the SOC channels: intracellular Ca^{2+} -chelation (EGTA), SERCA pump inhibition (thapsigargin), ER Ca^{2+} release (ionomycin).

IV. *Store-operated calcium channels*

As stated above, SOC channels are responsible for the SOCE, also called capacitative calcium entry (CCE). This particular calcium entry has been documented since the 1980s (Putney 2011; Putney 1990), but its mechanisms remained obscure until its molecular characterization almost 20 years later. Indeed, SOC channels are composed of two distinct proteins: Orai, the channel unit, and its activator STIM, an ER calcium sensor. There are three Orai isoforms and two STIM isoforms. In PCa, SOC channels have been shown to be constituted of Orai1 and STIM1. We therefore focused on these two isoforms in our studies.

1. *STIM1*

Stromal interaction molecule (STIM) was first identified in a screen for adhesion molecules in pre-B cells (Oritani and Kincade 1996). Its role was unknown for almost 10 years, until it was identified as a component of the SOC channels. Indeed, STIM acts as a calcium sensor in the ER (Liou et al. 2005; Roos et al. 2005).

There are two STIM isoforms, STIM1 (74k Da) and STIM2 (84 kDa), with relatively high homology. Even though both isoforms are ubiquitously expressed, STIM1 is generally expressed at higher levels, as it is the case in PCa cells. Moreover, the two isoforms can have distinct physiological roles. As stated above, STIM1 is the major component of SOC channels in PCa cells.

STIM1 is a type I single pass ER membrane protein with its N-terminal (Nt) end residing within ER lumen, whereas its C-terminal (Ct) end is in the cytoplasm (reviewed in Soboloff et al. 2012). On its luminal domain, STIM1 possesses a calcium-binding EF-hand associated to a sterile α -motif (SAM) domain, essential for its role as an ER calcium sensor. On its cytoplasmic side, STIM1 has three coiled-coil domains constituting the Orai1-activating small fragment (OASF) (detailed in [Figure 6](#)). Within the OASF, one can find the CAD/SOAR (CRAC-activation domain/STIM-Orai activating region) domain, containing the minimum fragment required for Orai1/STIM1 interaction.

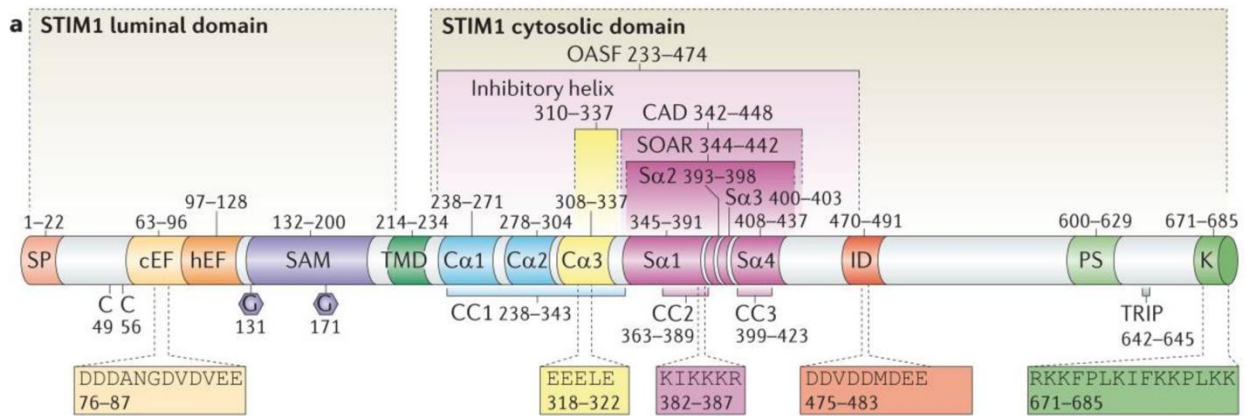


Figure 6: Molecular structure of STIM1
Soboloff et al. 2012

Molecular domains of STIM1, with the key residues underlined. At the Nt end, we have a signal peptide (SP), cleaved during translation. On its luminal domain, STIM1 possesses a Ca^{2+} -binding EF-hand domain conferring calcium sensor abilities. This is followed by a SAM (sterile α -motif) domain and a single transmembrane domain (TMD). The cytosolic domain of STIM1 contains three coiled-coil regions (CC1-3). SOAR (STIM-Orai activating region) is the sequence required to activate Orai1 via its underlined KIKKKR sequence. The SOAR is comprised of four α helices ($\text{S}\alpha$ 1-4) spanning from the CC2 to the CC3. The SOAR is located within the CAD (CRAC-activation domain), which is part of the OASF (Orai1-activating small fragment) together with the CC1. Upstream of the SOAR and within the CC1, one can find the $\text{C}\alpha$ 3 SOAR-inhibitory helix. Downstream of the SOAR, one can find the ID (inhibitory domain) responsible for the characteristic fast Ca^{2+} -dependent inactivation of Orai1. At the Ct end, STIM1 contains a proline/serine-rich domain (PS), a microtubule-interacting domain (TRIP for threonine-arginine-isoleucine-proline) and a lysine-rich domain (K) that allows interaction with the phospholipids of the PM.

2. *Orai1*

Orai, the channel unit of SOC channels, was identified a year after STIM1 (Feske et al. 2006; Prakriya et al. 2006). Over all, three highly homologous isoforms of Orai can be found (Orai1-3). Among them, Orai1 often presents the highest expression levels and is the best characterized.

Orai1 (33 kDa) is constituted by four transmembrane domains with both extremities facing the cytoplasm. Both C- and N-termini are required for STIM1 interaction (McNally et al. 2013), as shown in Figure 7. The crystal structure of drosophila Orai revealed an hexameric association to form a functional channel (Figure 7C) (Hou et al. 2012). The pore is constituted by the extended transmembrane Orai1 N-terminal domain (ETON), the first transmembrane domain (TM1) and the calcium accumulating region (CAR).

The channel formed by Orai1 is one of the most Ca^{2+} -selective channels, presents an inward rectification and an extremely low conductance (around 10 fS in 2 mM Ca^{2+}). In addition, SOC channels present low permeability for large ions with a $P_{\text{Cs}}/P_{\text{Na}} \approx 0.1$ (Lepple-Wienhues and Cahalan 1996).

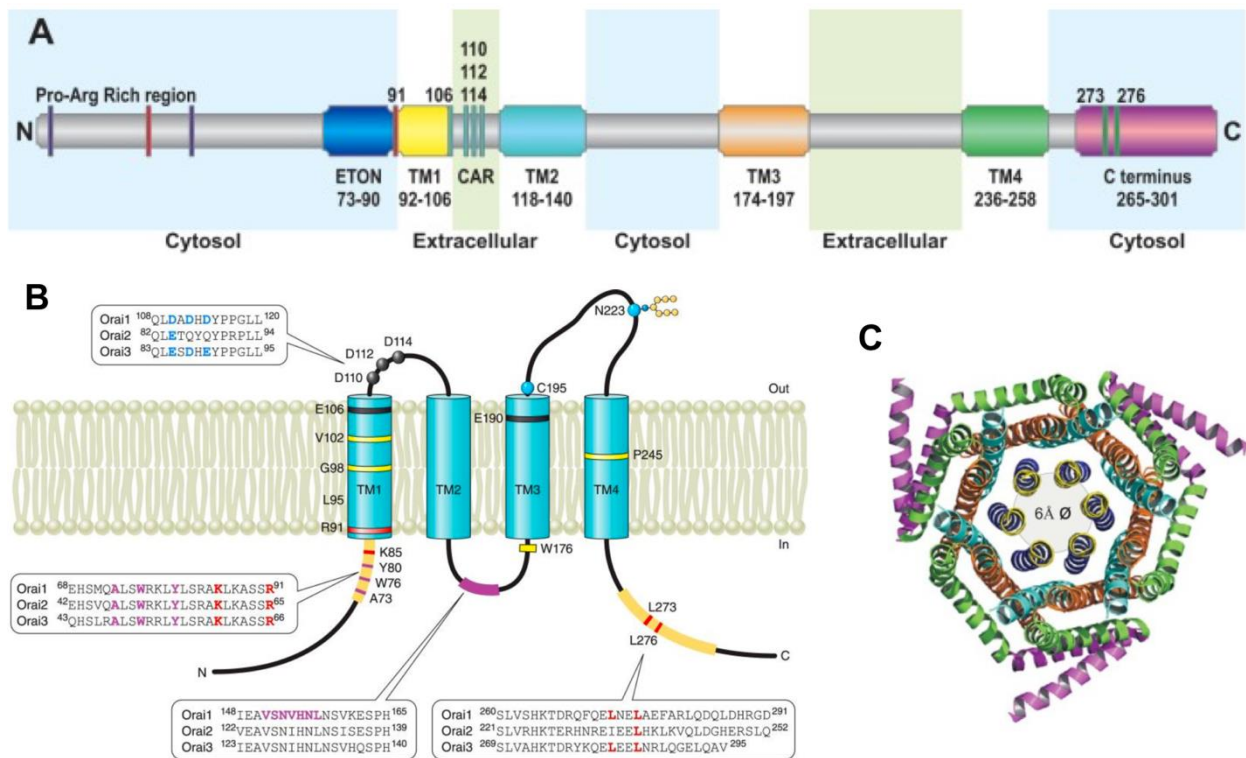


Figure 7: Molecular structure of Orai1

Adapted from Derler et al. 2016 and Prakriya and Lewis, 2015

A. Orai1 molecular structure; key residues are highlighted. Orai1 possesses 4 transmembrane domains (TM1-4). The pore of Orai1 is composed of the extended transmembrane Orai1 N-terminal domain (ETON), found upstream the first TM, and the Ca^{2+} accumulating region (CAR) found between TM1 and TM2. **B.** Topology of Orai1. Orai1-3 are highly conserved in their transmembrane regions (TM) but differ in their N- and C-termini, as showed in the compared sequences. The putative interaction sites with STIM1 are indicated in thick orange lines at both Nt and Ct. Yellow lines indicate the sites of gain of function mutations leading to STIM1-independent Orai1 activation. Red lines show loss-of function mutations. In black are the mutations affecting ion selectivity. The purple line shows the region regulating the Ca^{2+} -dependent inactivation. **C.** Hexameric assembly of Orai subunits based on the crystallography of drosophila Orai. Colors are the same as in A.

3. SOC activation mechanism

SOC channels have a unique activation mechanism. These channels are activated by ER calcium depletion detected by STIM1. This process is highly dynamic and involves the remodeling of both Orai1 and STIM1 in the PM and the ER membrane respectively.

In basal conditions, STIM1 is associated in dimers homogeneously distributed in the ER. The sensor binds calcium in the ER lumen via its EF-hand domain, stabilizing the EF-SAM structure in an inactive state. This process is reinforced by interactions in the cytoplasmic domains involving CC1 and CAD domains (Muik et al. 2009; Zhou et al. 2013): CC1 binds and retains the CAD domain, forming an inhibitory clamp (Figure 8).

STIM1 is activated by the loss of calcium binding to its EF-hand due to ER calcium store depletion. Calcium release triggers the unfolding of the EF-SAM domain resulting in conformational changes in both luminal and cytosolic parts of STIM1. In this process, the EF-SAM domain exposes hydrophobic surfaces allowing STIM1 oligomerization (Luik et al. 2008; Stathopoulos and Ikura 2013). On the cytoplasmic side, the inhibitory clamp formed by CC1 interacting with CAD is released, allowing CAD exposition for Orai1 activation (Covington et al. 2010; Fahrner et al. 2014). As a consequence, the cytosolic end of STIM1 extends towards the PM to bind Orai1 (Muik et al. 2011).

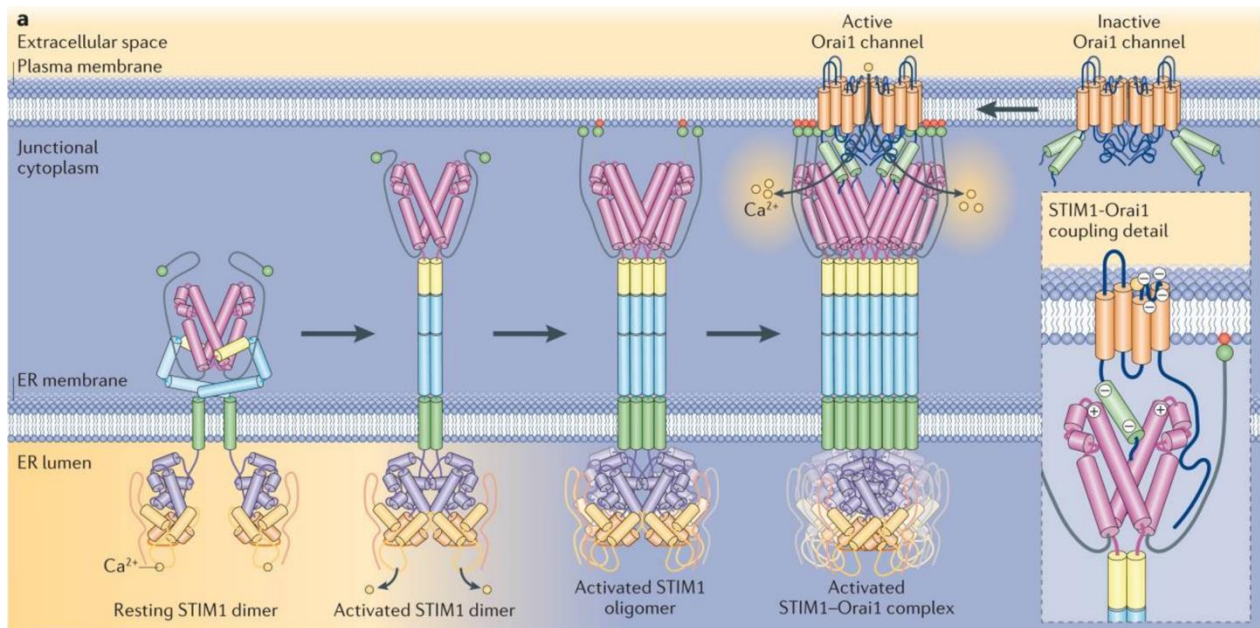


Figure 8: STIM1 activation sequence

Soboloff, et al. 2012

The colors for STIM1 domains are the same as in Figure 5. In resting STIM1 dimer, the TM domains (green) are separated. The EF-SAM domains (yellow and dark blue) are separated and bound to calcium. CC1 (light blue) binds and inhibits the CAD domain (in purple, inhibitory clamp), maintaining the cytosolic domain in a compact configuration. After ER store depletion, the calcium release from the EF-SAM domains triggers STIM1 activation. The TM and the EF-SAM domains of the dimer bind together, releasing the inhibitory clamp, allowing STIM1 extension in the cytoplasm towards the PM. STIM1 dimers oligomerize and diffuse to ER-PM junctions. The lysine-rich Ct end of STIM1 (green circle) binds PIP₂ at the PM (red circle). The Orai1/STIM1 interaction is shown on the left, with the SOAR of STIM1 binding to the Ct extension of Orai1.

In the meantime, Orai1 and STIM1 move by diffusion within their respective membranes to accumulate at ER-PM junctions (Wu et al. 2014; Wu et al. 2006a). This clustering of Orai1 and STIM1 will lead to the formation of characteristic structures called puncta (Figure 9).

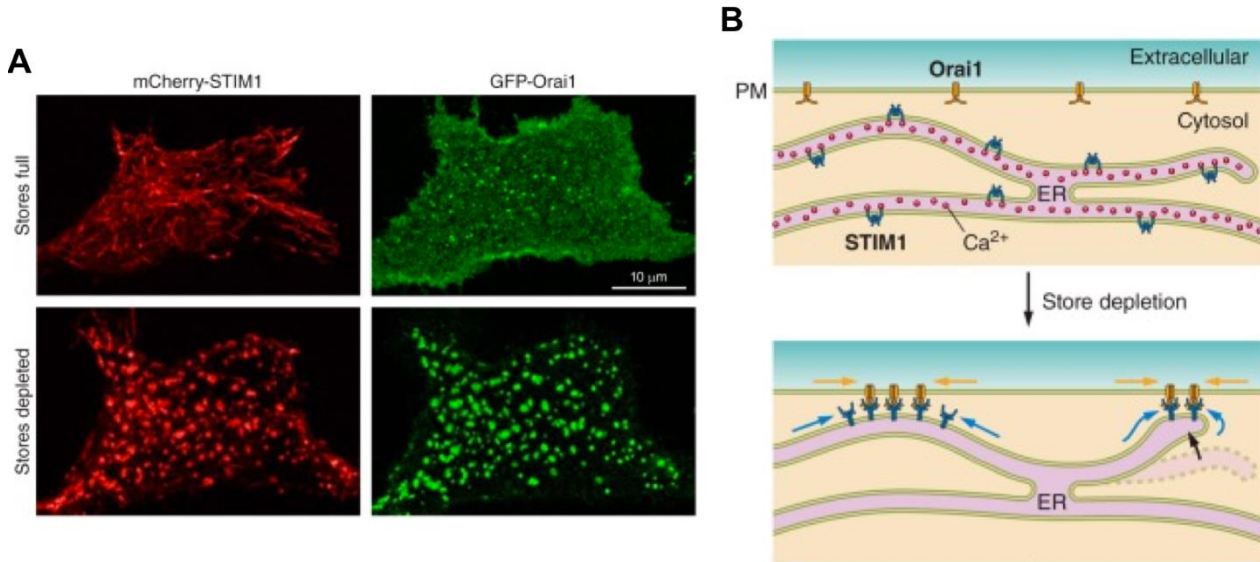


Figure 9: STIM1 and Orai1 co-clustering

Adapted from Prakriya and Lewis, 2015

A. Confocal images of mCherry-STIM1 and GFP-Orai1 in HEK-293 cells in resting conditions (top) or after calcium store depletion (bottom). **B.** Diagram showing STIM1 and Orai1 co-clustering

When STIM1 oligomers reach the ER-PM junctions, the lysine-rich region at the Ct end of STIM1 binds PIP₂ (phosphatidylinositol 4,5-bisphosphate) at the PM (Liou et al. 2007). Then, STIM1 binds and activates Orai1. STIM1 Ct has been shown to be sufficient to activate Orai1 (Huang et al. 2006). A few years later, the OASF was shown to be the minimal required fragment for Orai1 binding and activation (Kawasaki et al. 2009; Muik et al. 2009; Park et al. 2009; Yuan et al. 2009). Within the OASF, the CAD domain directly interacts with Orai1 Ct end, as well as the Nt end to a lesser extent. The coupling between STIM1 and Orai1 Ct, called the STIM1/Orai1 association pocket (SOAP), has been well resolved (Stathopoulos et al. 2013). The interaction between STIM1 and Orai1 Nt has been debated, and although STIM1 binding has not been ruled out, recent studies show that Orai1 Nt can in fact bind the loop between Orai1's TM2 and TM3, stabilizing the protein (Fahrner et al. 2018; Yeung et al. 2018).

Electrophysiology studies show that the hexameric channel formed by Orai1 is only fully functional when all six Ct are bound to STIM1 (Yen and Lewis 2018) (Figure 10A). There are currently two models proposed for STIM1/Orai1 binding: the monomeric or the dimeric model (Yen and Lewis 2019) (Figure 10B).

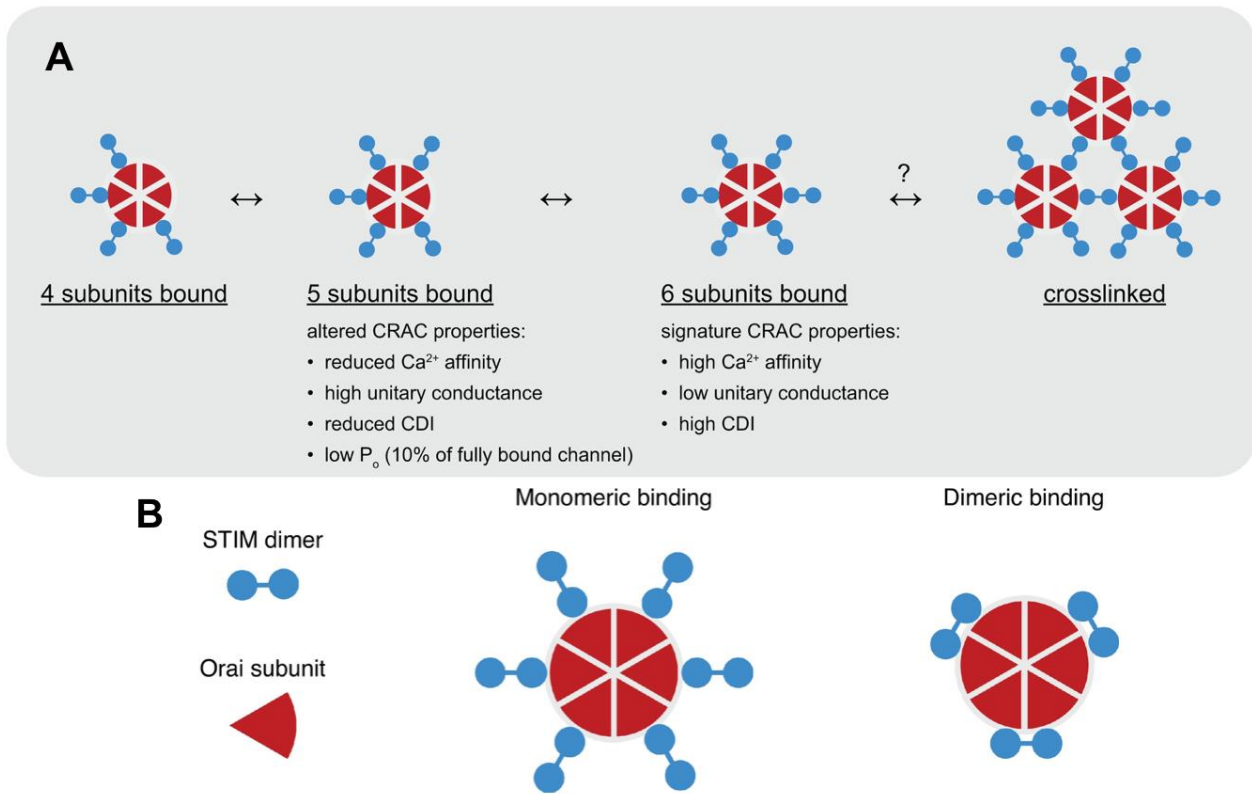


Figure 10: STIM1 and Orai1 binding models
Yen and Lewis, 2019

While the exact mechanisms of SOC channel gating remain to be identified, as the open state of Orai1 has not been resolved to this day, three putative gating models are proposed (reviewed in Qiu and Lewis 2019).

4. SOC inactivation mechanism

The SOC channels are characterized by an important feedback mechanism: Ca²⁺ entering the channel leads to a rapid Ca²⁺-dependent inactivation (CDI). This is a two-step process with a fast CDI (FCDI) and a slow CDI (SCDI) component (reviewed in Parekh 2017).

FCDI happens in a matter of milliseconds and is mediated by the inhibitory domain of STIM1 (also called CRAC modulatory domain, CMD) (Derler et al. 2009; Lee et al. 2009; Mullins et al. 2009).

Evidence suggests that this regulation takes place via an interaction with the Nt end of Orai1 (Mullins and Lewis 2016).

SCDI is observed minutes after channel opening, via Ca^{2+} -calmodulin (CaM) interaction with the CAD domain of STIM1, disrupting the Orai1/STIM1 complex (Li et al. 2017).

Furthermore, CDI has been shown to be regulated by SARAF, an ER resident protein that interacts with the CAD domain of STIM1 in the presence of Orai1/STIM1 complexes (Palty et al. 2012) (reviewed in Cao et al. 2015).

5. SOC modulation

The SOC channels can be modulated by multiple factors, as discussed below.

SOC activity can be regulated through phosphorylation: Orai1 can be inhibited via phosphorylation by the protein kinase C (PKC) (Kawasaki et al. 2010), and studies showed that STIM1 diffusion to the ER-PM junctions can be slowed down by phosphorylation.

Orai and STIM can be modulated by reactive oxygen species via cysteine residues (reviewed in Bogeski et al. 2012). Orai3 has been shown to be less sensitive than Orai1, due to the absence of some cysteine residues.

SOC channels have also been shown to be sensitive to pH (Mancarella et al. 2011) and temperature variations (Xiao et al. 2011).

Another major component in the regulation of SOC channel activity is the interaction with other proteins. Indeed, SOC binding to SARAF and CaM were already described above, but both Orai1 and STIM1 have been shown to interact with other proteins. For example, the cytoplasmic CRAC regulatory protein 2A (CRACR2A) has been shown to directly bind STIM1 and Orai1, promoting their association (Srikanth et al. 2010). This protein is inhibited by Ca^{2+} -binding on its cytosolic EF-hand.

6. SOC pharmacology

The complex activation mechanism of SOC channels allows its pharmacological targeting at different levels. Several SOC inhibitors have thus been developed, acting via either STIM1 inhibition, Orai1 inhibition or STIM1/Orai1 coupling inhibition (reviewed in Tian et al. 2016). Some of them will be briefly described below.

a. Lanthanides

Orai1 can be inhibited by trivalent cations such as La^{3+} and Gd^{3+} (Hoth and Penner 1993), but lanthanides can also inhibit other Ca^{2+} channels including members of the TRP family.

b. 2-aminoethyldiphenyl borate (2-APB)

2-APB has been widely used to study SOC channels. At low concentrations, this compound increases SOC activity, whereas high concentrations can have an inhibitory effect.

However, this compound can also affect the activity of SERCA pumps and ion channels of the TRP family.

c. 3,5-bis(trifluoromethyl)pyrazole (BTP2)

Also known as YM-58483, BTP2 inhibits SOCE through an unknown mechanism. However, it has been shown to modulate other calcium channels of the TRP family.

d. Synta66

A more recent compound similar to BTP2, Synta66, appears to be relatively specific. This inhibitor has been widely used in recent years to inhibit SOC channels.

e. GSK compounds

Other recent pyrazole derivatives, the GSK-5503A and GSK-7975A, are thought to inhibit SOCE via pore geometry alteration. Interestingly, these compounds have been shown to have little to no effect on other channels, except for TRPV6 (TRP vanilloid member 6).

f. RO2959

This Roche compound is another relatively selective pyrazole derivative inhibiting SOCE through an unknown mechanism.

7. Gene expression regulation via SOC channels

SOCE can have various long-term or short-term effects on cell physiology. One of the most documented long-term effect is the regulation of gene expression via the activation of the NFAT (nuclear factor of activated T cell) transcription factor (TF) (Hogan et al. 2003; Müller and Rao 2010). This pathway was first identified in immune cells (Feske et al. 2001), but was later shown to be present in most cell types, regulating various cellular processes. The NFAT family comprises five members: NFATc1 (also known as NFATc and NFAT2), NFATc2 (also known as NFATp and NFAT1), NFATc3 (also known as NFATx and NFAT4), NFATc4 (NFAT3) and NFAT5. Among these five members, only the first four are regulated by Ca^{2+} .

All NFAT proteins share a similar structure and are comprised of a regulatory domain (NFAT homology region, NHR) containing the transactivation domain (TAD), serine-rich regions (SRR), serine-proline-X-X repeat motifs (SP1-3) and docking sites. The NHR is followed by a DNA-binding domain (Rel-homology domain, RHD) and the Ct domain (Figure 11A).

In basal conditions, NFATs are phosphorylated and restricted to the cytoplasm. Upon SOCE, the rise in cytosolic Ca^{2+} will lead to the activation of calcineurin (CN), a CaM-dependent serine/threonine phosphatase. CN will then dephosphorylate NFAT on 13 of its phosphorylated residues, exposing its nuclear localization sequence (NLS) (Figure 11B) (Okamura et al. 2000).

Within the nucleus, NFAT is inactivated by phosphorylation via multiple kinases on its SRR and SP regions. These kinases fall in two different categories, depending on their localization. Export kinases are within the nucleus and allow the nuclear export of NFAT. Among these kinases, one can find the glycogen synthase kinase 3 (GSK3) (Beals et al. 1997), the casein kinase 1 (CK1)

(Okamura et al. 2004) and the dual-specificity tyrosine-phosphorylation regulated kinase (DYRK1). Maintenance kinases (CK1 and DYRK2) are cytoplasmic, and further phosphorylate NFAT in order to keep it in the cytoplasm. In the nucleus, NFAT has been shown to form a complex with NRON (non-coding RNA repressor of NFAT), IQGAP1 (IQ motif containing GTPase activating protein), CK1, GSK3 and DYRK (Sharma et al. 2011).

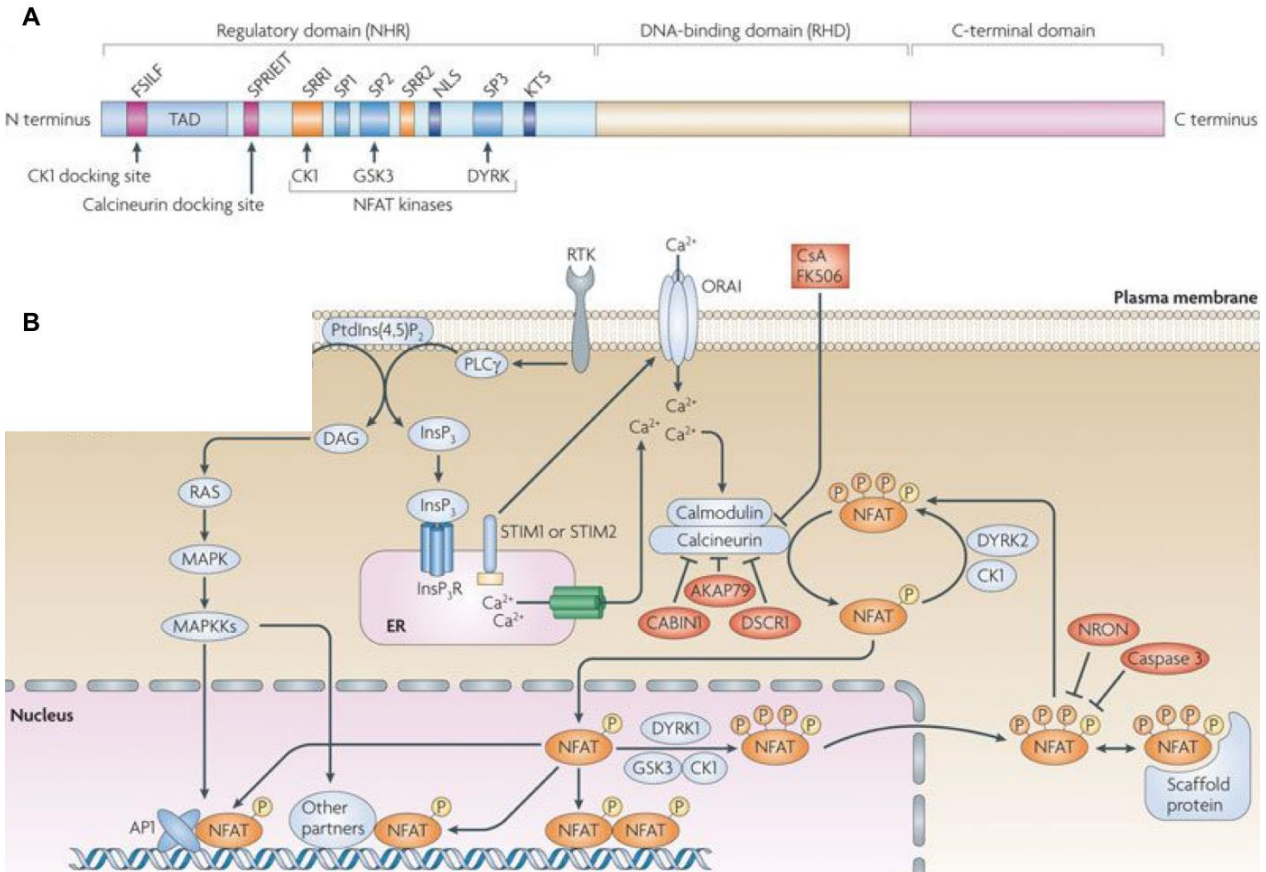


Figure 11: NFAT structure and activation pathway

Adapted from Müller and Rao 2010

A. Molecular structure of NFAT. The regulatory domain (NFAT homology region, NHR) contains a transactivation domain (TAD), docking sites, serine-rich motifs (SRR1-2, SP1-3, KTS) and a nuclear localization signal (NLS). **B.** Ca^{2+} entering the cell through SOC channels binds and activates the CaM, which in turn activates the phosphatase calcineurin (CN). CN dephosphorylates NFAT, allowing its nuclear translocation. In the nucleus, NFAT can cooperate with MAPK-activated transcription factors such as AP-1 to regulate gene expression. Within the nucleus, NFAT can be phosphorylated by casein kinase (CK1), dual specificity tyrosine phosphorylation-regulated kinase 1 and 2 (DYRK) and glycogen synthase kinase 3 (GSK3) resulting in its nuclear exclusion. The activity of CN can be inhibited by CABIN1 (CN-binding protein 1), AKAP79 (A-kinase anchor protein 79), DSCR1 (Down's syndrome critical region 1); or pharmacological inhibitor cyclosporine A (CsA) and FK506. NFAT can interact with scaffolding proteins such as NRON (non-coding RNA repressor of NFAT). NFAT can be inhibited by other mechanisms such as caspase 3 cleavage.

NFAT can be regulated by other mechanisms, such as cytoplasmic Homer binding (Huang et al. 2008), cleavage by caspase 3 (Wu et al. 2006b), ADP-ribosylation by poly-ADP-ribose polymerase (PARP) (Olabisi et al. 2008), ubiquitylation by murine double minute 2 (MDM2) (Yoeli-Lerner et al. 2005) or sumoylation (Terui et al. 2004).

Various inhibitors have been identified for CN: calcineurin-binding protein 1 (CABIN1) (Sun et al. 1998), the A-kinase anchor protein AKAP79 (Coghlan et al. 1995) and a DSCR (Down's syndrome critical region) (Rothermel et al. 2000).

Interestingly, Orai1 has been shown to be a more potent inducer of NFAT than Orai3. In this study, authors show that AKAP79 scaffolding protein brings CN in close contact with CaM and Orai1, facilitating the signaling pathway leading to NFAT activation (Kar et al. 2014).

NFATc2 and NFATc3 have been shown to have distinct kinetics: NFATc2 shows sustained nuclear translocation, whereas NFATc3 exhibits transient activation (Yissachar et al. 2013). Furthermore, although local Ca^{2+} variations are sufficient to activate NFATc2, NFATc3 requires a nuclear Ca^{2+} rise via the IP₃R as well to be activated (Kar et al. 2016; Kar and Parekh 2015).

Once in the nucleus, NFAT can regulate gene expression by working as a dimer. NFAT can also interact with other TF, such as AP1 (activator protein 1), formed by the association of Fos and Jun (Jain et al. 1992). This versatility allows for the regulation of a wide set of genes implicated in various cellular processes. NFAT thus plays a role in many physiological and pathological processes. Indeed, NFAT has been shown to play a role in cancer, as we will briefly describe below (reviewed in Mancini and Toker 2009).

8. SOC and cancer

A growing number of studies show the importance of SOC channels in cancer (reviewed in Fiorio Pla et al. 2016). These channels have been shown to have both pro- and anti-tumor roles. Depending on the signature of the Ca^{2+} signal, SOCE can influence cell fate via different Ca^{2+} -regulated pathways and have both long-term and short-term effects as shown in [Figure 12](#) (Monteith et al. 2017).

As previously stated, SOC channels can regulate gene expression via the NFAT pathway (reviewed in Pan et al. 2013), but other TF as well, such as CREB (cAMP response element binding protein) (König et al. 2013) and NF κ B (nuclear factor kappa B) (Berry et al. 2018). Via these TF, SOCE can, for example, increase the expression of genes implicated in the cell cycle, allowing a long-term increase in cell proliferation. Indeed, NFATc1 has been shown to have a pro-proliferative transforming potential in fibroblasts (Neal and Clipstone 2003; Robbs et al. 2008), pancreatic carcinoma (Buchholz et al. 2006), Burkitt lymphoma and T-cell acute lymphoblastic leukemia (Pham et al. 2005). On the other hand, NFATc2 activates other signaling pathways inducing cycle arrest and apoptosis (Robbs et al. 2008). NFAT has also been implicated in other

oncogenic mechanisms such as migration and angiogenesis (reviewed in Mancini and Toker 2009).

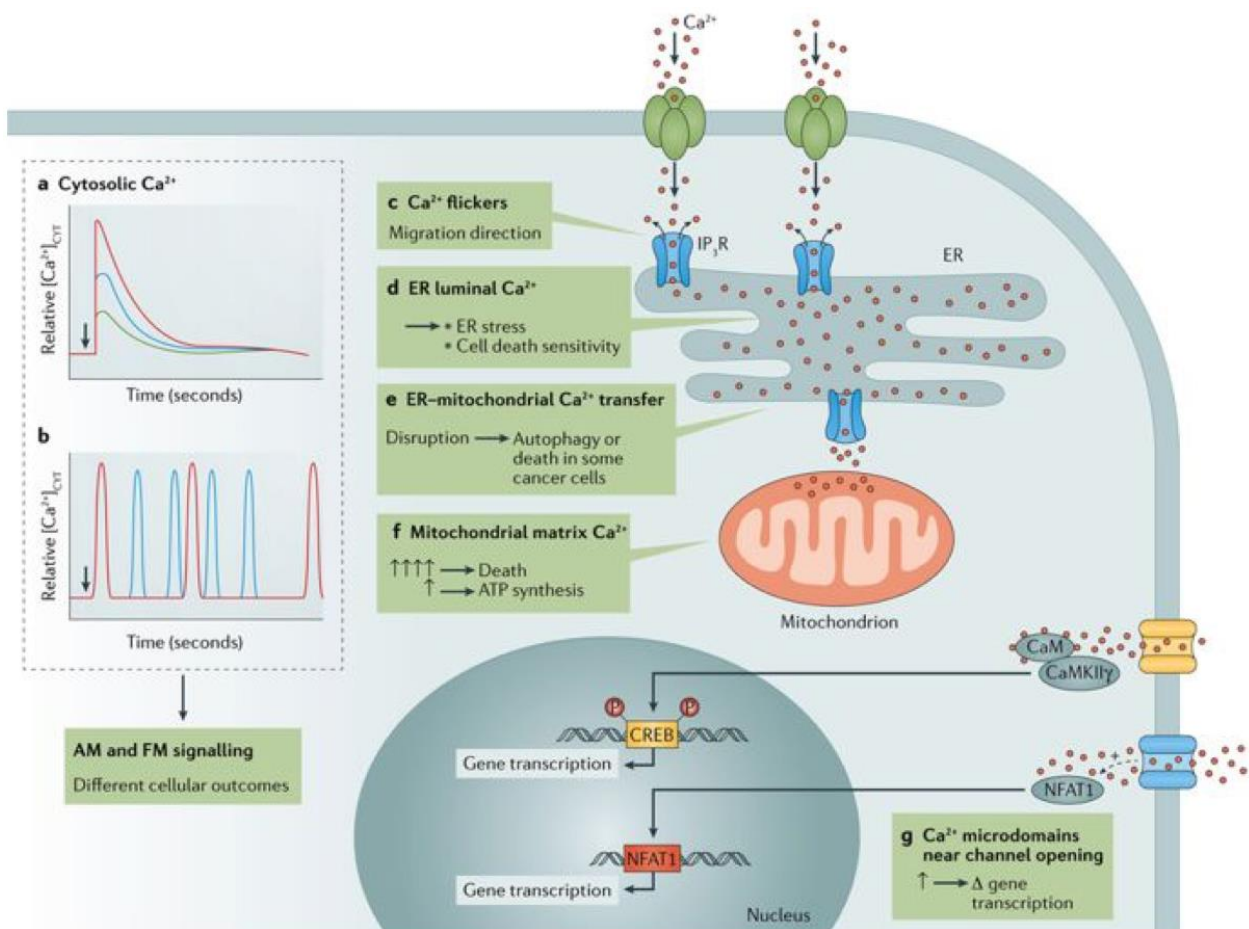


Figure 12: Calcium signaling and cancer

Adapted from Monteith et al. 2017

a. The amplitude and duration of the Ca²⁺ signal can determine cell fate (amplitude modulation, AM). **b.** The frequency of Ca²⁺ oscillations can also determine the outcome of the Ca²⁺ signaling (frequency modulation, FM). **c.** Localized and transient Ca²⁺ signals can activate cell migration. **d.** ER Ca²⁺ content can modulate ER stress and cell death. **e.** Ca²⁺ transfer from the ER to the mitochondria can determine autophagy and cell death. **f.** Moderate levels of Ca²⁺ in mitochondria modulates metabolism, whereas sustained increase can lead to cell death. **g.** Local calcium elevations can lead to specific TF activation in Ca²⁺ microdomains and gene regulation.

SOC channels can also have short-term effects. For example, SOCE can regulate focal adhesion kinases (FAK) and Src kinases, key regulators of the focal adhesion assembly/disassembly, essential for cell migration. This is the case in breast cancer (BCa) (Yang et al. 2009a), melanoma (Sun et al. 2014) and esophageal squamous cell carcinoma (Zhu et al. 2014).

Moreover, Orai proteins have been implicated in cancer through SOC-independent mechanisms: store-independent activation of Orai1 by secretory pathway Ca²⁺-ATPase 2 (SCPA2) increases proliferation (Feng et al. 2010).

Interestingly, tumor microenvironment (TME) has been shown to regulate SOC activity via reactive oxygen species (Frisch et al. 2019). Moreover, cancer-associated hypoxia can lead to the acidification of the TME, modulating SOC channel activity. TME can also influence cancer cells via the secretion of growth factors (GF) that can activate SOC channels through RTK or GPCR activation and IP₃ production.

Orai1 and STIM1 have been shown to regulate cancer cell proliferation in lung cancer (Hou et al. 2011), clear renal cell carcinoma (Kim et al. 2014), cervical cancer (Chen et al. 2011), glioblastoma (Liu et al. 2011), non-small cell lung cancer (SCLC) (Zhan et al. 2015) and esophageal squamous cell carcinoma (Zhu et al. 2014).

SOC have been extensively studied in BCa. High STIM1 levels and low STIM2 expression have been associated with poor prognosis (McAndrew et al. 2011). Moreover, Orai3 is overexpressed in BCa, due to its regulation by estrogens (Motiani et al. 2013). In this context, Orai3 participates in SOCE, increasing proliferation, apoptosis resistance and migration, via NFAT-regulated transcription and modulation of the FAK (Faouzi et al. 2013; Motiani et al. 2013). A similar role was documented for Orai3 in non-small-cell lung adenocarcinoma.

Interestingly, recent studies showed that SOC channels could regulate CSC physiology (Aulestia et al. 2018; Lee et al. 2016; reviewed in Terrié et al. 2019).

In PCa, NFAT was shown to regulate cell proliferation via TRPV6/Orai1 (Raphaël et al. 2014) and Orai3/Orai1 (Dubois et al. 2014), but not canonical SOC channels. Orai3, a protein known to form with Orai1 the ARC (arachidonic acid-regulated channels) store-independent channels (Thompson and Shuttleworth 2013), has been shown to be overexpressed in aggressive PCa (Dubois et al. 2014). Such remodeling disrupts the equilibrium of Orai channels and favors cell progression to a more aggressive pro-proliferative phenotype. Authors show that in aggressive PCa, Orai3 recruits Orai1 to form ARC channels leading to increased cell proliferation through activation of the NFAT pathway. This recruitment of Orai1 negatively regulates the SOCE, inhibiting PCa apoptosis sensitivity (Flourakis et al. 2010).

V. *The sigma 1 receptor*

1. *Identification and function*

Initially identified as an opioid receptor (Martin et al. 1976), the sigma 1 receptor (S1R, 25 kDa) can actually bind many different compounds. This unique protein has no homology with other Mammalian proteins. Unlike what its name suggests, the S1R does not act like a receptor in the way that ligand binding will lead to the activation of a signaling pathway. Instead, ligands will trigger a conformational change or a translocation of the S1R, which will in turn modulate its activity. This protein has been shown to act as a chaperone protein, able to bind and modulate many different proteins. Mostly known as an ER resident protein preferentially located in the mitochondria-associated membranes (MAM), the S1R has been extensively studied as a modulator of ER stress and ER-mitochondria Ca^{2+} signaling, particularly in neurons (reviewed in Hayashi and Su 2007; Penke et al. 2018; Su et al. 2016). Interestingly, the S1R is also able to translocate to the cytoplasm and the PM. Moreover, several studies showed that the S1R was able to modulate ion channels via direct or indirect interaction.

2. *S1R structure*

The structure of the S1R is still debated to this day. Initially thought to contain 2 TMD (Aydar et al. 2002; Hayashi and Su 2007), a recent study provided evidence of a single TMD (Schmidt et al. 2016). The orientation of the S1R has been disputed as well (Aydar et al. 2002; Hayashi and Su 2007), and although the crystal structure of the S1R indicated a cytoplasmic Ct, with the Nt residing in the lumen, a recent study showed otherwise (Mavylutov et al. 2018). Moreover, the S1R has been shown to function in different orders of oligomerization, depending on the cellular context (Gromek et al. 2014; Mishra et al. 2015; Schmidt et al. 2016).

3. *S1R and cancer*

The S1R has been shown to be overexpressed in cancer a long time ago (John et al. 1998; Vilner et al. 1995b), however, the ligands used in these studies were not quite specific of the S1R, and therefore precluded the identification of its roles in this pathology. This caveat was later overcome in some cancers with a more specific approach (Aydar et al. 2006). Several studies using S1R ligands showed that the chaperone protein could have a pro-survival effect in cancer cells (Achison et al. 2006; Spruce et al. 2004; Vilner et al. 1995a). However, the precise role(s) of the S1R remain(s) to be studied in cancer. Interestingly, a growing number of studies show that the S1R can have an effect in cancer cell physiology through the modulation of ion channels (reviewed in Soriani and Rapetti-Mauss 2017).

The S1R has first been shown to modulate potassium channels in cancer. The S1R drives BCa and colorectal cancer migration via the regulation of calcium homeostasis through SK3 channel (small-conductance calcium-activated K^+ channel) modulation (Gueguinou et al. 2017; Guéguinou

et al. 2016). The S1R can also regulate voltage-gated potassium channels such as hERG channels (human ether-à-go-go-related gene) in leukemic cells (Balasuriya et al. 2014; Crottès et al. 2011; Kinoshita et al. 2012). In SMLC and T-cell leukemia, the S1R has also been shown to regulate proliferation via Kv1.3 potassium channel modulation (Renaudo et al. 2004).

The S1R has also been linked with Nav1.5 sodium channels in a BCa cell line (Balasuriya et al. 2012).

Finally, the S1R regulates cell cycle via volume-regulated chloride channel modulation in SMLC and T-cell leukemia (Renaudo et al. 2007).

The S1R has been shown to regulate more types of ion channels in neurons or other cell types, however some of these targets have not been investigated in cancer yet. This is the case for SOC channels (Srivats et al. 2016).

4. S1R pharmacology

The S1R can bind many different ligands and thus possesses a rich pharmacology (Chu and Ruoho 2016). Indeed, many antipsychotics show high to moderate affinity for the S1R. The S1R can also bind neurosteroids such as progesterone. To this day, no endogenous ligand has been clearly identified, but among the candidates one can find the DMT (N,N-dimethyltryptamine) (Fontanilla et al. 2009; Frecska et al. 2013; Mavlyutov et al. 2012). Interestingly, the enzyme responsible for DMT production, INMT (indolethylamine-N-methyltransferase), is overexpressed in PCa (Larkin et al. 2012).

Aims of the thesis

Prostate cancer (PCa) is the most frequent and the third deadliest cancer in men in developed countries. As described before, there is still a need to develop new markers, more reliable than the controversial PSA, and able to better discriminate between the different stages of PCa progression. There is also a general need for new therapeutic strategies, especially for aggressive advanced stages. In our work, we focused on cancer stem cells (CSC), a rare subset of cancer cells with stem cell properties. CSCs are highly aggressive and resistant to conventional therapies (Nguyen et al. 2012; Reya et al. 2001), and have been proposed as the origin of tumor relapse. A better understanding of CSC regulation could therefore allow to address several clinically relevant issues, and potentially to target them in the context of the development of new therapeutic strategies.

Calcium is a highly versatile second messenger that can determine cell fate depending on its signaling properties. Although a few studies indicated the implication of calcium in the regulation of stemness, its role in this particular context is just beginning to unfold. However, calcium signaling has been shown to be in all the hallmarks of cancer (Monteith et al. 2017; Prevarskaya et al. 2018). This fact was confirmed by our laboratory, we showed the involvement of several calcium channels in prostate carcinogenesis, and the associated signaling pathways. Our first general aim was thus to study the calcium signature of prostate CSCs in order to identify the key calcium channels regulating their physiology. As previously stated, SOC channels have been shown to influence cancer cell physiology in many different cancer types. However, neither the role of SOCE in PCa cell proliferation, nor its possible implication in CSC physiology had been documented before this work. Indeed, although some data showed the possible implication of NFAT in CSC regulation (Horsley et al. 2008), its implication and roles remained to be studied. Finally, as mentioned above, although the pharmacology of the SOC channels is extensive, it only allows for inhibition. However, more and more studies show the importance of partner proteins in the regulation of ion channels (Gkika et al. 2015; Harteneck 2003; Radhakrishnan et al. 2010). It would thus be interesting to take advantage of these protein to indirectly modulate ion channels. Therefore, the second general objective of this project was to study the S1R, a chaperone protein that has been shown to modulate several ion channels in cancer (Soriani and Rapetti-Mauss 2017), as a potential modulator of the SOC channels in PCa.

I. Characterization of the calcium signature of stem-like cancer cells

The first objective of this work was to study the calcium signature of a rare subset of cancer cells presenting stem-like properties. To do so, we used two different models allowing us to isolate cells with stem-like properties in both prostate cancer and melanoma cell lines.

After the initial characterization of our models, we studied their calcium signature, with the aim of finding a common one. We used the technique of RT-qPCR that allowed us to compare the levels of mRNA expression of several key actors of calcium signaling between the stem-like cancer cells and their non-stem counterpart.

After this identification of the gene(s) differentially expressed between stem- and non-stem cancer cells, our next objective was to confirm our results at the functional level using calcium imaging, and to identify the effects on this (these) pathway(s) on cancer cell physiology. For this purpose, we used functional tests such as sphere formation assays, associated with the modulation of our targets to evaluate their role on the stemness of our cells (see section 1 of the results).

II. The S1R as a potential partner protein of calcium channels in PCa

1. Study of the S1R expression in PCa

Previous studies showed that the S1R is overexpressed in many cancers, including PCa (Aydar et al. 2006; Vilner et al. 1995b). We first aimed to confirm those results using human samples and PCa cell lines. We also performed experiments to determine if the expression of the S1R can be modulated by androgens, a critical factor in PCa cell regulation (see sections 2.1 and 2.2 of the results).

The expression of Orai and STIM have been previously studied in PCa samples. Interestingly, a previous study showed a possible regulation of Orai1 by androgens (Flourakis et al. 2010). Our objective was to confirm those results and verify the possibility of androgen-regulation for the other Orai/STIM isoforms implicated in PCa (see sections 2.3 of the results).

2. Functional and physiological impacts of the S1R on SOC channels in PCa cells

Our next goal was to evaluate the effects of the S1R on SOC activity in PCa cells by using patch-clamp to record the SOC currents and calcium imaging to measure the SOCE (see section 2.4 of the results).

After characterizing the functional effects of the S1R on SOC channels, we then aimed to decipher its mechanisms by studying S1R subcellular localization and protein-protein interactions (see sections 2.5 and 2.6 of the results).

SOC channels have been studied in different cancers, and they have been shown to be implicated in different hallmarks of cancer (Fiorio Pla et al. 2016). In PCa cells, previous studies have shown the implication of SOC channels in apoptosis resistance (Flourakis et al. 2010). Another study implicated Orai1 and Orai3 in PCa cell proliferation via their direct association to form the ARC

channels (Dubois et al. 2014). In light of these previous results, our aim was to study the effect of the S1R/SOC interaction on PCa cell proliferation, quiescence and apoptosis resistance (see sections 2.7 to 2.11).

3. Regulation of other calcium channels by the S1R in PCa

Finally, we aimed to study the potential effects of the S1R on the activity of other calcium channels previously shown by our lab as being implicated in PCa.

To do so, we performed some initial experiments in HEK-293 cells, in order to test the effect of S1R overexpression or inhibition on the activity of two calcium channels. We thus studied TRPV6 (transient receptor vanilloid 6), implicated in PCa cell proliferation and apoptosis (Raphaël et al. 2014), and TRPM8 transient receptor melastatin 8), a key regulator of PCa cell migration (Gkika et al. 2010) (see sections 2.12 and 2.13 of the results).

Material & Methods

I. Biological materials

In this section, we will detail the different samples and cells we used for this work. Overall, we used immortalized human cell lines for our studies, as well as two sets of human samples.

1. Human samples

We used two different sets of human samples to study S1R expression pattern in prostate cancer at protein and mRNA levels.

a. Tissues

We used 17 human prostate samples:

- 2 samples of healthy prostates (obtained from bladder cancer patients).
- 6 samples of benign prostatic hyperplasia (BPH).
- 6 samples of Gleason 7 prostate cancer.
- 3 samples of Gleason 9 prostate cancer.

The samples were obtained thanks to our collaboration with Pr Gosset and Dr Mihalache from Groupement des Hôpitaux de l'Institut Catholique de Lille, processed and stained automatically with a Ventana BenchMark XT (Roche). Paraffin-embedded prostate sections were subjected to standard deparaffinization (EZ prep solution, Ventana, Roche) followed by antigen retrieval using citrate buffer at 95°C. Samples were pretreated with basic Tris solution for 60 minutes with the CC1 program (Ventana). Endogenous peroxidase activity was blocked with hydrogen peroxide (8 minutes), and samples were exposed to primary antibodies (see [Table 4](#); 32 minutes). Signal was amplified with the Amplification kit (Ventana, Roche), endogenous biotin activity was blocked with the Endogenous biotin blocking kit (Ventana, Roche). Samples were incubated with horse radish peroxidase (HRP)-coupled secondary antibodies. Signal was detected with 3,3'-diaminobenzidine tetrahydrochloride and an IVIEW-DAB detection system (N760-500, Ventana, Roche). Tissues were counterstained with hematoxylin and the Bluing reagent (Ventana, Roche). After dehydration and xylene baths, slides were mounted for microscopy and analyzed with a Zeiss Axioscope microscope.

b. cDNA

We obtained cDNAs from 13 patients with prostate cancer (in collaboration with Cancéropôle Grand Ouest, Pr Gaëlle Fromont-Hankard; Gleason 6 to 9). For each patient, two separate samples were taken after histopathological analysis: one from a healthy part of the prostate, and another one from a cancerous area. The samples were then processed, subjected to qPCR (see section III) and analyzed by Dr Dimitra Gkika.

2. Cell lines

For this study, we used different immortalized cell lines that will be described below. First the HEK-293 model cell line allowed us to easily characterize the functional effect of the S1R on calcium channels. Then, we used more physiologically relevant models: prostate cancer and melanoma cell lines to study SOCE in cancer.

a. HEK-293 model cell line

We first used the well characterized cell line HEK-293 (human embryonic kidney) (purchased from the American Type Culture Collection (ATCC)). These cells express both S1R and SOC channels, thus enabling the study of their interaction in an endogenous context. Moreover, they can be easily transfected, thus allowing either the modulation of expression of our proteins of interest, or the heterologous expression of other channels and proteins.

b. Prostate cancer cell lines

For this study, we used two different prostate cancer cell lines (purchased from ATCC):

- The LNCaP (lymph node carcinoma of the prostate) cell line was established from the lymph node of a patient with prostate cancer. These cells express the androgen receptor (AR) and the prostate specific antigen (PSA) and are therefore considered as a common model for the androgen-sensitive stage of prostate cancer development. (van Bokhoven et al. 2003; Horoszewicz et al. 1980).
- The PC3 (Prostate Cancer 3) cell line was established from a bone metastasis of a patient with prostate cancer. These cells do not express the AR or the PSA and are therefore considered as a common model for the androgen-resistant stage of prostate cancer development (van Bokhoven et al. 2003; Kaighn et al. 1979).

We also used a PC3 clone stably expressing Luciferase (PC3-Luc) and a PC3 clone stably expressing luciferase and TRPM8 channel (PC3-M8-Luc) developed in our laboratory by Dr Guillaume Grolez.

c. Melanoma cell line

We used the human cutaneous melanoma cell line HBL which was established from a nodular malignant melanoma by the team of Pr Ghanem (Ghanem et al. 1988) (the cell line was a kind gift from the Pr Ghanem's lab). For our studies, we used a stable clone expressing H2B-GFP developed by our collaborators from Dr Renata Polakowska's team, described below (see section I.5.a.).

3. Adherent culture conditions

HEK-293 cells were maintained in DMEM GlutaMax™ high glucose medium (Gibco, Life Technologies) supplemented with 10 % fetal bovine serum (FBS; Gibco, Life Technologies) at 37°C in a humidified atmosphere containing 5 % CO₂.

Cancer cells were grown in the same conditions with RPMI-1640 medium (Gibco, Life Technologies) supplemented with 2 mM L-glutamine (Gibco, Life Technologies) and 10 % FBS. To study the androgen-dependence of our proteins in prostate cancer, we cultivated cells in steroid-deprived conditions. To do so, we used RPMI-1640 medium without phenol red, supplemented with 2 mM L-glutamine and 10% charcoal-stripped FBS.

When needed, cells were washed with PBS (phosphate-buffered saline; Gibco, Life Technologies) and dissociated using 0.05 % Trypsin-EDTA and mechanical trituration.

Cells were counted under a microscope with a 10x objective using a hemocytometer. We used Trypan blue (0.2 %, 2 minutes) exclusion to exclude dead cells.

For long term conservation, we froze cells in the Recovery™ cell culture freezing medium (Gibco, Life Technologies) at the concentration of 10^7 cells/ml.

4. *Sphere formation*

CSCs derived from solid tumors (such as melanoma and prostate cancer) have the particularity to be able to survive and proliferate in non-adherent cell culture, as opposed to the non-stem adherent cancer cells. In such culture conditions, CSCs will proliferate and form a sphere. Thus, suspension cell culture allows us to increase the proportion of CSC in our cancer cell population and to test the stemness of our cells through their ability to form spheres.

To generate spheres, cells were grown in 24-well plates (2×10^3 cells/well) treated with 5mg/ml poly(2-hydroxyethyl methacrylate) (pHEMA, Sigma) in 95% ethanol preventing cell adhesion. Cells are maintained in DMEM-F12 medium (Gibco, Life Technologies) supplemented with 20 ng/ml epidermal growth factor (EGF) (Stem cells technologies), 20 ng/ml recombinant human basic fibroblast growth factor (rHu bFGF) (PromoKine-PromoCell GmbH) and 2% B-27™ serum free supplement (Gibco, Life Technologies).

After 7 days, spheres were pelleted by centrifugation and dissociated (500 μ l of Trypsin-EDTA per 24-well plate). Before dissociation, spheres can be counted under microscope (Leica DMI8) to determine the sphere forming unit (SFU), in %, using the following formula:

$$\text{SFU} = (\text{number of spheres/number plated cells}) \times 100$$

5. Identification of quiescent/slow cycling cells and FACS sorting

a. Melanoma

For the tracing of slow cycling melanoma cells, we used the previously described HBL H2B-GFP cell line stably expressing the tetracycline-inducible histone 2B (H2B) fused with a green fluorescent protein (GFP) (Ostyn et al. 2014). With this construct, after 24 hours of treatment with 1 $\mu\text{g/ml}$ tetracycline (Sigma), all nuclei are GFP-positive. Then, following tetracycline removal from the medium, the GFP signal will be diluted by two after each cell division as pictured in Figure 1. After 7 days of dilution in sphere forming conditions (see section I.4.), the GFP-positive subpopulation (GFP^{hi}) and its GFP-negative counterpart (GFP^{lo}) were isolated by fluorescence-activated cell sorting (FACS) using a FACSAria™ III instrument (BD Biosciences).

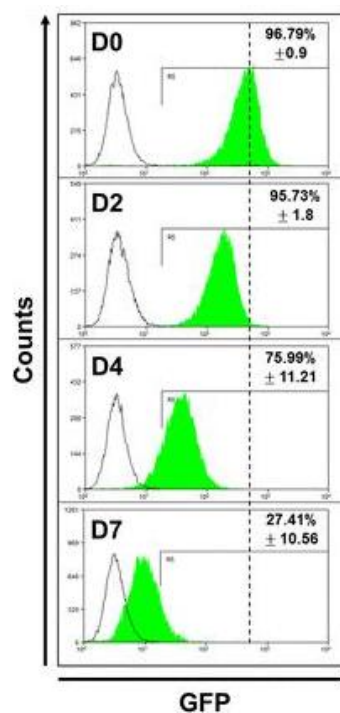


Figure 1: GFP dilution in HBL H2B-GFP cells

Flow cytometry profiles of the GFP signal dilution at days (D) 0, 2, 4 and 7 in HBL H2B-GFP cells after tetracycline induction (1 $\mu\text{g/ml}$, 24 hours). The non-induced HBL are used as the GFP-negative control reference population (black line) to gate the GFP-positive subset (green). The numbers indicate the percentage of GFP-positive cells (\pm SEM) in the total population. Adapted from Ostyn et al. 2014.

b. Prostate

To detect quiescent/slow cycling prostate cancer cells, PC3 cells resuspended in serum-free RPMI-1640 (10^6 cells/ml) were stained with 1 μ l/ml of Vybrant™ Dil (1,1'-Dioctadecyl-3,3,3',3'-tetramethylindocarbocyanine perchlorate, or DilC18(3)) labeling solution (Invitrogen™, ThermoFisher Scientific) for 25 min at 37°C. Labelled cells will then dilute the Dil with each cellular division as shown in Figure 2. Cells were then washed and used for sphere formation assay (see section I.4.). After 7 days of label dilution, the Dil-positive (Dil^{hi}) and negative (Dil^{lo}) subpopulations are isolated by FACS as described above (see section I.5.a.).

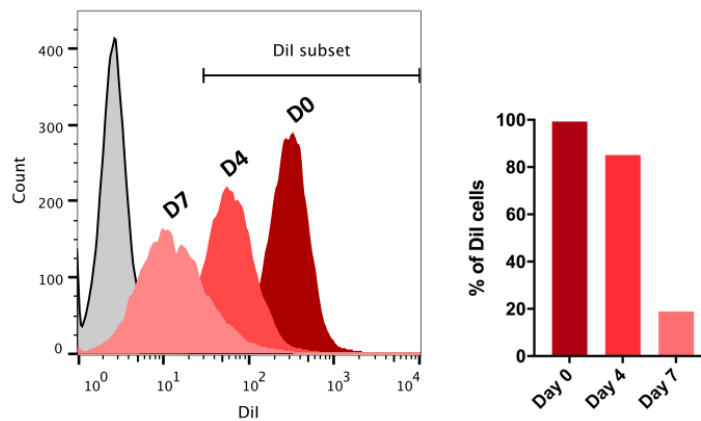


Figure 2: Dil dilution in PC3 cells

On the left, flow cytometry profiles of the Dil signal dilution at days (D) 0, 4 and 7 in PC3 cells. The unlabeled PC3 cells are used as the GFP-negative control reference population (grey) to gate the Dil-positive subset (shades of red). On the right, bars show the percentage of Dil-positive cells in the total population.

These experiments were carried out with the help of Dr Pilar Flamenco.

II. Transfection

Transfections allowed us to modulate the expression of our proteins of interest. We first used this technique to strongly decrease the expression of target proteins using siRNA. With this technique, we were also able to deliver plasmids to our cells. We used different constructs that enabled us to perform protein overexpression, heterologous expression of wild type, mutated or modified proteins fused to fluorescent proteins or tags for example.

We used lipofection to deliver siRNA, and either lipofection or nucleofection to deliver plasmids to our cells depending on the experimental design. Compared to nucleofection, lipofection is less efficient but gentler, making it the preferred method for sensitive cells and/or stressful conditions.

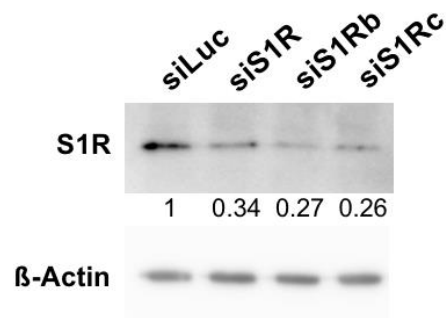
1. siRNA lipofection

siRNAs (50-100 nM) were lipofected using the HiPerFect reagent (Qiagen) according to manufacturer's instruction. We performed a reverse transfection for 96-well plates and a fast-forward transfection for bigger volumes. Reagent volumes were optimized for our cells as follows: 0.5 μ l per well for a 96-well plate, 9 μ l per well for a 6-well plate, 15 μ l for a 60 mm dish, 30 μ l for a 100 mm dish. This protocol led to a good inhibition of our proteins, as shown in Figure 3 for S1R where we were able to obtain a 70% inhibition of protein expression with three distinct siRNA sequences.

The siRNAs (custom, designed by Dr Dimitra Gkika, Eurogentec) used for our study are described in Table 1. For every siRNA silencing, we used a siRNA targeting the luciferase (siLuc), a gene not expressed in Mammalian cells as a control. For experiments combining luciferase and siRNAs, we used a scramble siRNA as control (siNeg; Eurogentec).

Figure 3: siS1R validation

Western blot analysis of S1R expression in LNCaP cells 3 days after lipofection with siLuc, siS1R, siS1Rb or siS1Rc (50 nM). S1R expression is normalized with β -actin.



Name	Sequence
siLuciferase	5'-CUUACGCUGAGUACUUCGA (dTdT)-3'
siAR	5'-GACUCAGCUGCCCAUCCA (dTdT)-3'
siOrai1	5'-UGAGCAACGUGCACAAUCU (dTdT)-3'
siOrai3	5'-UUGAAGCUGUGAGCAACAUA (dTdT)-3'
siS1R	5'-GGAUAUCCAUGCUUAUGUA (dTdT)-3'
siS1Rb	5'- CCATCATCTCTGGCACCTT (dTdT)-3'
siS1Rc	5'- GCTGAGATCTCGGATACCA (dTdT)-3'
siSTIM1	5'-GGCUCUGGAUACAGUGCUC (dTdT)-3'
siSTIM2	5'-AACUGAGAAGCAGUUGGUCUG (dTdT)-3'

Table 1: Name and sequence of siRNAs

2. *Plasmid transfection*

For plasmid transfections, we used an empty pcDNA4 or pmaxGFP plasmid (Lonza) as control. The amount of plasmid, ranging from 0.5 to 3 µg, was adjusted depending on the number of cells, the transfection method and the experimental design. We used either commercial plasmids, kind gifts from collaborators or plasmids created in our laboratory (see [Table 2](#)).

a. Plasmid lipofection

Different lipofection reagent were used depending on the cell line.

For LNCaP cells, we used the Lipofectamine® 3000 (ThermoFisher Scientific) according to manufacturer's instruction. Lipofectamine volume was optimized to 2 µl per well for a 6-well plate and 3.5 µl for a 60 mm dish.

PC3 cells were lipofected according to manufacturer's instructions using the X-tremeGENE 9 DNA Transfection Reagent (Roche) with a 3:1 ratio (µl of reagent : µg of plasmid).

For HEK-293 cells, we used the X-tremeGENE HP DNA Transfection Reagent (Roche) according to manufacturer's instructions with a 3:1 ratio.

b. Plasmid nucleofection

Nucleofection is an electroporation-based transfection method developed by Amaxa and marketed by Lonza. This method makes possible, in a reproducible and efficient way, to introduce plasmids, siRNAs and other nucleic materials directly into the nucleus of the cells. Practically, transfection was carried out on cells in suspension. After trypsinization and counting, 10⁶ cells were pelleted, resuspended in 100 µl of transfection buffer (V buffer for HEK-293 cells, R Buffer for LNCaP cells). For the detection of transfected cells during patch-clamp experiments, 0.25 µg of pmax-GFP (Lonza) plasmid were added to the buffer. The suspension obtained was then placed in an electroporation cuvette, and transferred into the Nucleofector™ (Amaxa, Lonza) where it was subjected to an electrical stimulation whose parameters are built-in and optimized for each cell line. 500 µL of warm culture medium was then added in order to increase cell recovery, and cuvettes were left for 5 minutes in an incubator prior to their seeding in culture dishes. Functional studies were typically performed 24 hours after nucleofection.

Plasmid	Origin
<i>pCMV-hS1R-cMyc</i>	Dr O. Soriani
<i>pcDNA4-hS1R-cMyc</i>	Laboratory
<i>phS1R-eGFP</i>	Dr O. Soriani
<i>phS1R-mCherry</i>	Dr O. Soriani
<i>pVLL-hS1R-SYFP</i>	Laboratory
<i>rS1R-V1</i>	Dr T.P. Su
<i>pVLL-hOrai1-mTurq</i>	Laboratory
<i>pVLL-hOrai3-SYFP</i>	Laboratory
<i>pVLL-hSTIM1-mTurq</i>	Laboratory
<i>luc2P-NFAT-RE</i>	Promega
<i>NFATc3-mCherry</i>	Laboratory
<i>NFATc3-eGFP</i>	Laboratory
<i>ER-DsRed</i>	Laboratory
<i>pcDNA4-hAR</i>	Laboratory
<i>pcDNA4-hTRPM8</i>	Laboratory
<i>pcDNA4-hTRPV6</i>	Laboratory

Table 2: List and origin of plasmids

III. Transcriptomics

We used transcriptomic methods to study the expression of our genes of interest. Gene expression was quantified at mRNA level by quantitative PCR after total RNA extraction and reverse transcription (RT).

1. RNA extraction

Total RNA was extracted with the NucleoSpin® RNA Plus kit (Macherey Nagel), or the NucleoSpin® RNA XS kit (Macherey Nagel) for small samples, according to the manufacturer's instructions. RNA quality was verified by checking the integrity of ribosomal RNAs (28S rRNA and 18S rRNA) on a 2 % agarose gel, and sample concentration was determined by absorption at 260 nm.

When needed, extracted samples were purified using the NucleoSpin® RNA Clean-Up kit (Macherey Nagel).

2. Reverse transcription

The extracted total RNA was then subjected to a reverse transcription (RT) to synthesize the complementary deoxyribonucleic acid (cDNA). For this purpose, 2 µg of extracted RNA was incubated with 3 µM [d(N)₆] random hexamers (used as primers for the RT) (Invitrogen) at 70°C for 10 minutes followed by 30 seconds on ice to denature RNAs and allow primer annealing. RT was then performed by adding 2.5 mM MgCl₂, 10 mM dNTP (2.5 mM per dNTP), 50 U MuLV, 20 U RNase inhibitor in the PCR buffer II (Applied Biosystems, Life Technologies). A first incubation at room temperature allowed primer extension (15 minutes). The samples were then incubated for 30 minutes at 42°C, the optimal polymerization temperature for the RNA-dependent DNA polymerase MuLV. The samples were then placed at 70°C for 10 minutes to stop the reaction.

3. Quantitative PCR

Real-time quantitative PCR (polymerase chain reaction; qPCR) allows for the relative quantification of gene expression. This technique uses a fluorescent nucleic acid dye that incorporates in the DNA synthesized by the polymerase allowing for monitoring of the amplification in real time. Here, we used the SsoFast™ EvaGreen® (Bio-Rad) supermix. The unbound EvaGreen® dye has a weak fluorescence that increases strongly when bound to DNA. To quantify gene expression, we used specific primer couples (custom designed by Dr Dimitra Gkika, Eurogentec) targeting the cDNA of mRNAs of interest (see [Table 3](#)). The primer couples were previously tested on serial dilution of cDNA or specific plasmid and we selected primers and conditions with an efficiency close to 100%.

The reaction was carried out in 20 µl volume, with 20-50 ng of cDNA, 300 nM primer concentration, with the CFX96 Real-Time PCR detection system (Bio-Rad).

qPCRs were performed in three steps: denaturation, amplification cycles and melting curve. We used a qPCR supermix featuring the hot-start system: the polymerase's enzymatic site is blocked by antibodies to avoid non-specific elongation. The first step of denaturation (30 seconds at 95°C) leads to the removal of these antibodies, activating the polymerase for the PCR. This first step was followed by 40 cycles of amplification: strand dissociation (5 seconds at 95°C) followed by annealing and extension (5 seconds at 60°C). The strong fluorescence emitted by the DNA-bound EvaGreen® dye was recorded at the end of each cycle. After the 40 cycles of amplification, we performed a melt curve of the amplicons (a ramp from 65°C to 95°C with an increment of 0.5°C, 5 seconds per step) to validate the specificity of the reaction.

HPRT and r18S were used as internal control to normalize variations in RNA quality and RT efficiency. To quantify the results, we used the comparative threshold cycle method described by Livak and Schmittgen (Livak and Schmittgen 2001).

Gene	Forward sequence	Reverse sequence
<i>RN18S</i>	5'-CAGCTTCCGGGAAACCAAAGTC-3'	3'-AATTAAGCCGCAGGCTCCACTC-5'
<i>AR</i>	5'-GCAGGAAGCAGTATCCGAAG-3'	3'-CTCTCGCCTTCTAGCCCTTT-5'
<i>HPRT</i>	5'-GGCGTCGTGATTAGTGATGAT-3'	5'-CGAGCAAGACGTTTCAGTCCT-5'
<i>ORAI1</i>	5'-ATGGTGGCAATGGTGGAG-3'	3'-CTGATCATGAGCGCAAACAG-5'
<i>ORAI3</i>	5'-GGCCAAGCTCAAAGCTTCC-3'	3'-CCTGGTGGGTACTCGTGGT-5'
<i>SIGMAR1</i>	5'-CAGTACGCTGGGCTGGAC-3'	3'-GAGCAGCACATACTCGGACA-5'
<i>STIM1</i>	5'-TGTGGAGCTGCCTCAGTATG-3'	3'-CTTCAGCACAGTCCCTGTCA-5'
<i>STIM2</i>	5'-GACGTCAGTATGCAGAACAG-3'	3'-GACCAACTGCTTAGTTC-5'

Table 3: Name and sequence of primers

IV. Proteomics

We used different techniques based on the immunodetection of proteins to study protein expression levels, intracellular localization and interactions. First, Western blot (WB) allowed us to study gene expression at protein level. We also used WB-derived techniques such as biotinylation to test the presence of proteins at the cell surface and coimmunoprecipitation (coIP) to investigate protein complexes.

We also performed immunocytochemistry (ICC) to identify protein expression patterns and subcellular localizations.

1. *Western blot and associated techniques*

We used the technique of Western blot (WB) to study protein expression. Here, cells are lysed in order to isolate and analyze the protein content. This technique relies on electrophoresis to separate protein according to their molecular weight and immunoreactivity to detect proteins of interest.

We also coupled WB to other techniques to study protein interactions and localizations. We used coimmunoprecipitation to study protein complexes and biotinylation to study the presence of proteins at cell surface.

a. Protein extraction

Cells were washed in PBS and lysed in RIPA buffer (10 mM Tris, 150 mM NaCl, 2 % sodium deoxycholate, 2 % Triton X100, pH 7.2) in the presence of an anti-protease cocktail (10 % v:v; Sigma). The sample was then centrifugated (10 minutes at 12,000 g) to isolate the total protein lysate in the supernatant.

The protein content of each sample was measured with the colorimetric BCA assay kit (Bicinchoninic assay; Pierce, ThermoFisher Scientific) using a standard curve of bovine serum albumin (BSA).

b. Western Blot

The protein extracts were analyzed by electrophoresis in denaturing conditions using the SDS-PAGE technique (sodium dodecyl sulfate polyacrylamide gel electrophoresis).

The samples (usually 40-50 µg) were prepared in the denaturing Laemmli loading buffer (200 mM Tris, 25 mM DTT, 4 % SDS, 2 % sucrose, bromophenol blue, pH 6.2) and heated at 37°C for 30 minutes. The concentration of the polyacrylamide gel was chosen according to the molecular weights of the proteins of interest. We used 4 – 20% gradient gels to study a wide range of protein weights (Bio-Rad). Migration was performed with fixed voltage in a Tris/glycine buffer (25 mM Tris, 192 mM glycine, 0.1 % SDS, pH 8.4). After electrophoresis, proteins were transferred on a methanol-activated (5 minutes) polyvinylidene fluoride membrane (PVDF; Amersham, GE Healthcare) by semi-dry transfer (G2 fast blotter, ThermoFisher Scientific). After the transfer, the membrane was blocked in 5 % milk prepared in Tris-NaCl-Tween buffer (TNT; 15 mM Tris, 140

mM NaCl, 0.05 % Tween 20, pH 7.4) during 1 hour, gently rocking, to prevent non-specific binding. We then exposed the membrane to the primary antibody targeting the protein of interest (see [Table 4](#) for antibodies; time and temperature of exposition were antibody-dependent) prepared in 1 % milk TNT. After three washes in TNT, membranes were exposed to a peroxidase-coupled secondary antibody (anti-mouse or anti-rabbit; Jackson Laboratories) prepared at 1:20,000 dilution in 1 % milk TNT during 1 hour, gently rocking, followed by three TNT washes. To detect the signal, membranes were exposed to an enhanced chemiluminescence (ECL) horse radish peroxidase (HRP) substrate (we used three different substrates, depending on the amount of protein and expected signal intensity: West Pico, West Dura and West Femto; ThermoFisher Scientific). The chemiluminescent signal resulting from HRP activity was recorded by a CCD-based imager (Amersham Imager 600, GE Healthcare). Relative quantification of proteins was obtained by densitometry using ImageJ software (NIH) (Schneider et al. 2012) and an appropriate control protein such as β -actin, calnexin or GAPDH.

c. Coimmunoprecipitation

By coupling specific antibodies to beads, coimmunoprecipitation (coIP) allows for the isolation of a specific protein. This crucial step of immunoprecipitation is performed in specific conditions preserving the integrity of protein complexes. Thus, by immunoprecipitating a specific protein, we are able to study the other proteins it directly or indirectly interacts with.

Specific antibodies (1 μ g) or control IgGs were incubated with 40 μ l of Protein A/G agarose beads (Pierce, ThermoFisher Scientific) in 500 μ l of IP buffer (150 mM NaCl, 20 mM NaH_2PO_4 , pH 8) for 1 hour at 4°C, in rotation. During this step, antibodies are bound to agarose beads thanks to a fusion protein of antibody binding domains of protein A and G. We then added protein samples (see section IV.1.a.) in equal amounts (0.5-1 mg) for 12 hours at 4°C, in rotation. Samples were then centrifugated (2 minutes at 2,000 g) to isolate two protein fractions:

- The **immunoprecipitated fraction**: pelleted fraction representing the protein of interest and any directly or indirectly interacting protein at the time of protein extraction.
- The supernatant containing all the other proteins of our sample.

After three washes in IP buffer, we used different methods to elute the protein samples from the immunoprecipitated fraction. We first used an acidity-based method with a 10 minutes incubation in a glycine buffer at pH 2.6 followed by the addition of equal amounts of a Tris buffer at pH 8 to cancel the acidity. After centrifugation, we retrieved the supernatant containing the proteins of interest. This procedure was repeated once, and the two elutions were pooled for WB analysis. This gentle elution allows the retrieval of most of the proteins of interest without the antibodies used for the coIP. This method was used to study S1R and Orai1 which molecular weights are close to the light chain of denaturated antibodies. When used, this elution was followed by a regular elution in Laemmli loading buffer without dithiothreitol (DTT) (10 minutes at 50°C). With this harsher elution, we were able to retrieve all the remaining proteins, but the samples were

contaminated by fragments of antibodies used for our experiment. A final elution was then performed, as a control, using Laemmli buffer (5 minutes at 96°C). All the samples were then prepared for WB analysis as previously described (see section IV.1.b.).

To validate the reproducibility of our results, we performed reverse colPs, targeting each protein of interest belonging to the same complex.

d. Biotinylation

Biotinylation uses the high affinity properties of biotin towards neutravidin, coupled with precipitation principles to isolate the proteins expressed at cell surface.

Cells were plated in 100 mm dishes (TPP) and used at 60-80 % confluence. After two washes with PBS-B (PBS supplemented with 1 mM MgCl₂ and 0.5 mM CaCl₂; pH 8), cells were incubated with biotin (0.5-1 mg/ml; EZ-Link NHS-LC-LC-Biotin, ThermoFisher Scientific) for 30 minutes at 4°C. During this time, biotin conjugates to the proteins exposed at cell surface. Cells were then washed twice with 0.1 M glycine (in PBS-B) to quench the unbound biotin. After a PBS wash, cells were lysed with lysis buffer (section IV.1.a.) for 1 hour at 4°C gently rocking. Cell lysate was then pelleted (10 minutes at 14,000 g) and we collected the supernatant containing the proteins. Protein concentration was measured as previously described (see section IV.1.a.). We exposed 0.5-1 µg protein to agarose bead coupled with neutravidin (Pierce NeutrAvidin™ Agarose, ThermoFisher Scientific) for 12 hours at 4°C, in rotation. With its strong affinity for neutravidin, the biotin binds to agarose beads allowing for the precipitation of the biotinylated fraction of our total protein lysate. This technique thus allowed us to isolate two protein fractions after centrifugation (2 minutes at 2,500 g):

- The **biotinylated fraction**: pelleted fraction representing the proteins expressed at cells surface coupled with the biotin-neutravidin-agarose beads.
- The **non-biotinylated fraction**: supernatant containing the proteins not exposed at cell surface.

The biotinylated fraction was washed five times in lysis buffer and prepared for WB analysis as previously described (see section IV.1.b.) in order to study the presence of our proteins of interest at the cell surface.

2. Immunocytochemistry

Immunocytochemistry (ICC) relies on the same principle of protein detection by specific antibodies, but without cell lysis. In this technique, cells are preserved and fixed with or without permeabilization and immunoreacted to detect specific proteins. Here, we performed immunofluorescence (IF) using primary or secondary antibodies coupled with fluorescent proteins. Samples were then analyzed by confocal microscopy or flow cytometry, depending on the experiment.

We used different protocols, depending on the target protein and/or the analysis method.

a. Standard protocol

Cells were prepared depending on the experiment. We used dissociated cells for flow cytometry analysis. For microscopy, cells were grown on 10mm slides in 12-well plates (2×10^4 cells per well).

When needed, plasma membrane was stained using Alexa 488-coupled wheat germ agglutinin (WGA; 2.5 $\mu\text{g/ml}$, 10 minutes at 37°C) prior to cell fixation.

Cells were washed in PBS and fixed in 4% paraformaldehyde (20 minutes). Samples were then blocked with 1.2 % gelatin, 0.1 % Triton X100, 0.2 % glycine, 10 % donkey serum (in PBS, 30-60 minutes at room temperature). Cells were then washed thrice with 1.2 % gelatin in PBS and exposed to the primary antibody at appropriate dilution in 1.2 % gelatin 0.1 % Triton X100 in PBS (see Table 4; 12 hours at 4°C). After three washes in PBS-gelatin, fluorescent protein-coupled secondary antibody was added at 1:2,000 dilution for 1 hour in 1.2 % gelatin 0.1 % Triton X100 in PBS (anti-mouse or anti-rabbit coupled to Alexa 488, Alexa 546, Alexa 594, Alexa 633 or Cy5; Life Technologies).

For flow cytometry analysis, cells were placed in 500 μl PBS and analyzed using a CyAn™ ADP (Beckman Coulter) analyzer or a LSRFortessa™ (BD) analyzer.

For confocal microscopy, nuclei were stained using DAPI or Hoechst 33342 (5 minutes, 0.5 $\mu\text{g/ml}$) and slides were mounted in Glycergel® (Dako, Agilent) or Vectashield® (Vector Laboratories). Slides were analyzed using a Zeiss LSM 700 confocal microscope.

b. Specific protocol for S1R

To study the S1R, we used a specific protocol adapted from Hayashi et al. 2011.

Cells were washed and fixed as previously described (see section IV.2.a.). Samples were then permeabilized with 0.1 % NP-40 (in PBS; 10 minutes). The free PFA was quenched with a 10 mM glycine solution (in PBS, pH 7.2; 10 minutes). This was followed by antigen retrieval using 6 M urea (in 0.1 M Tris, pH 9.5; 10 minutes at 80°C). After this step, the sample was blocked in 10 % milk (in PBS, 1 hour). After PBS washes, the sample was exposed to the primary antibody targeting the S1R at 1:500 dilution, prepared in 0.2 % BSA (in TBST (Tris-buffered saline with Tween 20; 25 mM Tris base, 137 mM NaCl, 3 mM KCl, 0.05% Tween 20, pH 7.4), 12 hours at 4°C). The sample was then washed three times (TBST, 10 minutes) and exposed to the secondary antibody targeting coupled with a fluorescent protein (see section IV.2.a.).

The samples were then prepared for confocal microscopy as described above (see section IV.2.a.).

Antigen	Species	Technique	Dilution	Size (kDa)	Supplier	Reference
<i>AR</i>	Rabbit	WB	1:400	110	Santa Cruz	sc-816
<i>β-actin</i>	Rabbit	WB	1:2,000	42	Sigma	A-2066
<i>Calnexin</i>	Mouse	WB	1:2,000	90	Millipore	MAB3126
<i>CBP</i>	Rabbit	IF	1:50	-	Santa Cruz	discontinued
<i>CD44-FITC</i>	Mouse	Flow Cy	1:500	-	Immunotools	21810443
<i>GAPDH</i>	Mouse	WB	1:2,000	36	Santa Cruz	ab8245
<i>Ki67</i>	Rabbit	IF	1:50	-	Abcam	ab15580
<i>Ki67</i>	Mouse	IHC	1:100	-	Dako	MIB-1
<i>Ki67-Alexa488</i>	Rabbit	Flow Cy	1:50	-	Abcam	ab197234
<i>Melan A</i>	Mouse	IF	1:50	-	Santa Cruz	sc-20032
<i>NFATc1</i>	Rabbit	IF	1:100	-	Abcam	ab25916
<i>NFATc3</i>	Mouse	IF	1:50	-	Abcam	ab219063
<i>Orai1</i>	Rabbit	WB	1:500	35	Alomone	ACC-060
<i>Orai1</i>	Mouse	IF	1:500	-	OriGene	TA320060
<i>Orai1</i>	Mouse	Flow cy	1:100	-	OriGene	TA320060
<i>PCNA</i>	Mouse	WB	1:500	30	Santa Cruz	sc-56
<i>PSA</i>	Mouse	WB	1:500	28	Santa Cruz	sc-69664
<i>PSA</i>	Rabbit	IHC	1:500	-	Dako	A0562
<i>STIM1</i>	Mouse	WB	1:1,000	80	Alomone	ACC-063
<i>S1R</i>	Mouse	WB	1:500	25	Santa Cruz	sc-137075
<i>S1R</i>	Mouse	IF/IHC	1:500	-	Santa Cruz	sc-166392

Table 4: List of antibodies used for western blot (WB), immunofluorescence (IF), immunohistochemistry (IHC) or flow cytometry (Flow Cy)

V. Functional studies

In this section, we will describe the different techniques used to functionally characterize our models.

First, we studied the activity of calcium channels with two complementary techniques, patch-clamp and calcium imaging.

We used confocal microscopy to study the dynamic subcellular localization of target proteins. The FRET-derived TD-FLIM imaging technique allowed us to analyze protein-protein interactions.

We then used different techniques to study cell physiology. First, we assessed cell viability, proliferation and cell death with specific assays and flow cytometry. We also evaluated the migration potential of our cells with the random migration assay.

Finally, we performed *in vivo* experiments to assess the tumorigenic potential of our models.

1. Calcium signaling

We used two different techniques to study the activity of calcium channels in our cells.

First, the electrophysiology technique of patch-clamp in its whole-cell configuration allowed us to record the current generated by our channels of interest.

We also performed calcium imaging using a ratiometric Ca^{2+} dye allowing us to measure cytosolic calcium levels.

a. Patch-clamp

The patch clamp technique was used to record transmembrane ion currents (Neher and Sakmann 1976). Generally speaking, this technique consists in applying a glass (borosilicate, World Precision Instruments) pipette (with a diameter in the micrometer range) to the surface of a cell using a MP-225 micromanipulator (Sutter Instruments). The pipettes (2-5 M Ω resistance) were obtained with a pipette puller (P-97, Sutter Instrument Company) and polished using a microforge (MF-900, Narishige, World Precision Instruments). After establishing a contact between the cell and the micropipette, a slight negative pressure is applied with an air pressure/vacuum application system connected to the pipette holder in order to electrically isolate a fragment (patch) of membrane in the pipette. The vacuum is maintained until a tight contact (or seal) is obtained between pipette and cell membrane. This process is monitored using a patch-clamp set-up (PC-9 amplifier, Heka Elektronik) and the Heka Pulse software, following pipette resistance as a reflection of the quality of this contact. When resistance was in the giga ohm order (G Ω), the contact (qualified as a giga seal), was considered as good enough to proceed with the next step consisting in “breaking” plasma membrane through short applications of negative pressure. We thus reach the “whole cell” configuration, allowing us to record the activity of all channels located in plasma membrane (illustrated in [Figure 4](#)).

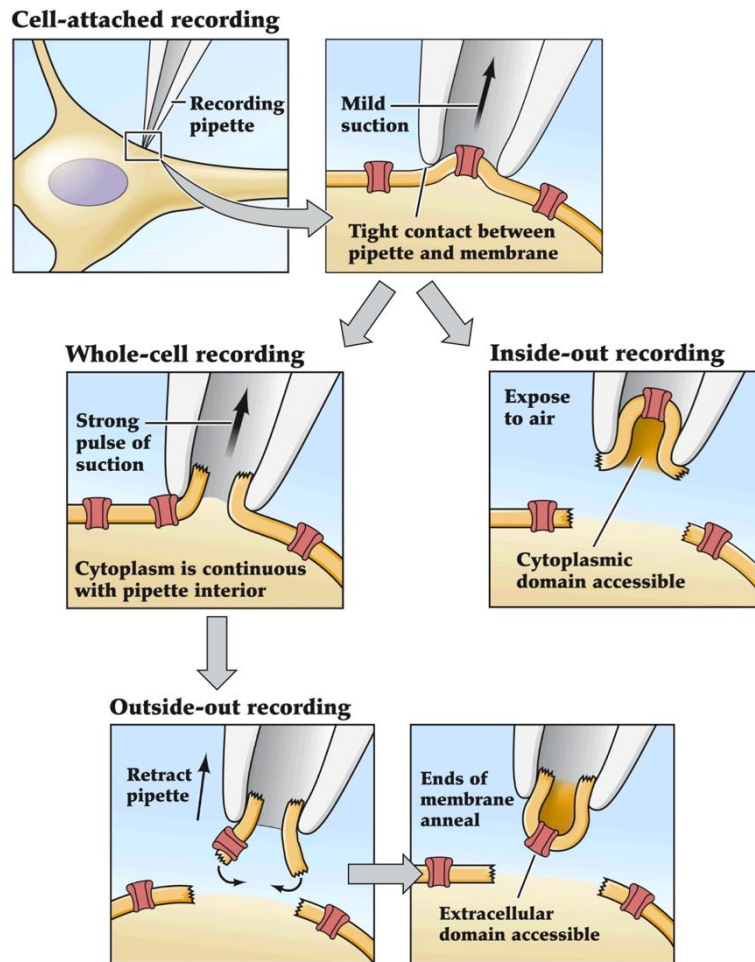


Figure 4: Schematic representation of the four main patch-clamp configurations
Adapted from Augustine et al., 2015

Membrane potential was clamped at 0 mV in all our experiments, and cells were subjected to voltage ramps ranging from -100 mV to +100 mV every 2 seconds for SOC recordings, and every 5 seconds for TRPV6/TRPM8 recordings. Time courses of current amplitude were thus generated, and corresponding figures are presented in the manuscript at -100 mV for SOC and TRPV6, and at +100 mV for TRPM8. At the end of each recording, cell capacitance was determined using the built-in Cslow compensation function of Heka Pulse software, and currents were normalized as to be expressed as current density (pA/pF).

For patch-clamp experiments, cells were plated in 35 mm dishes (Nunc), and the solutions we used are presented below, in Table 5 and Table 6.

	SOC	TRPV6	TRPM8
<i>CsCl</i>	150 mM	150 mM	150 mM
<i>BAPTA</i>	10 mM	10 mM	
<i>EGTA</i>			8 mM
<i>HEPES</i>	10 mM	10 mM	10 mM
<i>CaCl₂</i>			4 mM
<i>MgCl₂</i>	6 mM	6 mM	1 mM

Table 5: Composition of the intracellular solutions used during patch-clamp experiments

We adjusted the pH at 7.2 with CsOH, and the osmolarity at 290 mOsmol with D-mannitol.

	SOC	TRPV6 A	TRPV6 B	TRPM8
<i>NaCl</i>	150 mM	150 mM	150 mM	150 mM
<i>KCl</i>	5 mM	5 mM	5 mM	5 mM
<i>HEPES</i>	10 mM	10 mM	10 mM	10 mM
<i>EDTA</i>			100 μ M	
<i>Glucose</i>	10 mM	10 mM	10 mM	10 mM
<i>CaCl₂</i>	10 mM	10 mM	0 mM	2 mM
<i>MgCl₂</i>				1 mM
<i>TEA-Cl</i>	10 mM	10 mM	10 mM	10 mM

Table 6: Composition of the extracellular solutions used during patch-clamp experiments

We adjusted the pH at 7.3 with NaOH and the osmolarity at 320 mOsmol with D-mannitol.

For TRPV6 recordings, we used two distinct solutions: a solution with 10 mM CaCl_2 (solution A) to follow Ca^{2+} entry in the cells, and a divalent free solution (DVF, solution B) allowing Na^+ to permeate TRPV6 and leading to bigger currents.

b. Calcium imaging

Cytosolic calcium content was monitored using the calcium imaging technique with the ratiometric Ca^{2+} dye Fura2-AM (Interchim). Fura2 is coupled with acetoxymethyl ester (AM) groups allowing the dye to enter the cells. The dye is then retained within the cytoplasm after the AM group is cleaved by endogenous esterases.

Fura2 is composed by a fluorophore coupled to a Ca^{2+} -chelating structure derived from EGTA. This indicator emits at 510 nm, but it has two different excitation wavelengths depending on its bound or unbound state: unbound Fura2 is excited at 380 nm whereas Ca^{2+} -bound Fura2 is excited at 340 nm. Thus, the ratio between the fluorescence recorded after sequential excitation at 340 nm and 380 nm (F_{340}/F_{380}) allows us to monitor cytoplasmic Ca^{2+} variations.

Cells were plated on 30 mm diameter coverslips (VWR) and incubated with Fura2-AM (2 μ M, in the culture medium, for 45 minutes). Fura2-loaded cells were then washed twice and placed in an extracellular solution of the following composition (in mM) : 150 NaCl, 5 KCl, 10 HEPES, 10 glucose, 1 MgCl_2 , 2 CaCl_2). Cells were then washed and placed in a calcium-free extracellular solution.

Experiments were performed with an inverted microscope (Nikon Eclipse Ti) coupled to a DG4 illumination system (Sutter Instruments), a charge-coupled device (CCD) camera (QImaging). Experiments were monitored with the Metafluor Imaging System (Molecular Devices). Results are shown as the F_{340}/F_{380} ratio representing intracellular calcium contents.

2. *Confocal microscopy*

We performed dynamic confocal studies to study S1R localization and NFAT nuclear translocation. We also used the imaging technique of TD-FLIM to study direct interactions between our proteins of interest.

Prior to confocal imaging experiments, cells were plated on FluoroDish™ (World Precision Instruments).

a. Dynamics (S1R/NFAT)

The dynamic confocal studies were carried out by Dr Dmitri Gordienko. To do so, experimental chambers with the cells were placed on the stage of Axiovert 200M inverted microscope attached to an LSM 510 META laser-scanning unit (Zeiss). The confocal microscope was assisted by the LSM 510 software (Zeiss). During time series protocol, the x-y confocal images were acquired at 0.1–0.5 Hz using a Zeiss plan-Apochromat 40x 1.3 NA (numerical aperture) or 63x 1.4 NA oil-immersion objectives. The illumination intensity was attenuated to 0.5-6 % (depending on the laser line) with an acousto-optical tunable filter (Zeiss). To optimize signal quality the pinhole was set to provide a confocal optical section 0.5–1.8 μm , depending on experimental protocol. To avoid any bleed-through of the fluorescence signal in multi-staining experiments, fluorochromes with well separated excitation and emission spectra were used and imaging was performed using the frame-by-frame multitrack mode of the confocal scanner: sequential acquisition via well-separated optical channels of the x-y images produced by fluorescence of different fluorochromes. The photomultiplier gain and offset in each optical channel were set individually to achieve similar signal intensity at each channel and remove sub-signal noise from the images.

For some experiments, plasma membrane was stained with the CellMask™ Deep Red (Invitrogen™) according to manufacturer's instructions. When needed, cytoplasmic calcium contents were monitored with Cal-590.

b. Time domain – fluorescence lifetime-imaging microscopy (TD-FLIM)

We used the Förster resonance energy transfer (FRET)-based imaging technique of TD-FLIM (time domain – fluorescence-lifetime imaging microscopy) to study protein-protein interactions. These experiments were carried out in collaboration with Dr Alessandro Furlan and Dr Laurent Hélot from the PhLAM laboratory (Physique des Lasers, Atomes et Molécules, Lille).

This technique is based on the FRET principle of energy transfer between two fluorophores in close proximity with spectral overlap. Its high dependence on distance (FRET only occurs at 2-10 nm of distance) makes it a widely used technique to study protein-protein interactions.

Classically, FRET is performed with a CFP/YFP (cyan fluorescent protein and yellow fluorescent protein) pair which has a good spectral overlap as pictured in Figure 5: the emission of the CFP overlaps with the absorption of the YFP. In this context, if the two proteins are in close proximity, the donor (CFP) emission is transferred to the acceptor (YFP). To study interactions between two proteins of interest, each of the FP is fused to one of the protein. For our experiments, we used a modified CFP/YFP pair with enhanced fluorescent properties: mTurquoise and super YFP. We fused the fluorescent protein (FP) to our protein of interest, separating the two with a small linker allowing for FP movement, using the pVLL (variable length linker) plasmid (Bidaux et al. 2018b).

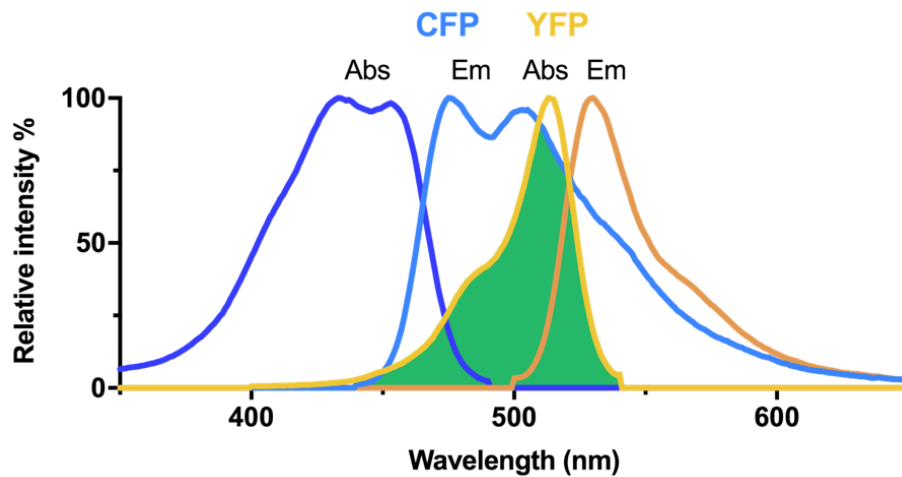


Figure 5: CFP and YFP spectra

Absorbance (Abs) and emission (Em) spectra of CFP (blue) and YFP (yellow). The spectral overlap between the two FP is shown in green.

There are different ways to record FRET efficiency: intensity and lifetime. We used the FLIM-FRET lifetime-based method that allows for a more accurate measurement avoiding FP bleed-through. Moreover, this technique is independent of donor concentration. The fluorescence lifetime is the average time the FP remains in the excited S1 state before returning to the S0 ground state. Fluorescence lifetime is an intrinsic characteristic of the FP, independent of its concentration and dependent on the molecular environment. Thus, when FRET occurs the fluorescence lifetime of the donor will be shortened. To perform these experiments, we used the time-domain FLIM method, TD-FLIM, in which the sample is excited by a pulsed laser and the fluorescence decay is recorded by high-speed detectors.

FLIM was performed with an A1 Nikon confocal head (Nikon Instruments) mounted on an inverted microscope (Nikon Eclipse Ti). A pulsed diode laser (PDL) 800-B (PicoQuant GMBH), delivered 20 MHz repetitive rate pulses at 405 nm. The confocal pinhole was set to 1 Airy, for a 0.921 μm optical slice. Single photons originating from the illuminated voxel were collected through a 40x 1.25 NA water-immersion objective and detected through a 483/32 single-bandpass filter (Semrock) on single photon avalanche photodiodes (SPAD) (PDM Series; PicoQuant GMBH). Arrival time of single photons was measured with a time-correlated single photon counting

(TCSPC) card (HydraHarp 400; Picoquant GMBH). Image size was setup to 128 x 128 pixels. Data were acquired using both SymPhoTime software (PicoQuant GMBH) and NIS software (Nikon Instruments). Since the statistical determination of the distribution of single photon arrival times requires a minimum of 100 photons per pixel which was reached in about 120 frames, therefore 120 frames were acquired at 2 Hz for each TCSPC recording.

3. *Cell viability and proliferation*

Cell viability and proliferation was assessed by a colorimetric cell viability assay coupled to cell counting.

We used the MTS (3-(4,5-dimethylthiazol-2-yl)-5-(3-carboxymethoxyphenyl)-2-(4-sulfophenyl)-2H-tetrazolium) assay based on a tetrazolium salt that is processed into a formazan dye soluble in culture media by mitochondrial oxidoreductases in metabolically active cells. This reaction needs the presence of phenazine methosulfate (PMS), that will act as an electron acceptor. To perform the experiment, we used the CellTiter 96® AQueous MTS reagent powder (Promega) and PMS powder (Sigma), prepared according to manufacturer's instructions. Cells were plated on transparent 96-well plates (TPP), with 6 to 12 wells per condition. The MTS/PMS mix was added directly into the medium and cells were incubated for 90 minutes, at 37°C, in the dark. We then measured the absorbance at 490 nm with a TriStar² LB 942 microplate reader (Berthold) after thorough homogenization. Values were normalized with the absorbance of cell-free wells containing culture medium incubated with the MTS/PMS mix.

The results obtained with the MTS assay were validated with cell counting (described in section I.3.).

4. *Cell cycle*

We studied cell cycle using different staining methods coupled with flow cytometry analysis. First, PI allowed us to have a first reading of cell cycle and cell death. We then coupled this staining with ki67 immunodetection to identify the quiescent cells. Finally, the EdU assay allowed to specifically detect the cells in the S phase of the cell cycle.

a. Propidium iodide

Propidium iodide (PI) is a membrane-impermeable DNA dye used to evaluate cell DNA content. This intercalating agent binds DNA at the concentration of one molecule every 4-5 base pair, allowing the separation of the cells in 4 phases according to their DNA content:

- subG1 (sub-gap 1): fragmented DNA (<2n DNA). Represents necrotic or apoptotic cells.
- G0/G1 (gap 0, gap 1): 2n DNA content. Represent the quiescent state (G0) or the first step of cell division before DNA replication (G1).
- S (synthesis): between 2n and 4n DNA. Represents the phase of DNA replication.
- G2/M (gap 2, mitosis): 4n DNA. Represents the final steps of the cell cycle.

PI staining thus allowed us to analyze cell cycle, and to evaluate cell death by the amount of fragmented DNA represented by the subG1 subset.

To perform the experiment, cells were dissociated and washed in PBS. Cells were then resuspended in 50-100 μ l PBS and fixed in 70% ice-cold ethanol (30 minutes, -20°C). Fixed cells were washed in PBS and treated with 1:500 RNase Cocktail™ Enzyme Mix (15 min; 1 U ribonuclease A, 40 U ribonuclease T1) for 15 minutes to remove RNA that PI is also able to bind. Cells were then stained with 50 $\mu\text{g}/\text{ml}$ PI for 30 minutes and analyzed by flow cytometry using a CyAn™ ADP (Beckman Coulter) analyzer or a LSRFortessa™ (BD) analyzer. Cells were gated on singlets to avoid any misinterpretation in DNA content due to cell aggregates.

b. PI-ki67 double staining

The PI staining alone does not allow the specific identification of quiescent cells. To identify this subset, we counterstained the cells with an antibody targeting the ki67, a protein specifically expressed during cell proliferation. This double staining allowed us to separate the cells in the G0 quiescent phase from the cells in the first step of the cell cycle preceding DNA replication (G1). Cells were prepared and fixed as previously described (see section V.4.a) and stained with an Alexa488-coupled ki67 antibody (see Table 4). Cells were then prepared for PI staining and analyzed by flow cytometry as described above (see section V.4.a).

c. EdU assay

As stated above, the PI staining does not allow a precise separation of cells between the different phases of the cell cycle. To have a better reading of the cell cycle, we used the EdU (5-ethynyl-2'-deoxyuridine) assay. EdU is a thymidine analog that is incorporated in newly synthesized DNA during the replication phase of the cell cycle (S phase). This method is an improved version of the BrdU assay (5-bromo-2'-deoxyuridine) allowing for easier and faster detection of proliferating cells. We used the Click-iT™ EdU Alexa Fluor™ 647 assay kit (Invitrogen™, ThermoFisher Scientific) based on click chemistry. The counterstaining with PI allows the separation between the different phases of cell cycle as described previously, with a more precise detection of the S phase by EdU. EdU incubation conditions were adjusted as follows: 5×10^5 cells per sample; 3 hours for PC3 cells and 4 hours for LNCaP cells. Cells were then fixed with ethanol as previously described (see section V.4.a) and Click reaction was performed according to manufacturer's instructions. Cells were then subjected to PI counterstaining when needed and analyzed by flow cytometry as previously described (see section V.4.a).

5. NFAT-Luciferase assay

In order to assess NFAT activity, we transfected our cells with the luc2P-NFAT-RE plasmid (see section II.2.). This construct is composed of the luciferase gene preceded by an NFAT response element. Thus, luciferase expression is proportional to NFAT activity in transfected cells. Luciferase activity was assessed 48 hours after transfection by the Luciferase Assay System

(Promega), according to manufacturer's instructions with a TriStar² LB 942 microplate reader (Berthold).

6. Apoptosis

Morphonuclear analysis allowed us to detect apoptotic cells with characteristic fragmented nucleus. We stained the nuclei with Hoechst 33342, a cell permeable DNA dye that binds the minor grooves of DNA with a higher affinity for adenine and thymine-rich regions.

Cells were fixed on microscopy slides in cold methanol for 20 minutes (-20°C), rinsed and stained with Hoechst 33342 (0.5 µg/ml in PBS, 20 minutes; InvitrogenTM, ThermoFisher Scientific). The slides were then mounted in Glycergel® (Dako, Agilent).

Samples were observed using a DMI8 (Leica) inverted microscope. We analyzed five random fields per condition using the Cell counter feature of ImageJ software (NIH) (Schneider et al. 2012).

7. Cell migration

We used random cell migration to study the effect of S1R on cell migration. With this technique, cells are plated at low density and followed with videomicroscopy.

Cells were plated at low density (10⁴ cells/well) in 1 % gelatin-coated 24-well plates 24 hours before the experiment. The plate was then placed in a videomicroscope (Eclipse Ti-E, Nikon) equipped with a cage incubator (Okolab) maintaining the temperature at 37°C with 5 % CO₂. We selected five positions at random in each well and acquired an image every 10 minute for 10 hours with an 10x objective.

Images were processed with the MtrackJ plugin (Meijering et al. 2012) on the ImageJ software (NIH) (Schneider et al. 2012). We only analyzed individual cells which stayed within the acquisition field during the 10 hours without dividing.

8. In vivo studies

We performed sub-cutaneous xenografts in immunodeficient mice to assess tumorigenic potentials. These experiments were carried out with the help of Dr Yasmine Touil, and following guidelines validated by the local ethics committee. Tumor growth was measured twice a week and estimated in mm³ using the following formula:

$$\text{Tumor volume (mm}^3\text{)} = (\text{length} \times \text{width} \times \text{width}) / 2$$

Mice were sacrificed before tumors reached 10 % of the animal's weight. Tumors were then extracted and preserved for further analysis.

For our studies, we used two different experimental protocols.

a. Cancer stem cell validation

We used *in vivo* experiments to confirm the increased tumorigenicity of our subpopulations with stem-like properties. To do so, we injected a very low number of cells (10^3 cells per mice) in 6 weeks old Nod-SCID-Gamma mice (we used females for melanoma and males for prostate cancer cells; the mice model was developed by Jackson Laboratories and purchased from Charles River). After FACS (see section I.5), cells were prepared in 50 % Matrigel® basement membrane matrix growth factor reduced, phenol red free (Corning) and 50 % PBS, and injected sub-cutaneously in the right flank of the animal.

b. S1R

We performed xenografts experiments to study the role of the S1R in tumor growth. 24 hours after transfection with siRNA, LNCaP or PC3 cells were prepared in 50 % Matrigel® basement membrane matrix high concentration, phenol red free (Corning) and 50 % PBS, and injected (3×10^6 cells per mice for LNCaP; 10^6 cells per mice for PC3) in the right flank of male NMRI Nude mice (6-8 weeks old).

VI. Data analysis and statistics

All results are expressed as mean \pm SEM. Statistical significance was assessed using Student's *t* test. For multiple comparisons, we performed a one-way analysis of variance (ANOVA) with Turkey's test. A *p* value < 0.05 was considered as significant. *p* values are shown as: **p* <0.05 ; ***p* <0.01 ; ****p* <0.01 .

Figures and statistical analysis were done using the Graphpad Prism 7 software and the Origin 6.1 software (OriginLab Corporation).

Flow cytometry data were analyzed using the FlowJo v10 software (BD).

Results

1. Orai1/NFAT pathway is a gatekeeper of cancer cell quiescence/activation transition

Lucile Noyer, Pilar Flamenco*, Yasmine Touil*, Christian Slomianny, Pauline Ostyn, Dimitra Gkika, Raja El Machhour, Jerome Vandomme, Pascaline Segard, Fabien Vanden Abeele, Pierre Formstecher, Bruno Quesnel, Renata Polakowska#, Natalia Prevarskaya#, Loic Lemonnier#*

**Equal contribution*

#Shared co-senior authorship

Article in preparation

Despite the establishment of the crucial role played by cancer stem cells (CSCs) in cancer progression, the mechanisms controlling CSCs quiescence/activation states remain poorly understood. Our aim was therefore to investigate the potential involvement in these phenomena of calcium channels previously identified as key players in cancer progression.

Prostate cancer (PC3) and melanoma (HBL) cell lines were used to generate tumour mimicking spheres from which quiescent/slow cycling cells with CSCs properties were sorted by FACS. Control and CSC-like cells were then further characterized by RT-qPCR, immunofluorescence, confocal microscopy, calcium imaging and flow cytometry.

We present here initial evidence that calcium channel Orai1 expression is down-regulated in prostate cancer and melanoma subpopulations presenting CSC-like properties. The low level of Orai1 is functionally associated with a major decrease in store-operated calcium entry and cytosolic calcium concentration. This in turn down-regulates the Ca^{2+} -calcineurin-NFAT/CBP signalling pathway. Furthermore, we demonstrate that the impairment of Orai1 activity in non-stem cells effectively increases stemness-defining sphere-forming capacity and expansion of the stem cell-like pool in both prostate cancer and melanoma cell lines. We also show that Orai1 suppression endows CSC-like cells with a chemotherapy-resistant phenotype.

Our findings therefore uncover a previously unknown Ca^{2+} -dependent regulatory mechanism governing CSC reactivation, and potentially associated with their propagation and consequent cancer relapse.

1. Orai1 expression and function decrease in prostate cancer cells with stem-like properties

Stem cells are mostly quiescent and rarely divide, displaying a slow cycling profile. This property has allowed their characterization as label retaining cells (LRCs) (Pece et al. 2010). We used the androgen-resistant prostate cancer PC3 cell line, labelled with a vital Dil dye to distinguish quiescent LRCs from the cycling population. Cycling cells dilute this dye by half with each cell division. After 7 days of dilution, about 15 % of the population was still Dil-positive (see section I.5.b. of the Material and Methods). In conjunction with the Dil labelling technique, we also used CD44, a well-known cell surface marker of prostate CSCs, shown to be enriched in sphere-forming cells (Garraway et al. 2010; Patrawala et al. 2007). The double labelling and sphere-forming capacity ensured an accurate identification of quiescent and/or slow cycling prostate stem-like cells. We isolated a subpopulation of CD44^{hi}/Dil^{hi} prostate stem-like cells (2.9 ± 0.8 %) by sorting dissociated sphere cells (Figure 1A). As shown in Figure 1B, after 7 days of dilution, the remaining Dil-positive cells exhibit a decreased expression of epithelial differentiation markers such as vimentin and E-cadherin. Moreover, when injected in small number (10^3 cells) in immunodeficient mice, the Dil^{hi} subpopulation is more aggressive, as shown by a faster tumor growth than with Dil^{lo} cells (Figure 1C), and an increased mean tumor weight upon sacrifice (Figure 1D, $1,245 \pm 121.3$ mg vs 603.7 ± 32.36 mg). Taken together, our results show that the Dil^{hi} subpopulation presents CSC-like properties, namely slow cell cycling and increased tumorigenicity.

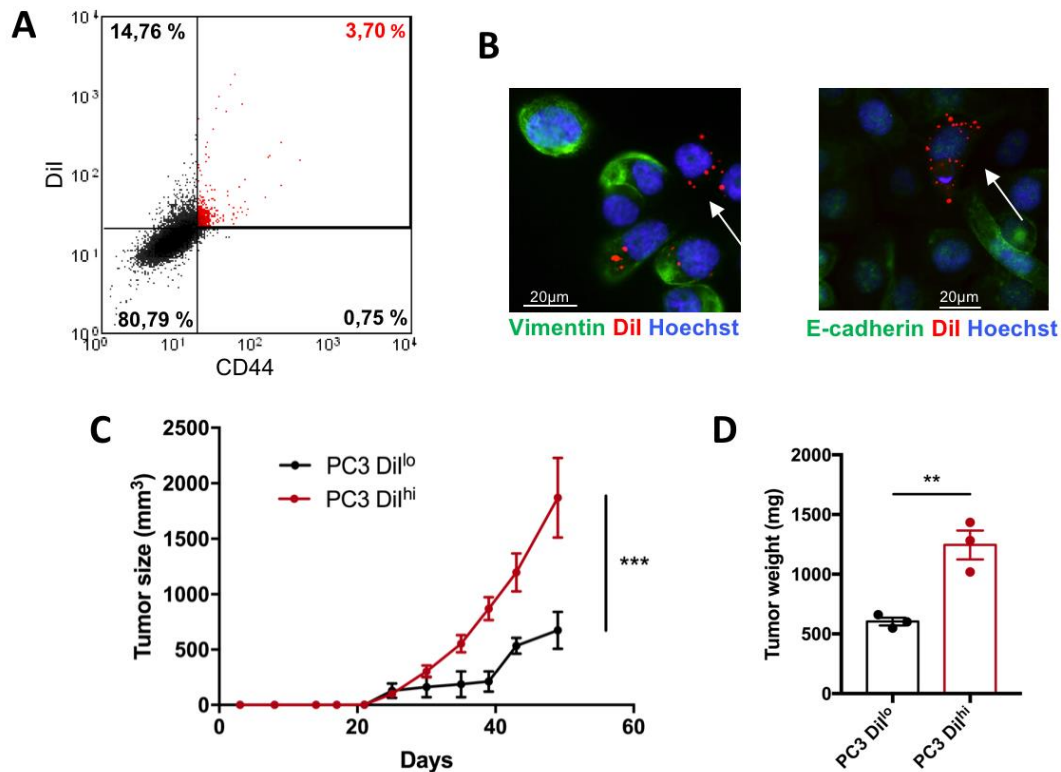


Figure 1: CD44-positive PC3 LRCs present stem-like properties

A. Two-color flow cytometry analysis of PC3 cells labelled with Dil and CD44 after 7 days of Dil dilution in spheres. The double positive population is shown in red. Representative image from 7 independent experiments. **B.** Confocal microscopy of PC3 total population after 7 days of Dil dilution in spheres. Shown are: Dil fluorescence (red) and immunofluorescence (green) with anti-Vimentin (left) or anti-E-cadherin (right) antibodies, nuclei were stained with Hoechst 33342 (blue). Scale bar: 20 μm. Representative images. **C, D.** Kinetics of tumor growth in male NSG mice injected (s.c.) with Dil^{hi} or Dil^{lo} PC3 cells (3 mice per condition), and corresponding tumor weights upon sacrifice. **p<0.01; ***p<0.001

The importance of calcium in cell physiology has been clearly stated in many cellular models (Clapham 2007; Monteith et al. 2017), but not in stem cells. We used RT-qPCR to evaluate the expression of Orai1 and STIM1, the main components of the store-operated calcium entry in prostate cancer (Dubois et al. 2014). The analysis determined a 3-fold decrease in Orai1 expression in CD44^{hi}/Dil^{hi} CSC-like prostate cells when compared to the CD44^{lo}/Dil^{lo} major subpopulation (Figure 2A). Interestingly, this was associated with a 3-fold decrease in STIM1 expression. The difference in Orai1 expression was confirmed at protein level using immunofluorescence and confocal microscopy (Figure 2B).

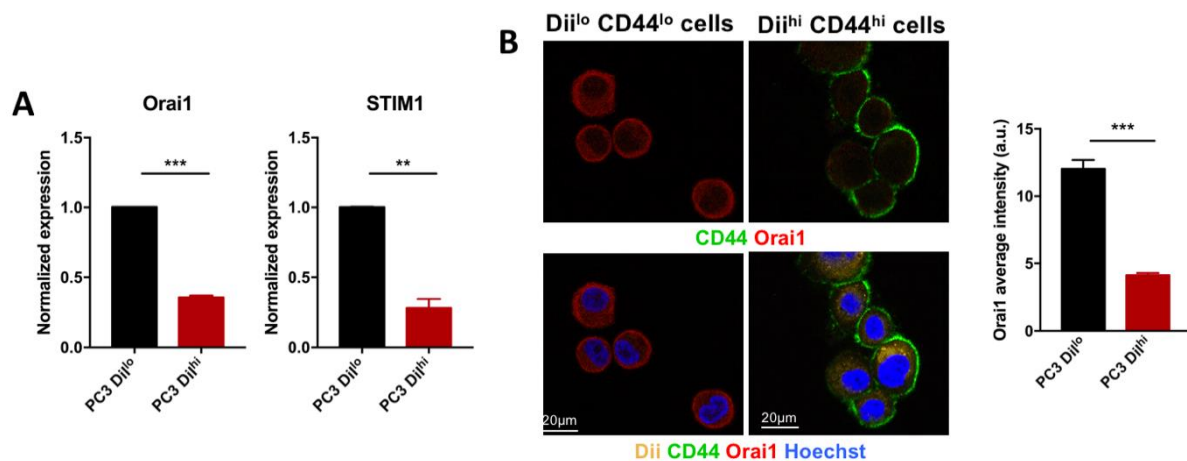


Figure 2: Orai1 expression is decreased in prostate cancer cells with stem-like properties

A. Real-time quantitative PCR showing the expression of Orai1 and STIM1 in PC3 Dil^{lo}/CD44^{lo} and PC3 Dil^{hi}/CD44^{hi} FACS-sorted subpopulations (n=3 and n=4 respectively). **B.** Confocal microscopy of PC3 cells. After 7 days of Dil dilution, cells were immuno-reacted with anti-CD44 antibody and then sorted. Shown are Dil fluorescence (orange) and indirect CD44 (green) and Orai1 (red) immunofluorescence, Hoechst 33342-stained nuclei are in blue. Scale bar: 20 μ m. Representative images of 4-6 fields from 3 independent experiments. Bars show the average \pm S.E.M of fluorescence intensities measured in PC3 cells. Data from three experiments. **p<0.01; ***p<0.001

The functional relevance of Orai1 and STIM1 expression decrease on store-operated calcium entry (SOCE) was examined using the calcium imaging technique (Kondratska et al. 2014). Values corresponding to the difference between the peak ratio and level before calcium add-back (referred to as ratio deltas) in non-stem (Dil^lo) and stem-like (Dil^hi) PC3 cells were respectively: 8.22 ± 0.28 and 5.97 ± 0.17 (Figure 3A). Summarized in Figure 3B, these data demonstrate that capacitative calcium entry in stem-like cells was significantly lower than in non-stem PC3 cells, a result associated with a significant decrease in basal calcium level (Figure 3C). Ratio values were: 1.28 ± 0.03 (Dil^lo) and 1.15 ± 0.02 (Dil^hi).

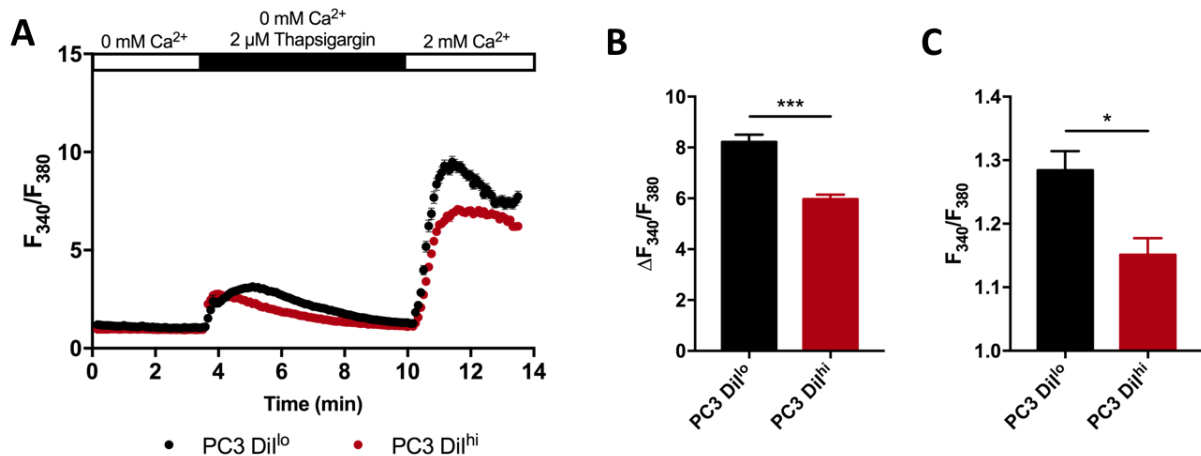


Figure 3: Orai1 function is decreased in prostate cancer cells with stem-like properties

A. Time course of cellular responses observed with calcium imaging technique. Thapsigargin and calcium add-backs are indicated by bars. **B.** Histogram summarizing deltas of ratio observed in A after calcium addition. **C.** Histogram presenting basal calcium levels in Dil^lo and Dil^hi PC3 cells as observed in A. *p < 0.05; ***p < 0.001.

2. *Orai1* expression and function are also down-regulated in melanoma cells with stem-like properties

To check whether low *Orai1*/calcium is restricted to prostate cancer stem-like cells, we used an unrelated model, melanoma. Our collaborators previously generated a Tet-ON controlled Histone 2B-GFP (H2B-GFP) fusion construct (Ostyn et al. 2014) (see section 1.5.a of the Material & Methods). We then labeled, isolated and characterized LRCs in this HBL melanoma cell line. After 7 days of dilution, the remaining GFP-positive cells (GFP^{hi}) show weak expression of the Melan A differentiation marker and Ki67 proliferation marker as compared to the GFP-negative cells (GFP^{lo}) (Figure 4A). Moreover, when injected in small number (10³ cells) in immunodeficient mice, the GFP^{hi} subpopulation displays a higher tumorigenic potential than the GFP^{lo}, as shown by the 2-fold increase in tumor growth (Figure 4B) and mean tumor weight upon sacrifice (Figure 4C, 753.8 ± 57.81 mg vs 353.9 ± 78.83 mg). Our results therefore show that the GFP^{hi} subpopulation presents stem-like properties, namely slow cell cycling and increased tumorigenicity.

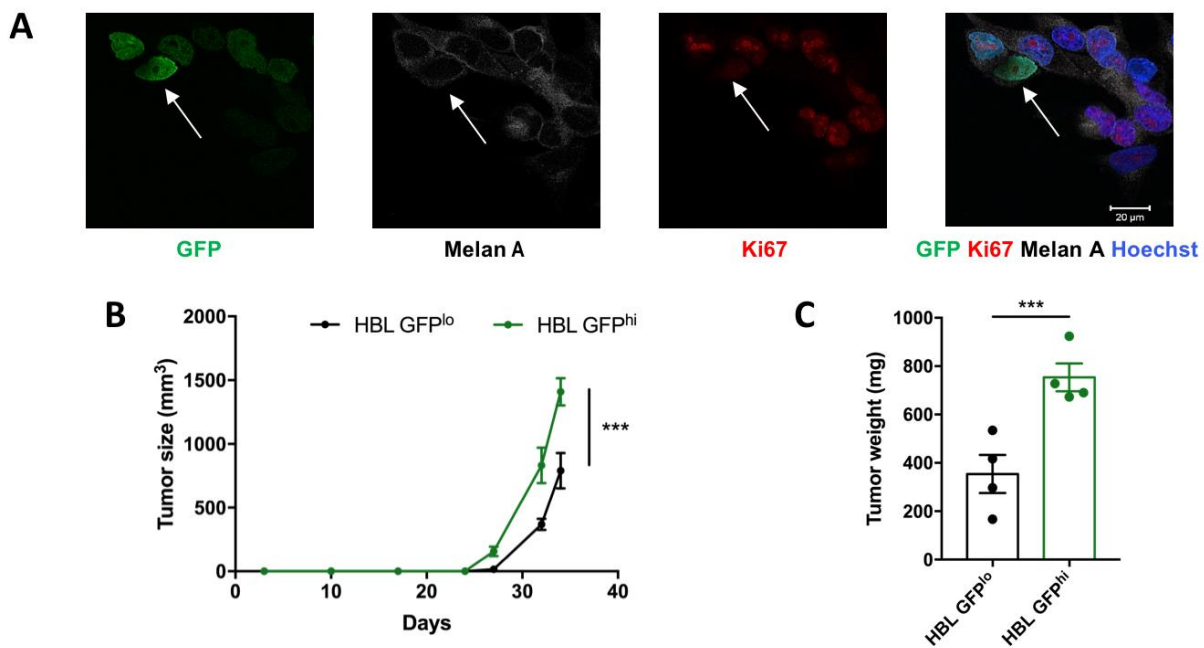


Figure 4: HBL LRCs present stem-like properties

A. Representative confocal microscopy images of HBL H2B-GFP total population after 7 days of GFP dilution in spheres. Shown are: H2B-GFP fluorescence (green) and immunofluorescence with anti-Melan A (white) and anti-Ki67 (red) antibodies, nuclei were stained with Hoechst 33342 (blue). Scale bar: 20 μm. **B, C.** Kinetics of tumor growth in female NSG mice injected (s.c.) with GFP^{hi} or GFP^{lo} HBL H2B-GFP cells (4 mice per condition), and corresponding tumor weights upon sacrifice. ***p < 0.001.

As in prostate cancer, RT-qPCR analysis showed a 3-fold lower Orai1 expression in the subpopulation of GFP^{hi} stem-like cells than in the GFP^{lo} non-stem major subpopulation (Figure 5A). This variation was specific to Orai1 transcript, since the expression of STIM1 did not differ between these two subpopulations. Confocal fluorescent immunocytochemistry (Figure 5B) confirmed that Orai1 expression was strongly decreased in the GFP^{hi} subpopulation as compared to GFP^{lo} cells.

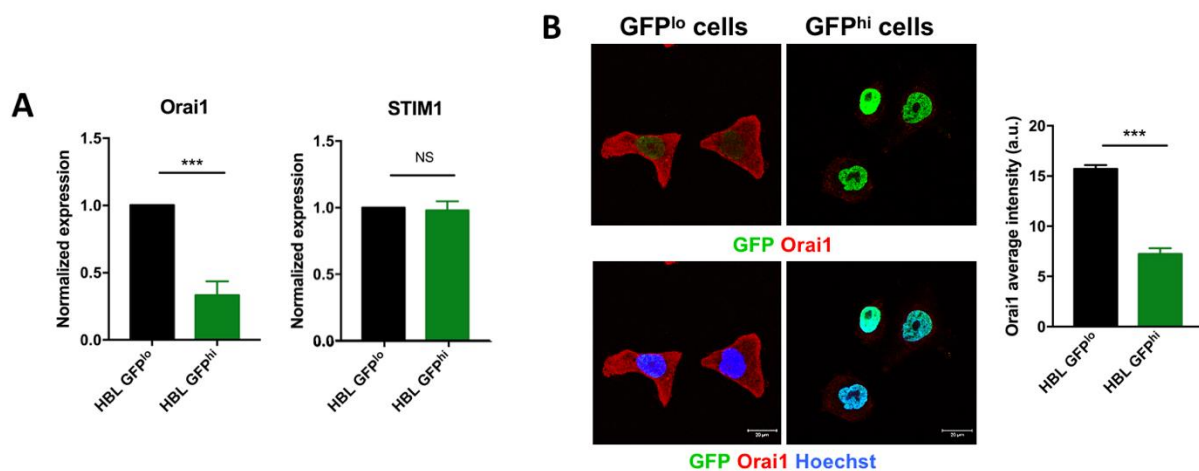


Figure 5: Orai1 expression is decreased in melanoma cells with stem-like properties

A. RT-qPCR showing relative expression of Orai1 and STIM1 in HBL GFP^{lo} and GFP^{hi} FACS-sorted subpopulations (n=8 and n=3 respectively). **B.** Confocal microscopy of HBL GFP^{lo} and GFP^{hi} cells. Sorted cells were immuno-reacted with anti-Orai1 antibody (red), H2B-GFP fluorescence is in green and Hoechst 33342-stained nuclei are in blue. Scale bar: 20 μ m. Representative images of 4-6 fields from 3 independent experiments. Bars show the average \pm S.E.M fluorescence intensities measured in cells from three independent experiments. *p<0.05; ***p<0.001.

As presented in [Figure 6A and 6B](#), GFP^{hi} HBL cells exhibited less SOCE than non-stem GFP^{lo} cells. Ratio deltas obtained during capacitative calcium entry in non-stem (GFP^{lo}) and stem-like (GFP^{hi}) HBL cells were respectively: 1.59 ± 0.12 , 1.11 ± 0.12 . In agreement with the observed decrease in SOCE, the GFP^{hi} HBL cells exhibited a small, albeit extremely significant, reduction in their basal calcium level when compared to GFP^{lo} cells ([Figure 6C](#)). Ratio values were: 1.205 ± 0.001 (GFP^{lo}) and 1.157 ± 0.001 (GFP^{hi}). Our results therefore associate melanoma stem-like phenotype with a general decrease in calcium level and Orai1 expression.

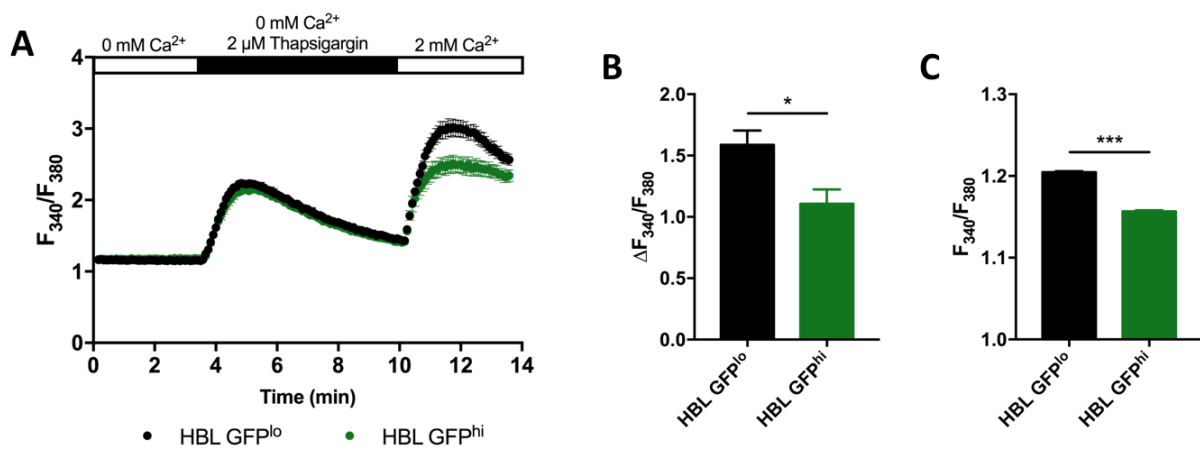


Figure 6: Orai1 function is decreased in melanoma cells with stem-like properties

A. Time course of calcium imaging in response to SERCA pump inhibitor thapsigargin in the absence of extracellular calcium. Thapsigargin and calcium add-backs are indicated by bars. **B.** Histogram summarizing deltas of ratio observed in **A** after calcium addition. **C.** Histogram presenting basal calcium levels in GFP^{lo} and GFP^{hi} HBL cells as observed in **A**. * $p < 0.05$; *** $p < 0.001$.

Taken together, our data indicate that a sub-population of cells exhibiting stem cell-like properties in two unrelated cancer models express low Orai1 levels and show a decrease in SOCE and basal calcium concentration.

3. *Orai1* is involved in SOCE in both non-stem and stem-like subpopulations

Although *Orai1* is generally accepted as being ubiquitously involved in SOCE, we used siRNA against this channel to confirm its importance in our models' SOCE.

As shown in **Figure 7A**, a 3-day treatment with *Orai1* siRNA (si*Orai1*) in non-stem PC3 cells significantly reduced SOCE when compared to cells treated with control siRNA (siLuc). Ratio deltas were: 8.22 ± 0.29 (siLuc) and 1.28 ± 0.16 (si*Orai1*). We obtained similar results in the PC3 stem-like subpopulation (**Figure 7B**), where ratio deltas were 5.99 ± 0.26 (siLuc) and 3.12 ± 0.19 (si*Orai1*). Those results, summarized in **Figure 7C**, confirm the importance of *Orai1* in the SOCE in prostate cancer as previously shown (Dubois et al. 2014), and indicate that the involvement of *Orai1* is maintained in the stem-like subpopulation.

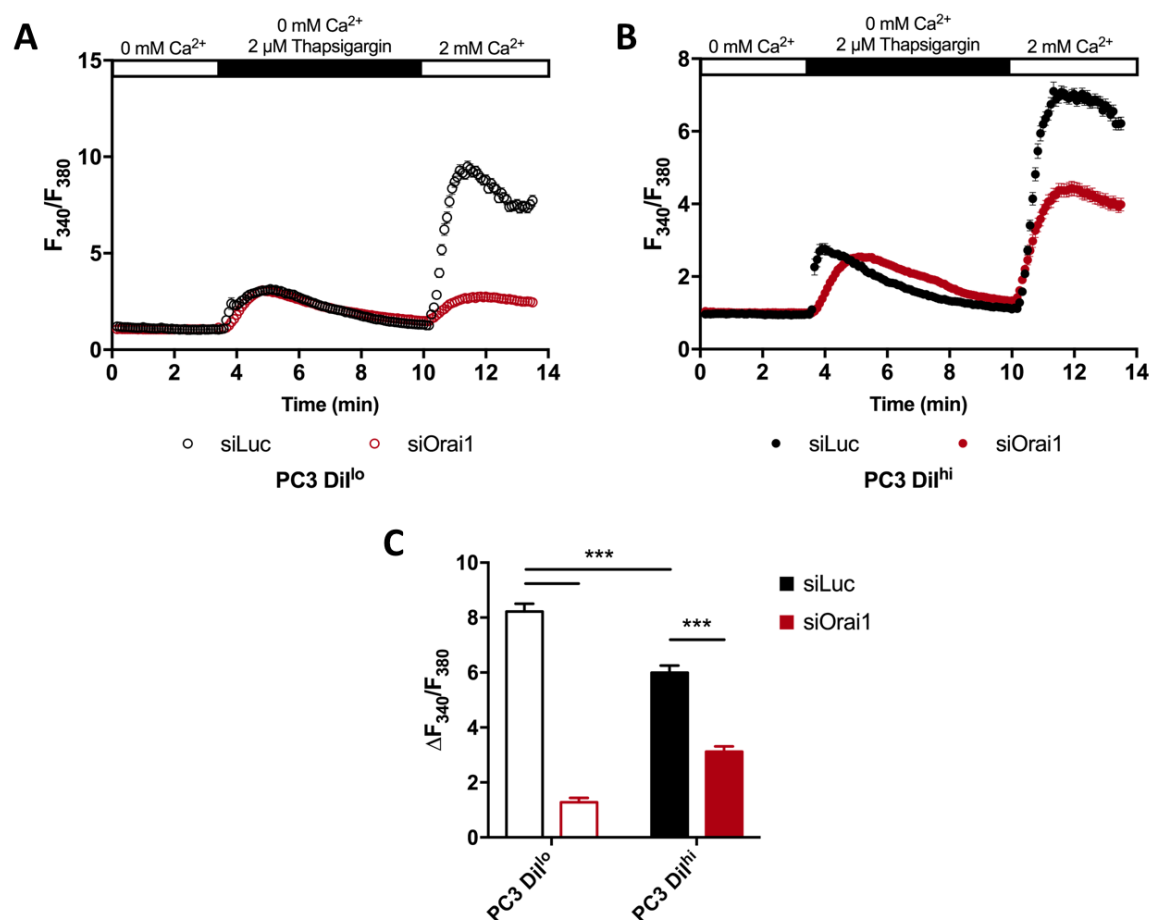


Figure 7: *Orai1* is a key actor in non-stem and stem-like PC3 cells SOCE

A, B. Time courses of calcium ratios after 3 days of treatment with siRNA targeting *Orai1* (si*Orai1*) or Luciferase (siLuc). Thapsigargin and calcium add-backs are indicated by bars. **C.** Histogram summarizing deltas of ratio observed in A and B after calcium addition. *** $p < 0.001$.

Although Orai1 implication in melanoma has been well documented (Stanisz et al. 2016; Umemura et al. 2014), no data were available about HBL cells. We therefore checked whether Orai1 was also a key actor of SOCE in this melanoma cell line. In the non-stem GFP^{lo} major subpopulation, siOrai1 significantly reduced SOCE (Figure 8A) with ratio deltas of 2.98 ± 0.27 (siLuc) and 1.39 ± 0.20 (siOrai1). We confirmed the involvement of Orai1 in the GFP^{hi} subpopulation as well (Figure 8B) with ratios of 1.85 ± 0.13 (siLuc) and 0.66 ± 0.07 (siOrai1). Our results, summarized in Figure 8C, confirm that Orai1 is a key element in SOCE in both stem-like and non-stem HBL cells.

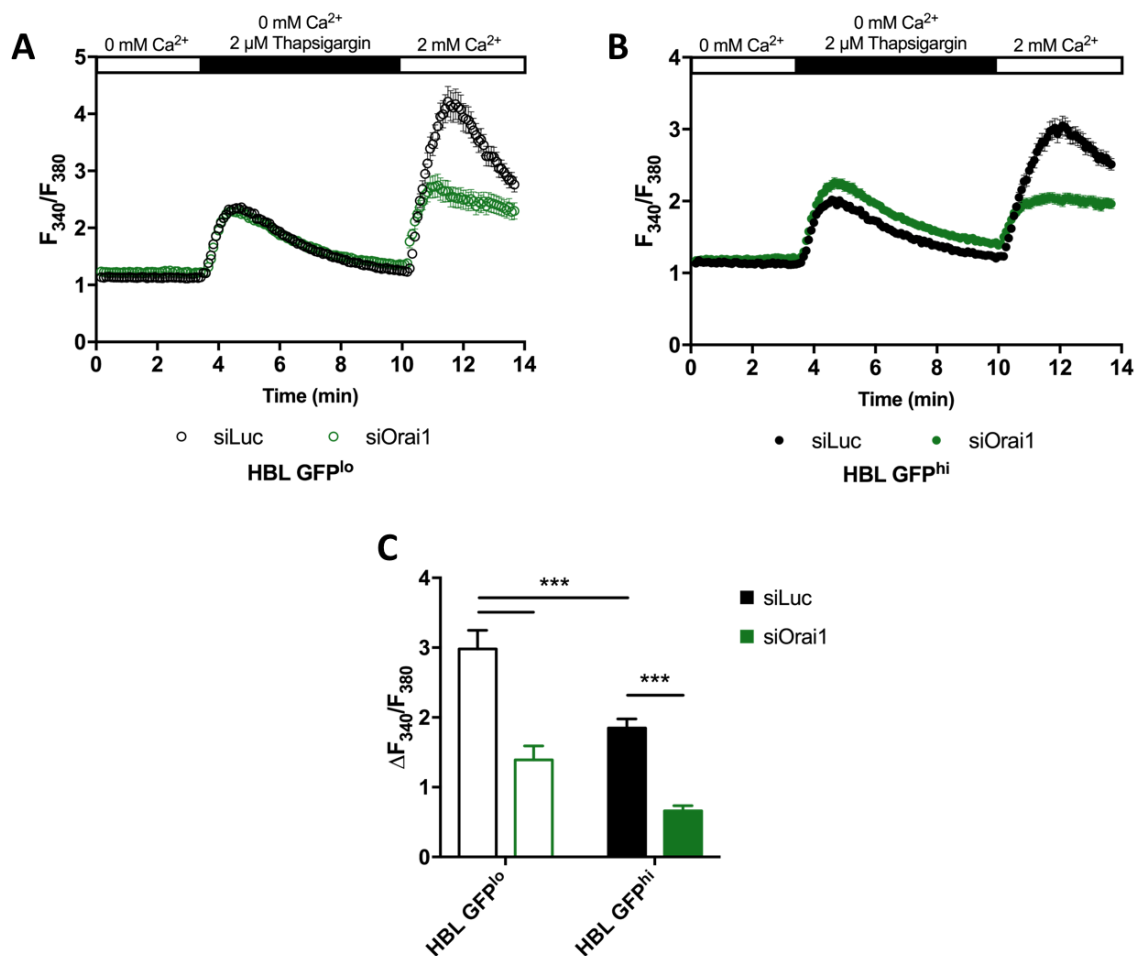


Figure 8: Orai1 is a key actor in HBL cells SOCE

A, B. Time courses of calcium ratios after 3 days of treatment with siRNA targeting Orai1 (siOrai1) or Luciferase (siLuc). Thapsigargin and calcium add-backs are indicated by bars. **C.** Histogram summarizing deltas of ratio observed in A and B after calcium addition. *** $p < 0.001$.

4. *Orai1* inhibition increases a pool of cells with stem-like properties

Having defined the involvement of *Orai1* in our models, we examined the effect of its inhibition on cell fate determination.

As shown in Figure 9A, the *Orai1* inhibitor BTP2 (10 μ M) almost completely abrogated SOCE in non-stem (Dil^{lo}) and stem-like (Dil^{hi}) prostate cancer cells with ratio deltas of 8.34 ± 0.77 vs 0.05 ± 0.10 for Dil^{lo} and 6.60 ± 0.34 and 0.05 ± 0.01 for Dil^{hi} . We then evaluated the effect of BTP2 during sphere formation. For this purpose, we labelled the PC3 cells with Dil and added 1 μ M of BTP2 in the medium during sphere formation. After 7 days of Dil dilution in sphere forming condition, flow cytometry analysis determined that BTP2 induces an increase in the size of the Dil^{hi} subpopulation (Figure 9B, 19.61 ± 0.5 % vs 17.08 ± 0.68 %). This suggests that the inhibition of *Orai1* increases the number of quiescent/slow cycling cells during sphere formation. Interestingly, spheres treated with BTP2 exhibited a significantly greater ability to form secondary spheres than control spheres (Figure 9C), thus confirming that a decrease in *Orai1* activity effectively raises the pool of stem-like prostate cancer cells.

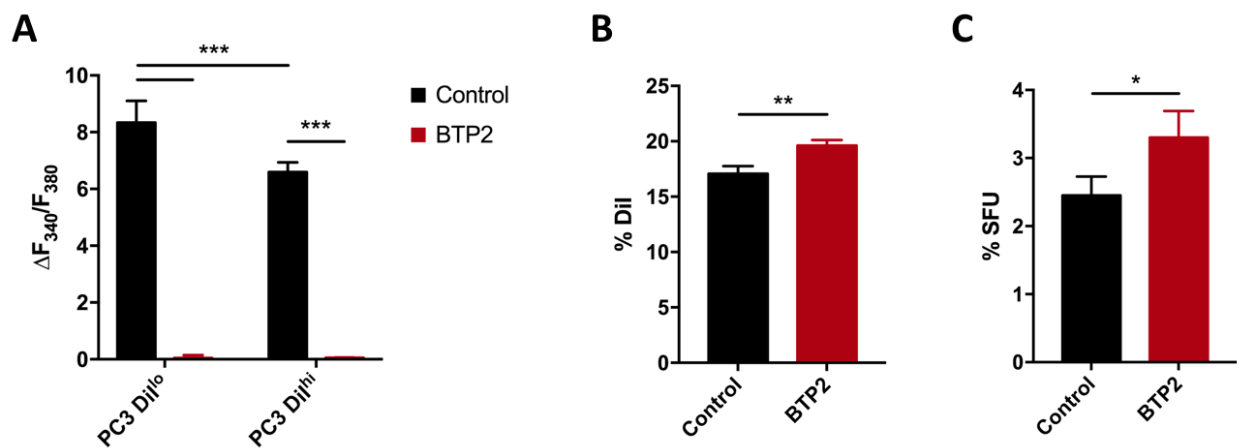


Figure 9: *Orai1* inhibition increases stemness in prostate cancer cells

A. Histograms summarizing deltas of calcium ratios observed in the presence or absence of 10 μ M BTP2 after calcium addition. **B.** Histogram showing the percentage of Dil positive cells after 7 days of sphere formation with or without 1 μ M BTP2 determined by flow cytometry (n=8). **C.** Quantification of SFU after 7 days of sphere formation with BTP2 or control. * $p < 0.05$; ** $p < 0.01$; *** $p < 0.001$.

Similarly, in HBL cells, BTP2 (10 μ M) strongly inhibited SOCE in both GFP^{lo} and GFP^{hi} subpopulations. Ratio deltas, summarized in Figure 10A, were as follows: 5.53 ± 0.21 (GFP^{lo} control), 0.06 ± 0.02 (GFP^{lo} BTP2); 1.76 ± 0.10 (GFP^{hi} ctrl), 0.18 ± 0.04 (GFP^{hi} BTP2). Subsequently to a 24-hour tetracycline-induction, BTP2 (1 μ M) was added to sphere cultures. After 7 days of GFP dilution in spheres, flow cytometry analysis showed that BTP2 increases the GFP^{hi} subpopulation as it was reported above for prostate cancer cells (Figure 10B, 14.56 ± 2.08 vs. 7.74 ± 1.04). We then confirmed those results by testing the secondary sphere forming capacities of treated cells. As expected, Orai1 inhibition led to an increased capacity to form second generation spheres (Figure 10C).

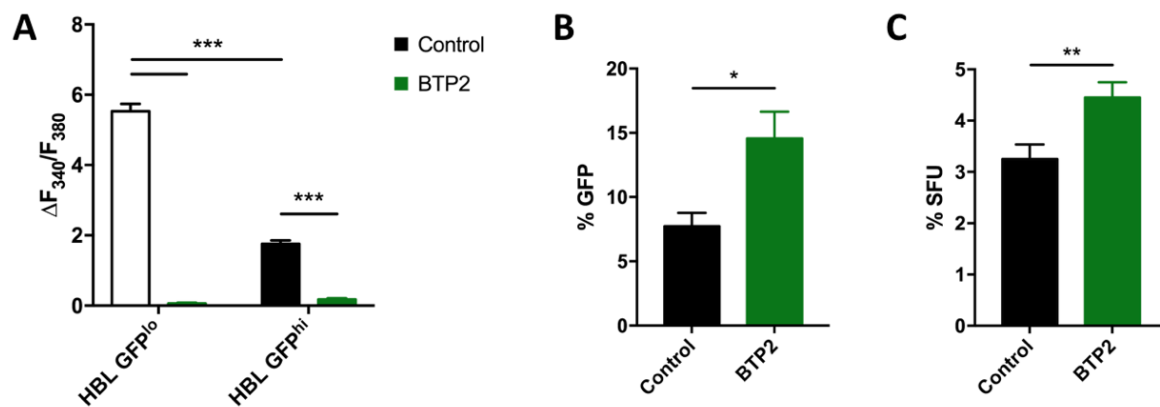


Figure 10: Orai1 inhibition increases stemness in melanoma cells

A. Histograms summarizing deltas of calcium ratios observed in the presence or absence of 10 μ M BTP2 after calcium addition. **B.** Histogram showing the percentage of GFP positive cells after 7 days of sphere formation with or without 1 μ M BTP2 determined by flow cytometry (n=8). **C.** Quantification of SFU after 7 days of sphere formation with BTP2 or control. *p<0.05; **p<0.01; ***p<0.001.

In summary, our results suggest that Orai1 plays a critical role in the control of SOCE in both melanoma and prostate cancer cells, and that low Orai1 expression level and activity are linked to a stem-like phenotype in both models.

5. *Orai1 regulates quiescence via calcineurin-NFAT modulation*

Our data suggest that Ca^{2+} entry via Orai1 controls the quiescence of a subpopulation of cells with stem-like properties by modulating SOCE. We have also shown that even in the absence of outside stimulation, stem-like cells have a lower level of basal calcium correlated to decreased Orai1 expression and activity. To explore the mechanistic relationship between Ca^{2+} , Orai1 and quiescence, we examined the calcineurin-NFAT pathway downstream of Orai1.

As shown in [Figures 11A and B](#), NFATc1, the major NFAT isoform in melanoma cells (Horsley et al. 2008; Levin-Gromiko et al. 2014), is predominantly located in the nucleus of proliferating HBL GFP^{lo} cells, while its distribution is homogenous throughout GFP^{hi} quiescent cells. When added to the medium during melanosphere formation, FK506, a calcineurin inhibitor that blocks NFAT nuclear translocation, augments the number of sphere forming units ([Figure 11C](#), 5.17 ± 0.42 % vs. 3.03 ± 0.25 %). This demonstrates the NFAT inactivation increases the pool and quiescence of melanoma stem-like cells.

We performed the same experiments on prostate cancer cells where NFATc3 is the predominant isoform (unpublished data). As previously observed with melanoma, NFAT inhibition during sphere formation led to an increased sphere forming capacity ([Figure 11D](#), 5.16 ± 0.63 % vs. 3.13 ± 0.40 %). These results show that the calcineurin-NFAT pathway is a key actor of quiescence/proliferation transition in both melanoma and prostate cancer cells.

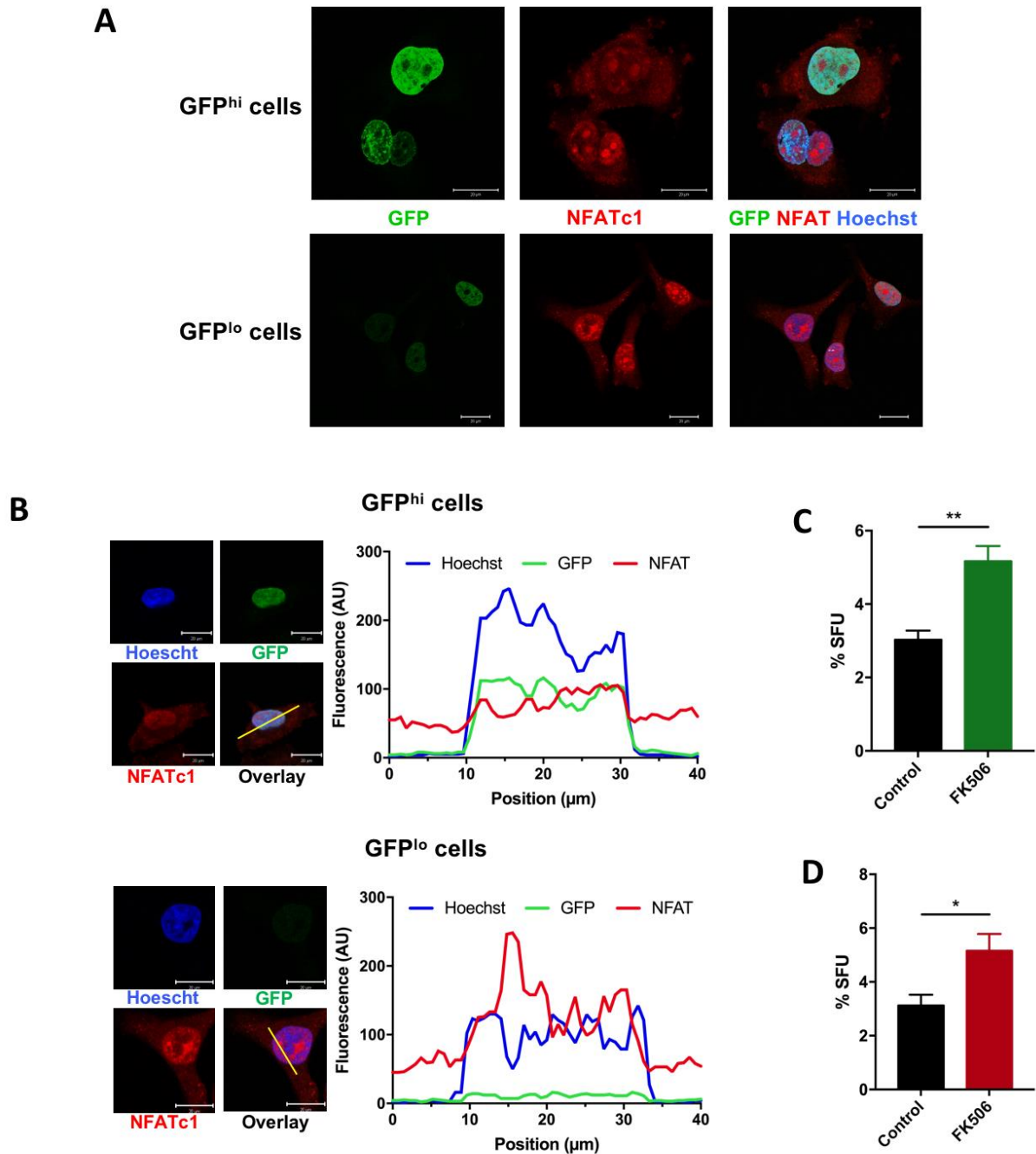


Figure 11: Orai1 regulates quiescence via calcineurin-NFAT modulation

A. Confocal microscopy of HBL GFP^{hi} and GFP^{lo} cells. Sorted cells were immuno-reacted with anti-NFATc1 antibody (red), nuclei were stained with Hoechst 33342 (blue), H2B-GFP fluorescence is shown in green. Representative images of 4-6 fields from 3 independent experiments. **B.** Representative images of cellular distribution of NFATc1 in GFP^{hi} cells (top) and GFP^{lo} cells (bottom). For each panel, galleries on the left show images of Hoechst 3342-stained nuclei fluorescence (blue), H2B-GFP fluorescence (green), NFATc1 immunofluorescence (red) and their overlay. On the right, spatial profiles of GFP (green curve), NFATc1 (red curve) and Hoechst 3342 (blue curve) fluorescence along the yellow line shown on the overlay image (left), respectively. Note the predominant translocation of NFAT to the nuclei in GFP^{lo} cells. **C.** Histogram of SFU in HBL cells after 7 days of treatment with 10 μ M FK506 (n=6). **D.** Histogram of SFU in PC3 cells after 7 days of treatment with 10 μ M FK506 (n=5). *p<0.05; **p<0.01.

While investigating for molecular targets of NFAT that could control the quiescence of the subpopulation of cells with stem-like properties, we concentrated on NFAT-controlled CBP (Matsubara et al. 2010), a transcriptional co-activator, and an important regulator of stemness in different cell types (Chitilian et al. 2014; Ring et al. 2014; Wang et al. 2013). As shown in [Figure 12A](#), CBP expression was higher in Dil^{hi} than in Dil^{lo} prostate cancer cells and this expression was further increased by BTP2 and FK506. Similar data were obtained with HBL cells ([Figure 12B](#)). This CBP upregulation was accompanied by Orai1 and NFAT inactivation, demonstrating their inverse relationship and thereby implying that Orai1-instigated signaling negatively regulates CBP linked to melanoma and prostate stem-like cells quiescence.

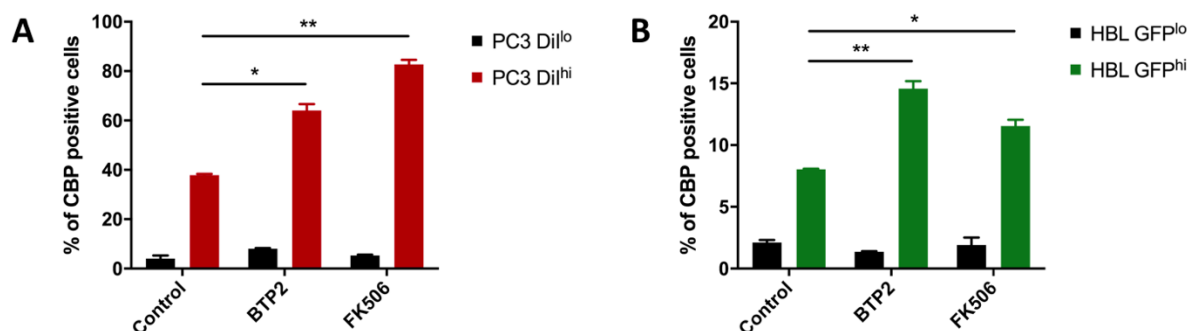


Figure 12: CBP is upregulated in cell populations with stem-like properties

A, B. Histograms showing the percentage of CBP-positive cells in PC3 Dil^{lo} and Dil^{hi} subpopulations and HBL GFP^{lo} and GFP^{hi} respectively in control conditions or after treatment with 1 μ M BTP2 or 10 μ M FK506. * $p < 0.05$; ** $p < 0.01$.

6. Chemotherapeutic stress induces quiescence and is associated with a decrease in Orai1 expression

The CSCs hypothesis portends that CSCs possess increased resistance to chemotherapy and thus serve as a reservoir for tumor repopulation after therapy (Alison et al. 2012). While recent studies have provided evidence that therapy resistance relates to the ability of CSCs to enter quiescence (Borst 2012; Ehninger et al. 2014; Touil et al. 2014), the underlying mechanistic relationship remains to be understood. Because our data point to the importance of Orai1 in controlling CSCs quiescence and Orai1 has been linked to apoptosis (Cui et al. 2013; Dubois et al. 2014; Henke et al. 2013), we investigated in our models whether cells with stem-like properties enter quiescence in response to DNA damage and stress-inducing chemotherapeutics, and whether this correlates with Orai1 expression levels.

We treated melanoma cells with 100 μ M 5-fluorouracil (5-FU) or 40 μ M oxaliplatin during 24 hours. This treatment significantly increased the quiescent G0 subpopulation from 12.17 ± 1.53 % in control to respectively 33.73 ± 4.50 % and 31.98 ± 5.19 % in 5-FU and oxaliplatin-treated cells respectively (Figure 13A). Moreover, the Orai1^{lo} subpopulation increased from 3.97 ± 0.78 % in control to 23.56 ± 2.74 % and 32.0 ± 2.2 % respectively in 5-FU and oxaliplatin treated cells (Figure 13B). As shown in Figure 13C, this Orai1^{lo} subpopulation was mainly in the G0 phase of the cell cycle.

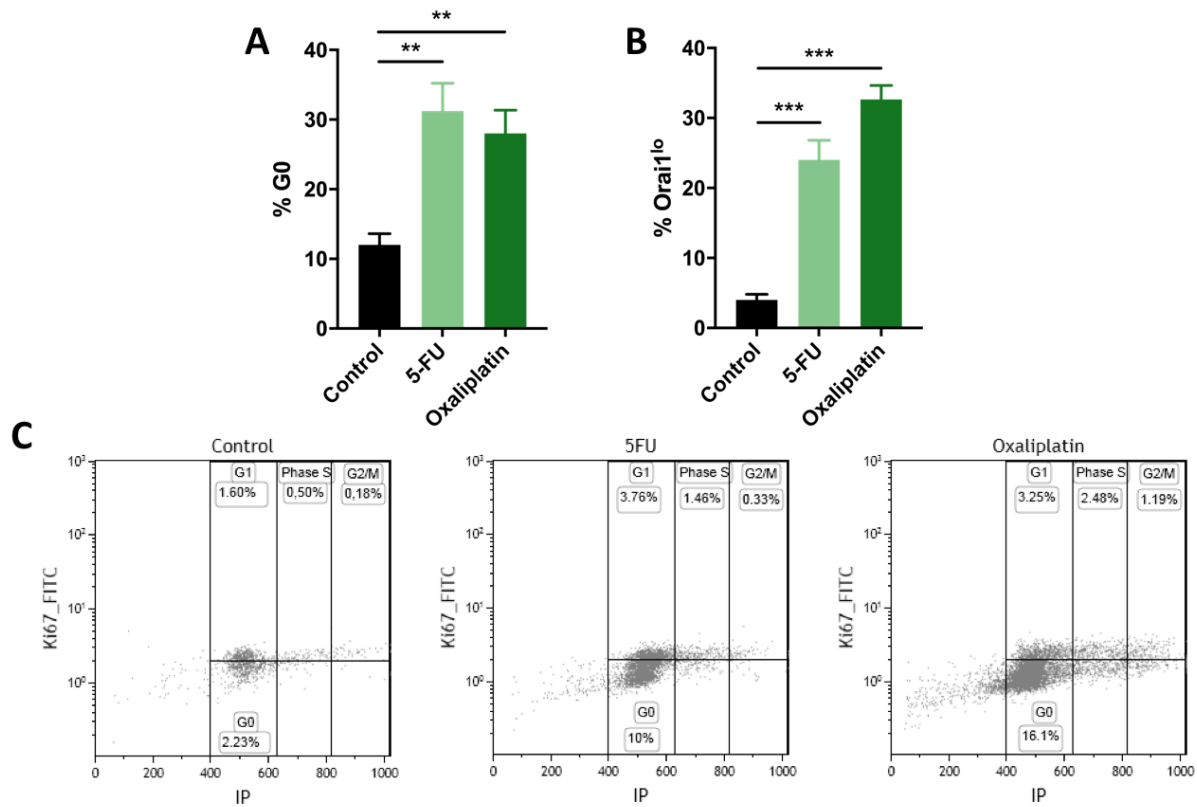


Figure 13: Chemotherapy induces quiescence and is associated with a decrease in Orai1 expression

A. HBL cells were treated with 100 μ M 5-FU or 40 μ M oxaliplatin. After 24 h, the percentage of quiescent cells was determined by flow cytometry and Ki67/IP staining (n=5). **B.** Orai1^{lo} subpopulation was analyzed by flow cytometry after 5-FU or oxaliplatin treatment (24 h, n=3). **C.** Cell cycle distribution gated in Orai1^{lo} subpopulation. 5-FU and oxaliplatin 24 h treatments increases the quiescent Orai1^{lo} subpopulation (representative results from three independent experiments). **p<0.01; ***p<0.001.

We are currently performing similar experiments to confirm these results in prostate cancer cells with docetaxel (DoceT, 10 nM).

Taken together, our results confirm that Orai1 downregulation induces cellular quiescence and suggest that this ability endows CSCs with a chemotherapeutic-resistant phenotype.

2. The sigma 1 receptor, a new partner protein of store-operated channels in prostate cancer

Lucile Noyer, Dmitri Gordienko, Alessandro Furlan, Alexandre Bokhobza, Yasmine Touil, Franck Borgese, Dimitra Gkika, Adriana Mihalache, V'yasheslav Lehen'kyi, Pascaline Segard, Mohamed El-Kadiri, Laurent Allart, Nathalie Ziental-Gelus, Pierre Gosset, Laurent Heliot, Olivier Soriani, Natalia Prevarskaya, Loic Lemonnier

Article in preparation

As stated in the introduction, calcium channels play a major role in prostate cancer (PCa), the most frequent and third deadliest cancer in men in developed countries. Among them, the store-operated channels (SOC), constituted by Orai1 and STIM1, have been shown to regulate apoptosis-sensitivity and, as described above, the quiescence/proliferation transition of cancer cells with stem-like properties. Unfortunately, SOC targeting is currently limited, with only the possibility of inhibition. We thus aimed to identify a partner protein to bypass these shortcomings. We took interest in the sigma 1 receptor (S1R), whose ability to modulate ion channels has been well documented over the years. Interestingly, the S1R has been shown to be overexpressed in many cancers, including PCa. Recent studies using overexpression in HEK-293 cells showed that S1R could modulate SOC activity, but there has been no such report in PCa, or in an endogenous setting.

We used hormone-sensitive (LNCaP) and resistant (PC3) PCa cell lines to show that S1R expression is regulated by androgens in PCa at both protein and mRNA levels. We also confirmed the previously reported regulation of Orai1 by androgens. Using specific techniques such as patch clamp, calcium imaging, confocal microscopy and TD-FLIM, we report here that upon store-operated calcium entry (SOCE) activation, the S1R translocates to the plasma membrane and interacts with Orai1, increasing SOC activity. These results were confirmed in both overexpressing and endogenous models of PCa. Finally, through the roles of SOC in PCa cells, this S1R modulation leads to an increased PCa cell proliferation associated with a decrease in the pool of cancer cells presenting stem-like properties and an enhanced sensitivity to apoptosis.

Our results uncover a new role for S1R in PCa, as a modulator of SOC and regulator of cell proliferation, and of tumor growth. We also present preliminary results showing that S1R is able to regulate other calcium channels implicated in prostate carcinogenesis, such as TRPV6 and TRPM8, reinforcing the importance of this chaperone protein in PCa.

1. The S1R is overexpressed in PCa

Previous studies showed that the S1R is overexpressed in many cancers, including PCa (John et al. 1998; Vilner et al. 1995b).

We used two different sets of patient samples to study the expression of the S1R in PCa at both mRNA and protein levels. In a first set of samples, immunohistochemistry experiments showed that the S1R is expressed in healthy prostate. S1R expression is slightly increased in benign prostatic hyperplasia (BPH), and further increased in PCa, in correlation with aggressiveness as shown by the stainings obtained on Gleason 7 and 9 (Figure 1A). It is important to note that all our cancer samples are hormone-sensitive PCa, as confirmed by the strong PSA staining.

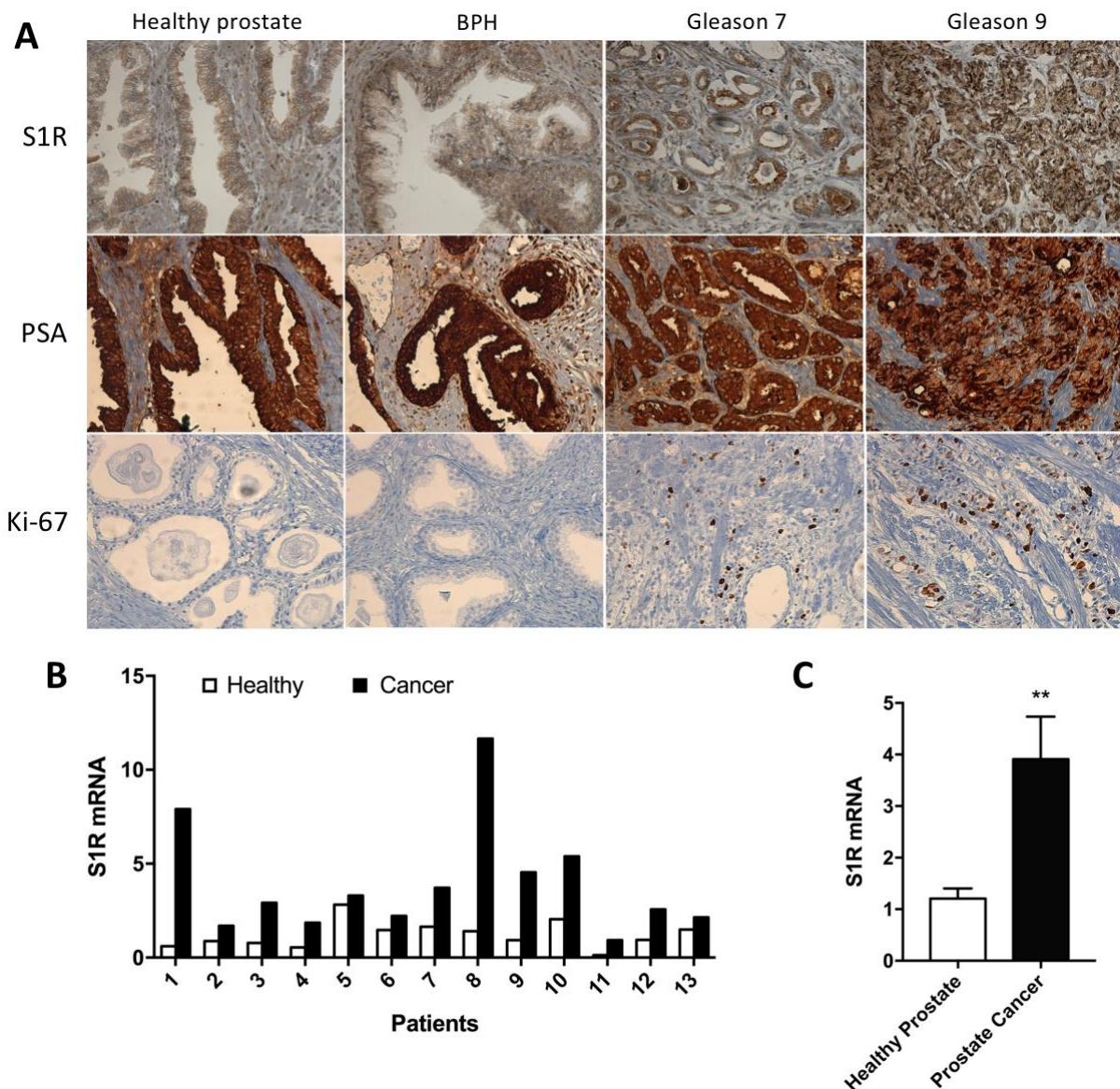


Figure 1: S1R expression is increased in prostate cancer

A. From top to bottom are shown immunohistochemistry staining of S1R, PSA and Ki-67, on healthy prostate, benign prostatic hyperplasia (BPH), Gleason 7 PCa and Gleason 9 PCa. Representative images (respectively n=2, n=6, n=6, n=3). **B.** RT-qPCR results showing S1R mRNA expression levels normalized on r18S in 13 PCa biopsies. For each patient, two separate samples were compared after histopathological analysis: healthy prostate tissue and prostate cancer. **C.** Summary of the results presented in B. **p<0.01

We were able to confirm S1R overexpression in PCa with a second set of samples in which we compared mRNA levels between healthy prostate tissue and prostate cancer in 13 patients with hormone-sensitive PCa (Gleason 6 to 9). RT-qPCR results show that, for every patient, S1R mRNA expression is higher in PCa tissue than in its healthy counterpart (Figure 1B). The mean expression of all 13 patients presented in Figure 1C shows a significant 3-fold overexpression of the S1R in PCa, with relative expressions of 1.20 ± 0.19 in healthy tissue and 3.90 ± 0.83 in cancer, confirming previously reported data.

We then examined the expression of the S1R in PCa cell lines by RT-qPCR and western blot. Our results show a strong expression of the S1R in LNCaP cells at both mRNA and protein levels (Figures 2A and 2B). Interestingly, the more aggressive PCa cell line PC3 presented a weaker expression of the S1R.

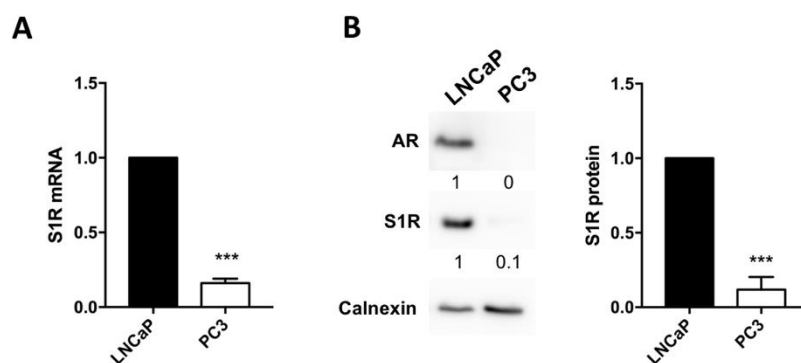


Figure 2: S1R expression in prostate cancer cell lines

A. RT-qPCR results of S1R mRNA expression normalized on r18S in LNCaP and PC3 cells (n=4).

B. On the left, representative image of a western blot experiment showing calnexin-normalized expression of AR and S1R in LNCaP and PC3 cells. On the right, S1R protein expression normalized on calnexin measured by western blot (n=3). ***p<0.001

2. S1R expression is positively regulated by androgens in PCa

The main difference between the LNCaP and PC3 cell lines is their dependence to androgens. Indeed, LNCaP are hormone-sensitive cells that express the androgen receptor (AR). These cells require androgens to proliferate and express classical androgen-regulated prostate markers such as the prostate specific antigen (PSA) (Schuurmans et al. 1988; Young et al. 1991). On the other hand, PC3 are hormone-resistant cells that do not express the AR nor the PSA (van Bokhoven et al. 2003). We thus investigated the possibility of S1R expression being regulated by androgens in PCa cells.

To do so, we treated the LNCaP hormone-sensitive cells with Casodex® (Bicalutamide), a pharmacological inhibitor of the AR. We also placed LNCaP cells in steroid-deprived medium with or without the addition of dihydrotestosterone (DHT), the active form of testosterone. After 3 days, Casodex® (10 μ M) led to a strong decrease in S1R mRNA and protein expression (Figure 3A and 3B). When LNCaP cells were placed in steroid-deprived medium, S1R mRNA and protein levels were decreased as well, and the addition of 100 nM DHT in the medium led to a significant

increase in S1R expression. Interestingly, this regulation seems to be indirect, as shown by the absence of effect after 4 hours of treatment in [Figure 3C](#). To confirm the implication of the AR in this regulation, we used a siRNA targeting the receptor to strongly decrease its expression in LNCaP cells. After 3 days of treatment, specific AR inhibition decreased the S1R mRNA

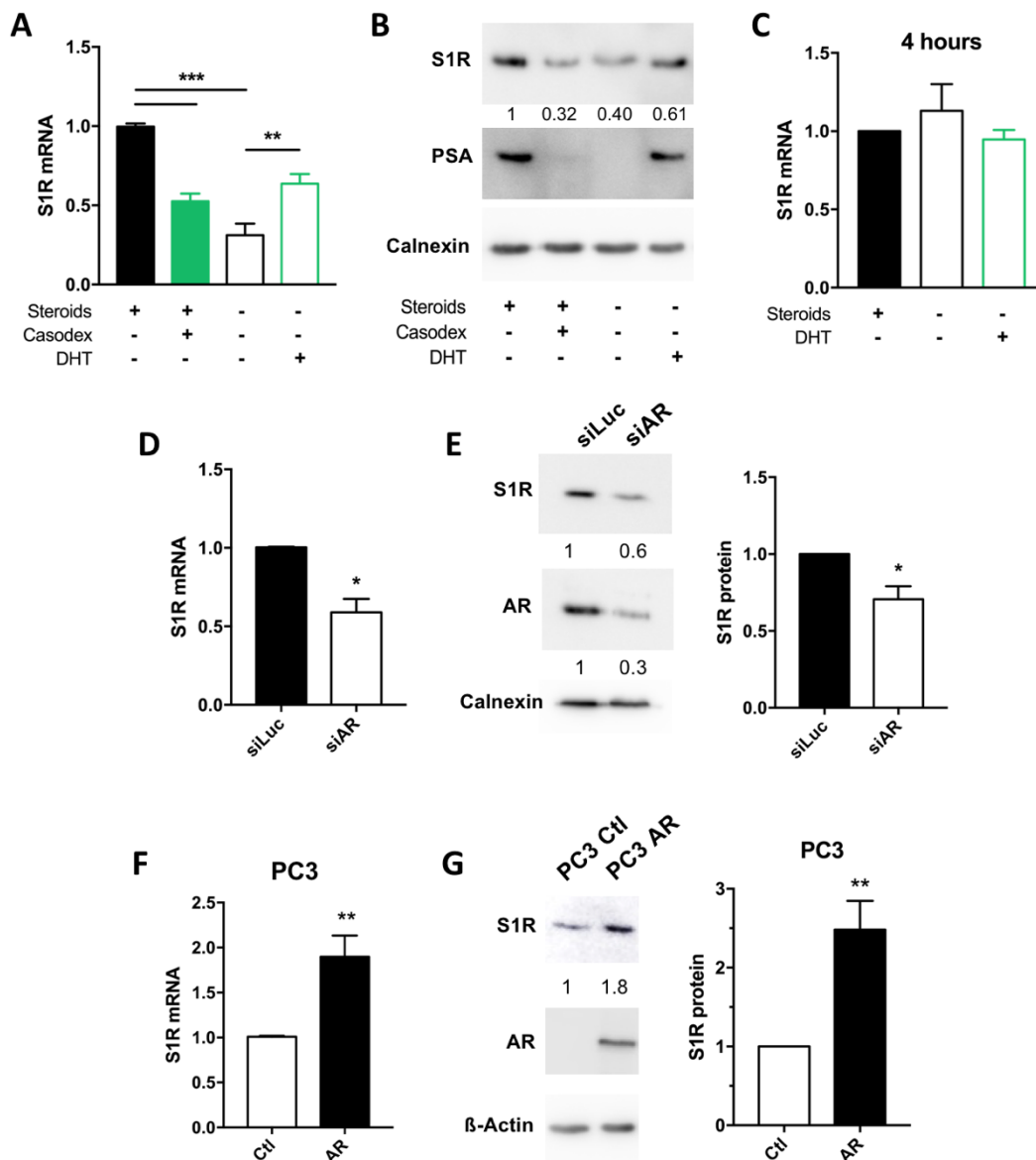


Figure 3: Androgens regulate S1R expression in PCa cells

A-B. LNCaP cells grown for 3 days in normal medium with or without 10 μ M Casodex®, or in steroid-deprived medium with or without 100 nM DHT. **A.** r18S-normalized S1R mRNA expression obtained by RT-qPCR (n=5). **B.** S1R protein expression normalized on calnexin, PSA expression was used as a control for androgen modulation, representative western blot experiment from three independent experiments. **C.** r18S-normalized S1R mRNA levels in LNCaP cells 4 hours after steroid-deprivation, with or without addition of 100 nM DHT (n=3). **D-E.** LNCaP cells, 3 days after transfection with a control siRNA (siLuc, 50 nM) or siAR (50 nM) in 2 % FBS medium. **D.** r18S-normalized S1R mRNA expression (n=3). **E.** On the left, representative western blot experiment showing S1R and AR expressions, calnexin was used as a control. On the right, S1R protein expression normalized on calnexin (n=3). **F-G.** PC3 cells 3 days after transfection with an empty vector (Ctl) or the AR. **F.** r18S-normalized S1R mRNA expression (n=4). **G.** On the left, representative western blot experiment showing S1R and AR expressions, β -actin was used as a control. On the right, S1R protein expression normalized on β -actin (n=3). *p<0.05; **p<0.01; ***p<0.001

expression from 1 to 0.59 ± 0.08 (Figure 3D). This was accompanied by a significant decrease in S1R protein level (Figure 3E).

We confirmed these results in another PCa cell model by re-expressing the AR in the hormone-resistant PC3 cells that do not express this receptor. As shown in Figures 3F and 3G, the re-expression of AR in these cells significantly increased the weak expression of the S1R after 3 days by at least 2-fold at both protein and mRNA levels.

Taken together, these results show that S1R expression is positively regulated by androgens in PCa cells. It is well known that androgen signaling is hyperactivated in hormone-sensitive PCa, cells and this could thus be responsible for the S1R overexpression we previously showed (Figure 1). These results also suggest that S1R expression would significantly drop in androgen-resistant PCa (castration-resistant PCa, CRPC), suggesting that the S1R could be an interesting marker for late stages of PCa.

3. *Androgens regulate Orai1 expression, but not Orai3 and STIM1*

Orai and STIM isoforms have been previously studied in PCa. The expression of Orai1 and STIM1, the major components of store-operated channels (SOC) in our models, remains unchanged in PCa (Dubois et al. 2014; Raphaël et al. 2014). Interestingly, a previous study also suggested that Orai1 could be regulated by androgens in PCa (Flourakis et al. 2010), similarly to our results above for the S1R. We thus repeated our experiments to confirm Orai1 regulation by androgens and to study the sensitivity of Orai1's activator, STIM1, to these steroids.

As shown in Figure 4A, Orai1 mRNA expression is significantly down-regulated in androgen-deprived culture conditions via both AR pharmacological inhibition and steroid removal from the medium. In steroid-deprived culture conditions, the addition of 100 nM DHT leads to a significant increase of Orai1 mRNA expression from 0.57 ± 0.08 to 0.90 ± 0.06 . This result was confirmed at protein level (Figure 4B). As previously shown for the S1R, no effect was detected on Orai1 mRNA levels after 4 hours of treatment (Figure 4C), hinting at an indirect regulation. As it was previously shown, AR knockdown by siRNA decreases Orai1 mRNA expression (Figure 4D). AR re-expression in PC3 cells further confirmed those results by significantly increasing Orai1 mRNA from 1 to 1.33 ± 0.10 (Figure 4E).

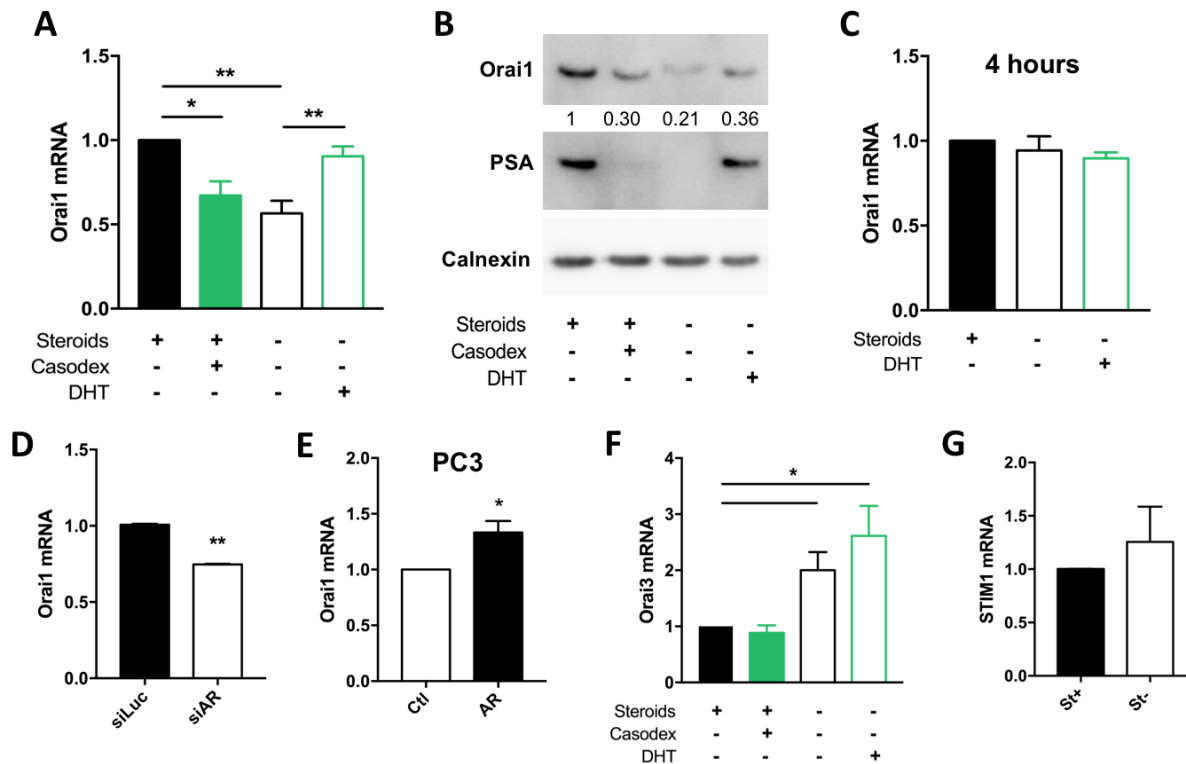


Figure 4: Androgens regulate Orai1 but not Orai3 and STIM1 in PCa cells

A-B. LNCaP cells grown for 3 days in normal medium with or without 10 μ M Casodex®, or in steroid-deprived medium with or without 100 nM DHT. **A.** r18S-normalized Orai1 mRNA expression obtained by RT-qPCR (n=5). **B.** Orai1 protein expression normalized on calnexin, PSA expression was used as a control for androgen modulation, representative western blot from three independent experiments. **C.** r18S-normalized Orai1 mRNA levels in LNCaP cells 4 hours after steroid-deprivation, with or without addition of 100 nM DHT (n=3). **D.** r18S-normalized relative Orai1 mRNA expression LNCaP cells, 3 days after transfection with a control siRNA (siLuc, 50 nM) or siAR (50 nM), in 2 % FBS medium (n=3). **E.** r18S-normalized Orai1 mRNA expression in PC3 cells 3 days after transfection with an empty vector (Ctl) or the AR (n=4). **F.** r18S-normalized Orai3 mRNA expression in LNCaP treated as in A-B (n=4). **G.** r18-normalized STIM1 mRNA levels in LNCaP grown in normal or steroid-deprived medium (3 days; n=4). *p<0.05; **p<0.01.

Orai3 was shown to be overexpressed in PCa, but this channel does not participate in SOC (Dubois et al. 2014). We also studied the expression of the Orai3 isoform in our model and found that Orai3 can be repressed by steroids other than androgens. Indeed, while Casodex® and DHT had no effect on Orai3 expression, the removal of steroids from the culture medium led to a significant 2-fold increase in Orai3 mRNA levels (Figure 4F).

Finally, as shown in Figure 4G, steroids did not have any effect on STIM1 mRNA expression in LNCaP cells after 3 days of treatment.

These results show that among the Orai and STIM isoforms implicated in PCa physiology, only Orai1 is regulated by androgens as previously suggested (Flourakis et al. 2010). Interestingly, Orai1 regulation by androgens presents a profile similar to the one we have identified for the S1R.

4. *The S1R positively regulates SOC channels in PCa cells*

Although S1R overexpression has been documented in many cancers, its precise role remains to be elucidated. Unlike what its name suggests, this protein does not act as a receptor, but as a chaperone able to bind and regulate many proteins (Su et al. 2016). Among its targets, some ion channels have been shown to be regulated by the S1R (Soriani and Rapetti-Mauss 2017). SOC channels having been implicated in cancer as key players of migration, proliferation, as well as apoptosis (reviewed in Fiorio Pla et al. 2016), we therefore investigated the possible regulation of the SOC channels by the S1R in PCa cells.

Patch-clamp recordings of the IP₃-activated SOC current presented in [Figures 5A and 5B](#) show that the overexpression of human S1R (hS1R) increases SOC activity in LNCaP cells. This result was confirmed using the calcium-imaging technique ([Figure 5D](#)): S1R overexpression also led to an increased store-operated calcium entry (SOCE).

Surprisingly, a previous study conducted in HEK-293 with the overexpression of the rat S1R (rS1R) has shown that the S1R inhibits SOC channels (Srivats et al. 2016), a result in apparent contradiction with our own. We thus tested the rS1R construct used for this study in our PCa cells, and we were able to confirm its inhibitory effect on SOC ([Figure 5C](#)). These results thus indicate that the hS1R and the rS1R have opposite effects of SOC channel activity. However, S1R sequence is highly conserved between the two species, with 93% of homology. Interestingly, sequence alignment showed that most of the modified residues are located within the putative transmembrane region of the S1R. We thus built a human/rat chimera construct by switching this region of interest between the two species, and we are currently assessing its effect on SOC channels.

Since our main question was to elucidate the role of the S1R in human PCa cells, for the rest of this study, we worked with the human variant of the S1R.

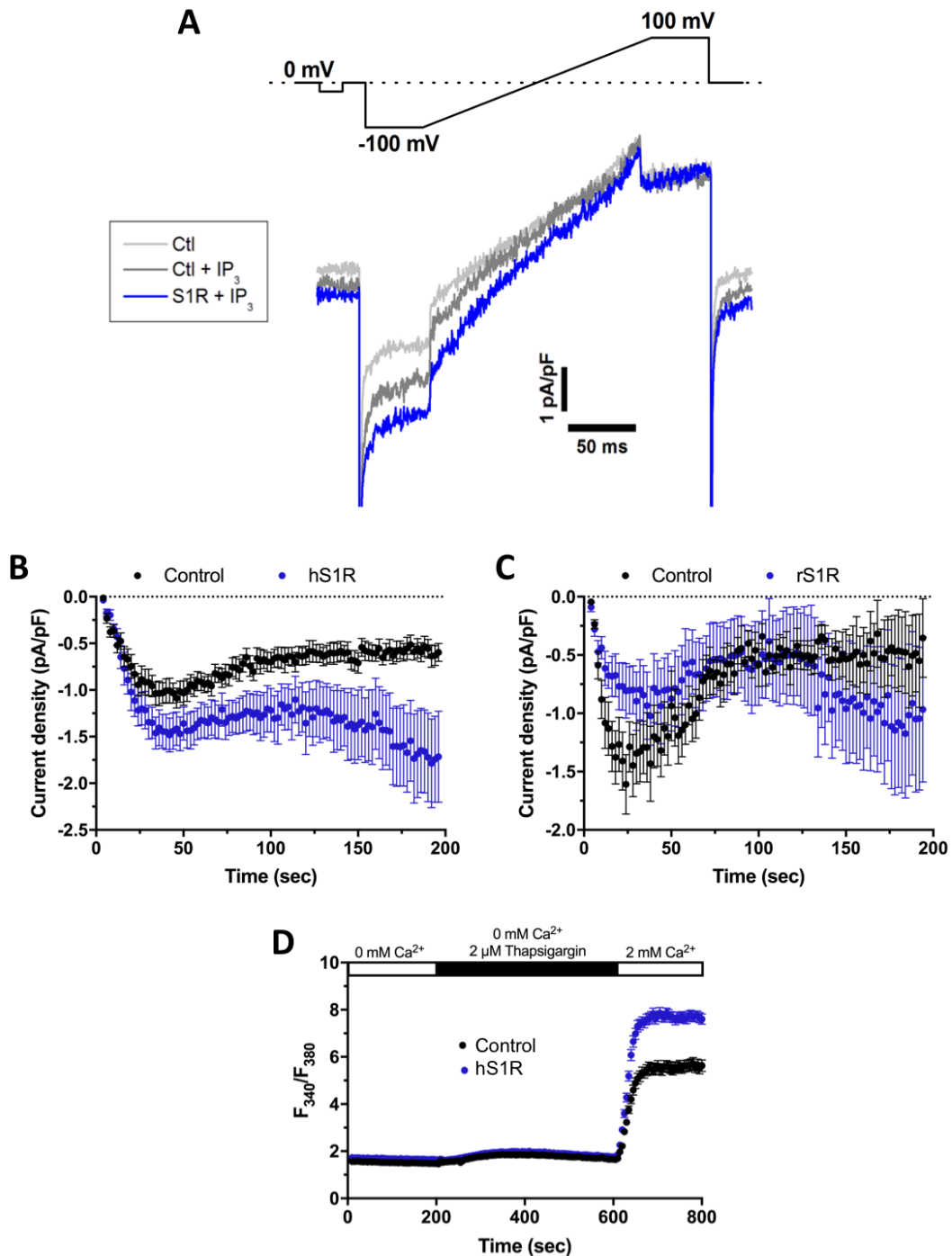


Figure 5: Human S1R overexpression increases SOC channel activity in LNCaP cells

A. Representative traces of control (light grey) and IP₃-activated (100 μM) I_{SOC} recorded in LNCaP cells transiently transfected with human S1R (S1R, in blue) or an empty vector (Ctl, in grey). The corresponding stimulation protocol is presented in the upper panel. **B-C.** Average time courses of IP₃-evoked I_{SOC} in LNCaP cells, currents are monitored at -100 mV. Peak I_{SOC} is typically reached between 25-40 seconds. **B.** LNCaP cell transiently transfected with an empty vector (control) or human S1R (hS1R). **C.** LNCaP cells transiently transfected with an empty vector or rat S1R (rS1R). **D.** Time course of calcium ratios obtained by calcium imaging. Thapsigargin and calcium addbacks are indicated by bars.

As reported above, S1R expression is already quite high in LNCaP cells (Figure 2A and 2B). We thus used RNA interference to evaluate the role of endogenous S1R on SOCE in these cells. As expected, S1R knockdown led to a significant decrease in SOC channel activity as shown in Figure 6.

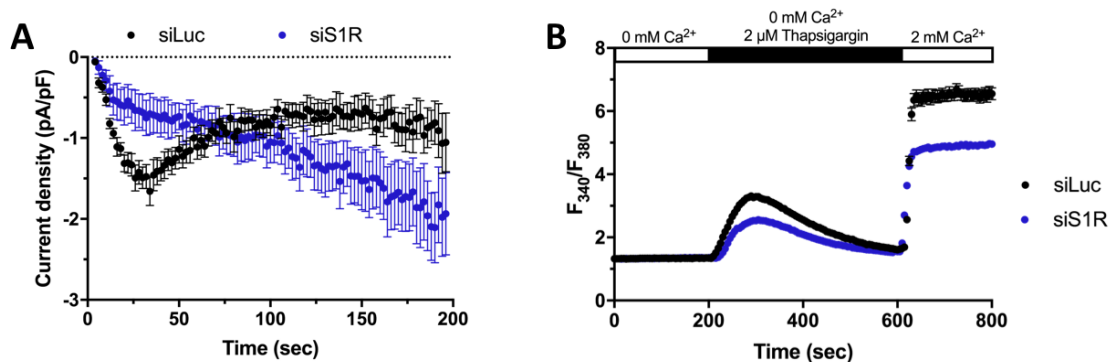


Figure 6: Endogenous S1R inhibition decreases SOC activity in LNCaP cells

A-B. LNCaP cells transfected with a control siRNA (siLuc, 50 nM) or siS1R (50 nM, 3 days). **A.** Average time courses of IP₃-evoked I_{SOC}. **B.** Time course of calcium ratios obtained by calcium imaging. Thapsigargin and calcium addbacks are indicated by bars.

One of the particularity of the S1R is its ability to bind many different compounds (reviewed in Chu and Ruoho 2016). It has been reported that upon ligand binding, the S1R can translocate, detach from protein or interact with new targets. We thus investigated the effect of different S1R ligands on SOC channels. We tested two S1R agonists, Igmesine and SKF-10047. As shown in Figure 7, acute treatment with S1R agonists (1 μM) increased SOC current and SOCE in LNCaP cells. This shows that upon ligand binding, the S1R can modulate SOC channel activity with a fast kinetic as the agonist were added mere minutes before SOC activation by either IP₃ or ER store depletion.

We then examined the effect of S1R ligands on SOC activity after chronic exposition, by adding them to the culture medium for 7 days. The results first results presented in Figure 8 show that long term exposition to S1R agonists (1 μM) increased SOC activity in LNCaP cells.

Taken together, these results show that SOC channel activity can be regulated via S1R pharmacological modulation, opening interesting new perspective for their targeting.

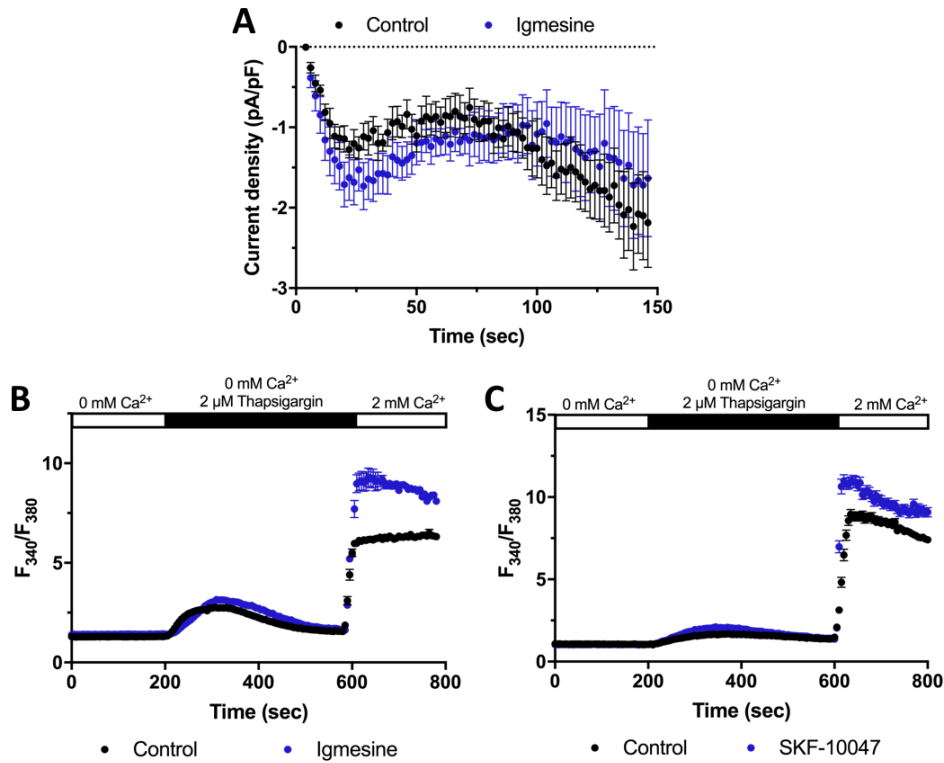


Figure 7: Acute exposure with S1R agonists increases SOC activity

A-B. LNCaP cells treated with 1 μM igmesine at t=0. **C.** LNCaP cells treated with 1 μM SKF-10047 at t=0. **A.** Average time course of IP₃-evoked I_{SOC}. **B-C.** Time courses of calcium ratios obtained by calcium imaging. Thapsigargin and calcium addbacks are indicated by bars.

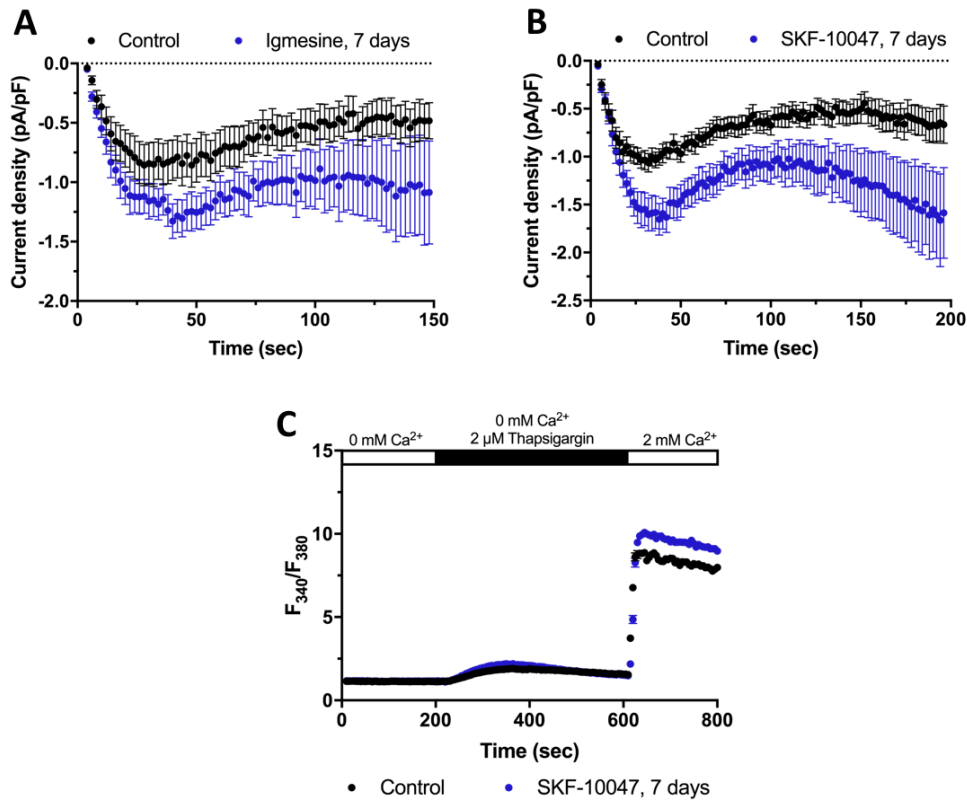


Figure 8: Chronic exposure with S1R agonists increases SOC activity

A. LNCaP cells treated with 1 μM igmesine at for 7 days. **B-C.** LNCaP cells treated with 1 μM SKF-10047 for 7 days. **A-B.** Average time courses of IP₃-evoked I_{SOC}. **C.** Time course of calcium ratios obtained by calcium imaging. Thapsigargin and calcium addbacks are indicated by bars.

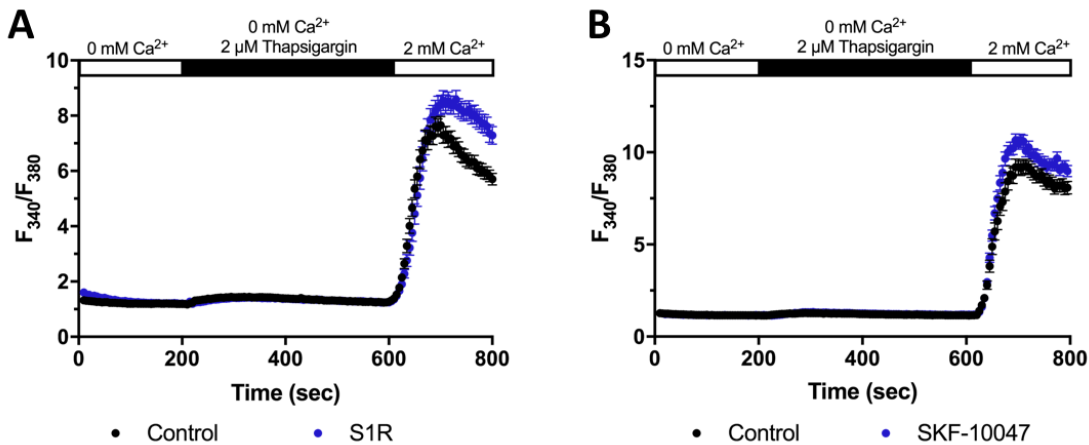


Figure 9: S1R is a positive modulator of SOCE in PC3 cells

A-B. Time course of calcium ratios obtained by calcium imaging. Thapsigargin and calcium addbacks are indicated by bars. **A.** PC3 cells transiently transfected with an empty vector (Control) or the S1R. **B.** PC3 cells were incubated or not with 1 μ M SKF-10047 (added at $t=0$).

Although S1R expression and SOCE are weaker in PC3 cells, we were able to show that the positive modulation of the S1R on SOC channel activity was also present in these cells, to a lesser extent (Figure 9). Since SOC activity is too small to be recorded by patch-clamp in PC3 cells, only SOCE is shown, monitored through calcium imaging.

All of our results show the effect of the S1R on induced SOC channel activity. We therefore also used ionomycin, a calcium ionophore, to evaluate the ER Ca^{2+} stores of our cells by calcium imaging. Indeed, as SOCE is the main Ca^{2+} entry pathway in non-excitable cells, ER Ca^{2+} content can reflect the basal SOC channel activity in our cells. Our results show that S1R overexpression significantly increased ER calcium content in both LNCaP (Figure 10A) and PC3 cells (Figure 10B), thus confirming our hypothesis that basal SOC activity is also increased by S1R overexpression.

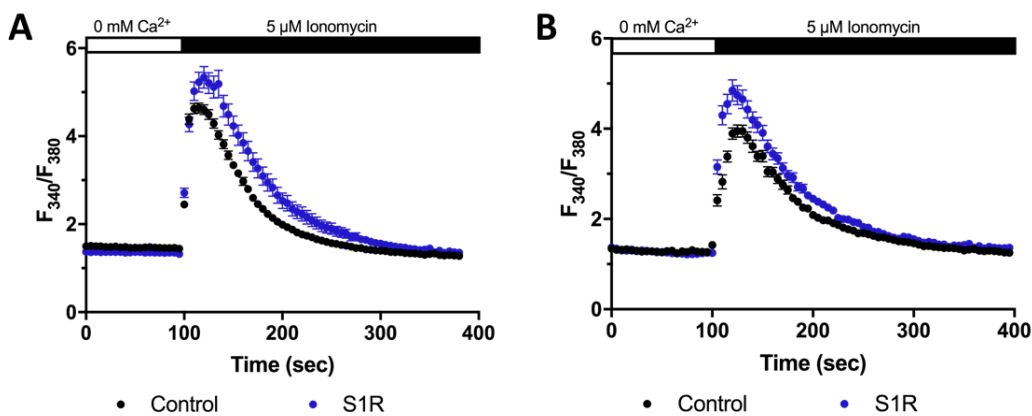


Figure 10: S1R overexpression increases ER calcium content in PCa cells

A-B. Time course of calcium ratios obtained by calcium imaging. Ionomycin addbacks are indicated by bars. **A.** LNCaP cells transiently transfected with an empty vector (Control) or the S1R. **B.** PC3 cells transiently transfected with an empty vector (Control) or the S1R.

5. The S1R translocates to the plasma membrane (PM) upon SOCE activation

SOC channels are mainly composed of two proteins: the pore-forming channel unit Orai and its activator STIM. Orai is located at the plasma membrane (PM), allowing calcium entry from outside of the cell into the cytoplasm when activated. STIM, on the other hand, is inserted in the endoplasmic reticulum (ER) membrane. In order to decipher the mechanism of SOC regulation by the S1R, we first investigated its subcellular localization. The S1R is indeed mainly known as an ER resident protein, preferentially located in the mitochondria-associated membranes (MAM) (Hayashi and Su 2007). But this localization is not exclusive, and studies have shown that the S1R is able to translocate to other regions upon specific signaling or ligand binding. Presence of the chaperone in the plasmalemmal ER region and in the PM have thus been reported (Su et al. 2016; Su et al. 2010).

We first performed biotinylation experiments to isolate the proteins that are located in the PM. As shown in Figure 11, the S1R can be found in PCa cells' PM in basal conditions. Interestingly, when we performed the same experiment after SOC activation through ER calcium store depletion, the S1R presence increased at cell surface. However, biotinylation is carried out in non-denaturing conditions, meaning that the S1R could not be directly in the PM, but simply part of a complex containing a PM-resident protein. For example, the ER-resident STIM can also be detected by biotinylation through its interaction with Orai.

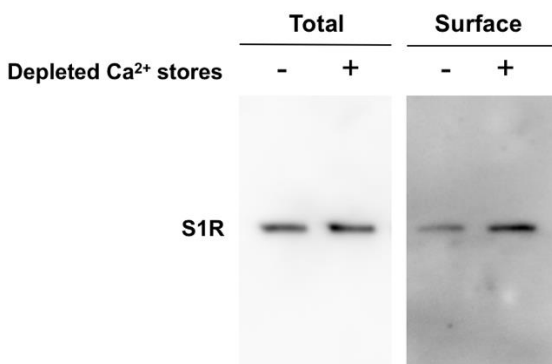


Figure 11: S1R presence increases in the biotinylated fraction upon SOCE activation

Western blot image showing S1R expression in the total protein lysate (left) and biotinylated fraction (right) in basal conditions or after ER Ca²⁺ store depletion (50 μ M CPA in a calcium-deprived extracellular solution, 2 hours). Representative image from three independent experiments.

We conducted additional experiment to study S1R localization in LNCaP cells upon SOCE. Using fluorescent constructs, we were able to study the dynamic localization of the S1R in live cells during SOC channel activation by confocal microscopy. We used a S1R-eGFP fusion protein, the ER-DsRed construct to visualize the ER (DsRed fluorescent protein fused to an ER-localization signal) and the membrane was stained with the CellMaskTM dye. We then followed S1R localization within the cells in basal conditions and during the activation of SOCE. Pictured in Figure 12 are representative images from the beginning of the experiment, with intact ER Ca²⁺

stores, and at the end of the experiment with depleted ER Ca^{2+} stores. In basal conditions, most of the S1R is inside the cell, colocalizing with the ER, and we can see little colocalization with the PM (Figures 12A-C). Interestingly, after ER store depletion, S1R seem to redistribute in clusters colocalizing with the PM (Figures 12D-F), resembling the characteristic puncta of Orai/STIM co-clustering observed upon SOC channel activation (Liou et al. 2005; Zhang et al. 2005).

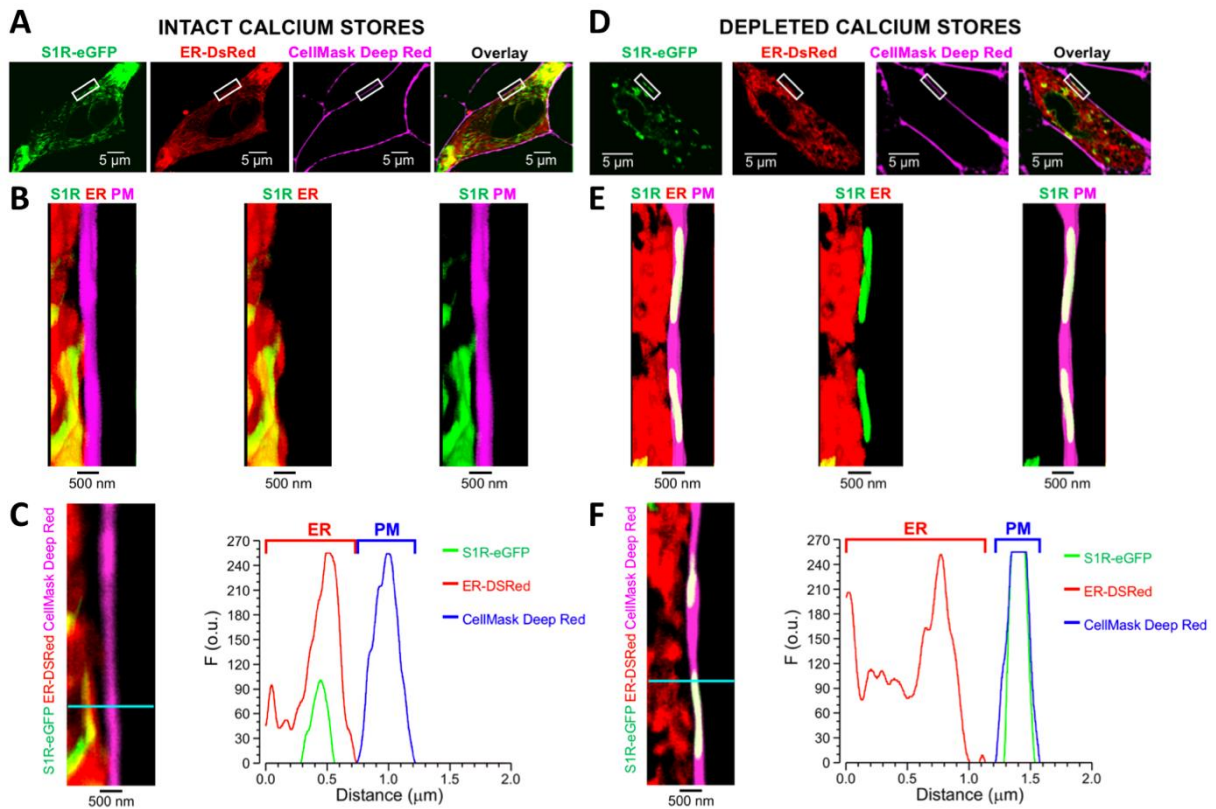


Figure 12: Dynamic confocal studies show that S1R translocates to the PM during ER Ca^{2+} store depletion

Representative confocal images of LNCaP cells expressing S1R-eGFP (green), ER-DsRed (red) and CellMask Deep Red PM stain (pink). **A-C**. Basal conditions, with intact ER calcium stores. **D-F**. Cells after ER calcium store depletion (50 μM CPA, 1-2 hours). **A, D**. Whole cell, overlay on the right. **B, E**. Images zoomed-in on a membrane portion indicated by the white box in whole cell images (A, D). **C, F**. Color profile of the fluorescence intensity along the blue line traced on the image on the left.

However, the overexpression of a protein can lead to aberrant clustering and localization. Our next step was therefore to detect endogenous S1R in LNCaP cells in basal conditions and after ER Ca^{2+} store depletion by immunofluorescence. The representative confocal images presented in Figure 13 show that, while we were also able to detect small amounts of S1R colocalizing with the PM in basal conditions (Figure 13A-C), a strong PM translocation of the S1R was observed after ER calcium store depletion (Figure 13D-F).

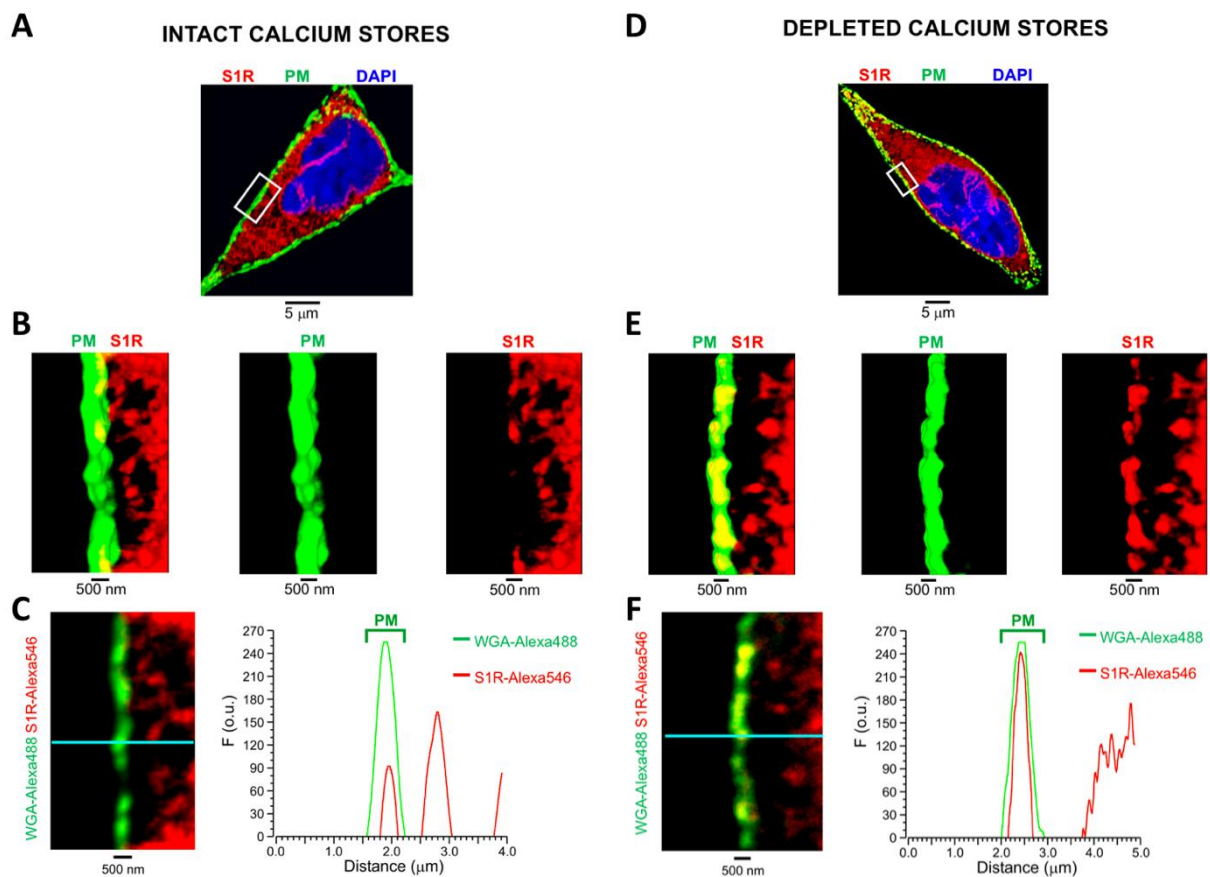


Figure 13: Endogenous S1R translocates to the PM during ER Ca^{2+} store depletion

Representative confocal images of LNCaP cells immunoreacted with anti-S1R antibody (red), PM was stained by Alexa488-coupled wheat-germ agglutinin (WGA, in green), nucleus was stained with DAPI (blue). **A-C**. Basal conditions, with intact ER calcium stores. **D-F**. Cells after ER calcium stores depletion (50 μM CPA, 2 hours). **A, D**. Whole cell overlay. **B, E**. Images zoomed-in on a membrane portion indicated by the white box in whole cell images (A, D). **C, F**. Color profile of the fluorescence intensity along the blue line traced on the image on the left.

Altogether, these results show that the S1R translocates toward PM upon SOC channel activation. Although our experiences cannot definitively conclude on S1R insertion within the plasma membrane itself due to their limitations in terms of spatial resolution, it is however clear that the S1R translocates to a region at least tightly associated with PM.

6. The S1R directly interacts with Orai1 to modulate SOCE

Our next step to decipher how the S1R is able to modulate SOC channels was to investigate protein-protein interactions.

To do so, we first performed co-immunoprecipitations experiments targeting the S1R and Orai1. As shown in [Figure 14](#), endogenous Orai1 and S1R coimmunoprecipitate, showing that they (directly or indirectly) interact together. In these same experiments, we were also able to detect STIM1 (data not shown), a protein known to interact with Orai1 (Park et al. 2009).

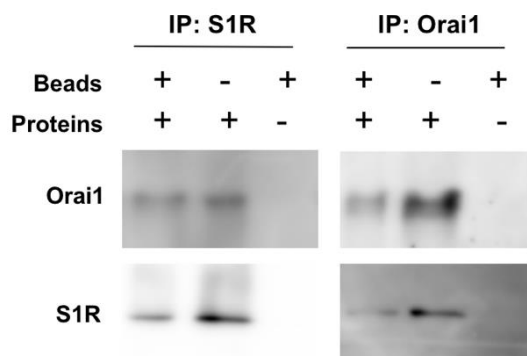


Figure 14: The S1R and Orai1 are found within the same protein complex

Western blot images showing S1R and Orai1 expression levels in coimmunoprecipitation experiments in LNCaP cells. S1R was immunoprecipitated on the left panel and Orai1 on the right panel. For each experiment, the first line was loaded with the immunoprecipitated fraction, the second line with the total protein lysate and the third line with the beads alone. Representative image from three independent experiments.

In order to determine whether Orai1 and S1R interact directly, we then used the FRET-based technique of TD-FLIM (time domain – fluorescence lifetime imaging microscopy). For this purpose, we fused each of our protein of interest to one of the following two fluorescent proteins (FP) with spectral overlap: mTurquoise, the donor, and sYFP, the acceptor. When the constructs are expressed in the cell, FRET will only occur if the target proteins directly interact with each other, bringing the two FP close together. In TD-FLIM experiments, we monitor the fluorescence lifetime of the donor FP that will decrease in the occurrence of FRET. Thus, a significant decrease in fluorescence half-time shows a direct interaction between the two proteins studied.

We first examined the interaction between the S1R and STIM1, the two ER resident proteins. The results presented in [Figure 15A](#) show a significant decrease in the donor fluorescence half-time when both construct were expressed within the cell as compared to the donor alone (S1R, here), representing a direct interaction between the two proteins in basal conditions. Interestingly, this interaction was lost upon SOC channel activation via ER calcium store depletion (50 μ M CPA) as shown by the fluorescence lifetime increase back to the basal level.

It is important to note that in these experiments, we used a construct with the sYFP fused with the N-terminal ER luminal extremity of STIM1. The loss of interaction between the two proteins therefore confirms our previous results showing that S1R leaves ER upon SOC activation, as it is well known that STIM1 stays in the ER throughout SOCE. However, in order to completely rule out the possibility that S1R and STIM1 still interact together after SOC activation, we have built a

construct of the sYFP fused with the C-terminus of STIM1, and we are currently testing this construct in TD-FLIM experiments.

In a second set of experiments, we studied the interaction between Orai1 and the S1R. This time, we could not detect any direct interaction in the basal conditions (Figure 15B). However, our results confirm that Orai1 and S1R interact together when SOC channels are activated through ER store depletion.

Taken together, these results show that in basal conditions, the S1R is mainly located in the ER where it interacts with STIM1. Then, upon SOC activation, S1R dissociates from STIM1 and translocates to the PM to interact with Orai1. This interaction between Orai1 and S1R in the PM then leads to an increased SOCE.

In PCa cells, Orai3 has been shown to inhibit SOCE by oligomerizing with Orai1 to form arachidonic acid-regulated calcium channels (ARC) (Dubois et al. 2014). We thus used the FLIM technique to determine if the S1R affect this interaction. As expected, we detected a strong interaction between Orai1 and Orai3 when the two constructs were expressed in our cells, and this interaction was significantly decreased upon SOC activation (Figure 15C). Interestingly, the overexpression of the S1R also decreased Orai1/Orai3 interaction, and this effect was more pronounced with concomitant ER store depletion.

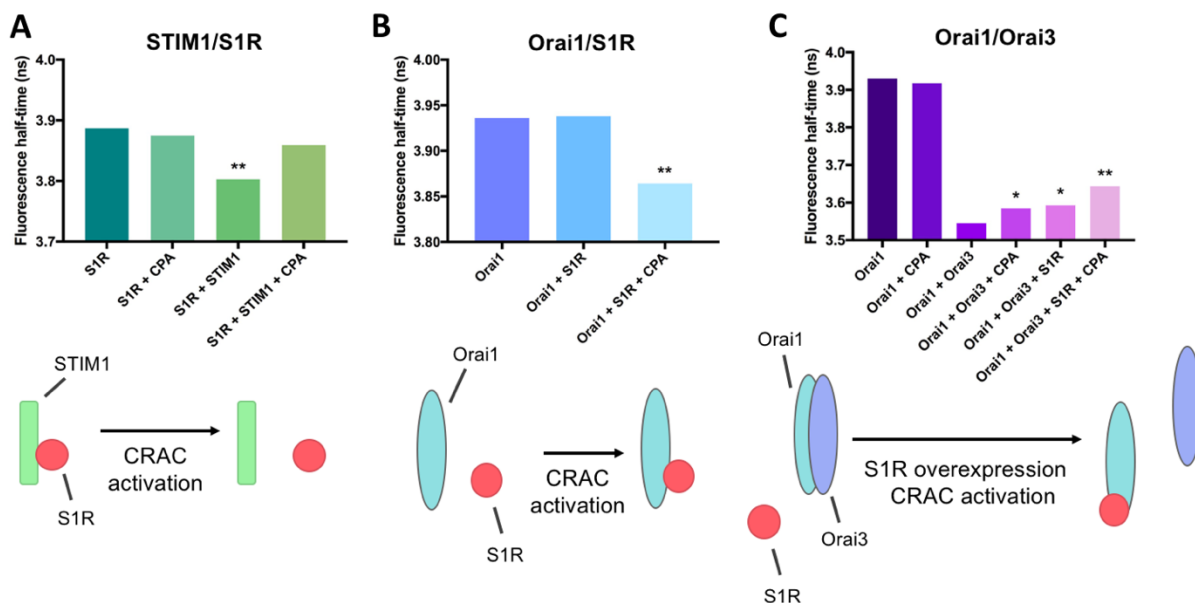


Figure 15: TD-FLIM experiments show that S1R interacts with STIM1 and Orai1

Top panel shows TD-FLIM recordings of the fluorescence lifetime of the donor FP in LNCaP cells transfected with the fluorescent constructs. For each histogram, the first bar shows the basal fluorescence lifetime of the donor expressed alone in the cells. Each experiment was conducted in basal conditions and after ER Ca²⁺ store depletion (CPA, 50 μM). Schematic illustrations of the results are depicted at the bottom. **A.** Experiment with S1R-mTurquoise as a donor, STIM1-sYFP as an acceptor. **B.** Experiments with Orai1-mTurquoise as a donor, S1R-sYFP as an acceptor. **C.** Experiments with Orai1-mTurquoise as a donor, Orai3-sYFP as an acceptor. These experiments were conducted with or without overexpression of the S1R.

These results suggest that the S1R could increase SOCE in part by promoting Orai1 to take part in SOC channels rather than in ARC channels.

Unfortunately, the difficulties of S1R immunostaining did not make it possible to confirm these results with endogenous proteins using the antibody-based proximity-ligation assay. However, for all our TD-FLIM experiment, we limited the amount of transfected plasmid as much as possible to limit abnormal localization due to an excess of proteins.

7. *The S1R increases PCa proliferation*

Our next step was to study the effect of the S1R in PCa cell physiology. Because of the implication of the SOC channels in PCa proliferation we showed above, we first focused on this cellular process.

We first used the MTS and Trypan blue viability assays to evaluate the effect of S1R on LNCaP cells. Our results show that S1R inhibition (siRNA, 50 nM, 4 days) significantly decreased the MTS readings as compared to the control condition (siLuc) (Figure 16A). Live cell counting with the Trypan blue exclusion method first showed that S1R inhibition did not induce cell death (data not shown). Moreover, the results we obtained indicate that the total number of cells was significantly decreased after 4 days in siS1R-transfected cells as compared to siLuc-transfected cells (Figure 16B). Taken together, these results show that the inhibition of the S1R decreases LNCaP cell proliferation. To confirm these data, we used the EdU assay to study cell cycle. As shown in Figure 16C, S1R inhibition significantly decreased the number of cells in the S phase of the cell cycle. Furthermore, siS1R significantly decreased the expression of the proliferation marker PCNA (proliferating cell nuclear antigen) (Figure 16D).

We then performed *in vivo* experiments with subcutaneous xenografts of LNCaP cells transfected with control siLuc or siS1R in male NMRI Nude mice. As presented in Figures 16E and F, the tumors generated by the siS1R-transfected cells were detected significantly later with a mean latency of detection of 61.67 ± 9.45 days as compared to 39.0 ± 2.6 days in control. Moreover, tumor growth was significantly decreased, nearly reaching a plateau towards the end of the experiment.

We confirmed our results with the PC3 cells using the same techniques. Indeed, S1R knockdown in these cells also significantly decreased cell proliferation assed by MTS assay (Figure 17A), Trypan blue cell counting (data not shown) and EdU assay (Figure 17B). These results were confirmed with *in vivo* tumor growth as well. Although tumors were detected in the same timeframe for both control and siS1R, tumor growth was significantly reduced when we inhibited the S1R as shown in Figure 17C, a result confirmed by the endpoint tumor weights (Figure 17D).

Overall, our data show that the S1R plays an important role in the regulation of PCa cell proliferation.

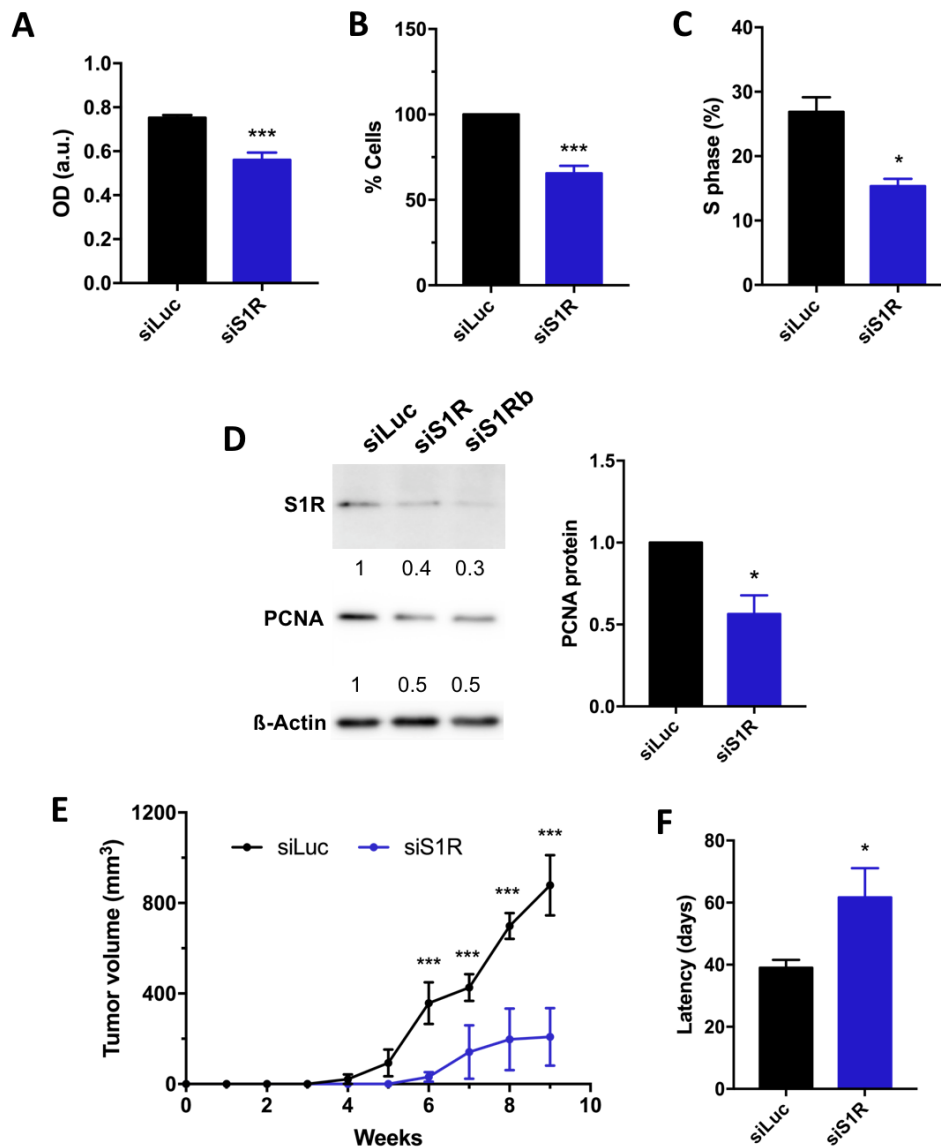


Figure 16: SIR inhibition decreases LNCaP cell proliferation and in vivo tumor growth

A. Optical density results of MTS viability assay, 4 days after transfection with a control siRNA (siLuc, 50 nM) or siS1R (n=3). **B.** Live cell counting (normalized to control condition) using Trypan blue, 4 days after siRNA transfection (n=13). **C.** Number of cells in S phase assessed by EdU assay, 4 days after siRNA transfection (n=3). **D.** Protein expression of the PCNA proliferation marker assessed by western blot, 4 days after transfection with a control siRNA (siLuc) or S1R targeting siRNAs (siS1R and siS1Rb). Representative image on the left, mean results on the right (n=4). **E.** Tumor growth in NMRI Nude mice subcutaneously injected with LNCaP cells transfected with siLuc or siS1R (50 nM) 16 hours prior to injection, 6 mice per condition. **F.** Latency of tumor detection in *in vivo* experiments showed in E. *p<0.05; ***p<0.001.

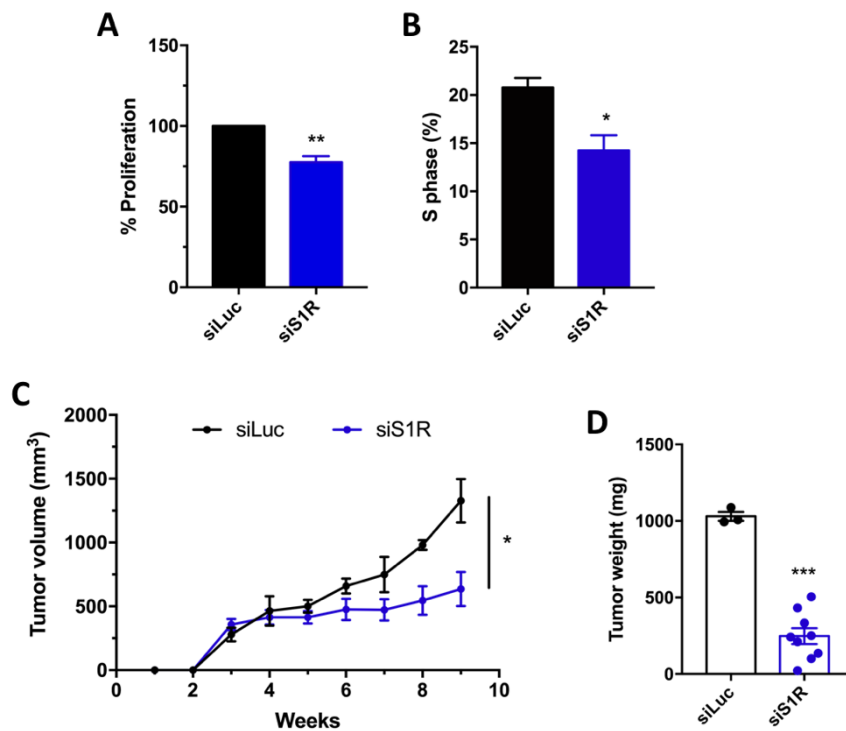


Figure 17: SIR inhibition decreases PC3 cell proliferation and in vivo tumor growth

A. Result obtained by MTS viability assay, 4 days after transfection with a control siRNA (siLuc, 50 nM) or siS1R (n=3). **B.** Number of cells in S phase determined by EdU assay, 4 days after siRNA transfection (n=3). **C.** Tumor growth in NMRI Nude mice subcutaneously injected with PC3 cells transfected with siLuc or siS1R (50 nM) 16 hours prior to injection (n=3 and n=9 respectively). **D.** Tumor weights upon sacrifice of the mice showed in C. *p<0.05; **p<0.01; ***p<0.001.

8. The S1R modulates PCa proliferation via SOC channels

We previously showed that Orai1 can regulate prostate CSC quiescence/proliferation transition, and that the S1R is a positive modulator of SOC channel in PCa cells. We therefore investigated whether the effect of the S1R on PCa cell proliferation implicated SOC channels. To do so, we inhibited the S1R and Orai isoforms, independently and in combination, and we assessed their impact on cell proliferation and viability with the MTS assay (Figure 18).

Our results first show that both Orai1 and Orai3 are implicated in LNCaP cell proliferation (Figure 18B) as it was previously reported (Dubois et al. 2014). Interestingly, Orai3 inhibition had significantly more effect than Orai1 inhibition alone, and similar effect than combined Orai1/Orai3 inhibition. Having confirmed the implication of Oraids in PCa proliferation, we then combined their inhibition with S1R inhibition.

First, when compared to S1R inhibition alone, Orai1 inhibition further decreased LNCaP cell proliferation from 0.56 ± 0.03 to 0.31 ± 0.04 (Figure 18C). Interestingly, the combined inhibition of

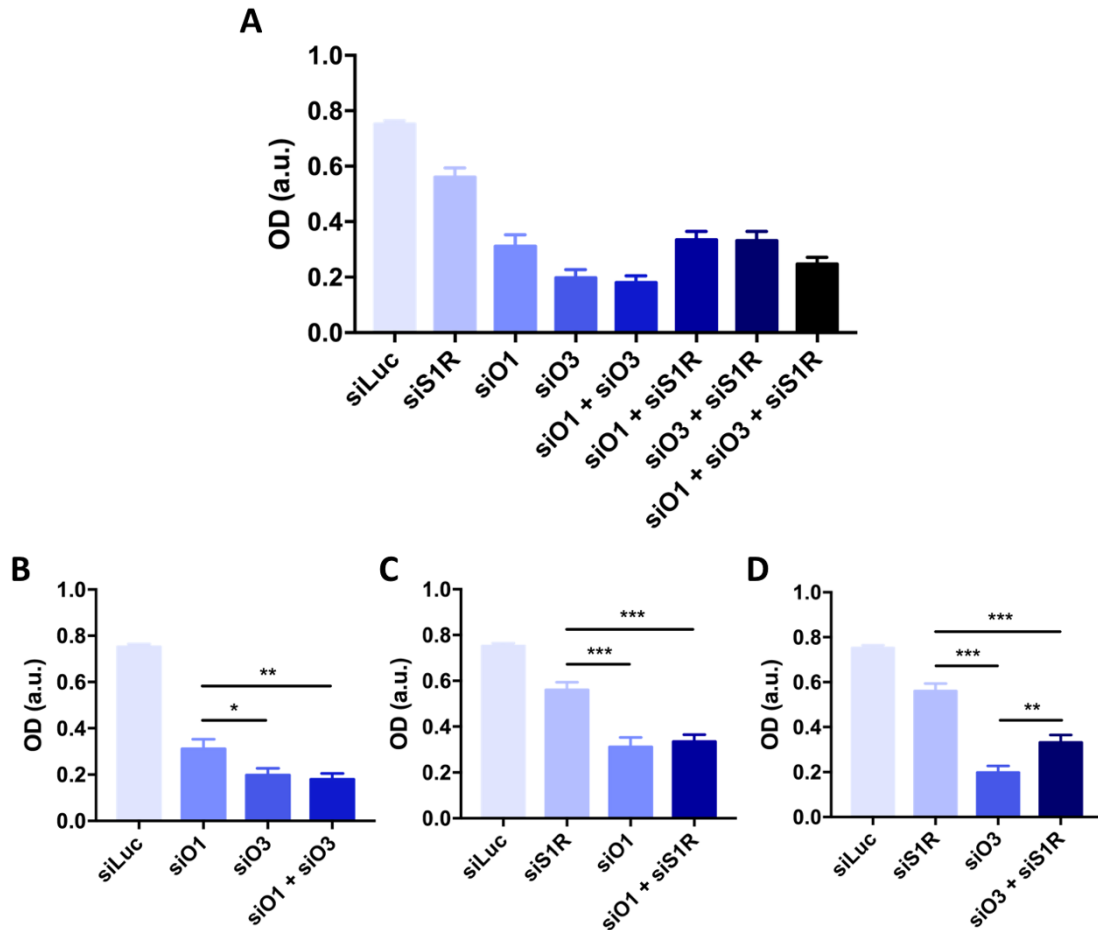


Figure 18: Effect of combined inhibition of the S1R and Orais

Optical density result obtained by MTS viability assay, 7 days after siRNA transfection (50 nM), siLuc was used as a control (n=4). **A.** Global results with all the conditions, detailed in B-D. All conditions are significantly different to control (siLuc) with $p < 0.001$. **B.** Comparison of Orai1 and Orai3 inhibition alone, and together. **C.** Comparison of S1R and Orai1 inhibition alone, and together. **D.** Comparison of S1R and Orai3 inhibition alone, and together. * $p < 0.05$; ** $p < 0.01$; *** $p < 0.001$.

S1R and Orai1 did not show any additive effect, i.e. did not decrease cellular proliferation any further. This result suggests that S1R's effect on LNCaP cells proliferation involves the SOC channels.

As previously stated, Orai3 recruits Orai1 to form ARC channels leading to SOCE inhibition. Those store-independent channels were previously shown to regulate PCa cell proliferation (Dubois et al. 2014). As our previous results indicate that the S1R is able to decrease Orai1/Orai3 association (Figure 15C), we wanted to see how they impacted PCa cell proliferation. As shown in Figure 18D, Orai3's effect on cell proliferation was significantly greater than S1R's with values of 0.20 ± 0.03 and 0.56 ± 0.03 respectively. However, the combined inhibition of Orai3 and the S1R increased cell proliferation as compared to Orai3 inhibition alone from 0.20 ± 0.03 to 0.33 ± 0.03 . Taken

together, our results support the idea that the S1R inhibits Orai3/Orai1 association to form ARC channels and decreases Orai3-mediated proliferation.

Reinforcing this hypothesis, the triple inhibition of Orai1, Orai3 and the S1R significantly decreased cell proliferation as compared to the double inhibition of Orai3 and the S1R from 0.33 ± 0.03 to 0.25 ± 0.02 ($p < 0.05$) (Figure 18A). Moreover, this triple inhibition was not significantly different from the combined inhibition of both Orai isoforms, showing that the S1R does not seem to influence PCa cell proliferation in the absence of Orai1 and Orai3.

It is important to note that these first results obtained with the MTS viability assay can also reflect altered cellular viability or mitochondrial activity. We are currently confirming these results with cell cycle and viability analysis (PI, EdU).

Although we have previously shown the importance of S1R alone in PCa growth, we are currently conducting *in vivo* experiments to confirm these results combined with Orai isoforms modulations.

9. *The S1R modulates NFATc3 nuclear translocation*

The Ca^{2+} -activated calcineurin-NFAT pathway has been shown to regulate PCa cells proliferation by our laboratory (Dubois et al. 2014; Raphaël et al. 2014; Thebault et al. 2006). As this transcription factor is a downstream target of the calcium entering the cells through SOCE, we evaluated its regulation by the S1R in our cells.

We used the NFATc3-mCherry construct to follow its cellular localization by confocal microscopy. When LNCaP cells were transfected with siS1R, NFATc3 nuclear translocation events were significantly decreased in basal conditions as shown by the representative images in Figure 19A & B, and the mean results in Figure 19C.

To confirm these results, we used a reporter construct with the luciferase gene preceded by an NFAT response element. By expressing this construct in our cells, endogenous NFAT activation leads to luciferase production, allowing to assess NFAT activity by measuring the luminescence produced by luciferin substrate processing. Confirming our previous results, S1R inhibition by siRNA significantly reduced NFATc3 activity in both LNCaP and PC3 cells (Figure 19D).

We also conducted dynamic studies of NFATc3 nuclear translocation upon SOCE using the NFATc3-eGFP fusion protein. Interestingly, S1R inhibition drastically affected NFATc3 nuclear translocation dynamics in our cells. As pictured in Figure 20, S1R knockdown accelerates SOCE-induced translocation of NFATc3 to the nucleus but curtails its nuclear retention. Indeed, the results summarized in Figure 20C clearly show that S1R inhibition leads to a rapid but transient NFATc3 nuclear translocation as compared to the control where the translocation is slower but sustained.

These results show that the S1R plays a crucial role in NFATc3 signaling. Indeed, NFAT activity as a transcription factor is highly dependent on the time spent activated within the nucleus. The highly transient NFAT translocation we witnessed with S1R inhibition would drastically change its

role within the nucleus and consequently shape the cellular response. This is well illustrated by our results presented in Figure 19D.

The S1R receptor thus seems to be a key protein allowing a sustained NFATc3 nuclear translocation. Taken together, our results show that the S1R regulated PCa cell proliferation via the SOC channels and their downstream regulation of NFATc3 translocation.

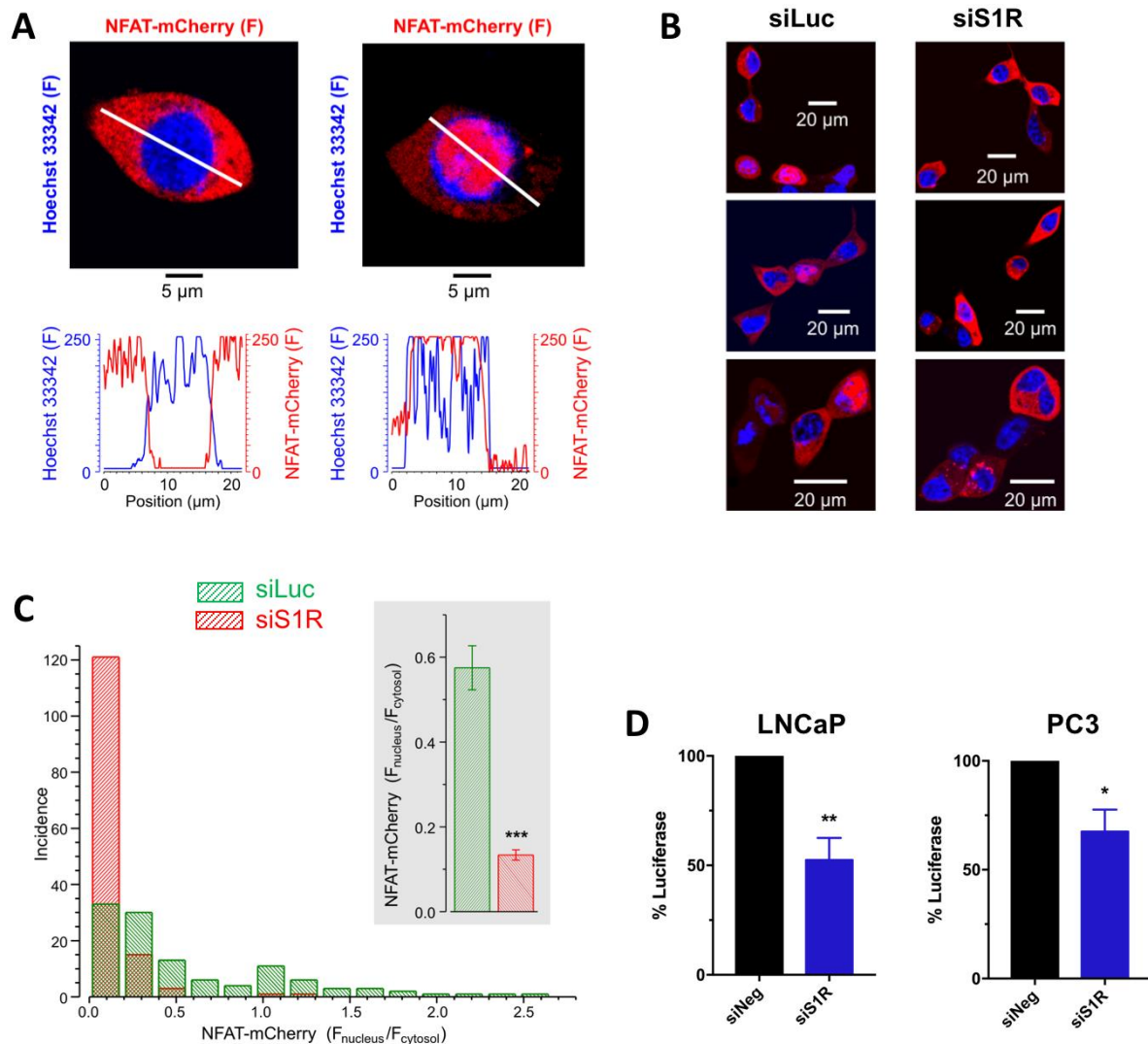


Figure 19: S1R inhibition decreases NFATc3 nuclear translocation and activity

A-C. NFATc3 nuclear translocation in basal conditions in LNCaP cells transfected with the NFATc3-mCherry construct (48 h), with Hoechst 33342-stained nuclei, followed by confocal microscopy. **A.** Representative images of NFATc3 translocation (top). On the bottom are showed fluorescence intensities along the white line represented in the images above. **B.** Representative images of NFATc3 localization in LNCaP cells transfected with control siLuc or siS1R (50 nM, 3 days). **C.** Mean results of NFATc3-mCherry translocation. **D.** Luciferase activity represented by the luminescence measured after incubation on total cell lysates with luciferin (normalized on control) in LNCaP cells (left, n=6) and PC3 cells (right, n=5), four days after transfection with either siNeg (control scramble siRNA) or siS1R (50 nM), 2 days after transfection with the luc2P-NFAT-RE construct.

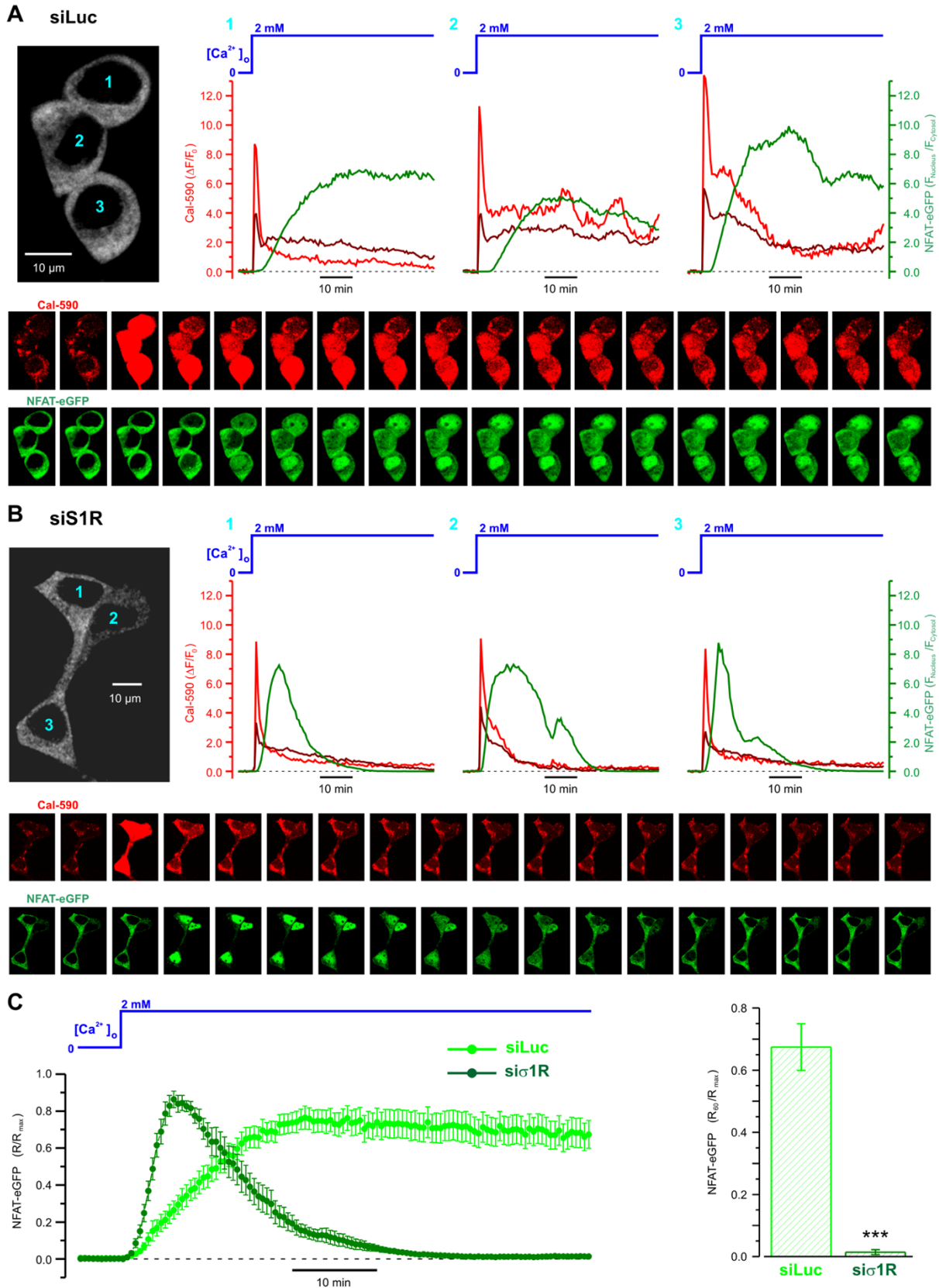


Figure 20: The S1R affects the dynamics of SOCE-induced nuclear translocation and retention of NFATc3 in LNCaP cells

The Ca^{2+} store depletion in LNCaP cells expressing NFATc3-eGFP was achieved by 20 min incubation in Ca^{2+} -free solution supplemented with 0.1 mM EGTA and 50 μM CPA. Following CPA washout, SOCE was activated by Ca^{2+} readmission (blue bars). **A-B.** Kinetics of SOCE-induced

Ca²⁺ responses in the nuclear region (red trace) and outside of the nucleus (wine trace), reported by relative changes in Cal-590 fluorescence ($\Delta F/F_0$; left axis), to the dynamics of NFATc3 translocation to the nucleus (olive trace), reported by the ratio of eGFP fluorescence inside and outside of the nucleus ($F_{\text{Nucleus}}/F_{\text{Cytosol}}$; right axis), in LNCaP cells pre-treated with either siLuc (A) or siS1R (B) for 48 hours. The plots are related to corresponding cells (images left) by the numbers (cyan). The galleries (bottom) show every 6th image of Cal-590 and eGFP fluorescence, as indicated. **C.** The plot (left) relates mean traces of self-normalized eGFP fluorescence ratio (R/R_{max} , where $R = F_{\text{Nucleus}}/F_{\text{Cytosol}}$ and R_{max} is the maximum of R detected in particular cell) obtained from siLuc- (green; n=18) and siS1R-treated (olive; n=12) cells. The bar diagram plot (right) compares corresponding fractions of the maximal response (R_{max}) remaining at the 60th min of the imaging protocol (57 min after stimulation). *** $p < 0.001$.

10. The S1R modulates prostate cancer cell quiescence via Orai1

As we previously reported, Orai1 plays a key role in the regulation of the quiescence/proliferation transition of prostate cancer cells presenting stem-like properties via the NFAT pathway. We thus wanted to check if the S1R could also have an effect in this particular subtype of cancer cells. Using our model of prostate LRCs, we are currently testing the effect of the S1R on PCa cell quiescence. To do so, we transfected PC3 cells with siRNAs targeting Orai1 or the S1R, and placed the cells in sphere forming conditions. Our preliminary results shown in [Figure 21](#) indicate that the inhibition of the S1R in PCa spheres increases the Dil-positive stem-like subpopulation after 7 days of sphere formation. Interestingly, the effect of S1R inhibition was similar to the one obtained with Orai1 inhibition, suggesting the involvement of the same pathway.

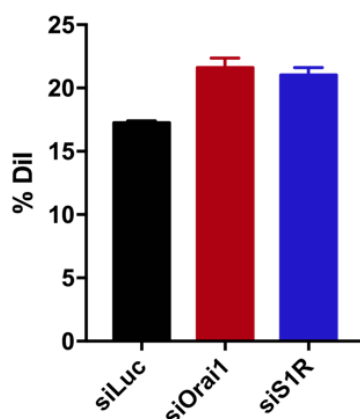


Figure 21: S1R inhibition increases the quiescent Dil-positive subpopulation

Histogram showing the percentage of Dil positive cells after 7 days of sphere formation with cells transfected with 100 nM of either control siLuc, siOrai1 or siS1R, determined by flow cytometry (n=2).

11. The S1R participates in apoptosis

Previous studies have shown that SOC channels are key regulators of PCa cell apoptosis (Flourakis et al. 2010). Indeed, extended activation of the SOC channels can lead to cytosolic Ca^{2+} accumulation that can then trigger apoptosis.

Flow cytometry analysis of cell DNA content (PI staining) indicated that S1R inhibition (siRNA, 48 h prior to cell death induction) significantly increased LNCaP cell resistance to thapsigargin-induced apoptosis (2 μM , 24 h), as shown by the decreased number of cells with fragmented DNA assessed by PI staining and flow cytometry ($18.20 \pm 0.82\%$ to $14.66 \pm 0.94\%$; Figure 22A). This result was confirmed by morphonuclear detection of apoptotic nuclei where the number of apoptotic cells was decreased from $16.67 \pm 1.06\%$ to $9.42 \pm 1.03\%$ (Figure 22B).

Interestingly, we obtained preliminary results indicating that the pro-apoptotic effect of the S1R can also be found in response to docetaxel (DoceT), a chemotherapy drug widely used to treat PCa (Figure 22C).

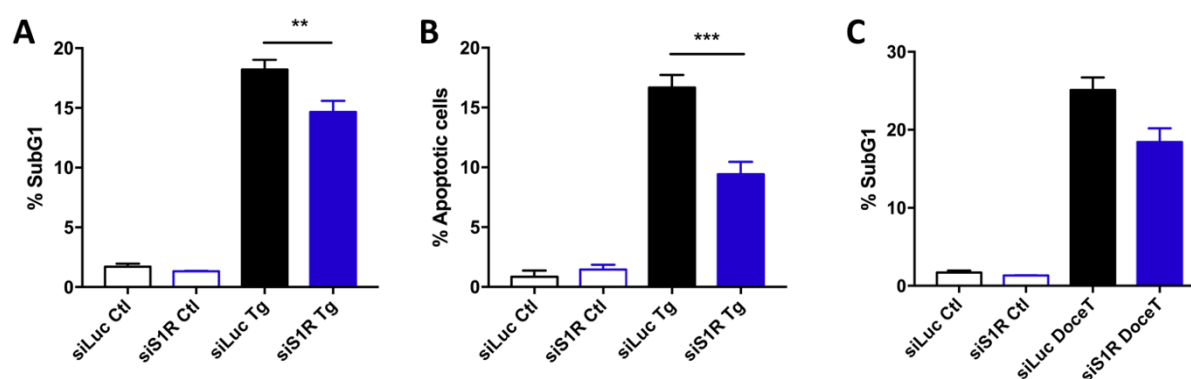


Figure 22: S1R inhibition increases apoptosis resistance in LNCaP cells

A-C. LNCaP cells transfected with either siLuc or siS1R (50 nM, 48 h). **A-B.** Cells were treated with 2 μM thapsigargin for 24 h, or DMSO (at equivalent volume) as a control. **A.** Flow cytometry results of cell cycle analysis in PI stained cells. Histogram show the number of cells (% from the total population) in the SubG1 phase with fragmented DNA (n=4). **B.** Histogram show the percentage of apoptotic cells assessed by morphonuclear analysis of Hoechst 33342-stained cells. **C.** Flow cytometry results of cell cycle analysis in PI stained cells. Histogram show the number of cells (% from the total population) in the SubG1 phase with fragmented DNA. LNCaP cells were treated with docetaxel (DoceT, 10 nM, 24 h) or DMSO as a control (n=2). **p<0.01; ***p<0.001.

12. The S1R is also able to modulate the activity of TRPV6

Previous studies have shown that calcium channels other than Orais play key roles in prostate carcinogenesis (Monteith et al. 2017). Among them, we can find TRPV6 (transient receptor potential vanilloid 6). Absent in healthy prostate and BPH, TRPV6 is upregulated with PCa and correlates with aggressiveness (Fixemer et al. 2003; Wissenbach et al. 2004). Previous results showed that this channel is implicated in PCa cell proliferation and apoptosis via its late recruitment to participate in SOCE (Lehen'kyi et al. 2007; Raphaël et al. 2014). Indeed, authors showed that upon SOC channel activation, TRPV6 is recruited to the PM and contributes to increase cell proliferation and enhance apoptosis resistance.

Because of the effect of the S1R on SOCE, we investigated the effect of this chaperone protein on TRPV6 activity. Our preliminary results show that S1R overexpression strongly inhibits TRPV6 activity in HEK-293 cells (Figure 23).

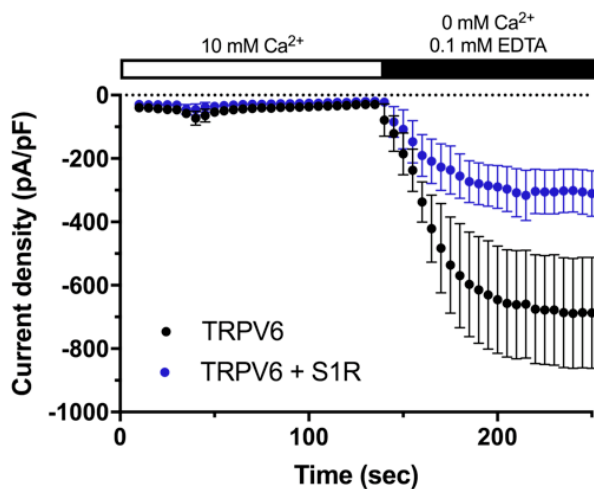


Figure 23: The S1R decreases TRPV6 activity in HEK-293 cells

Results of whole-cell patch-clamp experiments in HEK-293 cells transiently transfected with TRPV6 alone (black) or with the S1R (blue). Average time-course of Ca^{2+} I_{TRPV6} with 10 mM Ca^{2+} , followed by Na^{+} I_{TRPV6} in divalent free solution, currents are monitored at -100 mV.

These results show that S1R modulation of SOCE in PCa is more complex than we initially thought, as the S1R is able to shape the SOCE in additional ways via TRPV6. It would therefore be interesting to elucidate the modalities and physiological consequences of this modulation in prostate cancer.

13. The S1R increases TRPM8 activity, enhancing its antimigratory effect in PCa

The TRPM8 (transient receptor potential melastatin 8) calcium channel is mainly known as a cold receptor in the peripheral nervous system, but it was originally identified in prostate (Tsavaler et al. 2001). Interestingly, TRPM8's expression is positively regulated by androgens (Bidaux et al. 2007), and as a consequence, this channel is overexpressed in androgen-sensitive PCa, but its expression is decreased after androgen-deprivation therapy (Henshall et al. 2003). Moreover, TRPM8 was shown to have an inhibitory role on PCa cell migration (Gkika et al. 2010; Yang et al. 2009b).

We performed patch clamp experiments to study the effect of the S1R on TRPM8 activity in HEK-293 cells transiently transfected with TRPM8. As shown in Figure 24, the overexpression of the S1R increases TRPM8 activity in these cells.

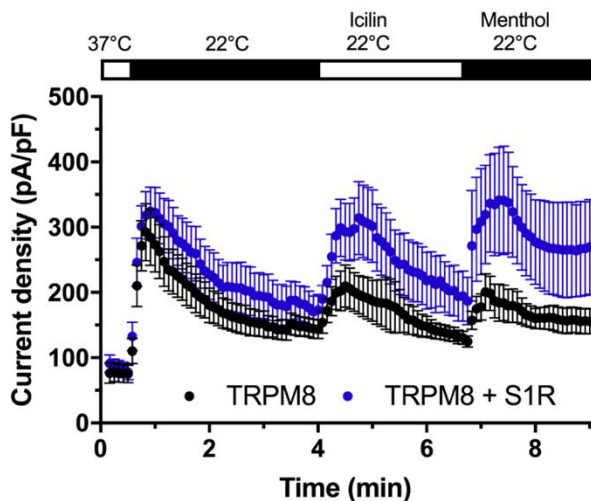


Figure 24: The S1R increases TRPM8 activity in HEK-293 cells

Results of whole-cell patch-clamp experiments in HEK-293 cells transiently transfected with TRPM8 alone (black) or with the S1R (blue). Average time-course of I_{TRPM8} sequentially activated by cold (22°C), icilin (10 μ M) and menthol (200 μ M), currents are monitored at +100 mV.

We then used a PC3 cell line stably expressing TRPM8 developed in our laboratory to show that this effect was also found in PCa cells. Indeed, the inhibition of the S1R by siRNA led to a decreased calcium entry by TRPM8 in response to menthol activation (Figure 25A).

As previously stated, TRPM8 inhibits PCa cell migration, and as expected, the inhibition of the S1R by siRNA lead to an increased migration of PC3-M8 cells (Figure 25B). We also overexpressed the S1R in this cell model and confirmed its anti-migratory through the modulation of TPM8 activity (Figure 25C).

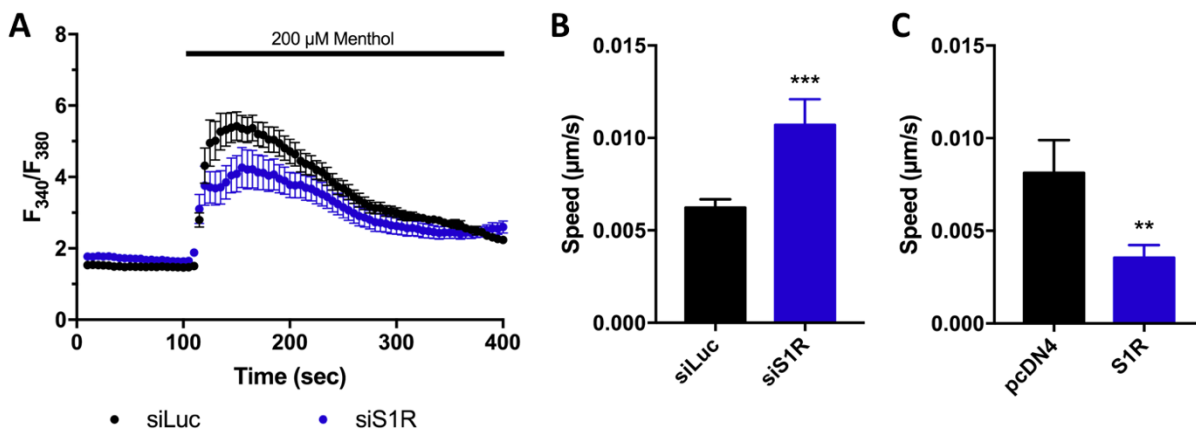


Figure 25: The S1R increases TRPM8-mediated inhibition of PCa cell migration

A. Time course of calcium ratios obtained by calcium imaging in PC3-TRPM8 cells transfected with siLuc or siS1R (50 nM, 3 days), menthol application is indicated by the bar. **B-C.** Average cell migration speed in random migration assays on PC3-TRPM8 cells transfected with siLuc or siS1R (B, n=3) or with an empty vector or the S1R in (C, n=3).

Taken together, our results suggest that the expression of both S1R and TRPM8 in early hormone-dependent prostate cancer could have a protective effect by preventing PCa migration. Then, when PCa progresses towards advanced hormone-resistant stages, the strong decrease in TRPM8 and S1R expressions could favor cancer cell migration and subsequent metastasis development. This hypothesis, while promising, will need further studies that are however beyond the scope of this work.

Discussion

In this work, we first identified a calcium-dependent signaling pathway governing cancer cell stemness. We also show that this same pathway, implicating the SOC channels and NFAT, is able to regulate PCa cell proliferation. Interestingly, our data indicate that this pathway can be regulated by the S1R via direct interaction with STIM1 and Orai1, offering new SOC-targeting possibilities.

1. Orai1/NFAT pathway is a key player of the proliferation/quiescence transition

In this study, we first present new data supporting the idea of cytoplasmic calcium presiding over CSCs' determination toward either proliferation or quiescence. Using two cancer models as different as neural crest-derived melanoma and epithelial prostate cancer, we conclude that the Orai1 calcium channel and its classic downstream calcineurin-NFAT signaling, are the key actors responsible for a Ca^{2+} -mediated switch between stem-like cells quiescence and activation in stem-like cells.

Furthermore, our data suggest that Orai1/calcineurin/NFAT signals exert their regulatory function by cooperating with CBP transcriptional coactivator, which segregates with an inactive Orai1/NFAT signal. This suggests that the $CBP^{hi}/Orai1^{lo}/NFAT^{inactive}$ phenotype is a new marker for melanoma and prostate stemness.

It has been suggested that calcium channels display a functional specificity in the activation of Ca^{2+} -dependent transcription factors and gene expression. Consistent with this hypothesis, NFAT translocation and NFAT-dependent gene expression have been shown to be dependent on Orai1-mediated Ca^{2+} entry (Kar et al. 2014; Ong et al. 2012). NFAT is regulated by the Ca^{2+} concentration achieved locally near the Orai1 channel, likely due to a co-localization of calmodulin-calcineurin-NFAT within the Orai1-associated nanodomain, in such a way that Ca^{2+} entering via Orai1 can be locally detected by the calcium sensor. It has been proposed that NFAT activation, strictly dependent on Orai1, follows an "all-or-none" mode. If an insufficient number of Orai1 channels are activated, NFAT dephosphorylation is not completed and nuclear translocation does not occur (Ong et al. 2012). Our result that NFAT is predominantly localized in the nucleus of proliferating cells, whilst its distribution is mainly in the cytoplasm in quiescent cells, could therefore be explained by the reduced number of activated Orai1 channels in a quiescent stem-like cell population.

We show that when activated, NFAT cooperates with CBP to control quiescence and the pool of stem-like cells. The influence of CBP in CSC's fate does not appear to be exceptional. CBP and its homolog p300 protein were shown to balance self-renewal and differentiation of hematopoietic stem cells (Rebel et al. 2002), to maintain the self-renewal and pluripotency of embryonic stem cells (Fang et al. 2014) and to govern quiescence, proliferation and differentiation of normal and tumor stem cells (Kida and Kahn 2013; Wang et al. 2013). Our study mechanistically links CBP to calcium signaling and suggests that CBP interacts with the NFAT transcription factor to balance

stem-like cells' quiescence/activation state and determine stem or non-stem cells' fates. Thus, we provide one possible explanation of how Ca^{2+} is capable of contributing to cellular processes as diametrically opposed as quiescence, proliferation and differentiation.

Interestingly, inhibitors of Orai1 (BTP2), as well as calcineurin (FK506), both inactivated NFAT and significantly increased the stem-like cells compartment encompassing both quiescent G0 and slow cycling cells at the expense of the fast proliferating cell compartment, thus demonstrating that Orai1-signaling activates quiescent cells with stem-like properties and stimulates their exit from the stem cell compartment. As these phenotypic changes are accompanied by variations in Ca^{2+} influx and its intracellular concentration, it becomes clear that Orai1 is at the top of the signaling network that controls stem like cells' cycling activity and determines their fate. We are currently confirming these results using Orai1 targeting siRNAs. Evidence corroborating this interpretation is provided by a direct relationship between Orai1/SOCE and entry into quiescence of melanoma and prostate stem-like cells in response to stress-inducing chemotherapeutics. This is an important observation given that Orai1 function was linked to apoptosis (Cui et al. 2013; Flourakis et al. 2010; Henke et al. 2013), so its downregulation may represent an important mechanism of drug resistance acquired by cellular retraction into a reversible quiescence, an attribute of stem cells (Borst 2012). This result is in agreement with a previous report (Jia et al. 2011), where it was shown that PCa cells overexpressing the stem cells marker SOX2, were exhibiting a reduced expression of Orai1 as well as a decreased SOCE. As in our case, these features were associated with a higher resistance of cells to apoptotic inducers, confirming that the Orai1^{lo} phenotype is a new marker of stemness, at least in melanoma and PCa.

Various studies have clearly stated that inhibition of Orai1 blocks both SOCE and proliferation in cancer cells (Dubois et al. 2014; Umemura et al. 2014). Our data suggest that, rather than a decrease in cell proliferation as in non-CSCs, a loss of SOCE in CSCs elicits an increase in their quiescence. Therefore, while targeting Orai1 would eradicate proliferating cells, it would also increase the pool of drug-resistant CSCs constituting a reservoir of dormant tumor-initiating cells underlying tumor dormancy. If controlled, Orai1-inactivation would therefore offer an anticancer therapy by chronic tumor cell dormancy, potentially preventing tumor relapse. On the other hand, Orai1 activation would force the cell towards a proliferative phenotype, allowing their targeting by conventional chemotherapy.

Interestingly, our data show a common mechanism for quiescence regulation of both melanoma and PCa stem-like cells. It would be interesting to see if this mechanism can be observed in other CSC models.

II. The S1R, a new partner of SOC channels in PCa

1. S1R expression is regulated by androgens in PCa cells

We show here for the first time that S1R expression is regulated by androgens in PCa cells. We have confirmed at mRNA and protein levels that the S1R is overexpressed in PCa using two different cohorts of human samples. Interestingly the removal of the androgen stimulus significantly decreases the expression of the S1R in PCa cells. The S1R has been shown to bind neurosteroids such as progesterone, but there is no evidence of testosterone binding (Su et al. 1988). Our experiments show that both DHT and the AR are required to maintain high S1R expression in androgen-sensitive LNCaP cells. Moreover, our results here indicate that this regulation is not direct, as 4 hours of treatment do not affect S1R mRNA levels. Moreover, these results were confirmed by reintroducing the AR in the androgen-resistant PC3 cell line, which led to a significant increase in S1R expression. Interestingly, when S1R sequence was first analyzed, authors identified a steroid responsive element (Prasad et al. 1998). Additional studies will however be needed to understand how the androgens are able to regulate S1R expression in PCa cells.

Interestingly, a recent study showed that the S1R, acting as a chaperone protein, is able to stabilize the AR in PCa cells (Thomas et al. 2017). Authors show that S1R inhibition leads to inactivation and degradation of the AR, thus affecting PCa physiology. When combined with our results, these data suggest the existence of a positive feedback mechanism maintaining a strong expression of the S1R in androgen-sensitive PCa cells via AR signaling. It is important to note that, in our hands, S1R inhibition by siRNA did not cause the loss of AR or the development of an androgen-deprived (i.e. neuroendocrine) phenotype in LNCaP cells, suggesting that although AR stabilization may decrease, the associated signaling pathway remains sufficient to maintain a strong AR expression and a differentiated phenotype. A plausible explanation for this absence of effect of a siRNA targeting S1R could be the relatively high expression level of this protein in LNCaP cells. Indeed, generation of LNCaP cells stably expressing a shRNA against S1R showed us the difficulty to reduce S1R expression to a low enough level associated with phenotypic changes. We hope that the generation of a KO LNCaP cell model using CRISPR/Cas9 technology (clustered regularly interspaced short palindromic repeats/CRIPR-associated protein 9; in collaboration with Dr Soriani, iBV Nice, France) will allow us to overcome this caveat, and will provide us with a clean background in which we will further decipher the interaction between AR and S1R.

Our results show that the S1R is overexpressed in the early androgen-sensitive stages of PCa in correlation with aggressiveness, and then, during ADT, the expression of the S1R decreases ([Figure 1](#)). However, the expression in androgen-resistant PCa cells evading ADT remains to be determined using human samples. PCa cells can evade ADT in different ways, via either AR-dependent or independent pathways (reviewed in Crona and Whang 2017). Thus, the study of

S1R in CRPC samples could lead to mixed results, dependent on the dominant mechanism of resistance in the tumor tested.

2. *Orai1 expression is regulated by androgens in PCa cells*

A previous study showed that the expression of Orai1 could also be androgen-sensitive in PCa cells. Our results clearly confirm Orai1 dependence on androgens, with treatments such as steroid removal or direct AR inhibition (siRNA or Casodex®) leading to Orai1 down-regulation in LNCaP cells, and reintroduction of the AR in PC3 cells increasing Orai1 expression (Figure 1). It is well known that prostate CSCs are less differentiated and express little to no AR. Indeed, through the AR, androgens promote the differentiation and proliferation of prostate epithelial cells. This was recently confirmed in a study, along with the identification of the mechanisms responsible for AR degradation in prostate CSCs, maintaining their stemness (Vummidi Giridhar et al. 2019). This work is therefore in good accordance with our results on prostate stem-like cells, where we showed that quiescent cells exhibit low Orai1 expression and activity. This decrease could also be associated, in a more physiological context (i.e. tumors), to a down-regulation of the AR and androgens.

We also performed experiments to study STIM1 and Orai3 expressions in PCa. STIM1, whose expression remains unchanged in PCa (Dubois et al. 2014), does not appear to be regulated by AR, DHT or steroids in general (Figure 1). Orai3, on the other hand, has been shown to be overexpressed in PCa, in correlation with aggressiveness. Our results show that neither Casodex® nor DHT impacted this channel's expression, whereas steroids seemed to have an effect (Figure 1). Indeed, steroids removal from the culture medium significantly increased Orai3 expression in androgen-sensitive LNCaP cells. However, steroids, more precisely estrogens, have been shown to positively regulate the channel's expression in BCa cells (Motiani et al. 2013). It would thus be interesting to perform additional experiments in order to understand what happens in PCa cells regarding Orai3 modulation.

Altogether, these data allow us to present a potential expression profile of Orai1, Orai3, STIM1 and the S1R during PCa progression towards late androgen-resistant stages (Figure 1). However, due to the difficulties to obtain samples of patients with CRPC, data are lacking for the advanced stages. It would be especially interesting to confirm our *in vitro* data on patients undergoing androgen-removal treatments, and to follow the expression of these proteins during the onset of castration resistance. This is indeed a necessary step before proposing any of these proteins as new markers, and to potentially target them during the different stages of PCa progression.

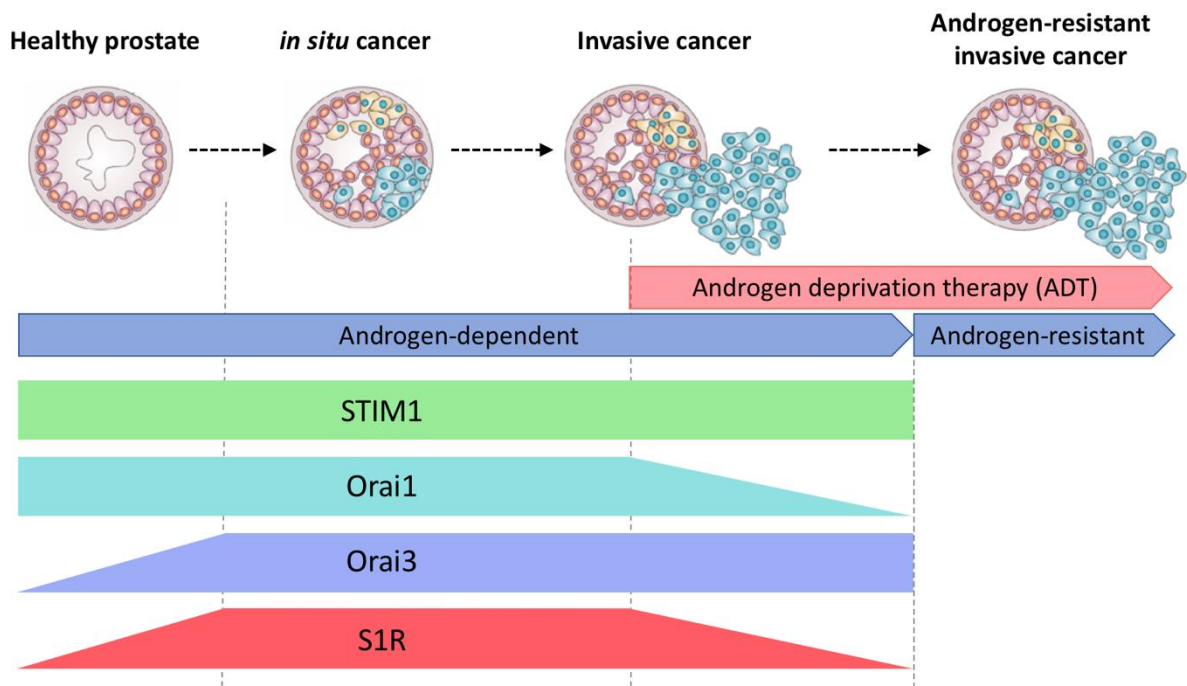


Figure 1: Expression profile of our proteins of interest during PCa progression
Adapted from Witte 2009

3. The S1R positively modulates SOC channels in PCa cells

In the second part of this study, we identified a new partner protein for SOC channels in PCa: the S1R.

Our data here show that in basal conditions, the S1R binds STIM1 in the ER. Then, upon SOC channel activation via ER calcium store depletion, the S1R translocates towards the PM and interacts with Orai1. Our current results point towards a dissociation between the S1R and STIM1 upon SOC activation, but further characterization will be necessary to conclude on this point because our current construct do not take into account the dramatic conformational change STIM1 undergoes to activate Orai1. From our results so far, two hypotheses can be outlined: during SOC activation. S1R could stay bound to STIM1, and the two proteins could diffuse together towards ER-PM junctions where both S1R and STIM1 bind Orai1. Another hypothesis would be the loss of the STIM1/S1R interaction during the conformational change STIM1 undergoes during its activation, this loss of interaction could trigger S1R translocation towards the PM to interact with Orai1 independently of STIM1.

Furthermore, our results indicate that through its interaction with Orai1, the S1R is able to increase SOC channel activity and SOCE in PCa cells. This result comes in opposition with a recent finding showing that the S1R inhibits SOC channels (Srivats et al. 2016). However, our data shows that the hS1R is capable of positive SOC modulation, as opposed to the rS1R, used for the study cited

above, which exerts an inhibitory effect in our cells. The origin of this difference is unclear, as the S1R is highly conserved between the two species and sequence alignment did not allow us to understand its opposed effect on SOC in our cells. To better understand this mechanism, we are currently building a rat/human chimera of the S1R that we will characterize functionally using patch-clamp and calcium imaging.

The precise mechanism by which the S1R is able to increase SOC activity remains to be elucidated. Our results indicate that the S1R could have both fast and long-term effects on SOCE. It would be interesting to do additional experiments to better understand these effects. Using the microscopy technique of FCCS (fluorescence cross-correlation spectroscopy) that follows the movement of fluorescent proteins within a small volume, we could see if the S1R influences STIM1 and/or Orai1 diffusion towards ER-PM junctions. This technique could also indicate if STIM1/S1R or Orai1/S1R move together during SOCE activation. We are currently conducting experiments to see if the S1R is able to affect STIM1 and Orai1 expressions at both mRNA and protein levels, as well as Orai1 presence at the PM. Indeed, the S1R has been shown to positively regulate ion channels by helping their maturation within the ER and their trafficking towards the PM (Crottès et al. 2011). We are also planning to perform TD-FLIM experiments to evaluate the effect of the S1R on Orai1/STIM1 coupling.

Interestingly, our results show that although S1R expression is low in androgen-resistant PC3 cells, due to the absence of the AR, S1R also has a significant effect on SOCE in these cells as well, reinforcing its importance.

Finally, our data show that the S1R decreases Orai1/Orai3 interaction. As previously reported, Orai1/Orai3 heteromers may form the store-independent ARC channels in PCa cells (Dubois et al. 2014). The S1R could thus favor the recruitment of Orai1 to form homohexamers participating in SOCE at the detriment of ARC channels. These results show that the S1R should decrease ARC channel activity in PCa cells. However, this effect on ARC activity still needs to be confirmed, as we were not able to reproducibly record any arachidonic acid-activated current or associated calcium entry in our cells.

Together with expression profiles, these data allow us to draw a profile of SOC and ARC activity during the initial stages of PCa development ([Figure 2](#)). In untreated androgen-sensitive PCa, Orai3 overexpression increases ARC channel activity. Although Orai1 and STIM1 expressions remain unchanged, S1R overexpression will allow a strong SOC channel activity. Then, during ADT, both S1R and Orai1 expressions will drop, whereas Orai3 expression remains unchanged. As a consequence, SOC activity would drop and ARC activity would increase leading to the oncogenic switch previously described (Dubois et al. 2014).

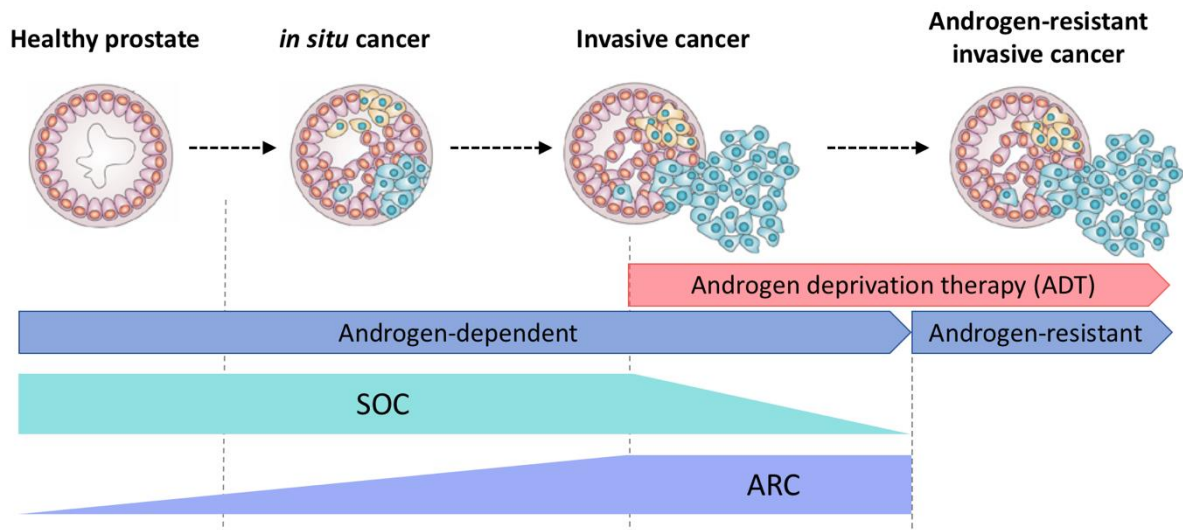


Figure 2: Activity profiles of SOC and ARC channels during PCa progression
Adapted from Witte 2009

4. S1R modulates PCa proliferation via the SOC/NFAT pathway

Finally, our results show that through its modulation of the SOCE, the S1R regulates PCa proliferation, quiescence and apoptosis.

Previous studies showed that S1R pharmacology can modulate cell proliferation and apoptosis in other cancers (Brent et al. 1996; Brent and Pang 1995; Kim and Maher 2017; Moody et al. 2000; Spruce et al. 2004; Vilner et al. 1995a). However, in these studies, no precise mechanism was identified. Here, we first show that S1R inhibition (siRNA) decreases PCa cell proliferation *in vitro* and tumor growth *in vivo*, without affecting basal viability. Furthermore, we show that Orai1 inhibition further decreases PCa cell proliferation and that the combination with S1R inhibition has no additive effect. These results, that we are currently validating *in vitro* (cell cycle) and *in vivo*, show that, in LNCaP cells, the S1R modulates proliferation via SOC channels. Furthermore, our results indicate that the S1R has a dramatic impact on NFAT nuclear translocation. Indeed, S1R inhibition prevents sustained nuclear translocation of NFATc3, the major isoform involved in PCa cells, and the time NFAT spends active in the nucleus plays a critical role to determine which set of genes it will activate. These results show how the S1R can shape cell fate via the NFAT transcription factor. Interestingly, it was recently shown that the NFATc3 isoform translocation requires both calcium from sub-plasmalemmal microdomains and calcium mobilization from the nuclear envelope via the IP₃R (Kar et al. 2016). As the role of the S1R in IP₃R modulation has been extensively documented (Su et al. 2016), it comes to question how the S1R modulates NFAT activation in PCa cells: via its positive modulation of the SOC channels, of the IP₃R, or both? We performed confocal dynamic experiments to evaluate NFATc3 translocation in LNCaP with or without IP₃R inhibition (xestospongin C) and saw no effect on NFATc3 nuclear translocation.

These results show that IP₃R are not required to induce NFATc3 translocation in our cells, and that the S1R modulates NFAT via direct interaction with Orai1 and SOCE modulation. Furthermore, as previously mentioned, the S1R is able to stabilize the AR in PCa cells. Thus, S1R inhibition can also decrease PCa cell proliferation and tumor growth by reducing AR signaling (Salvino et al. 2017; Thomas et al. 2017). However, the fact that S1R knockdown also inhibits *in vitro* proliferation and *in vivo* tumor growth in AR-lacking PC3 cells strengthen the importance of the SOC/NFAT pathway in the control of proliferation.

Moreover, we show that S1R inhibition increases apoptosis resistance by limiting SOCE, an important factor to trigger apoptosis via cellular calcium overload. These results are in line with previous reports showing that decreased SOCE leads to apoptosis resistance in PCa cells (Flourakis et al. 2010).

Finally, we present first results showing that SOCE modulation by the S1R could also regulate stem-like cell quiescence via the mechanism characterized in the first part of this work, although additional experiments will be needed to confirm it.

Taken together our data thus show that, through SOC modulation, the S1R plays a critical role in PCa cell physiology.

On the other hand, a previous study showed that ARC channels were also able to regulate PCa cell proliferation via the NFAT pathway (Dubois et al. 2014). As previously stated, our results show that the S1R reduces Orai1/Orai3 interaction, indicating that the S1R could limit ARC-regulated PCa cell proliferation. We present first data here supporting this possibility: we show that Orai3 inhibition decreases PCa cell proliferation significantly more than combined S1R/Orai3 inhibition. To better understand what happens, it is essential to put these data in perspective with the expression profiles and consequent channel activities we have identified so far during PCa evolution (Figure 3). Our data indicate that during androgen-sensitive PCa, the strong SOC channel activity will lead to a high proliferation associated with an elevated sensitivity to apoptosis. However, during ADT, the balance between SOC/ARC activities will switch towards a predominant ARC profile (the oncogenic switch described by Dubois and colleagues) due to AR signaling impairment. As a result, PCa cell will present a more aggressive profile with high proliferation associated with apoptosis resistance. Moreover, by decreasing Orai1 expression, ADT could favor the development of highly aggressive stem-like PCa cells.

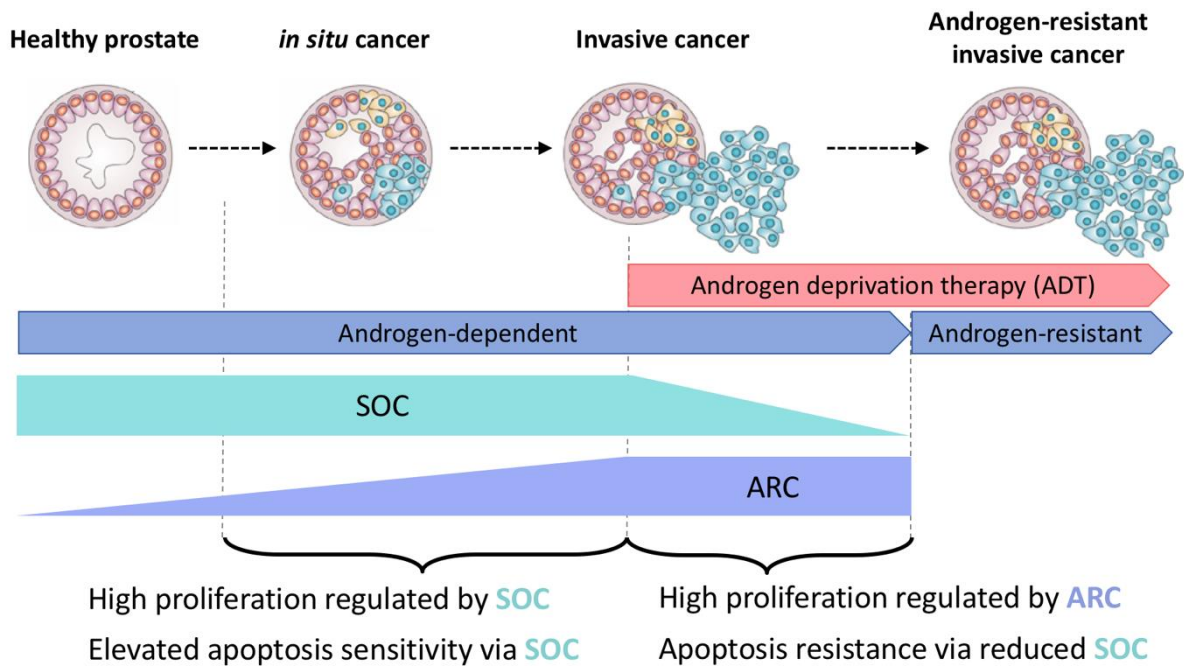


Figure 3: Physiological consequences of the SOC/ARC balance during PCa progression
Adapted from Witte 2009

5. S1R modulates other calcium channels in PCa cells

S1R being a chaperone protein, it can target and modulate other proteins, leading to a situation more complex than the “simple” modulation of Orais in PCa.

The regulation of IP₃R by the S1R has been well documented over the years in neurons (Su et al. 2016). As regulators of the ER calcium content, IP₃R can have a key role in SOC channels modulation. It would thus be interesting to investigate the relationship between IP₃R and the S1R in the context of PCa. Although we ruled out IP₃R implication in the regulation of NFAT translocation, it would be interesting to determine if the effect of the S1R on apoptosis is also partly mediated by IP₃R. Interestingly, IP₃R have been shown to be implicated in PCa apoptosis resistance via androgens signaling (Boutin et al. 2015).

Moreover, we showed preliminary results indicating that the S1R could also inhibit the TRPV6 channel, a secondary participant of SOCE that has been shown to regulate proliferation and apoptosis in PCa (Lehen'kyi et al. 2007; Raphaël et al. 2014). These data show that the S1R has a more complex effect on general SOCE in PCa than initially expected. TRPV6, absent in healthy prostate, is expressed in high levels in PCa cells in correlation with aggressiveness (Fixemer et al. 2003; Wissenbach et al. 2004) (Figure 4). Although the androgen-dependency of this channel has been debated, there has been no evidence of direct modulation of TRPV6 by the AR. The regulation of TRPV6 by the S1R should therefore be studied to better understand the general effect of the S1R on SOCE and its physiological consequences. If TRPV6 inhibition by the S1R is confirmed in PCa, we could hypothesize that in hormone-resistant advanced PCa, when SOCE is

strongly decreased due to the decreased expression of both S1R and Orai1, TRPV6 could participate to the regulation of PCa proliferation.

We also obtained results indicating that the S1R is able to increase TRPM8 activity. Furthermore, our data indicate that this modulation enhances TRPM8's anti-migratory effects in PCa cells (Gkika et al. 2010; Yang et al. 2009b). Interestingly, TRPM8's expression has been shown to be regulated by androgens in PCa cells, and thus present an expression profile similar to the S1R's (Bidaux et al. 2007; Henshall et al. 2003) (Figure 4). Moreover, TRPM8 has been shown to have many different isoforms, some of them crucial for ER-mitochondria calcium signaling (Bidaux et al. 2018a), the main subcellular localization of the S1R. Further investigation will be necessary to elucidate TRPM8 regulation by the S1R and understand its consequences.

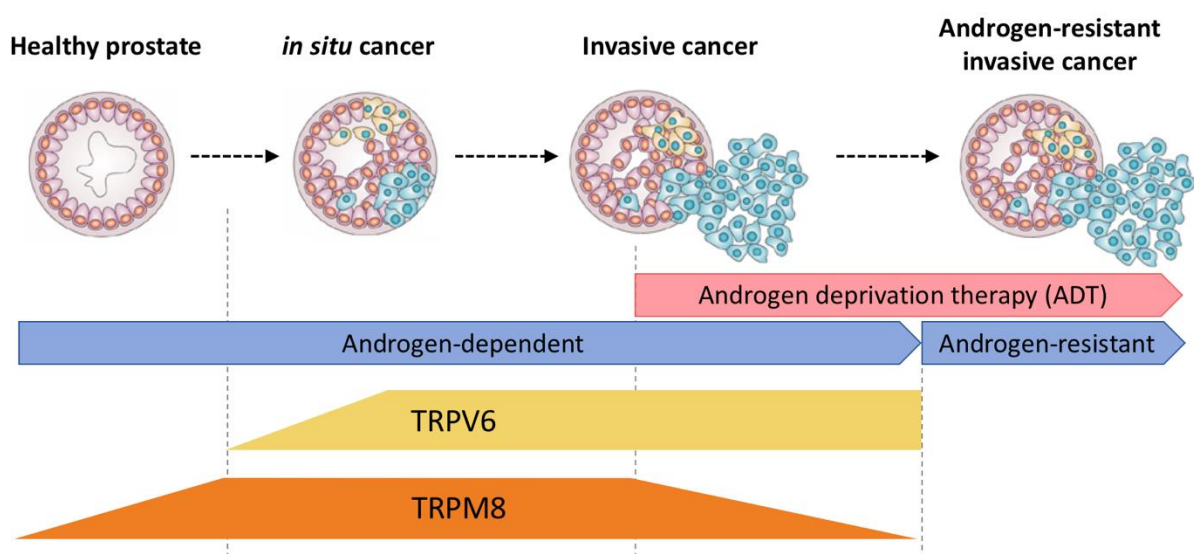


Figure 4: TRPV6 and TPM8 expression profiles during PCa progression
Adapted from Witte 2009

Altogether, these data show that the S1R, through the modulation of various proteins, has a complex role in PCa that we are only starting to unravel (Figure 5).

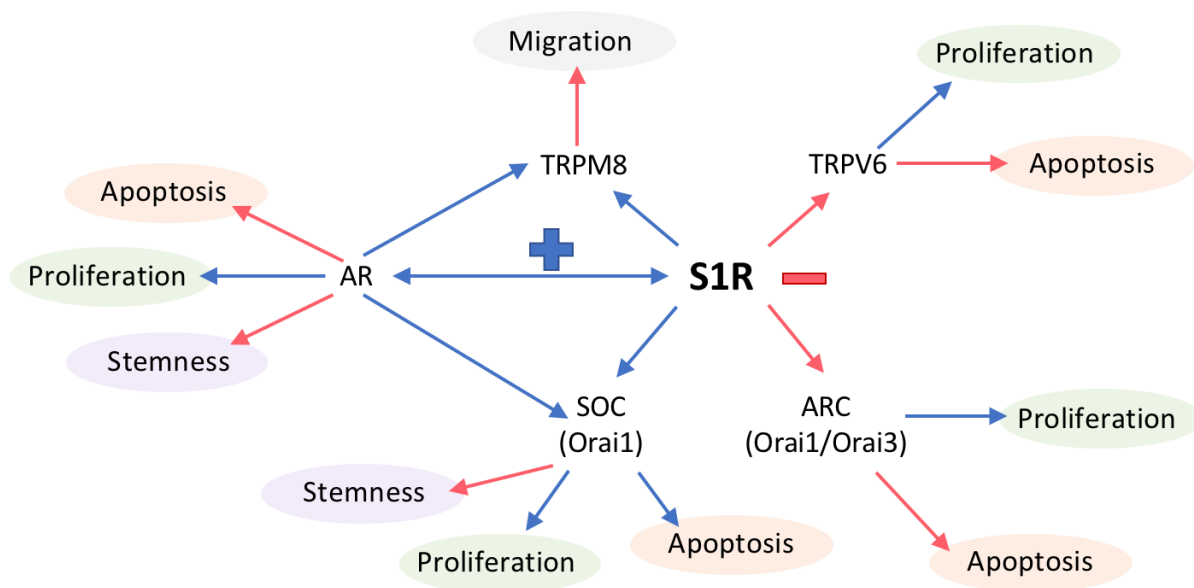


Figure 5: Potential roles of the S1R in PCa
Positive regulations are in blue, negative regulations are in red.

6. *The S1R: a new pharmacological target for PCa treatment?*

For all of the reasons mentioned above, the S1R is an exciting new target for PCa treatment. As stated before, the S1R can bind many different compounds, some already used in clinics. We show in this study results indicating that S1R ligands such as Igmesine and SKF10047 are able to increase SOCE in PCa, either during acute or chronic treatments. These first results indicate that S1R pharmacology could have an interesting potential allowing to increase SOCE channel activity. It would thus be interesting to validate the effects of S1R ligands in PCa cell physiology both *in vitro* and *in vivo*, to develop new therapeutic strategies for the treatment of PCa. S1R ligands have already been tested in different cancers, showing various effects on cell proliferation and viability (Brent et al. 1996; Brent and Pang 1995; Kim and Maher 2017; Moody et al. 2000; Spruce et al. 2004; Vilner et al. 1995a). The potential of S1R targeting has been recently investigated in PCa, as it was shown to stabilize the AR (Salvino et al. 2017). In this study, authors show a decreased PCa cell proliferation and tumor growth using small S1R inhibitors, showing the potential of a therapy targeting this chaperone protein. Thus, if S1R ligands prove to be potent regulator of PCa cell physiology *in vitro* and *in vivo*, new anticancer therapeutic strategies could be proposed with the S1R ligands already clinically used. Moreover, S1R modulation could also be useful to increase the efficiency of ion channel targeting.

To this day, no endogenous ligand of the S1R has been clearly identified, but among the candidates one can find the DMT (N,N-dimethyltryptamine) (Fontanilla et al. 2009; Frecska et al. 2013; Mavlyutov et al. 2012). Interestingly, the enzyme responsible for DMT production, INMT (indolethylamine-N-methyltransferase), is overexpressed in PCa, in correlation with

aggressiveness (Larkin et al. 2012). Further investigation of this potential endogenous compound and its enzyme are crucial to fully understand S1R regulation and roles during PCa progression.

III. General conclusion and perspectives

Altogether, our results shed light on the central role of the SOC/NFAT pathway in the regulation of prostate cancer cell proliferative state and switch to the quiescent state. Interestingly, we show that this pathway is directly regulated by the S1R chaperone protein, opening new therapeutic perspectives. Moreover, our preliminary data indicate that the S1R is able to modulate the activity of other calcium channels implicated in PCa cells, such as TRPV6 and TRPM8.

Overall, our results show that it would be possible to modulate calcium channel activity by targeting the S1R in PCa cells. According to these data, S1R activation would first lead to an increased PCa cell proliferation via SOC channels and the NFAT pathway. However, it would also activate the quiescent cancer cells with stem-like properties, pushing them towards proliferation. Moreover, our results indicate that S1R activation could also sensitize PCa cells to apoptosis and cell death by increased SOCE, enhancing chemotherapy efficiency. Finally, our preliminary data indicate that S1R activation could also increase TRPM8 activity and limit PCa cell migration. Thus, S1R receptor activation combined with chemotherapy could increase chemotherapy efficiency and, by activating the CSC cells, S1R activation could also allow their elimination by chemotherapy, avoiding relapse. Moreover, these effects would be strengthened via AR stabilization, increasing PCa cell proliferation and leading to the differentiation of PCa stem-like cells with a loss of stem properties.

All of these elements show that S1R plays a complex role in PCa that we only began to unfold. However, it is clear from our results that the inhibition of S1R decreases PCa cell proliferation and tumor growth and increases apoptosis-resistance.

References

Achison M, Boylan MT, Hupp TR, Spruce BA. HIF-1 α contributes to tumour-selective killing by the sigma receptor antagonist rimcazole. *Oncogene*. 2006 Aug 21;26(8):1137–46.

Alison MR, Lin W-R, Lim SML, Nicholson LJ. Cancer stem cells: in the line of fire. *Cancer Treat. Rev*. 2012 Oct;38(6):589–98.

Ammon J, Karstens JH, Rathert P. [TNM-system orientated radiological therapy in prostatic carcinoma (author's transl)]. *Urol. Ausg A*. 1977 Mar;16(2):73–82.

Askew EB, Gampe RT, Stanley TB, Faggart JL, Wilson EM. Modulation of androgen receptor activation function 2 by testosterone and dihydrotestosterone. *J. Biol. Chem*. 2007 Aug 31;282(35):25801–16.

Augustine GJ, Fitzpatrick D, Hall W, LaMantia A-S, Purves D, White L. *Neurosciences*. De Boeck Superieur; 2015.

Aulestia FJ, Néant I, Dong J, Haiech J, Kilhoffer M-C, Moreau M, et al. Quiescence status of glioblastoma stem-like cells involves remodelling of Ca²⁺ signalling and mitochondrial shape. *Sci. Rep*. 2018 Jun 27;8(1):9731.

Aydar E, Onganer P, Perrett R, Djamgoz MB, Palmer CP. The expression and functional characterization of sigma (sigma) 1 receptors in breast cancer cell lines. *Cancer Lett*. 2006 Oct 28;242(2):245–57.

Aydar E, Palmer CP, Klyachko VA, Jackson MB. The sigma receptor as a ligand-regulated auxiliary potassium channel subunit. *Neuron*. 2002 Apr 25;34(3):399–410.

Balasuriya D, D'Sa L, Talker R, Dupuis E, Maurin F, Martin P, et al. A direct interaction between the sigma-1 receptor and the hERG voltage-gated K⁺ channel revealed by atomic force microscopy and homogeneous time-resolved fluorescence (HTRF®). *J. Biol. Chem*. 2014 Sep 29;jbc.M114.603506.

Balasuriya D, Stewart AP, Crottès D, Borgese F, Soriani O, Edwardson JM. The Sigma-1 Receptor Binds to the Nav1.5 Voltage-gated Na⁺ Channel with 4-Fold Symmetry. *J. Biol. Chem*. 2012 Oct 26;287(44):37021–9.

Barron DA, Rowley DR. The reactive stroma microenvironment and prostate cancer progression. *Endocr. Relat. Cancer*. 2012 Dec;19(6):R187-204.

Beals CR, Sheridan CM, Turck CW, Gardner P, Crabtree GR. Nuclear export of NF-ATc enhanced by glycogen synthase kinase-3. *Science*. 1997 Mar 28;275(5308):1930–4.

Berridge MJ, Bootman MD, Roderick HL. Calcium signalling: dynamics, homeostasis and remodelling. *Nat. Rev. Mol. Cell Biol*. 2003 Jul;4(7):517–29.

Berry CT, May MJ, Freedman BD. STIM- and Orai-mediated calcium entry controls NF- κ B activity and function in lymphocytes. *Cell Calcium*. 2018;74:131–43.

Bidaux G, Flourakis M, Thebault S, Zholos A, Beck B, Gkika D, et al. Prostate cell differentiation status determines transient receptor potential melastatin member 8 channel subcellular localization and function. *J. Clin. Invest*. 2007 Jun;117(6):1647–57.

Bidaux G, Gordienko D, Shapovalov G, Farfariello V, Borowiec A-S, Iamshanova O, et al. 4TM-TRPM8 channels are new gatekeepers of the ER-mitochondria Ca²⁺ transfer. *Biochim. Biophys. Acta Mol. Cell Res*. 2018a;1865(7):981–94.

- Bidaux G, Le Nézet C, Pisfil MG, Henry M, Furlan A, Bensaude O, et al. FRET Image Correlation Spectroscopy Reveals RNAPII-Independent P-TEFb Recruitment on Chromatin. *Biophys. J.* 2018b 06;114(3):522–33.
- Bogeski I, Kilch T, Niemeyer BA. ROS and SOCE: recent advances and controversies in the regulation of STIM and Orai. *J. Physiol.* 2012 Sep 1;590(17):4193–200.
- van Bokhoven A, Varella-Garcia M, Korch C, Johannes WU, Smith EE, Miller HL, et al. Molecular characterization of human prostate carcinoma cell lines. *The Prostate.* 2003 Nov 1;57(3):205–25.
- Borst P. Cancer drug pan-resistance: pumps, cancer stem cells, quiescence, epithelial to mesenchymal transition, blocked cell death pathways, persists or what? *Open Biol.* 2012 May;2(5):120066.
- Boutin B, Tajeddine N, Monaco G, Molgo J, Vertommen D, Rider M, et al. Endoplasmic reticulum Ca(2+) content decrease by PKA-dependent hyperphosphorylation of type 1 IP3 receptor contributes to prostate cancer cell resistance to androgen deprivation. *Cell Calcium.* 2015 Apr;57(4):312–20.
- Brent PJ, Pang G, Little G, Dosen PJ, Van Helden DF. The sigma receptor ligand, reduced haloperidol, induces apoptosis and increases intracellular-free calcium levels [Ca²⁺]_i in colon and mammary adenocarcinoma cells. *Biochem. Biophys. Res. Commun.* 1996 Feb 6;219(1):219–26.
- Brent PJ, Pang GT. σ Binding site ligands inhibit cell proliferation in mammary and colon carcinoma cell lines and melanoma cells in culture. *Eur. J. Pharmacol.* 1995 May 15;278(2):151–60.
- Buchholz M, Schatz A, Wagner M, Michl P, Linhart T, Adler G, et al. Overexpression of c-myc in pancreatic cancer caused by ectopic activation of NFATc1 and the Ca²⁺/calcineurin signaling pathway. *EMBO J.* 2006 Aug 9;25(15):3714–24.
- Cao X, Choi S, Maléth JJ, Park S, Ahuja M, Muallem S. The ER/PM microdomain, PI(4,5)P₂ and the regulation of STIM1-Orai1 channel function. *Cell Calcium.* 2015 Oct;58(4):342–8.
- Catalona WJ, Smith DS, Ratliff TL, Dodds KM, Coplen DE, Yuan JJ, et al. Measurement of prostate-specific antigen in serum as a screening test for prostate cancer. *N. Engl. J. Med.* 1991 Apr 25;324(17):1156–61.
- Chen CD, Welsbie DS, Tran C, Baek SH, Chen R, Vessella R, et al. Molecular determinants of resistance to antiandrogen therapy. *Nat. Med.* 2004 Jan;10(1):33–9.
- Chen Y-F, Chiu W-T, Chen Y-T, Lin P-Y, Huang H-J, Chou C-Y, et al. Calcium store sensor stromal-interaction molecule 1-dependent signaling plays an important role in cervical cancer growth, migration, and angiogenesis. *Proc. Natl. Acad. Sci. U. S. A.* 2011 Sep 13;108(37):15225–30.
- Cheng L, Montironi R, Bostwick DG, Lopez-Beltran A, Berney DM. Staging of prostate cancer. *Histopathology.* 2012 Jan;60(1):87–117.
- Cheng T, Rodrigues N, Shen H, Yang Y, Dombkowski D, Sykes M, et al. Hematopoietic stem cell quiescence maintained by p21^{cip1/waf1}. *Science.* 2000 Mar 10;287(5459):1804–8.
- Cheung TH, Rando TA. Molecular regulation of stem cell quiescence. *Nat. Rev. Mol. Cell Biol.* 2013 Jun;14(6):329–40.

- Chitilian JM, Thillainadesan G, Manias JL, Chang WY, Walker E, Isovich M, et al. Critical components of the pluripotency network are targets for the p300/CBP interacting protein (p/CIP) in embryonic stem cells. *Stem Cells Dayt. Ohio*. 2014 Jan;32(1):204–15.
- Chu UB, Ruoho AE. Biochemical Pharmacology of the Sigma-1 Receptor. *Mol. Pharmacol.* 2016 Jan;89(1):142–53.
- Clapham DE. Calcium signaling. *Cell*. 2007 Dec 14;131(6):1047–58.
- Clapham DE, Runnels LW, Strübing C. The TRP ion channel family. *Nat. Rev. Neurosci.* 2001 Jun;2(6):387–96.
- Coghlan VM, Perrino BA, Howard M, Langeberg LK, Hicks JB, Gallatin WM, et al. Association of protein kinase A and protein phosphatase 2B with a common anchoring protein. *Science*. 1995 Jan 6;267(5194):108–11.
- Coller HA, Sang L, Roberts JM. A new description of cellular quiescence. *PLoS Biol.* 2006 Mar;4(3):e83.
- Collins AT, Berry PA, Hyde C, Stower MJ, Maitland NJ. Prospective identification of tumorigenic prostate cancer stem cells. *Cancer Res.* 2005 Dec 1;65(23):10946–51.
- Covington ED, Wu MM, Lewis RS. Essential role for the CRAC activation domain in store-dependent oligomerization of STIM1. *Mol. Biol. Cell.* 2010 Jun 1;21(11):1897–907.
- Crona DJ, Whang YE. Androgen Receptor-Dependent and -Independent Mechanisms Involved in Prostate Cancer Therapy Resistance. *Cancers [Internet]*. 2017 Jun 12 [cited 2019 Jun 16];9(6). Available from: <https://www.ncbi.nlm.nih.gov/pmc/articles/PMC5483886/>
- Crottès D, Martial S, Rapetti-Mauss R, Pisani DF, Loriol C, Pellissier B, et al. Sig1R Protein Regulates hERG Channel Expression through a Post-translational Mechanism in Leukemic Cells. *J. Biol. Chem.* 2011 Aug 12;286(32):27947–58.
- Cui W, Ma J, Wang X, Yang W, Zhang J, Ji Q. Free fatty acid induces endoplasmic reticulum stress and apoptosis of β -cells by Ca^{2+} /calpain-2 pathways. *PloS One*. 2013;8(3):e59921.
- Culig Z, Hobisch A, Cronauer MV, Radmayr C, Trapman J, Hittmair A, et al. Androgen receptor activation in prostatic tumor cell lines by insulin-like growth factor-I, keratinocyte growth factor, and epidermal growth factor. *Cancer Res.* 1994 Oct 15;54(20):5474–8.
- Dehm SM, Tindall DJ. Molecular regulation of androgen action in prostate cancer. *J. Cell. Biochem.* 2006;99(2):333–44.
- Denmeade SR, Isaacs JT. A history of prostate cancer treatment. *Nat. Rev. Cancer.* 2002 May;2(5):389–96.
- Derler I, Fahrner M, Muik M, Lackner B, Schindl R, Groschner K, et al. A Ca^{2+} release-activated Ca^{2+} (CRAC) modulatory domain (CMD) within STIM1 mediates fast Ca^{2+} -dependent inactivation of ORAI1 channels. *J. Biol. Chem.* 2009 Sep 11;284(37):24933–8.
- Derler I, Jardin I, Romanin C. Molecular mechanisms of STIM/Orai communication. *Am. J. Physiol. - Cell Physiol.* 2016 Apr 15;310(8):C643–62.
- Dubois C, Vanden Abeele F, Lehen'kyi V, Gkika D, Guarmit B, Lepage G, et al. Remodeling of channel-forming ORAI proteins determines an oncogenic switch in prostate cancer. *Cancer Cell*. 2014 Jul 14;26(1):19–32.

- Ehninger A, Boch T, Medyouf H, Müdder K, Orend G, Trumpp A. Loss of SPARC protects hematopoietic stem cells from chemotherapy toxicity by accelerating their return to quiescence. *Blood*. 2014 Jun 26;123(26):4054–63.
- English HF, Kyprianou N, Isaacs JT. Relationship between DNA fragmentation and apoptosis in the programmed cell death in the rat prostate following castration. *The Prostate*. 1989;15(3):233–50.
- Fahrner M, Muik M, Schindl R, Butorac C, Stathopoulos P, Zheng L, et al. A coiled-coil clamp controls both conformation and clustering of stromal interaction molecule 1 (STIM1). *J. Biol. Chem*. 2014 Nov 28;289(48):33231–44.
- Fahrner M, Pandey SK, Muik M, Traxler L, Butorac C, Stadlbauer M, et al. Communication between N terminus and loop2 tunes Orai activation. *J. Biol. Chem*. 2018 26;293(4):1271–85.
- Fang F, Xu Y, Chew K-K, Chen X, Ng H-H, Matsudaira P. Coactivators p300 and CBP maintain the identity of mouse embryonic stem cells by mediating long-range chromatin structure. *Stem Cells Dayt. Ohio*. 2014 Jul;32(7):1805–16.
- Faouzi M, Kischel P, Hague F, Ahidouch A, Benzerdjeb N, Sevestre H, et al. ORAI3 silencing alters cell proliferation and cell cycle progression via c-myc pathway in breast cancer cells. *Biochim. Biophys. Acta*. 2013 Mar;1833(3):752–60.
- Feldman BJ, Feldman D. The development of androgen-independent prostate cancer. *Nat. Rev. Cancer*. 2001 Oct;1(1):34–45.
- Feng M, Grice DM, Faddy HM, Nguyen N, Leitch S, Wang Y, et al. Store-Independent Activation of Orai1 by SPCA2 in Mammary Tumors. *Cell*. 2010 Oct 1;143(1):84–98.
- Feske S, Giltnane J, Dolmetsch R, Staudt LM, Rao A. Gene regulation mediated by calcium signals in T lymphocytes. *Nat. Immunol*. 2001 Apr;2(4):316–24.
- Feske S, Gwack Y, Prakriya M, Srikanth S, Puppel S-H, Tanasa B, et al. A mutation in Orai1 causes immune deficiency by abrogating CRAC channel function. *Nature*. 2006 May 11;441(7090):179–85.
- Fiorio Pla A, Kondratska K, Prevarskaya N. STIM and ORAI proteins: crucial roles in hallmarks of cancer. *Am. J. Physiol. Cell Physiol*. 2016 Apr 1;310(7):C509-519.
- Fixemer T, Wissenbach U, Flockerzi V, Bonkhoff H. Expression of the Ca²⁺-selective cation channel TRPV6 in human prostate cancer: a novel prognostic marker for tumor progression. *Oncogene*. 2003;22(49):7858–61.
- Flourakis M, Lehen'kyi V, Beck B, Raphaël M, Vandenberghe M, Abeele FV, et al. Orai1 contributes to the establishment of an apoptosis-resistant phenotype in prostate cancer cells. *Cell Death Dis*. 2010;1:e75.
- Fontanilla D, Johannessen M, Hajipour AR, Cozzi NV, Jackson MB, Ruoho AE. The Hallucinogen N,N-Dimethyltryptamine (DMT) Is an Endogenous Sigma-1 Receptor Regulator. *Science*. 2009 Feb 13;323(5916):934–7.
- Foradori CD, Weiser MJ, Handa RJ. Non-genomic actions of androgens. *Front. Neuroendocrinol*. 2008 May;29(2):169–81.
- Frecska E, Szabo A, Winkelman MJ, Luna LE, McKenna DJ. A possibly sigma-1 receptor mediated role of dimethyltryptamine in tissue protection, regeneration, and immunity. *J. Neural Transm*. 2013 Sep 1;120(9):1295–303.

- Frisch J, Angenendt A, Hoth M, Prates Roma L, Lis A. STIM-Orai Channels and Reactive Oxygen Species in the Tumor Microenvironment. *Cancers*. 2019 Mar 30;11(4).
- Garraway IP, Sun W, Tran CP, Perner S, Zhang B, Goldstein AS, et al. Human prostate sphere-forming cells represent a subset of basal epithelial cells capable of glandular regeneration in vivo. *The Prostate*. 2010 Apr 1;70(5):491–501.
- Ghanem GE, Comunale G, Libert A, Vercammen-Grandjean A, Lejeune FJ. Evidence for alpha-melanocyte-stimulating hormone (alpha-MSH) receptors on human malignant melanoma cells. *Int. J. Cancer*. 1988 Feb 15;41(2):248–55.
- Gkika D, Flourakis M, Lemonnier L, Prevarskaya N. PSA reduces prostate cancer cell motility by stimulating TRPM8 activity and plasma membrane expression. *Oncogene*. 2010 Aug 12;29(32):4611–6.
- Gkika D, Lemonnier L, Shapovalov G, Gordienko D, Poux C, Bernardini M, et al. TRP channel-associated factors are a novel protein family that regulates TRPM8 trafficking and activity. *J. Cell Biol.* 2015 Jan 5;208(1):89–107.
- Gleason DF, Mellinger GT. Prediction of prognosis for prostatic adenocarcinoma by combined histological grading and clinical staging. *J. Urol.* 1974 Jan;111(1):58–64.
- Goldstein AS, Huang J, Guo C, Garraway IP, Witte ON. Identification of a cell of origin for human prostate cancer. *Science*. 2010 Jul 30;329(5991):568–71.
- Gromek KA, Suchy FP, Meddaugh HR, Wrobel RL, LaPointe LM, Chu UB, et al. The oligomeric states of the purified sigma-1 receptor are stabilized by ligands. *J. Biol. Chem.* 2014 Jul 18;289(29):20333–44.
- Gueguinou M, Crottès D, Chantôme A, Rapetti-Mauss R, Potier-Cartreau M, Clarysse L, et al. The SigmaR1 chaperone drives breast and colorectal cancer cell migration by tuning SK3-dependent Ca²⁺ homeostasis. *Oncogene*. 2017 22;36(25):3640–7.
- Guéguinou M, Harnois T, Crottes D, Uguen A, Deliot N, Gambade A, et al. SK3/TRPC1/Orai1 complex regulates SOCE-dependent colon cancer cell migration: a novel opportunity to modulate anti-EGFR mAb action by the alkyl-lipid Ohmlin. *Oncotarget*. 2016 Jun 14;7(24):36168–84.
- Harteneck C. Proteins modulating TRP channel function. *Cell Calcium*. 2003 Jun;33(5–6):303–10.
- Hayashi T, Lewis A, Hayashi E, Betenbaugh MJ, Su T-P. Antigen retrieval to improve the immunocytochemistry detection of sigma-1 receptors and ER chaperones. *Histochem. Cell Biol.* 2011 Jun;135(6):627–37.
- Hayashi T, Su T-P. Sigma-1 Receptor Chaperones at the ER- Mitochondrion Interface Regulate Ca²⁺ Signaling and Cell Survival. *Cell*. 2007 Nov 2;131(3):596–610.
- Heinlein CA, Chang C. Androgen receptor in prostate cancer. *Endocr. Rev.* 2004 Apr;25(2):276–308.
- Henke N, Albrecht P, Bouchachia I, Ryazantseva M, Knoll K, Lewerenz J, et al. The plasma membrane channel ORAI1 mediates detrimental calcium influx caused by endogenous oxidative stress. *Cell Death Dis.* 2013 Jan 24;4:e470.
- Henshall SM, Afar DEH, Hiller J, Horvath LG, Quinn DI, Rasiah KK, et al. Survival Analysis of Genome-Wide Gene Expression Profiles of Prostate Cancers Identifies New Prognostic Targets of Disease Relapse. *Cancer Res.* 2003 Jul 15;63(14):4196–203.

- Hogan PG, Chen L, Nardone J, Rao A. Transcriptional regulation by calcium, calcineurin, and NFAT. *Genes Dev.* 2003 Sep 15;17(18):2205–32.
- Horoszewicz JS, Leong SS, Chu TM, Wajzman ZL, Friedman M, Papsidero L, et al. The LNCaP cell line--a new model for studies on human prostatic carcinoma. *Prog. Clin. Biol. Res.* 1980;37:115–32.
- Horsley V, Aliprantis AO, Polak L, Glimcher LH, Fuchs E. NFATc1 balances quiescence and proliferation of skin stem cells. *Cell.* 2008 Jan 25;132(2):299–310.
- Hoth M, Penner R. Calcium release-activated calcium current in rat mast cells. *J. Physiol.* 1993 Jun;465:359–86.
- Hou M-F, Kuo H-C, Li J-H, Wang Y-S, Chang C-C, Chen K-C, et al. Orai1/CRACM1 overexpression suppresses cell proliferation via attenuation of the store-operated calcium influx-mediated signalling pathway in A549 lung cancer cells. *Biochim. Biophys. Acta.* 2011 Dec;1810(12):1278–84.
- Hou X, Pedi L, Diver MM, Long SB. Crystal structure of the calcium release-activated calcium channel Orai. *Science.* 2012 Dec 7;338(6112):1308–13.
- Huang GN, Huso DL, Bouyain S, Tu J, McCorkell KA, May MJ, et al. NFAT binding and regulation of T cell activation by the cytoplasmic scaffolding Homer proteins. *Science.* 2008 Jan 25;319(5862):476–81.
- Huang GN, Zeng W, Kim JY, Yuan JP, Han L, Muallem S, et al. STIM1 carboxyl-terminus activates native SOC, I(crac) and TRPC1 channels. *Nat. Cell Biol.* 2006 Sep;8(9):1003–10.
- Huggins C, Stevens RE, Hodges CV. STUDIES ON PROSTATIC CANCER: II. THE EFFECTS OF CASTRATION ON ADVANCED CARCINOMA OF THE PROSTATE GLAND. *Arch. Surg.* 1941 Aug 1;43(2):209–23.
- Hurt EM, Kawasaki BT, Klarmann GJ, Thomas SB, Farrar WL. CD44+ CD24(-) prostate cells are early cancer progenitor/stem cells that provide a model for patients with poor prognosis. *Br. J. Cancer.* 2008 Feb 26;98(4):756–65.
- Jain J, McCaffrey PG, Valge-Archer VE, Rao A. Nuclear factor of activated T cells contains Fos and Jun. *Nature.* 1992 Apr 30;356(6372):801–4.
- Jia X, Li X, Xu Y, Zhang S, Mou W, Liu Y, et al. SOX2 promotes tumorigenesis and increases the anti-apoptotic property of human prostate cancer cell. *J. Mol. Cell Biol.* 2011 Aug;3(4):230–8.
- John CS, Gulden ME, Li J, Bowen WD, McAfee JG, Thakur ML. Synthesis, in vitro binding, and tissue distribution of radioiodinated 2-[125I]N-(N-benzylpiperidin-4-yl)-2-iodo benzamide, 2-[125I]BP: a potential sigma receptor marker for human prostate tumors. *Nucl. Med. Biol.* 1998 Apr;25(3):189–94.
- Kaighn ME, Narayan KS, Ohnuki Y, Lechner JF, Jones LW. Establishment and characterization of a human prostatic carcinoma cell line (PC-3). *Invest. Urol.* 1979 Jul;17(1):16–23.
- Kallio HML, Hieta R, Latonen L, Brofeldt A, Annala M, Kivinummi K, et al. Constitutively active androgen receptor splice variants AR-V3, AR-V7 and AR-V9 are co-expressed in castration-resistant prostate cancer metastases. *Br. J. Cancer.* 2018 Aug;119(3):347–56.
- Kar P, Mirams GR, Christian HC, Parekh AB. Control of NFAT Isoform Activation and NFAT-Dependent Gene Expression through Two Coincident and Spatially Segregated Intracellular Ca²⁺ Signals. *Mol. Cell.* 2016 Nov 17;64(4):746–59.

- Kar P, Parekh AB. Distinct Spatial Ca²⁺ Signatures Selectively Activate Different NFAT Transcription Factor Isoforms. *Mol. Cell.* 2015 Apr 16;58(2):232–43.
- Kar P, Samanta K, Kramer H, Morris O, Bakowski D, Parekh AB. Dynamic Assembly of a Membrane Signaling Complex Enables Selective Activation of NFAT by Orai1. *Curr. Biol.* 2014 Jun 16;24(12):1361–8.
- Kawasaki T, Lange I, Feske S. A minimal regulatory domain in the C terminus of STIM1 binds to and activates ORAI1 CRAC channels. *Biochem. Biophys. Res. Commun.* 2009 Jul 17;385(1):49–54.
- Kawasaki T, Ueyama T, Lange I, Feske S, Saito N. Protein kinase C-induced phosphorylation of Orai1 regulates the intracellular Ca²⁺ level via the store-operated Ca²⁺ channel. *J. Biol. Chem.* 2010 Aug 13;285(33):25720–30.
- Kida A, Kahn M. Hypoxia selects for a quiescent, CML stem/leukemia initiating-like population dependent on CBP/catenin transcription. *Curr. Mol. Pharmacol.* 2013 Nov;6(3):204–10.
- Kim FJ, Maher CM. Sigma1 Pharmacology in the Context of Cancer. *Handb. Exp. Pharmacol.* 2017;244:237–308.
- Kim J, Coetzee GA. Prostate specific antigen gene regulation by androgen receptor. *J. Cell. Biochem.* 2004 Oct 1;93(2):233–41.
- Kim J-H, Lkhagvadorj S, Lee M-R, Hwang K-H, Chung HC, Jung JH, et al. Orai1 and STIM1 are critical for cell migration and proliferation of clear cell renal cell carcinoma. *Biochem. Biophys. Res. Commun.* 2014 May 23;448(1):76–82.
- Kinoshita M, Matsuoka Y, Suzuki T, Mirrieles J, Yang J. Sigma-1 receptor alters the kinetics of Kv1.3 voltage gated potassium channels but not the sensitivity to receptor ligands. *Brain Res.* 2012 May 3;1452:1–9.
- Kondratska K, Kondratskyi A, Yassine M, Lemonnier L, Lepage G, Morabito A, et al. Orai1 and STIM1 mediate SOCE and contribute to apoptotic resistance of pancreatic adenocarcinoma. *Biochim. Biophys. Acta.* 2014 Oct;1843(10):2263–9.
- König S, Browne S, Doleschal B, Scherthaner M, Poteser M, Mächler H, et al. Inhibition of Orai1-mediated Ca²⁺ entry is a key mechanism of the antiproliferative action of sirolimus in human arterial smooth muscle. *Am. J. Physiol. Heart Circ. Physiol.* 2013 Dec 1;305(11):H1646-1657.
- Larkin SET, Holmes S, Cree IA, Walker T, Basketter V, Bickers B, et al. Identification of markers of prostate cancer progression using candidate gene expression. *Br. J. Cancer.* 2012 Jan 3;106(1):157–65.
- Lee KP, Yuan JP, Zeng W, So I, Worley PF, Muallem S. Molecular determinants of fast Ca²⁺-dependent inactivation and gating of the Orai channels. *Proc. Natl. Acad. Sci. U. S. A.* 2009 Aug 25;106(34):14687–92.
- Lee SH, Rigas NK, Lee C-R, Bang A, Srikanth S, Gwack Y, et al. Orai1 promotes tumor progression by enhancing cancer stemness via NFAT signaling in oral/oropharyngeal squamous cell carcinoma. *Oncotarget.* 2016 Jul 12;7(28):43239–55.
- Lehen'kyi V, Flourakis M, Skryma R, Prevarskaya N. TRPV6 channel controls prostate cancer cell proliferation via Ca²⁺/NFAT-dependent pathways. *Oncogene.* 2007 Nov 15;26(52):7380–5.
- Lepple-Wienhues A, Cahalan MD. Conductance and permeation of monovalent cations through depletion-activated Ca²⁺ channels (ICRAC) in Jurkat T cells. *Biophys. J.* 1996 Aug;71(2):787–94.

- Levin-Gromiko U, Koshelev V, Kushnir P, Fedida-Metula S, Voronov E, Fishman D. Amplified lipid rafts of malignant cells constitute a target for inhibition of aberrantly active NFAT and melanoma tumor growth by the aminobisphosphonate zoledronic acid. *Carcinogenesis*. 2014 Nov 1;35(11):2555–66.
- Li X, Wu G, Yang Y, Fu S, Liu X, Kang H, et al. Calmodulin dissociates the STIM1-Orai1 complex and STIM1 oligomers. *Nat. Commun*. 2017 19;8(1):1042.
- Liou J, Fivaz M, Inoue T, Meyer T. Live-cell imaging reveals sequential oligomerization and local plasma membrane targeting of stromal interaction molecule 1 after Ca²⁺ store depletion. *Proc. Natl. Acad. Sci. U. S. A.* 2007 May 29;104(22):9301–6.
- Liou J, Kim ML, Heo WD, Jones JT, Myers JW, Ferrell JE, et al. STIM is a Ca²⁺ sensor essential for Ca²⁺-store-depletion-triggered Ca²⁺ influx. *Curr. Biol. CB*. 2005 Jul 12;15(13):1235–41.
- Liu H, Hughes JD, Rollins S, Chen B, Perkins E. Calcium entry via ORAI1 regulates glioblastoma cell proliferation and apoptosis. *Exp. Mol. Pathol.* 2011 Dec;91(3):753–60.
- Livak KJ, Schmittgen TD. Analysis of relative gene expression data using real-time quantitative PCR and the 2⁻(Delta Delta C(T)) Method. *Methods San Diego Calif*. 2001 Dec;25(4):402–8.
- Luik RM, Wang B, Prakriya M, Wu MM, Lewis RS. Oligomerization of STIM1 couples ER calcium depletion to CRAC channel activation. *Nature*. 2008 Jul 24;454(7203):538–42.
- Mancarella S, Wang Y, Deng X, Landesberg G, Scalia R, Panettieri RA, et al. Hypoxia-induced acidosis uncouples the STIM-Orai calcium signaling complex. *J. Biol. Chem.* 2011 Dec 30;286(52):44788–98.
- Mancini M, Toker A. NFAT proteins: emerging roles in cancer progression. *Nat. Rev. Cancer*. 2009 Nov;9(11):810–20.
- Martin WR, Eades CG, Thompson JA, Huppler RE, Gilbert PE. The effects of morphine- and nalorphine- like drugs in the nondependent and morphine-dependent chronic spinal dog. *J. Pharmacol. Exp. Ther.* 1976 Jun 1;197(3):517–32.
- Matsubara T, Ikeda F, Hata K, Nakanishi M, Okada M, Yasuda H, et al. Cbp recruitment of Csk into lipid rafts is critical to c-Src kinase activity and bone resorption in osteoclasts. *J. Bone Miner. Res. Off. J. Am. Soc. Bone Miner. Res.* 2010 May;25(5):1068–76.
- Mavlyutov TA, Epstein ML, Liu P, Verbny YI, Ziskind-Conhaim L, Ruoho AE. DEVELOPMENT OF THE SIGMA-1 RECEPTOR IN C-TERMINALS OF MOTONEURONS AND COLOCALIZATION WITH THE N,N'-DIMETHYLTRYPTAMINE FORMING ENZYME, INDOLE-N-METHYL TRANSFERASE. *Neuroscience*. 2012 Mar 29;206:60–8.
- Mavylutov T, Chen X, Guo L, Yang J. APEX2- tagging of Sigma 1-receptor indicates subcellular protein topology with cytosolic N-terminus and ER luminal C-terminus. *Protein Cell*. 2018;9(8):733–7.
- McAndrew D, Grice DM, Peters AA, Davis FM, Stewart T, Rice M, et al. ORAI1-mediated calcium influx in lactation and in breast cancer. *Mol. Cancer Ther.* 2011 Mar;10(3):448–60.
- McNally BA, Somasundaram A, Jairaman A, Yamashita M, Prakriya M. The C- and N-terminal STIM1 binding sites on Orai1 are required for both trapping and gating CRAC channels. *J. Physiol.* 2013 Jun 1;591(11):2833–50.
- McNeal JE. Normal histology of the prostate. *Am. J. Surg. Pathol.* 1988 Aug;12(8):619–33.

- Meijering E, Dzyubachyk O, Smal I. Methods for cell and particle tracking. *Methods Enzymol.* 2012;504:183–200.
- Miller WL, Auchus RJ. The molecular biology, biochemistry, and physiology of human steroidogenesis and its disorders. *Endocr. Rev.* 2011 Feb;32(1):81–151.
- Mishra AK, Mavlyutov T, Singh DR, Biener G, Yang J, Oliver JA, et al. The sigma-1 receptors are present in monomeric and oligomeric forms in living cells in the presence and absence of ligands. *Biochem. J.* 2015 Mar 1;466(2):263–71.
- Monteith GR, Prevarskaya N, Roberts-Thomson SJ. The calcium-cancer signalling nexus. *Nat. Rev. Cancer.* 2017;17(6):367–80.
- Moody TW, Leyton J, John C. Sigma ligands inhibit the growth of small cell lung cancer cells. *Life Sci.* 2000 Apr 7;66(20):1979–86.
- Motiani RK, Zhang X, Harmon KE, Keller RS, Matrougui K, Bennett JA, et al. Orai3 is an estrogen receptor α -regulated Ca^{2+} channel that promotes tumorigenesis. *FASEB J. Off. Publ. Fed. Am. Soc. Exp. Biol.* 2013 Jan;27(1):63–75.
- Muik M, Fahrner M, Derler I, Schindl R, Bergsmann J, Frischauf I, et al. A Cytosolic Homomerization and a Modulatory Domain within STIM1 C Terminus Determine Coupling to ORAI1 Channels. *J. Biol. Chem.* 2009 Mar 27;284(13):8421–6.
- Muik M, Fahrner M, Schindl R, Stathopoulos P, Frischauf I, Derler I, et al. STIM1 couples to ORAI1 via an intramolecular transition into an extended conformation. *EMBO J.* 2011 May 4;30(9):1678–89.
- Müller MR, Rao A. NFAT, immunity and cancer: a transcription factor comes of age. *Nat. Rev. Immunol.* 2010 Sep;10(9):645–56.
- Mullins FM, Lewis RS. The inactivation domain of STIM1 is functionally coupled with the Orai1 pore to enable Ca^{2+} -dependent inactivation. *J. Gen. Physiol.* 2016 Feb;147(2):153–64.
- Mullins FM, Park CY, Dolmetsch RE, Lewis RS. STIM1 and calmodulin interact with Orai1 to induce Ca^{2+} -dependent inactivation of CRAC channels. *Proc. Natl. Acad. Sci. U. S. A.* 2009 Sep 8;106(36):15495–500.
- Neal JW, Clipstone NA. A constitutively active NFATc1 mutant induces a transformed phenotype in 3T3-L1 fibroblasts. *J. Biol. Chem.* 2003 May 9;278(19):17246–54.
- Neher E, Sakmann B. Single-channel currents recorded from membrane of denervated frog muscle fibres. *Nature.* 1976 Apr 29;260(5554):799–802.
- Nguyen LV, Vanner R, Dirks P, Eaves CJ. Cancer stem cells: an evolving concept. *Nat. Rev. Cancer.* 2012 12;12(2):133–43.
- Okamura H, Aramburu J, García-Rodríguez C, Viola JP, Raghavan A, Tahiliani M, et al. Concerted dephosphorylation of the transcription factor NFAT1 induces a conformational switch that regulates transcriptional activity. *Mol. Cell.* 2000 Sep;6(3):539–50.
- Okamura H, Garcia-Rodriguez C, Martinson H, Qin J, Virshup DM, Rao A. A conserved docking motif for CK1 binding controls the nuclear localization of NFAT1. *Mol. Cell. Biol.* 2004 May;24(10):4184–95.
- Olabisi OA, Soto-Nieves N, Nieves E, Yang TTC, Yang X, Yu RYL, et al. Regulation of transcription factor NFAT by ADP-ribosylation. *Mol. Cell. Biol.* 2008 May;28(9):2860–71.

- Ong HL, Jang S-I, Ambudkar IS. Distinct contributions of Orai1 and TRPC1 to agonist-induced $[Ca^{2+}]_i$ signals determine specificity of Ca^{2+} -dependent gene expression. *PLoS One*. 2012;7(10):e47146.
- Oritani K, Kincade PW. Identification of stromal cell products that interact with pre-B cells. *J. Cell Biol.* 1996 Aug;134(3):771–82.
- Ostyn P, El Machhour R, Begard S, Kotecki N, Vandomme J, Flamenco P, et al. Transient TNF regulates the self-renewing capacity of stem-like label-retaining cells in sphere and skin equivalent models of melanoma. *Cell Commun. Signal. CCS*. 2014 Sep 17;12:52.
- Palty R, Raveh A, Kaminsky I, Meller R, Reuveny E. SARAF inactivates the store operated calcium entry machinery to prevent excess calcium refilling. *Cell*. 2012 Apr 13;149(2):425–38.
- Pan M-G, Xiong Y, Chen F. NFAT gene family in inflammation and cancer. *Curr. Mol. Med.* 2013 May;13(4):543–54.
- Parekh AB. Regulation of CRAC channels by Ca^{2+} -dependent inactivation. *Cell Calcium*. 2017;63:20–3.
- Park CY, Hoover PJ, Mullins FM, Bachhawat P, Covington ED, Raunser S, et al. STIM1 clusters and activates CRAC channels via direct binding of a cytosolic domain to Orai1. *Cell*. 2009 Mar 6;136(5):876–90.
- Patrawala L, Calhoun-Davis T, Schneider-Broussard R, Tang DG. Hierarchical organization of prostate cancer cells in xenograft tumors: the CD44+ α 2beta1+ cell population is enriched in tumor-initiating cells. *Cancer Res*. 2007 Jul 15;67(14):6796–805.
- Pece S, Tosoni D, Confalonieri S, Mazzarol G, Vecchi M, Ronzoni S, et al. Biological and molecular heterogeneity of breast cancers correlates with their cancer stem cell content. *Cell*. 2010 Jan 8;140(1):62–73.
- Penke B, Fulop L, Szucs M, Frecska E. The Role of Sigma-1 Receptor, an Intracellular Chaperone in Neurodegenerative Diseases. *Curr. Neuropharmacol.* 2018;16(1):97–116.
- Pham LV, Tamayo AT, Yoshimura LC, Lin-Lee Y-C, Ford RJ. Constitutive NF-kappaB and NFAT activation in aggressive B-cell lymphomas synergistically activates the CD154 gene and maintains lymphoma cell survival. *Blood*. 2005 Dec 1;106(12):3940–7.
- Pilepich MV, Krall JM, al-Sarraf M, John MJ, Doggett RL, Sause WT, et al. Androgen deprivation with radiation therapy compared with radiation therapy alone for locally advanced prostatic carcinoma: a randomized comparative trial of the Radiation Therapy Oncology Group. *Urology*. 1995 Apr;45(4):616–23.
- Prakriya M, Feske S, Gwack Y, Srikanth S, Rao A, Hogan PG. Orai1 is an essential pore subunit of the CRAC channel. *Nature*. 2006 Sep 14;443(7108):230–3.
- Prakriya M, Lewis RS. Store-Operated Calcium Channels. *Physiol. Rev.* 2015 Oct;95(4):1383–436.
- Prasad PD, Li HW, Fei Y-J, Ganapathy ME, Fujita T, Plumley LH, et al. Exon-Intron Structure, Analysis of Promoter Region, and Chromosomal Localization of the Human Type 1 σ Receptor Gene. *J. Neurochem.* 1998;70(2):443–51.
- Prevarskaya N, Skryma R, Shuba Y. Ion Channels in Cancer: Are Cancer Hallmarks Oncochannelopathies? *Physiol. Rev.* 2018 01;98(2):559–621.

Putney JW. Capacitative calcium entry revisited. *Cell Calcium*. 1990 Dec;11(10):611–24.

Putney JW. Origins of the concept of store-operated calcium entry. *Front. Biosci. Sch. Ed.* 2011;3:980–4.

Qiu R, Lewis RS. Structural features of STIM and Orai underlying store-operated calcium entry. *Curr. Opin. Cell Biol.* 2019 Apr 1;57:90–8.

Radhakrishnan K, Hescheler J, Schneider T. Heat shock proteins and ion channels. Functional interactions and therapeutic consequences. *Curr. Pharm. Biotechnol.* 2010 Feb;11(2):175–9.

Ragde H, Grado GL, Nadir B, Elgamal AA. Modern prostate brachytherapy. *CA. Cancer J. Clin.* 2000 Dec;50(6):380–93.

Raphaël M, Lehen'kyi V, Vandenberghe M, Beck B, Khalimonchik S, Vandenberghe F, et al. TRPV6 calcium channel translocates to the plasma membrane via Orai1-mediated mechanism and controls cancer cell survival. *Proc. Natl. Acad. Sci. U. S. A.* 2014 Sep 16;111(37):E3870-3879.

Rawla P. Epidemiology of Prostate Cancer. *World J. Oncol.* 2019 Apr;10(2):63–89.

Rebel VI, Kung AL, Tanner EA, Yang H, Bronson RT, Livingston DM. Distinct roles for CREB-binding protein and p300 in hematopoietic stem cell self-renewal. *Proc. Natl. Acad. Sci. U. S. A.* 2002 Nov 12;99(23):14789–94.

Renaudo A, L'Hoste S, Guizouarn H, Borgès F, Soriani O. Cancer Cell Cycle Modulated by a Functional Coupling between Sigma-1 Receptors and Cl⁻ Channels. *J. Biol. Chem.* 2007 Jan 26;282(4):2259–67.

Renaudo A, Watry V, Chassot A-A, Ponzio G, Ehrenfeld J, Soriani O. Inhibition of tumor cell proliferation by sigma ligands is associated with K⁺ Channel inhibition and p27kip1 accumulation. *J. Pharmacol. Exp. Ther.* 2004 Dec;311(3):1105–14.

Reya T, Morrison SJ, Clarke MF, Weissman IL. Stem cells, cancer, and cancer stem cells. *Nature.* 2001 Nov 1;414(6859):105–11.

Ring A, Kim Y-M, Kahn M. Wnt/catenin signaling in adult stem cell physiology and disease. *Stem Cell Rev.* 2014 Aug;10(4):512–25.

Robbs BK, Cruz ALS, Werneck MBF, Mognol GP, Viola JPB. Dual roles for NFAT transcription factor genes as oncogenes and tumor suppressors. *Mol. Cell. Biol.* 2008 Dec;28(23):7168–81.

Roos J, DiGregorio PJ, Yeromin AV, Ohlsen K, Lioudyno M, Zhang S, et al. STIM1, an essential and conserved component of store-operated Ca²⁺ channel function. *J. Cell Biol.* 2005 May 9;169(3):435–45.

Rothermel B, Vega RB, Yang J, Wu H, Bassel-Duby R, Williams RS. A protein encoded within the Down syndrome critical region is enriched in striated muscles and inhibits calcineurin signaling. *J. Biol. Chem.* 2000 Mar 24;275(12):8719–25.

Salvino JM, Srikanth YVV, Lou R, Oyer HM, Chen N, Kim FJ. Novel small molecule guanidine Sigma1 inhibitors for advanced prostate cancer. *Bioorg. Med. Chem. Lett.* 2017 May 15;27(10):2216–20.

Schmidt HR, Zheng S, Gurpinar E, Koehl A, Manglik A, Kruse AC. Crystal structure of the human σ 1 receptor. *Nature.* 2016 Apr 28;532(7600):527–30.

- Schneider CA, Rasband WS, Eliceiri KW. NIH Image to ImageJ: 25 years of image analysis. *Nat. Methods*. 2012 Jul;9(7):671–5.
- Schuurmans AL, Bolt J, Mulder E. Androgens stimulate both growth rate and epidermal growth factor receptor activity of the human prostate tumor cell LNCaP. *The Prostate*. 1988;12(1):55–63.
- Sharma S, Findlay GM, Bandukwala HS, Oberdoerffer S, Baust B, Li Z, et al. Dephosphorylation of the nuclear factor of activated T cells (NFAT) transcription factor is regulated by an RNA-protein scaffold complex. *Proc. Natl. Acad. Sci. U. S. A.* 2011 Jul 12;108(28):11381–6.
- Soboloff J, Rothberg BS, Madesh M, Gill DL. STIM proteins: dynamic calcium signal transducers. *Nat. Rev. Mol. Cell Biol.* 2012 Sep;13(9):549–65.
- Soriani O, Rapetti-Mauss R. Sigma 1 Receptor and Ion Channel Dynamics in Cancer. *Adv. Exp. Med. Biol.* 2017;964:63–77.
- Spruce BA, Campbell LA, McTavish N, Cooper MA, Appleyard MVL, O'Neill M, et al. Small Molecule Antagonists of the σ -1 Receptor Cause Selective Release of the Death Program in Tumor and Self-Reliant Cells and Inhibit Tumor Growth in Vitro and in Vivo. *Cancer Res.* 2004 Jul 15;64(14):4875–86.
- Srikanth S, Jung H-J, Kim K-D, Souda P, Whitelegge J, Gwack Y. A novel EF-hand protein, CRACR2A, is a cytosolic Ca²⁺ sensor that stabilizes CRAC channels in T cells. *Nat. Cell Biol.* 2010 May;12(5):436–46.
- Srivats S, Balasuriya D, Pasche M, Vistal G, Edwardson JM, Taylor CW, et al. Sigma1 receptors inhibit store-operated Ca²⁺ entry by attenuating coupling of STIM1 to Orai1. *J. Cell Biol.* 2016 Apr 11;213(1):65–79.
- Stanisz H, Vultur A, Herlyn M, Roesch A, Bogeski I. The role of Orai-STIM calcium channels in melanocytes and melanoma. *J. Physiol.* 2016 01;594(11):2825–35.
- Stathopoulos PB, Ikura M. Structural aspects of calcium-release activated calcium channel function. *Channels Austin Tex.* 2013 Oct;7(5):344–53.
- Stathopoulos PB, Schindl R, Fahrner M, Zheng L, Gasmi-Seabrook GM, Muik M, et al. STIM1/Orai1 coiled-coil interplay in the regulation of store-operated calcium entry. *Nat. Commun.* 2013;4:2963.
- Steers WD. 5 α -reductase activity in the prostate. *Urology*. 2001 Dec;58(6 Suppl 1):17–24; discussion 24.
- Su T-P, Hayashi T, Maurice T, Buch S, Ruoho AE. The sigma-1 receptor chaperone as an inter-organelle signaling modulator. *Trends Pharmacol. Sci.* 2010 Dec;31(12):557–66.
- Su TP, London ED, Jaffe JH. Steroid binding at sigma receptors suggests a link between endocrine, nervous, and immune systems. *Science*. 1988 Apr 8;240(4849):219–21.
- Su T-P, Su T-C, Nakamura Y, Tsai S-Y. The Sigma-1 Receptor as a Pluripotent Modulator in Living Systems. *Trends Pharmacol. Sci.* 2016 Apr;37(4):262–78.
- Sun J, Lu F, He H, Shen J, Messina J, Mathew R, et al. STIM1- and Orai1-mediated Ca(2+) oscillation orchestrates invadopodium formation and melanoma invasion. *J. Cell Biol.* 2014 Nov 24;207(4):535–48.
- Sun L, Youn HD, Loh C, Stolow M, He W, Liu JO. Cabin 1, a negative regulator for calcineurin signaling in T lymphocytes. *Immunity*. 1998 Jun;8(6):703–11.

Terrié E, Coronas V, Constantin B. Role of the calcium toolkit in cancer stem cells. *Cell Calcium*. 2019 Jun;80:141–51.

Terui Y, Saad N, Jia S, McKeon F, Yuan J. Dual role of sumoylation in the nuclear localization and transcriptional activation of NFAT1. *J. Biol. Chem.* 2004 Jul 2;279(27):28257–65.

Thebault S, Flourakis M, Vanoverberghe K, Vandermoere F, Roudbaraki M, Lehen'kyi V, et al. Differential Role of Transient Receptor Potential Channels in Ca²⁺ Entry and Proliferation of Prostate Cancer Epithelial Cells. *Cancer Res.* 2006 Feb 15;66(4):2038–47.

Thomas JD, Longen CG, Oyer HM, Chen N, Maher CM, Salvino JM, et al. Sigma1 Targeting to Suppress Aberrant Androgen Receptor Signaling in Prostate Cancer. *Cancer Res.* 2017 01;77(9):2439–52.

Thompson JL, Shuttleworth TJ. Molecular basis of activation of the arachidonate-regulated Ca²⁺ (ARC) channel, a store-independent Orai channel, by plasma membrane STIM1. *J. Physiol.* 2013 Jul 15;591(14):3507–23.

Tian C, Du L, Zhou Y, Li M. Store-operated CRAC channel inhibitors: opportunities and challenges. *Future Med. Chem.* 2016 May;8(7):817–32.

Touil Y, Igoudjil W, Corvaisier M, Dessein A-F, Vandomme J, Monté D, et al. Colon cancer cells escape 5FU chemotherapy-induced cell death by entering stemness and quiescence associated with the c-Yes/YAP axis. *Clin. Cancer Res. Off. J. Am. Assoc. Cancer Res.* 2014 Feb 15;20(4):837–46.

Tsavalier L, Shapero MH, Morkowski S, Laus R. Trp-p8, a novel prostate-specific gene, is up-regulated in prostate cancer and other malignancies and shares high homology with transient receptor potential calcium channel proteins. *Cancer Res.* 2001 May 1;61(9):3760–9.

Umemura M, Baljinnyam E, Feske S, De Lorenzo MS, Xie L-H, Feng X, et al. Store-operated Ca²⁺ entry (SOCE) regulates melanoma proliferation and cell migration. *PLoS One.* 2014;9(2):e89292.

Veldscholte J, Ris-Stalpers C, Kuiper GG, Jenster G, Berrevoets C, Claassen E, et al. A mutation in the ligand binding domain of the androgen receptor of human LNCaP cells affects steroid binding characteristics and response to anti-androgens. *Biochem. Biophys. Res. Commun.* 1990 Dec 14;173(2):534–40.

Vilner BJ, Costa B de, Bowen WD. Cytotoxic effects of sigma ligands: sigma receptor-mediated alterations in cellular morphology and viability. *J. Neurosci.* 1995a Jan 1;15(1):117–34.

Vilner BJ, John CS, Bowen WD. Sigma-1 and Sigma-2 Receptors Are Expressed in a Wide Variety of Human and Rodent Tumor Cell Lines. *Cancer Res.* 1995b Jan 15;55(2):408–13.

Vummidi Giridhar P, Williams K, VonHandorf AP, Deford PL, Kasper S. Constant Degradation of the Androgen Receptor by MDM2 Conserves Prostate Cancer Stem Cell Integrity. *Cancer Res.* 2019 Mar 15;79(6):1124–37.

Waltering KK, Urbanucci A, Visakorpi T. Androgen receptor (AR) aberrations in castration-resistant prostate cancer. *Mol. Cell. Endocrinol.* 2012 Sep 5;360(1–2):38–43.

Wang F, Marshall CB, Ikura M. Transcriptional/epigenetic regulator CBP/p300 in tumorigenesis: structural and functional versatility in target recognition. *Cell. Mol. Life Sci. CMLS.* 2013 Nov;70(21):3989–4008.

Wissenbach U, Niemeyer B, Himmerkus N, Fixemer T, Bonkhoff H, Flockerzi V. TRPV6 and prostate cancer: cancer growth beyond the prostate correlates with increased TRPV6 Ca²⁺ channel expression. *Biochem. Biophys. Res. Commun.* 2004 Oct 1;322(4):1359–63.

Witte JS. Prostate cancer genomics: towards a new understanding. *Nat. Rev. Genet.* 2009 Feb;10(2):77–82.

Wright AS, Thomas LN, Douglas RC, Lazier CB, Rittmaster RS. Relative potency of testosterone and dihydrotestosterone in preventing atrophy and apoptosis in the prostate of the castrated rat. *J. Clin. Invest.* 1996 Dec 1;98(11):2558–63.

Wu MM, Buchanan J, Luik RM, Lewis RS. Ca²⁺ store depletion causes STIM1 to accumulate in ER regions closely associated with the plasma membrane. *J. Cell Biol.* 2006a Sep 11;174(6):803–13.

Wu MM, Covington ED, Lewis RS. Single-molecule analysis of diffusion and trapping of STIM1 and Orai1 at endoplasmic reticulum-plasma membrane junctions. *Mol. Biol. Cell.* 2014 Nov 5;25(22):3672–85.

Wu W, Misra RS, Russell JQ, Flavell RA, Rincón M, Budd RC. Proteolytic regulation of nuclear factor of activated T (NFAT) c2 cells and NFAT activity by caspase-3. *J. Biol. Chem.* 2006b Apr 21;281(16):10682–90.

Xiao B, Coste B, Mathur J, Patapoutian A. Temperature-dependent STIM1 activation induces Ca²⁺ influx and modulates gene expression. *Nat. Chem. Biol.* 2011 Jun;7(6):351–8.

Yang S, Zhang JJ, Huang X-Y. Orai1 and STIM1 are critical for breast tumor cell migration and metastasis. *Cancer Cell.* 2009a Feb 3;15(2):124–34.

Yang Z-H, Wang X-H, Wang H-P, Hu L-Q. Effects of TRPM8 on the proliferation and motility of prostate cancer PC-3 cells. *Asian J. Androl.* 2009b Mar;11(2):157–65.

Yen M, Lewis RS. Physiological CRAC channel activation and pore properties require STIM1 binding to all six Orai1 subunits. *J. Gen. Physiol.* 2018 Oct 1;150(10):1373–85.

Yen M, Lewis RS. Numbers count: How STIM and Orai stoichiometry affect store-operated calcium entry. *Cell Calcium.* 2019 May;79:35–43.

Yeung PS-W, Yamashita M, Ing CE, Pomès R, Freymann DM, Prakriya M. Mapping the functional anatomy of Orai1 transmembrane domains for CRAC channel gating. *Proc. Natl. Acad. Sci.* 2018 May 29;115(22):E5193–202.

Yissachar N, Sharar Fischler T, Cohen AA, Reich-Zeliger S, Russ D, Shifrut E, et al. Dynamic response diversity of NFAT isoforms in individual living cells. *Mol. Cell.* 2013 Jan 24;49(2):322–30.

Yoeli-Lerner M, Yiu GK, Rabinovitz I, Erhardt P, Jauliac S, Toker A. Akt blocks breast cancer cell motility and invasion through the transcription factor NFAT. *Mol. Cell.* 2005 Nov 23;20(4):539–50.

Young CY, Montgomery BT, Andrews PE, Qui SD, Bilhartz DL, Tindall DJ. Hormonal regulation of prostate-specific antigen messenger RNA in human prostatic adenocarcinoma cell line LNCaP. *Cancer Res.* 1991 Jul 15;51(14):3748–52.

Yuan JP, Zeng W, Dorwart MR, Choi Y-J, Worley PF, Muallem S. SOAR and the polybasic STIM1 domains gate and regulate Orai channels. *Nat. Cell Biol.* 2009 Mar;11(3):337–43.

Zhan Z-Y, Zhong L-X, Feng M, Wang J-F, Liu D-B, Xiong J-P. Over-expression of Orai1 mediates cell proliferation and associates with poor prognosis in human non-small cell lung carcinoma. *Int. J. Clin. Exp. Pathol.* 2015;8(5):5080–8.

Zhang SL, Yu Y, Roos J, Kozak JA, Deerinck TJ, Ellisman MH, et al. STIM1 is a Ca²⁺ sensor that activates CRAC channels and migrates from the Ca²⁺ store to the plasma membrane. *Nature.* 2005 Oct 6;437(7060):902–5.

Zheng X, Bi C, Brooks M, Hage DS. Analysis of Hormone–Protein Binding in Solution by Ultrafast Affinity Extraction: Interactions of Testosterone with Human Serum Albumin and Sex Hormone Binding Globulin. *Anal. Chem.* 2015 Nov 17;87(22):11187–94.

Zhou Y, Srinivasan P, Razavi S, Seymour S, Meraner P, Gudlur A, et al. Initial activation of STIM1, the regulator of store-operated calcium entry. *Nat. Struct. Mol. Biol.* 2013 Aug;20(8):973–81.

Zhu H, Zhang H, Jin F, Fang M, Huang M, Yang CS, et al. Elevated Orai1 expression mediates tumor-promoting intracellular Ca²⁺ oscillations in human esophageal squamous cell carcinoma. *Oncotarget.* 2014 Jun 15;5(11):3455–71.

Annexes

During my PhD, I have participated to several collaborative projects, either in the lab or abroad, that will be presented in this section.

First, I will briefly summarize an ongoing project initiated in collaboration with Sakai's laboratory (IIS, UTokyo, Japan). The aim of this project is to identify the calcium signature of hepatocytes undergoing differentiation. For this project, I obtained a 3 months fellowship from the JSPS (Japan Society for the Promotion of Science). My main results and hypothesis are presented in the following section (section 1).

I will then present the published papers I have co-authored, with first a review on the role of TRPM8 channel in prostate cancer (section 2), followed by three research papers I have collaborated to during my PhD (sections 3-5).

1. Identification of the calcium signature during hiPS differentiation into mature functional hepatocytes

Lucile Noyer, Mathieu Dannoy, Dimitra Gkika, Myriam L Bernier, Yasuyuki Sakai, Loic Lemonnier, Eric Leclerc

Within the frame of a collaboration with Japan, I have obtained a fellowship from the Japan Society for the Promotion of Science (JSPS) to work on a research project aiming to identify the calcium signature of hepatocytes undergoing differentiation. For this purpose, I was hosted in 2018 by Pr Yasuyuki Sakai's laboratory (Institute of Industrial Science, University of Tokyo) where I worked with the team of Dr Eric Leclerc for three months.

Background

Liver is a key organ for drug metabolism and elimination. The evaluation of liver metabolism thus constitutes an essential part of drug development. Currently, the most used *in vitro* liver models are cell lines and primary rat hepatocytes. However, those models present important limitations. There is indeed a need for more physiologically relevant models. Moreover, mature hepatocytes do not proliferate, thus preventing cellular expansion, and drastically limiting the available material. One of the approaches to improve current liver models is the use of micro-scale bioreactors that can mimic *in vivo*-like physiological conditions. The Yasuyuki Sakai laboratory, my host in Japan, has developed biochips with micro-flow that allow 3D tissue organization, high oxygenation, dynamic nutrient supply and waste removal. Biochips provide a specific microenvironment that has been showed to permit higher hepatocyte functionality of mature hepatocytes as compared to plated culture. Thus, liver biochips are a promising tool for predictive toxicology.

On the other hand, the scientific community has been looking for other cell sources to address the scarcity of mature hepatocytes. The generation of functional liver cells from human induced pluripotent stem cells (hiPSC) differentiation seems to be a promising strategy. hiPSC are able to proliferate indefinitely while keeping their ability to differentiate in different cell types (pluripotency). Several studies showed encouraging results, but, to this day, the generation of fully differentiated hepatocytes from hiPSC remains a major challenge. Indeed, the current differentiation protocols lead to the production of hepatocyte-like cells expressing specific adult liver markers and exhibiting hepatic functions (Si Tayeb, 2010). However, those cells still harbor signs of immaturity. To address this issue, my host laboratory in Japan is currently working on the differentiation of hiPSC in biochips. They have shown that the differentiation in biochips allows a more complex multicellular differentiation more representative of liver physiology (Leclerc, 2017). However, the hepatocyte-like cells still shown signs of immaturity. There is thus a strong need to develop the current knowledge on hepatocyte differentiation in order to improve the current protocols.

My host laboratory in France is specialized in the study of calcium channels and calcium homeostasis. Calcium is the most tightly regulated ion within the cell and represents a highly versatile second messenger controlling key physiological processes. Indeed, previous studies conducted in my lab have shown that calcium channels can control cell proliferation and

differentiation. Other studies have also shown the importance of calcium homeostasis and calcium channels in hepatocyte physiology (reviewed in Rychkov and Barritt, 2011; Barritt, 2008). Indeed, some studies have reported the presence of functional store-operated channels (SOC) in mature hepatocytes with an important role in the regulation of bile flow. The expression of TRP (Transient Receptor Potential) calcium channels was also described in these cells, but without defining their exact role. Moreover, previous work in our lab showed that SOC and TRPC6 (TRP Canonical 6) channels control malignant hepatoma cell proliferation (El Boustany, 2008). However, so far, very few studies have focused on the implication of calcium channels in hepatocyte differentiation. In fact, to this day, TRPM7 (TRP Melastatin 7) is the only calcium channel that has been studied in this context. This channel shows a decreased expression and activity in mature non-proliferating rat hepatocytes and is thus believed to participate in hepatocyte proliferation. There is therefore a flagrant lack of data on human and primary cells, as many of those studies have been conducted in rat hepatocytes and/or immortalized cell lines. A better understanding of the calcium signaling in human hepatocyte differentiation could allow us to increase the current knowledge on the subject and to improve the current protocols.

The frame of this fellowship was to start a collaborative project between our two labs with the goal to investigate the calcium signature in hiPSC differentiation in hepatocytes.

Research methodology

For this study, we used hiPSC provided from the stem cell bank of the Institute of Medical Science of the University of Tokyo (TkDN-4M clones; Takayama, 2010).

After a step of initial expansion, we followed a previously published 4 step differentiation protocol adapted from Si Tayeb (2010) to produce hepatocyte-like cells. For the final step of the differentiation, the cells were either kept on Petri dish, or detached and seeded in a biochip (Figure 1). Each differentiation step requires specific culture conditions, and medium was changed daily during the whole process.

The effectiveness of the differentiation protocol was evaluated through the determination of the expression levels of specific mature hepatocyte markers (Albumin, AFP, HNF-4; by RT-qPCR).

Samples were collected at the end of each differentiation step in order to investigate their calcium signature.

For that purpose, we first used RT-qPCR and specific primers to assess the expression of 35 genes known to be involved in calcium homeostasis: Orai channels and their activators STIMs; IP₃Receptors; TRP channels. As a control, we used commercially available samples of total RNA from human livers.

Secondly, we investigated the calcium signature associated with hepatocyte differentiation, by applying protocols routinely used in my French host lab. In order to monitor intracellular calcium stores, we applied on the cells ionomycin (5μM), a calcium ionophore. In order to follow the

process of capacitive calcium entry, which represents one of the main calcium entry pathway in non-excitable cells, I used thapsigargin (2 μ M). Changes in intracellular calcium concentration were monitored using a specific fluorescent calcium dye (Fluo-4) and confocal microscopy.

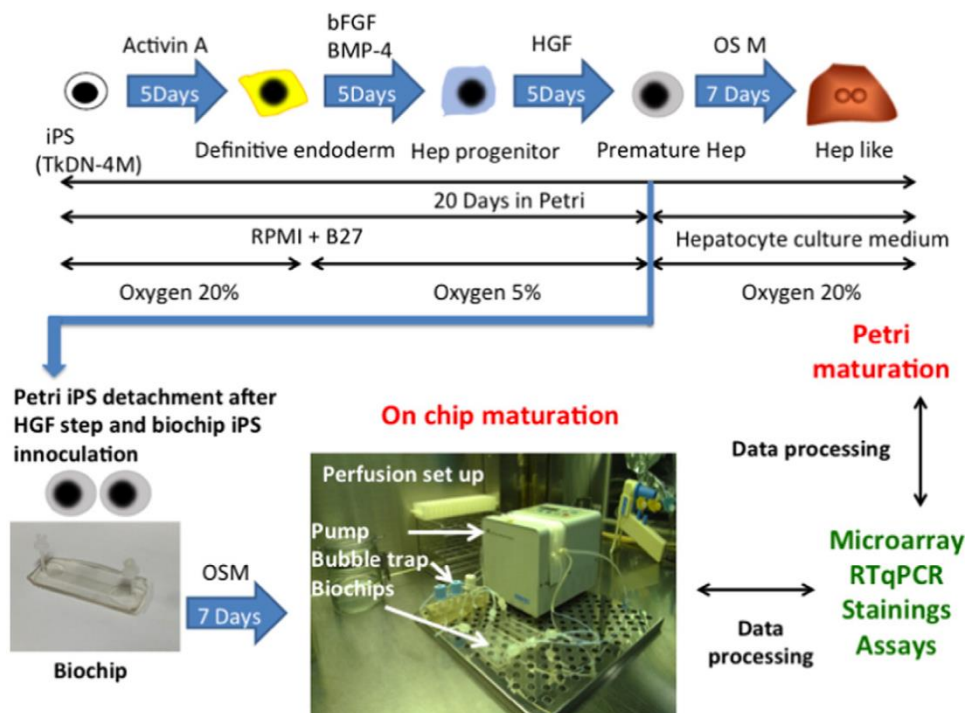


Figure1 : General experimental procedure
Leclerc, 2017

Results

This project allowed us to identify the calcium signature associated with each stage of hiPSC differentiation into hepatocyte-like cells.

First, we validated the differentiation experiment using a specific hepatic marker, albumin (RT-qPCR). As shown in Figure 2A, albumin is not expressed in hiPSC, and its expression increases throughout the differentiation process, thus confirming that it was successful.

Secondly, we evaluated the content of the intracellular calcium stores that are mainly comprised of the endoplasmic reticulum with confocal microscopy. As pictured in Figure 2B, cellular calcium stores vary between each differentiation step, showing a fine tuning of the calcium homeostasis throughout the whole differentiation process.

Finally, we assessed the level of expression of 35 genes involved in calcium homeostasis (Orais, STIMs, IP₃Rs, TRPs; RT-qPCR) at each step of the differentiation into hepatocyte-like cells. In Figures 2C & 2D we show the first heat maps obtained from the expression of the 26 most relevant calcium markers. Those results will allow us to identify the set of calcium channels involved in each differentiation step prior to further investigation.

We also compared three different culture conditions for the final step: Petri dish and two different types of biochips.

During this fellowship, we obtained a large amount of data that we are still analyzing. Moreover, we also have access to microarray data from previous experiments performed before my stay in Japan (Leclerc, 2017). These data will provide us additional information that we will use to fine-tune the final analysis.

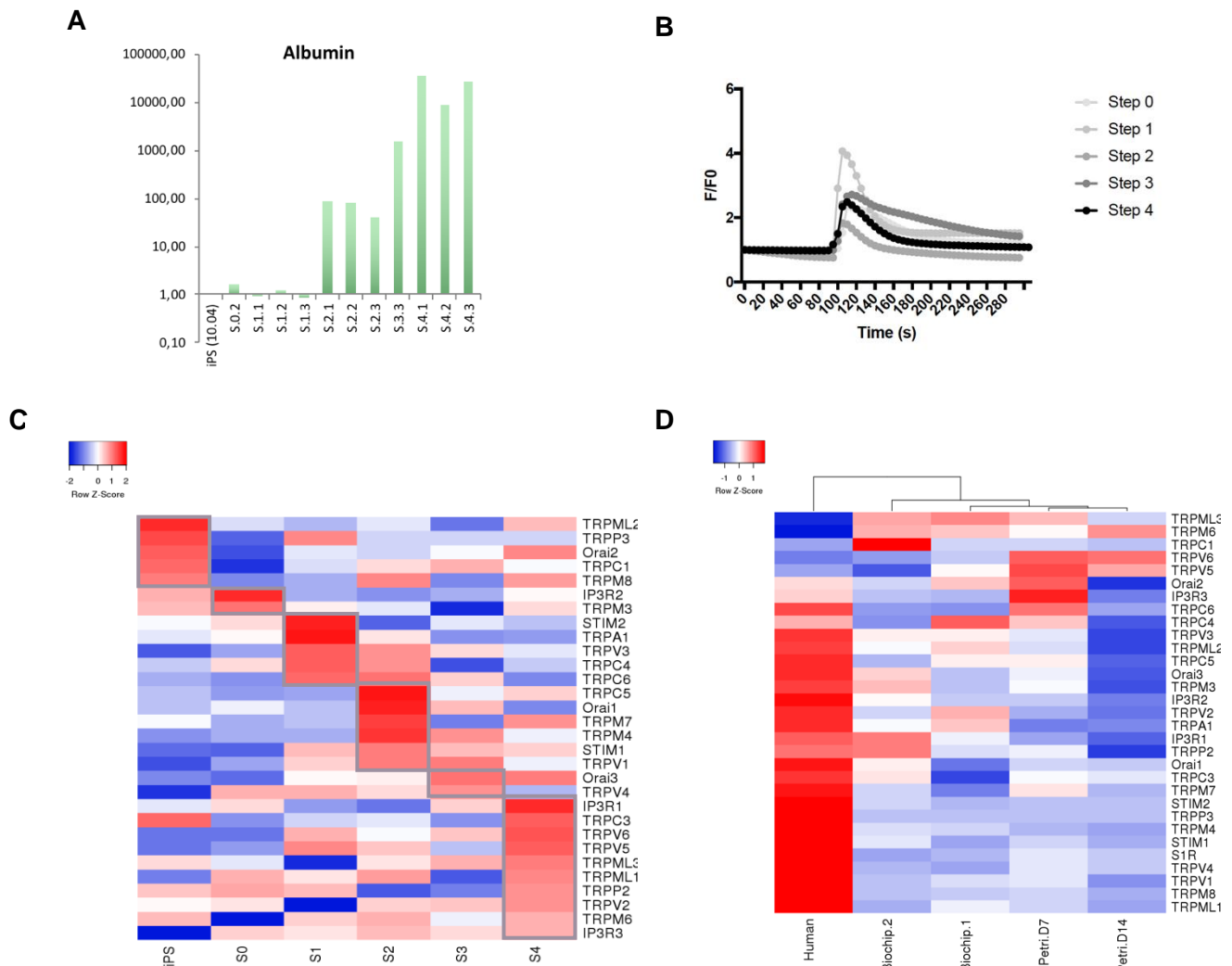


Figure 2: Step by step results obtained on 3 hiPSC differentiations in hepatocytes

A. Expression of the hepatic marker Albumin obtained by RT-qPCR (mRNA levels as a ratio to β -actin control, normalized on iPS condition). **B.** Endoplasmic reticulum calcium content measured by confocal microscopy (Fluo-4 probe) as a ratio of fluorescence (F) on basal fluorescence (F0), after addition of ionomycin (5 μ M) at 100s. **C.** Heatmap of relative mRNA expression levels during hepatocyte differentiation. **D.** Heatmap of relative mRNA expression levels comparing differentiation protocols and human total liver RNA.

All those results will allow us to define a general calcium signature of the cell during each step of the differentiation process into hepatocyte-like cells. After careful processing, these data will be valorized via the publication of a paper currently in preparation.

References

- Barritt GJ, Chen J, Rychkov RY. Ca(2+)-permeable channels in the hepatocyte plasma membrane and their roles in hepatocyte physiology. *Biochim Biophys Acta*. 1783(5):651-72. 2008.
- El Boustany C, Bidaux G, Enfissi A, Delcourt P, Prevarskaya N, Capiod T. Capacitative calcium entry and transient receptor potential canonical 6 expression control human hepatoma cell proliferation. *Hepatology*. 47(6):2068-77. 2008.
- Leclerc E, Kimura K, Shinohara M, et al. Comparison of the transcriptomic profile of hepatic human induced pluripotent stem like cells cultured in plates and in a 3D microscale dynamic environment. *Genomics*. 2017 Jan;109(1):16-26.
- Rychkov GY, Barritt GJ. Expression and function of TRP channels in liver cells. *Adv Exp Med Biol*. 704:667-86. 2011.
- Si Tayeb K, Noto KF, Nagaoka M, et al. Highly efficient generation of human hepatocyte-like cells from induced pluripotent stem cells. *Hepatology*. 2010 Jan;51(1):297-305.
- Takayama N, Nishimura S, Nakamura S, et al. Transient activation of c-MYC expression is critical for efficient platelet generation from human induced pluripotent stem cells. *J Exp Med*. 2010 Dec 20; 207(13):2817-2830.

2. TRPM8 and prostate: a cold case?

Lucile Noyer^{1,2*}, Guillaume P Grolez^{1,2*}, Natalia Prevarskaya^{1,2}, Dimitra Gkika^{1,2*},
Loic Lemonnier^{1,2*}

1: Inserm, U1003, Laboratory of Cell Physiology, University Lille Nord de France, 59655 Cedex, Villeneuve d'Ascq, France.

2: Laboratory of Excellence, Ion Channels Science and Therapeutics, Villeneuve d'Ascq, France.

*: Equal contribution

Invited Review

Pflugers Arch. 2018 Oct;470(10):1419-1429.

doi: 10.1007/s00424-018-2169-1.

Epub 2018 Jun 20.

Available at: <https://link.springer.com/article/10.1007%2Fs00424-018-2169-1>

While originally cloned from the prostate in 2001, transient receptor potential, melastatin member 8 (TRPM8) has since been identified as the cold/menthol receptor in the peripheral nervous system. This discovery has led to hundreds of studies regarding the role of this channel in pain and thermosensation phenomena, while relegating TRPM8 involvement in cancer to a secondary role. Despite these findings, there is growing evidence that TRPM8 should be carefully studied within the frame of carcinogenesis, especially in the prostate, where it is highly expressed and where many teams have confirmed variations in its expression during cancer progression. Its regulation by physiological factors, such as PSA and androgens, has proved that TRPM8 can exhibit an activity beyond that of a cold receptor, thus explaining how the channel can be activated in organs not exposed to temperature variations. With this review, we aim to provide a brief overview of the current knowledge regarding the complex roles of TRPM8 in prostate carcinogenesis and to show that this research path still represents a "hot" topic with potential clinical applications in the short term.

Key words: TRPM8, prostate, cancer, calcium, migration

Introduction

TRPM8 (Transient Receptor Potential, Melastatin member 8) channel stands apart from other TRP channels since, even though this channel is considered to be the predominant detector of cold temperatures in vivo [4, 22, 23], it is also expressed in sensory fibers innervating visceral organs [52, 82] and in epithelia such as the prostate, bladder, testis and skin [25, 61, 65]. A weak expression was also observed in the liver and pulmonary smooth muscle cells [19]. The broad expression pattern of TRPM8 implies that, aside from cold sensing, this channel has additional important functions and modes of activation.

TRPM8 cDNA was initially cloned during a screen for mRNA up-regulated in prostate cancer, and it is not exclusively overexpressed in malignant tissue of the prostate but also in other primary cancers, including melanoma, colorectal adenocarcinoma and breast carcinoma [65]. In the prostate, TRPM8 expression increases in both benign prostate hyperplasia and in prostate carcinoma cells, which both presented high androgen levels [65], and anti-androgen therapy greatly reduced the expression of TRPM8 [37]. It appears that the androgen dependency of TRPM8 expression is related to the differentiation degree of prostate epithelial cells [11, 13]. Furthermore, hormonal regulation by androgens apparently defines TRPM8 localization. Channel expression on the plasma or endoplasmic reticulum (ER) membrane depends on the differentiation and oncogenic status of prostate epithelial cells, probably mediated by two isoforms that are differentially regulated by androgens [11]. Highly differentiated prostate epithelial luminal cells express functional plasma membrane TRPM8, while endoplasmic reticulum TRPM8 remains functional irrespective of the prostate cells' differentiation status [11]. Although TRPM8 is considered a promising target for pharmaceutical, immunological, and genetic interventions in prostate cancer treatment [81], its biological function and physiological modulators in this organ remain elusive. With this review, we aim to give a brief overview of the current knowledge we and others have gathered over the years regarding the involvement of TRPM8 in prostate cancer and to show that this research still represents a “hot” topic with potential clinical applications in the short-term.

I. TRPM8 modulation: from neuronal cold menthol receptor to prostate-specific regulation

TRPM8 pharmacological modulators

Many chemical compounds are known to activate TRPM8. The most well-known of these are menthol, eucalyptol, and chemicals that elicit sensations of cold [54], while various other substances exist, such as the supercooling icilin, the selective agonists WS-12 and CPS-369, which are two menthol derivatives, and D-3263 [5, 6, 15, 21, 24, 49, 54]. Experimental evidence has shown that activation of TRPM8 is induced by all these compounds through different mechanisms and different binding sites in the TRPM8 channel due to the chemical structure of

these compounds and of TRPM8. This channel, like all TRP channels, is comprised of six transmembrane (TM) domains with cytoplasmic N and C-termini, and the functional channel is formed by the homotetrameric assembly of four subunits [48, 76, 78]. Concerning the distinct mechanisms of TRPM8 activation induced by different compounds, it has been shown that TRPM8 activation by icilin depends on intracellular Ca²⁺ levels, in contrast to its activation by menthol and WS-12, which are effective even in the absence of intracellular Ca²⁺ [21, 49]. Despite their different mechanisms for activating TRPM8, chemical compounds generally serve as positive allosteric modulators. More specifically, since activation of TRPM8 is also voltage-dependent, agonists shift the activation threshold towards more negative potentials, whereas antagonists exert their effect by shifting the voltage dependence of TRPM8 activation towards more positive potentials [17, 26, 68]. Regarding the selectivity of TRPM8 to the three most well-known and commonly used compounds, menthol, icilin, and WS-12, it has already been shown that the EC₅₀ for menthol is 10.4 μM and that the EC₅₀ for icilin is 10 times less (1.4 μM) and 100 times less for WS-12 (EC₅₀ = 193 nM) [15]. In view of these EC₅₀, WS-12 clearly appears to be the most potent agonist of TRPM8. In terms of specificity, WS-12 also emerges as the most specific agonist, with no reported activation of other channels induced by this compound so far. In contrast, it has been reported that menthol and icilin can activate other TRPs and ion channels. For example, it has been shown that menthol can activate the TRPA1 channel [38, 71] and the TRPV3 channel [43]. Moreover, menthol was also shown to induce calcium release from the ER and Golgi via a TRPM8-independent pathway when applied at high concentrations, probably through lipid membrane destabilization [44]. Concerning icilin specificity, it has been shown that icilin can also activate TRPA1 channels [39, 62]. Taking into account its high sensitivity and high selectivity for TRPM8, WS-12 appears to be the most efficient TRPM8 agonist and could therefore be used as a therapeutic agent targeting TRPM8 during prostate carcinogenesis. A great number of TRPM8 antagonists have also been characterized over the years; these molecules exhibit various levels of specificity towards this channel. Among these TRPM8 inhibitors are BCTC, thio-BCTC, capsazepine, SKF96365, AMTB, and M8-B [6, 41, 46, 50]. They have been shown to block TRPM8 activity with IC₅₀ of 0.8 ± 1 μM, 3.5 ± 1 μM, 18 ± 1 μM, 40 ± 1 μM, 65 ± 8 nM, and 10.9 ± 2.6 nM, respectively [6, 46, 51, 53]. In terms of their specificity towards TRPM8, M8-B and AMTB are currently the most specific antagonists of TRPM8 [41, 50], with no reported effect on any other TRP channels so far. In contrast, BCTC, thio-BCTC, and capsazepine were shown to also inhibit TRPV1 [6, 70] with IC₅₀ of 34.9 ± 19.4 nM, 54.3 ± 21.8 nM, and 2.6 ± 1.2 μM, respectively [6], making them better TRPV1 inhibitors than TRPM8 inhibitors. Moreover, capsazepine was also reported to inhibit TRPV4 with an IC₅₀ of 18.6 μM [67]. Finally, SKF96365, while blocking TRPM8 activity, is a long-known inhibitor of capacitative calcium entry in store-depleted cells [63], as well as a partial inhibitor of TRPC3 and TRPC6 channels when used at concentrations in the micromolar range [36].

TRPM8 structure-function relationship

Concomitant to the identification of TRPM8 chemical modulators, many teams were trying to determine the channel's structure and to uncover key residues conferring sensitivity to these modulators. The main approach used was point mutagenesis based on predictive models derived from the structures of other available channels, such as potassium channels. From these early experiments, a general consensus appeared regarding the key amino acids involved in TRPM8 response to its main activators. Namely, R842, Y745, and Y1005 were associated with menthol binding [47, 69], while N799, D802, and G805 were proposed to bind icilin [21]. Interestingly, during these studies, Y745 was shown to be not only important for the menthol-induced activation of the channel but also for some of its inhibitors, especially SKF96365 and to a lesser extent capsazepine, clotrimazole, and econazole [47]. The goal of our own experiments was to better understand the structure-function relationship inside the TRPM8 pore region. To do this, we used a homology model of the human TRPM8 pore region based on the then newly released TRPV1 structure obtained by cryo-electron microscopy (cryo-EM). Predictions made from this model were then confirmed by functional studies of the mutants thus generated [11]. Our results show that the previously undescribed point mutation Y908A induces a nearly complete loss of sensitivity to cold and menthol while preserving responsiveness to icilin. This would indicate that the TRPM8 P-helix region is important for cold/menthol sensitivity and that the conformational shift elicited by these two stimuli is different from the one induced by icilin. Since then, the first cryo-EM TRPM8 structure has been published using the collared flycatcher *Ficedula albicollis* TRPM8 [76]. While promising, this initial structure is based on a channel presenting 83% sequence identity with its human counterpart, so it will need to be confirmed with the latter, and a highly resolved density map of the pore region will be required before the next step can be taken to study the impact of TRPM8 chemical modulators on its structure and determine once and for all how they interact.

Endogenous agonists of TRPM8 in the prostate

A key aspect of the modulation of TRPM8 activity is the question of its regulation by endogenous factors. Indeed, as indicated before, TRPM8 was initially cloned in the prostate, where its primary agonist in the peripheral nervous system, i.e., cold, is unlikely to play any physiological role. Early on, several teams showed that, similarly to many other TRP channels, TRPM8 is positively modulated by PIP2 [42, 60]. In line with those results, PLC δ 4 was recently identified as a negative modulator of TRPM8 activity in neurons, with its activation leading to a localized depletion of PIP2 [79]. Despite these promising data, signaling pathways leading to the activation of TRPM8 through an increase in PIP2 production have been considered as a potential way to modulate channel activity in the long term rather than as a way to acutely open the channel in response to agonists. However, our results have shown that lysophospholipids (LPLs) could represent more direct agonists of TRPM8. Indeed, we observed the activation of iPLA2 in TRPM8-overexpressing HEK cells in response to depletion of ER calcium stores, which led to the production of lysophosphatidylinositol (LPI) and lysophosphatidylcholine (LPC) as well as the

subsequent activation of TRPM8 [66]. Our excised patch clamp experiments indicate that this activation most likely represents a direct effect of LPI and LPC on the channel lipid microenvironment. Indeed, both LPLs are known to incorporate into the plasma membrane, where they can act as cup formers that bend the membrane and therefore create a force that is able to mechanically open channels such as TREK [45]. Altogether, our results suggest that any stimulation of ER calcium store depletion could potentially lead to TRPM8 activation. However, in the case of PLC activation, the balance between its positive effect through IP₃ production and IP₃R-mediated ER calcium release and its negative effect via the concomitant decrease in PIP₂ concentration would probably induce variable responses depending upon the immediate surroundings of TRPM8. It would therefore be highly interesting to further explore the nature of the microdomains in TRPM8 in order to better understand its responses to the physiological agonists and growth factors that induce PLC activation and/or depletion of ER calcium stores.

Early detection of prostate cancer is associated with direct palpation and an increase in PSA (prostate-specific antigen) blood levels. More generally, PSA, the third member of the serine protease kallikrein family, represents a highly versatile tool used to monitor the emergence, the recurrence, and the responsiveness to therapies of prostate cancer. However, there is no clear role attributed to PSA during prostate cancer progression. Based on a previous report showing that kallikreins can modulate TRP channel activity through a B₂R (bradykinin 2 receptor)-dependent mechanism [32], we investigated the potential role of PSA on TRPM8. Our results show that, at a concentration found in prostate lumen, PSA can stimulate TRPM8 through two distinct pathways. Indeed, long-term treatments were shown to increase the number of channels found in the plasma membrane, thus leading to increased TRPM8 responses to its classical agonists, cold, menthol, and icilin. Moreover, an acute application of PSA was also shown to induce TRPM8 activation through a B₂R-dependent pathway. To our knowledge, this was the first indication of an endogenous agonist of TRPM8 in prostate cells, and we were then able to link PSA to an inhibition of cell migration [33]. There is little doubt regarding the existence of other endogenous modulators of TRPM8, and more efforts should be devoted to their identification in order to better understand the function of TRPM8 in the context of prostate cancer progression.

II. Pathophysiological impact of TRPM8 in prostate carcinogenesis

TRPM8 inhibits cell migration

As mentioned above, TRPM8 expression is strongly up-regulated in numerous cancers, including prostate cancer, while it is dramatically reduced during metastasis [37, 65, 75]. This expression pattern makes it an interesting candidate as a diagnostic marker for detection of cancer and as a prognosis marker for evaluating the outcome of epithelial cancers [80]. We propose that TRPM8 could also have a protective role in metastatic prostate cancer [30, 35], since recent data show that it blocks cancer cell migration in prostate cells [33, 34, 74, 83]. In particular, overexpression of TRPM8 in prostate cancer cells reduces cell motility through the inactivation of FAK (focal adhesion kinase) [74]. FAK is a non-receptor protein tyrosine kinase that localizes in cellular focal adhesions or cell contacts within the extracellular matrix, participates in growth factor receptor-mediated signaling pathways, and plays essential roles in cell survival, proliferation, migration, and invasion. Moreover, it seems that, outside of any stimulation, the presence of TRPM8 on the plasma membrane is sufficient to reduce migration, suggesting that the basal activity of TRPM8 is possibly affecting FAK phosphorylation, while activation of TRPM8 by icilin, one of its agonists, further reduces cell motility [33]. As mentioned before, the well-known prostate cancer marker PSA, which is secreted in the prostatic acini and is therefore in contact with the extracellular portion of TRPM8, activates the channel and decelerates cell migration by inducing its plasma membrane accumulation [33]. We could thus speculate that PSA activation of TRPM8 could sustain dormancy of prostate hyperplasia by reducing cell mobility and migration. In line with this assumption is the gradual loss of plasma membrane TRPM8 during tumor progression towards the late and invasive prostate cancer stage [37]. Furthermore, two other studies demonstrate that TRPM8 significantly inhibits migration in PC3 cells through the inactivation of FAK [74, 83]. In addition, overexpression of TRPM8 induced significant cell cycle arrest in the G0/G1 stage and facilitated the apoptosis of cells induced by starvation.

TRPM8 and angiogenesis

It was recently shown that TRPM8 expression has a negative effect on angiogenesis. Indeed, nude mice transplanted with prostate cancer cells overexpressing TRPM8 develop tumors that are less vascularized than control tumors. The lower microvascular density of TRPM8 xenografts can be explained by their lower expression of FAK and VEGF, one of the most potent angiogenic factors [83]. Our recent results further show the mechanism underlying the anti-angiogenic effect of TRPM8 through the trapping of the small GTPase, Rap1, and subsequent inhibition of endothelial cell migration [28]. More precisely, in addition to the loss of TRPM8 expression in refractory cancer, we have shown that its expression is also dramatically down-regulated in tumor-derived endothelial cells when compared to their healthy counterparts. In endothelial cells, TRPM8 only presents a reticular localization, in contrast to its dual localization in both reticular and plasma membranes in epithelial cells. Our data indicate that TRPM8 plays

the same role in both cell types, independently of its cellular localization, as overexpression or activation of the channel by its agonists inhibited cell adhesion and migration in both models. In this study, the role of TRPM8 was shown in healthy endothelial cells from macro- (human umbilical vein endothelial cells) and micro-circulation (human microvascular endothelial cells), suggesting a similar mechanism for prostate vasculature. These experimental data were also supported by a modeling approach showing that cell adhesion and migration are strictly dependent on basal TRPM8 activity and on its expression levels rather than its localization. Importantly, we have shown that the expression and constitutive activity of TRPM8 are sufficient to exert its functional effects, inhibiting endothelial cell adhesion to the extracellular matrix and, therefore, endothelial cell migration. We further unraveled the molecular mechanism underlying this inhibitory effect by showing that TRPM8 acts as a Rap1 GTPase inhibitor. Rap is a small G protein that is implicated in a variety of integrin-mediated “inside-out” signaling events [18, 20, 40, 58]. Rap1 cycles between inactive GDP-bound forms and active GTP-bound forms [16]. TRPM8 interacts preferentially with the GDP-bound state of Rap1, thus preventing its cytoplasm-plasma membrane trafficking. In turn, this mechanism impairs the activation of a major inside-out signaling pathway that triggers the conformational activation of integrins and, consequently, cell adhesion, migration, *in vitro* endothelial tube formation, and vessel sprouting [28]. One of the most interesting novelties of this work was the pore-independent function of TRPM8 on endothelial migration, since inhibition of migration using a dead-pore mutant TRPM8 channel was still observed to an extent similar to the one observed with wild-type TRPM8. These data raise the question of the possible roles of TRPM8 agonists, such as icilin and menthol, on channel function apart from pore gating. Indeed, these modulators could lead to conformational changes, inducing major rearrangements in the channel’s interactome. The recent resolution of the structure of TRPM8 will without doubt facilitate the understanding of allosteric coupling between channel domains and TRPM8 partner proteins. Taken together, these results suggest that TRPM8 could play a protective role in prostate cancer progression by reducing both cell migration and angiogenesis, making this channel an attractive target for therapeutics, with several regulatory agents that could be used to prevent the metastatic evolution of prostate cancer when diagnosed. In support of this hypothesis, a preclinical assay with a TRPM8 agonist (D-3263) shows that TRPM8 activation decreases mice prostate hyperplasia [24]. Moreover, recent advances in pharmacology and biotechnology have demonstrated the use of nanocarriers to deliver pharmacological compounds using plasma membrane protein targeting [77]. In this way, nanocarriers targeting membrane receptors such as HER2 and EGFR [29, 59] or targeting ion channels by using curcumin, a TRPA1 activator [73], were developed and used in the context of breast and prostate cancer treatment. Due to its plasma membrane localization, the TRPM8 channel is a promising target for nanocarriers, and as such, TRPM8 agonist encapsulation into nanocarriers could be developed to improve the delivery of TRPM8 agonists and the anti-metastatic effect induced by TRPM8 activation.

III. The next level in TRPM8 modulation: localization, partner proteins, and short isoforms

Intracellular localization of TRPM8 in ER membranes

Over the years, our understanding of how ion channels work has greatly evolved, from a model where they are simply inserted into the plasma membrane waiting to be activated to a complex array of microdomains including channels, various receptors, and their associated signaling pathways, specific lipids, and cytoskeleton elements, the whole of which contributes to the formation of a “channel signalplex” associated with complex physiological responses (for review, see [56, 57]). Among the many structures found in these signalplexes, partner proteins have been shown to control the insertion of TRP channels into the plasma membrane [72], as well as their activity [31, 32]. This question was of particular interest for TRPM8 in the context of prostate cancer. Indeed, an early report showed that in androgen-dependent human prostate cancer LNCaP cells, TRPM8 was almost exclusively located in ER membranes, with no detectable activity in the plasma membrane as proved by the absence of any classical TRPM8 current in response to cold and menthol application [64]. After ruling out the possibility of a mutation in TRPM8 in LNCaP and showing that the channel cloned from LNCaP cells can be found in the plasma membrane when expressed in a heterologous system such as HEK293, we were left with the possibility of a retention factor keeping the channel in ER membranes. Moreover, activation of this intracellular TRPM8 induces an ER calcium release leading to the activation of SOC (store-operated calcium channels), which could in turn impact cell proliferation and apoptosis resistance. The presence of the ER-bound TRPM8 has since then been confirmed [2, 3], but these studies did not discriminate between the physiological impact of the two localizations, if any. However, they linked plasma membrane localization to a higher apoptosis rate and suggested that cancer progression could be associated with the internalization of the channel through ubiquitination/degradation. There is therefore a clear need to further study the impact of TRPM8 intracellular localization on prostate cancer cells in order to understand how all these mechanisms lead to cancer progression before eventually proposing treatments targeting this channel.

TRPM8 partner proteins

As indicated before, partner proteins could be important when explaining the intracellular distribution of channels or even in controlling their activity. However, no such partners had been described for TRPM8 when we tried to address this issue. To identify these partners within the frame of prostate cancer, we used a GST pull-down strategy where N- and C-termini of human TRPM8 were exposed to mice prostate lysates. Proteins interacting with TRPM8 extremities were then identified by mass spectrometry, leading to the creation of a database of several hundred proteins. As it would have been difficult at that time to screen all those proteins for their effect on TRPM8 activity, we selected a few of them based on available literature and tested the impact of their overexpression and silencing on TRPM8. From these experiments, we have identified EAPA2

(experimental autoimmune prostatitis antigen 2) as a promising target. Indeed, this protein was initially described as being specifically expressed in the prostate and as being potentially regulated by androgens, two traits that are particularly interesting in regard to our knowledge of how TRPM8 is modulated during prostate cancer progression [27]. By sequence homology with mouse EAPA2, we were then able to identify two previously unknown human proteins that we named TCAF1 and TCAF2, for TRP channel-associated factors 1 and 2 [34]. While we have shown that both TCAF1 and TCAF2 induce a similar increase in TRPM8 translocation to the plasma membrane, we were surprised to see that they induce opposite effects on the channel's activity. Indeed, TCAF1 increases TRPM8 activity, whereas TCAF2 inhibits it, and this difference arises from a key domain missing in TCAF2, namely, a PI3K homology domain only found in the TCAF1 C-terminus. We have shown that a mutant of TCAF1 lacking this PI3K homology domain exhibits properties resembling those of TCAF2, suggesting that the activating effect of TCAF1 on TRPM8 is most likely due to the channel being phosphorylated. Moreover, the expression pattern of TCAF1 during prostate cancer progression closely resembles that of TRPM8, with an initial increase during the early androgen-dependent stages and a strong decrease when the cancer becomes androgen-independent. Finally, we have shown that the physiological impact of TCAFs is to modulate cell migration in conjunction with TRPM8, even if our observations suggest that TCAFs could also interact with other partners. Taken together, our data show that both TCAFs promote TRPM8 translocation to the plasma membrane and that TCAF1 is necessary for channel activation, probably through phosphorylation, while TCAF2 prevents its activity. To our knowledge, this was the first report describing partner proteins for TRPM8, and our data support the idea that TCAFs could be targeted independently from TRPM8 in order to prevent prostate cancer cell migration.

TRPM8 short isoforms

Another level of complexity in TRPM8 regulation was revealed when we started identifying short isoforms of the channel in prostate cancer cells. Indeed, on top of the “normal” full-length channel of 128 kDa, shorter truncated TRPM8 proteins were shown in our models. Most notably, we have characterized two short isoforms cloned from prostate cancer epithelial cells [9]. These two splice variants, named TRPM8 α and TRPM8 β , possess two and one alternate ATG, respectively, leading to the synthesis of two short proteins of 6 and 18 kDa, named sM8-6 and sM8-18, respectively. These short isoforms correspond to fragments of the TRPM8 N-terminus, a cytosolic domain, suggesting that they are primarily found in cytosol. Interestingly, both isoforms are absent from DRG neurons but can be found in other tumors such as melanoma, colon cancer, and endometrial adenocarcinoma, an observation that raises the question of their potential role in cancer but for which there is currently no response. When we tried to determine the functional impact of these isoforms, we observed a complex modulation of TRPM8. Indeed, while they both induced a significant decrease in TRPM8 activity in response to its agonists cold, menthol, and LPI, their effects on icilin-induced currents were the opposite, with sM8-6 increasing and sM8-18 decreasing current amplitude. Moreover, our biotinylation experiments have shown that the

overexpression of both isoforms resulted in a small increase in the amount of TRPM8 found in the plasma membrane, therefore ruling out the possibility that isoforms inhibit TRPM8 activity by preventing its translocation to cell surface. To understand these results, we tried to determine whether the short isoforms can directly bind the channel, using FRET (Förster resonance energy transfer) as our main technical approach. Our results show that sM8-6 and sM8-18 both bind the C-terminus of the full-length TRPM8, with little to no interaction with the channel N-terminus, and that this interaction is temperature dependent, i.e., inhibited by cold. Moreover, at the single-channel level, sM8-6 and sM8-18 were both shown to stabilize the channel in a closed state, making its activation by cold and agonists more difficult. Our interpretation of these results is that both isoforms share the same core property of binding to the TRPM8 C-terminus and that this interaction results in a conformational change that stabilizes the channel in a closed state. Upon cold application, TRPM8 undergoes a conformational change resulting in the dislodgement of the isoforms, as suggested by the loss of FRET signal. However, how these conformational changes lead to an increase in the response to icilin remains an open question for which additional studies will be required. While this last point still needs to be addressed, recent work by Peng et al. has confirmed that these short isoforms have a physiological impact on prostate cancer cells. Indeed, overexpression of sM8-18 leads to an increase in prostate cancer cell migration and invasiveness through the activation of MMP-2 [55]. This effect could also result from sM8-18 inhibiting full-length TRPM8, as we have shown that the channel negatively regulates migration [34], even if the interaction between short isoforms and ER-located TRPM8 has not yet been confirmed.

More recently, other types of short TRPM8 isoforms have been identified in prostate cancer cells [12, 14]. The most important ones appear to be truncated channels lacking the N-terminal section of the protein as well as the first two transmembrane domains, resulting in channels with four transmembrane domains instead of the usual six, notated 4TM-TRPM8 or eTRPM8 due to their exclusive localization in ER membranes. These isoforms are very similar to those previously described in keratinocytes, where they control the balance between proliferation and differentiation by modulating the shuttling of calcium between ER and mitochondria in a cold-dependent manner [10, 13]. In the prostate, we have identified at least three 4TM-TRPM8 isoforms of 35, 38, and 40 kDa found in ER membranes and showed their localization in MAMs (mitochondria-associated membranes), where they work as calcium leak channels that deplete ER calcium stores and increase mitochondria calcium content, leading to increased ATP production. Electrophysiological studies of purified 4TM-TRPM8 in giant unilamellar vesicles indicate that these isoforms represent fully functional channels that respond to classical TRPM8 modulators (e.g., icilin, menthol, WS12, BCTC). While their similarities make them difficult to study due to a lack of specific modulators, their physiological functions appear to be the control of proliferation and apoptosis, mostly through their interaction with sM8 isoforms. Indeed, silencing of sM8 isoforms resulted in an increase in p21 expression associated with an inhibition of proliferation and an increase in apoptosis, most likely due to oxidative stress and protein unfolding

in mitochondria in primary human prostate cancer cells, as well as in cell lines [12]. Interestingly, the effect of sM8 silencing was highly dependent on the type of TRPM8 isoforms expressed in the cells, indicating the potential presence of a very complex array of interactions and physiological responses depending on the expression of different isoform subtypes.

Conclusion

While originally cloned in the prostate in 2001 [65], TRPM8 has since then been identified as the cold/menthol receptor in the peripheral nervous system [49]. This discovery led to hundreds of studies regarding the role of this channel in the peripheral nervous system and the associated pain and thermosensation phenomena, while relegating the involvement of TRPM8 in cancer to a secondary place and relative neglect. Despite this fact, there is growing evidence that TRPM8 should be carefully studied within the frame of carcinogenesis, especially in the prostate, where it is highly expressed and where many teams have confirmed variations in its expression during cancer progression. With this review, we show that TRPM8 plays a critical role in many pathophysiological processes (Fig. 1) and that this diversity comes from the presence of many isoforms of the channel. Since these isoforms have been neglected so far in most models, including neurons, it is our hope that this work will prompt more teams to start investigating them in their respective models in order to better understand their general roles beyond the ones described here in the prostate.

Among many other points that still need to be addressed, the question of endogenous modulators of TRPM8 in the prostate and of their mechanisms of action is a critical one. Evidence of regulation by physiological factors such as PSA, androgens, and LPL has proved that TRPM8 can exhibit an activity beyond that of cold receptor, thus explaining how the channel can be activated in organs not exposed to temperature variations. The exact nature of this regulation is still a matter of intense debate, as is the physiological impact of TRPM8 activation in prostate cancer cells. Indeed, while TRPM8 expression is generally acknowledged as being androgen-dependent, direct modulation of the channel by testosterone has been reported by Zakharian's team [1]. In their hands, testosterone and its active form DHT (dihydrotestosterone) directly bind to TRPM8 and open it, with EC₅₀ of 64.9 pM and 21.4 nM, respectively. The physiological relevance of this discovery is still unclear since the same team then showed that this direct effect of steroids, when applied at a non-physiological concentration of 1 μM on TRPM8, disappears in the presence of the androgen receptor (AR) [2]. Indeed, since AR and TRPM8 expression are closely linked in prostate cancer cells, this would mean that, if this hypothesis is correct, TRPM8 activity would constantly be repressed by steroids, leading to an increase in cell migration [33, 34]. This apparent contradiction will need to be addressed before validating the concept of TRPM8 targeting in the treatment of prostate cancer, but an interesting possibility is that even if steroids indeed inhibit TRPM8 activity, agonists such as PSA and LPLs could still bind the channel and induce a conformational change

that could be sufficient to activate the signaling pathway leading to the inhibition of cell migration [28].

As stated above, the physiological function of TRPM8 in prostate cancer cells is not yet completely understood, and literature shows controversial data presenting the channel as controlling proliferation, apoptosis, survival, and/or migration depending on cell type and investigator. However, very few studies thus far have considered TRPM8 short isoforms or the impact of their localization beyond the plasma membrane. Since tools such as siRNA will target a large number of isoforms beyond the wild-type channel, one should be extremely careful when drawing conclusions from TRPM8 silencing. Indeed, siRNA targeting the N-terminal region of TRPM8 will not only affect the wild-type channel but also sM8 isoforms. On the other hand, siRNA targeting the pore region will prevent wild-type and 4TM-TRPM8 expression. Knowing that these isoforms have distinct impacts on cell fates, a close study of their respective abundance in any given cell type should be considered a necessity prior to drawing any conclusion. Similarly, while we have shown that 4TM-TRPM8 and wild-type TRPM8 exhibit the same core properties in terms of responsiveness to classical TRPM8 agonists and antagonists, it is still too early to say that they are perfectly identical in regard to their pharmacology. Further studies will need to address that point in order to make sure that a compound designed to block cancer cell migration and angiogenesis does not stimulate proliferation.

A final point we wish to make is about the recent publication of the first cryo-EM TRPM8 structure [76]. Indeed, for many years, TRP channel structures remained elusive, and most hypotheses relied on comparative models using other available crystal structures. While this first structure offers new information regarding the spatial organization of TRPM8 N- and C-termini, the pore region and other critical parts of the channel were not sufficiently resolved to be described. We therefore hope that the next technological developments in cryo-EM will provide the scientific community with a complete structure of TRPM8 in the years to come, which will better define the domains of the channel and shed light on the activation mechanisms of agonists such as menthol and WS-12. Indeed, when generalized, cryo-EM technology will provide us with a powerful tool allowing for the understanding of the interplay between wild-type TRPM8, 4TM-TRPM8, short isoforms, partner proteins such as TCAFs, AR, and steroids.

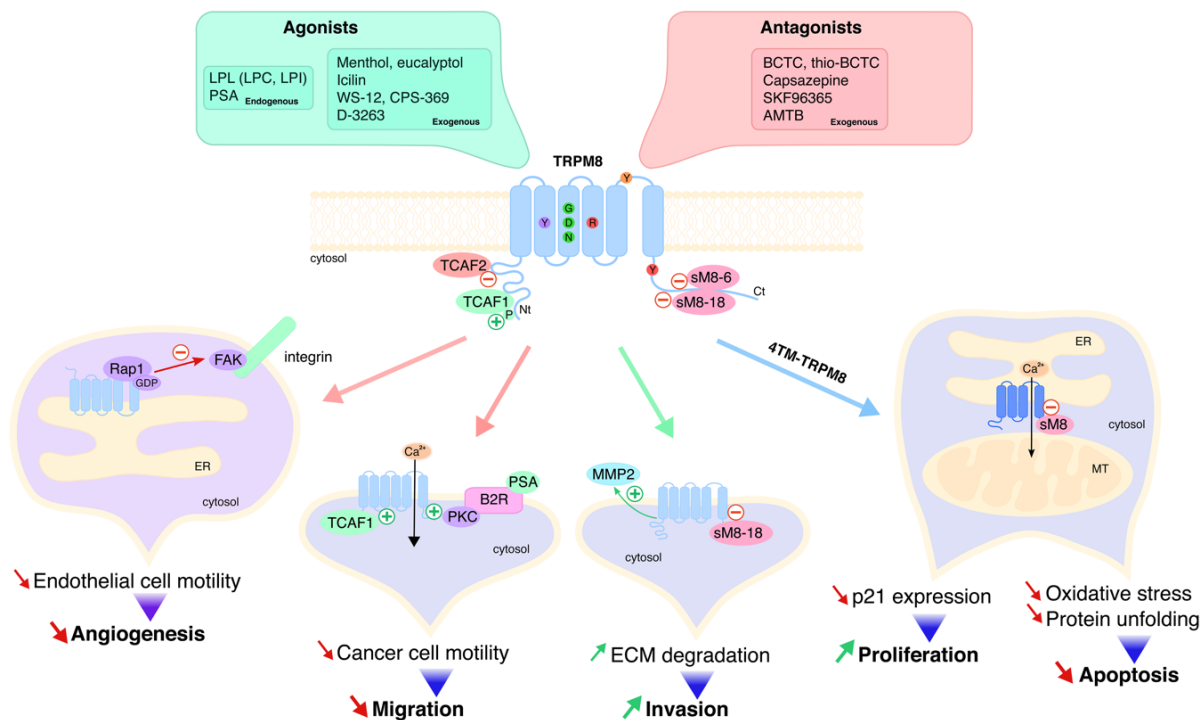


Figure 1. TRPM8 plays a central role in prostate cancer. The upper part of the scheme focuses on the main TRPM8 modulators that are discussed in this review. In the center, key amino acids involved in the responses of TRPM8 to its modulators are highlighted: N799, D802, and G805 for icilin binding (green); R842 and Y1005 for menthol binding (red); Y908 for cold sensitivity (orange); and Y745 for the binding of menthol and some antagonists (purple). Key interacting proteins directly binding and modulating TRPM8 are also presented. First, the TCAF partner proteins, which interact preferentially with the TRPM8 N-terminus. TCAF1 increases the channel activity via phosphorylation, whereas TCAF2 inhibits TRPM8. Second, the TRPM8 short isoforms sM8, sM8-6, and sM8-18, which interact with the TRPM8 C-terminus and stabilize the channel in a closed state. The major physiopathological impacts of TRPM8 in prostate carcinogenesis are presented in the lower part of the scheme. From left to right: 1. activation of TRPM8 traps the small GTPase Rap1 in its GDP-binding state in tumor-derived endothelial cells, preventing its participation in FAK/integrin signaling. This leads to decreased endothelial cell motility, inhibiting angiogenesis. 2. Activation of TRPM8 by its classical exogenous agonists (menthol, icilin) or endogenous agonists (PSA via B2R activation, TCAF1 via direct interaction) leads to decreased cancer cell motility, inhibiting prostate cancer migration. 3. TRPM8 inhibition by its small isoform sM8-18 leads to increased prostate cancer cell invasion via MMP-2 activation. 4. Located in the MAMs, the short isoforms 4TM-TRPM8 act as calcium leak channels between ER and mitochondria. Here, 4TM-TRPM8 can be inhibited by sM8 isoforms, leading to decreased p21 expression and a consequent increase in prostate cancer cell proliferation. sM8 inhibition of 4TM-TRPM8 also prevents apoptosis induced by oxidative stress and protein unfolding.

Authors' contributions

L. N., G. G., N. P., D. G., and L. L. wrote the paper.

Funding information

Our work was supported by funds from INSERM, University Lille Nord de France, Ministère de l'Education Nationale, LabEx ICST, Ligue Contre le Cancer, Fondation ARC pour la recherche sur

le cancer (PJA 20141202010), Agence Nationale pour la Recherche, the Region Hauts de France, SIRIC ONCOLille, Canceropole Nord Ouest, Association pour la Recherche sur les Tumeurs de la Prostate, and the Institut National du Cancer (INCa-PLBIO14-213).

References

1. Asuthkar S, Demirkhanyan L, Mueting SR, Cohen A, Zakharian E (2017) High-throughput proteome analysis reveals targeted TRPM8 degradation in prostate cancer. *Oncotarget* 8:12877–12890. doi: 10.18632/oncotarget.14178
2. Asuthkar S, Demirkhanyan L, Sun X, Elustondo PA, Krishnan V, Baskaran P, Velpula KK, Thyagarajan B, Pavlov EV, Zakharian E (2015) The TRPM8 protein is a testosterone receptor: II. Functional evidence for an ionotropic effect of testosterone on TRPM8. *J Biol Chem* 290:2670–2688. doi: 10.1074/jbc.M114.610873
3. Asuthkar S, Velpula KK, Elustondo PA, Demirkhanyan L, Zakharian E (2015) TRPM8 channel as a novel molecular target in androgen-regulated prostate cancer cells. *Oncotarget* 6:17221–17236. doi: 10.18632/oncotarget.3948
4. Bautista DM, Siemens J, Glazer JM, Tsuruda PR, Basbaum AI, Stucky CL, Jordt S-E, Julius D (2007) The menthol receptor TRPM8 is the principal detector of environmental cold. *Nature* 448:204–208. doi: 10.1038/nature05910
5. Beck B, Bidaux G, Bavencoffe A, Lemonnier L, Thebault S, Shuba Y, Barrit G, Skryma R, Prevarskaya N (2007) Prospects for prostate cancer imaging and therapy using high-affinity TRPM8 activators. *Cell Calcium* 41:285–294. doi: 10.1016/j.ceca.2006.07.002
6. Behrendt H-J, Germann T, Gillen C, Hatt H, Jostock R (2004) Characterization of the mouse cold-menthol receptor TRPM8 and vanilloid receptor type-1 VR1 using a fluorometric imaging plate reader (FLIPR) assay. *Br J Pharmacol* 141:737–745. doi: 10.1038/sj.bjp.0705652
7. Bidaux G, Beck B, Zholos A, Gordienko D, Lemonnier L, Flourakis M, Roudbaraki M, Borowiec A-S, Fernandez J, Delcourt P, Lepage G, Shuba Y, Skryma R, Prevarskaya N (2012) Regulation of activity of transient receptor potential melastatin 8 (TRPM8) channel by its short isoforms. *J Biol Chem* 287:2948–2962. doi: 10.1074/jbc.M111.270256
8. Bidaux G, Borowiec A, Gordienko D, Beck B, Shapovalov GG, Lemonnier L, Flourakis M, Vandenberghe M, Slomianny C, Dewailly E, Delcourt P, Desruelles E, Ritaine A, Polakowska R, Lesage J, Chami M, Skryma R, Prevarskaya N (2015) Epidermal TRPM8 channel isoform controls the balance between keratinocyte proliferation and differentiation in a cold-dependent manner. *Proc Natl Acad Sci U S A* 112:E3345–3354. doi: 10.1073/pnas.1423357112
9. Bidaux G, Borowiec A-S, Dubois C, Delcourt P, Schulz C, Vanden Abeele F, Lepage G, Desruelles E, Bokhobza A, Dewailly E, Slomianny C, Roudbaraki M, Heliot L, Bonnal J-L, Mauroy B, Mariot P, Lemonnier L, Prevarskaya N (2016) Targeting of short TRPM8 isoforms induces 4TM-

- TRPM8-dependent apoptosis in prostate cancer cells. *Oncotarget* 7:29063–29080. doi: 10.18632/oncotarget.8666
10. Bidaux G, Borowiec A-S, Prevarskaya N, Gordienko D (2016) Fine-tuning of eTRPM8 expression and activity conditions keratinocyte fate. *Channels Austin Tex* 10:320–331. doi: 10.1080/19336950.2016.1168551
11. Bidaux G, Flourakis M, Thebault S, Zholos A, Beck B, Gkika D, Roudbaraki M, Bonnal J-L, Mauroy B, Shuba Y, Skryma R, Prevarskaya N (2007) Prostate cell differentiation status determines transient receptor potential melastatin member 8 channel subcellular localization and function. *J Clin Invest* 117:1647–1657. doi: 10.1172/JCI30168
12. Bidaux G, Gordienko D, Shapovalov G, Farfariello V, Borowiec A-S, Iamshanova O, Lemonnier L, Gueguinou M, Guibon R, Fromont G, Paillard M, Gouriou Y, Chouabe C, Dewailly E, Gkika D, Lopez-Alvarado P, Carlos Menendez J, Heliot L, Slomianny C, Prevarskaya N (2018) 4TMTRPM8 channels are new gatekeepers of the ER-mitochondria Ca(2+) transfer. *Biochim Biophys Acta* 1865:981–994. doi: 10.1016/j.bbamcr.2018.04.007
13. Bidaux G, Roudbaraki M, Merle C, Crepin A, Delcourt P, Slomianny C, Thebault S, Bonnal J-L, Benahmed M, Cabon F, Mauroy B, Prevarskaya N (2005) Evidence for specific TRPM8 expression in human prostate secretory epithelial cells: functional androgen receptor requirement. *Endocr Relat Cancer* 12:367–382. doi: 10.1677/erc.1.00969
14. Bidaux G, Sgobba M, Lemonnier L, Borowiec A-S, Noyer L, Jovanovic S, Zholos AV, Haider S (2015) Functional and Modeling Studies of the Transmembrane Region of the TRPM8 Channel. *Biophys J* 109:1840–1851. doi: 10.1016/j.bpj.2015.09.027
15. Bodding M, Wissenbach U, Flockerzi V (2007) Characterisation of TRPM8 as a pharmacophore receptor. *Cell Calcium* 42:618–628. doi: 10.1016/j.ceca.2007.03.005
16. Bourne HR, Sanders DA, McCormick F (1990) The GTPase superfamily: a conserved switch for diverse cell functions. *Nature* 348:125–132. doi: 10.1038/348125a0
17. Brauchi S, Orio P, Latorre R (2004) Clues to understanding cold sensation: thermodynamics and electrophysiological analysis of the cold receptor TRPM8. *Proc Natl Acad Sci U S A* 101:15494–15499. doi: 10.1073/pnas.0406773101
18. Carmona G, Gottig S, Orlandi A, Scheele J, Bauerle T, Jugold M, Kiessling F, Henschler R, Zeiher AM, Dimmeler S, Chavakis E (2009) Role of the small GTPase Rap1 for integrin activity regulation in endothelial cells and angiogenesis. *Blood* 113:488–497. doi: 10.1182/blood-2008-02-138438
19. Cheung WYW, Ha N-R, Suen MWH, Xu CL, Yang CWT (2007) Warming up the cold reception at a TRPM8 function. *J Neurosci Off J Soc Neurosci* 27:7617–7618. doi: 10.1523/JNEUROSCI.2353-07.2007
20. Chrzanowska-Wodnicka M, Kraus AE, Gale D, White GC 2nd, Vansluys J (2008) Defective angiogenesis, endothelial migration, proliferation, and MAPK signaling in Rap1b-deficient mice. *Blood* 111:2647–2656. doi: 10.1182/blood-2007-08-109710

21. Chuang H, Neuhausser WM, Julius D (2004) The super-cooling agent icilin reveals a mechanism of coincidence detection by a temperature-sensitive TRP channel. *Neuron* 43:859–869. doi: 10.1016/j.neuron.2004.08.038
22. Colburn RW, Lubin ML, Stone DJJ, Wang Y, Lawrence D, D'Andrea MR, Brandt MR, Liu Y, Flores CM, Qin N (2007) Attenuated cold sensitivity in TRPM8 null mice. *Neuron* 54:379–386. doi: 10.1016/j.neuron.2007.04.017
23. Dhaka A, Murray AN, Mathur J, Earley TJ, Petrus MJ, Patapoutian A (2007) TRPM8 is required for cold sensation in mice. *Neuron* 54:371–378. doi: 10.1016/j.neuron.2007.02.024
24. Duncan D, Stewart F, Frohlich M, Urdal D (2009) PRECLINICAL EVALUATION OF THE TRPM8 ION CHANNEL AGONIST D-3263 FOR BENIGN PROSTATIC HYPERPLASIA. *J Urol* 181:503. doi: 10.1016/S0022-5347(09)61422-1
25. Facer P, Casula MA, Smith GD, Benham CD, Chessell IP, Bountra C, Sinisi M, Birch R, Anand P (2007) Differential expression of the capsaicin receptor TRPV1 and related novel receptors TRPV3, TRPV4 and TRPM8 in normal human tissues and changes in traumatic and diabetic neuropathy. *BMC Neurol* 7:11. doi: 10.1186/1471-2377-7-11
26. Fernandez JA, Skryma R, Bidaux G, Magleby KL, Scholfield CN, McGeown JG, Prevarskaya N, Zholos AV (2011) Voltage- and cold-dependent gating of single TRPM8 ion channels. *J Gen Physiol* 137:173–195. doi: 10.1085/jgp.201010498
27. Fujimoto N, Akimoto Y, Suzuki T, Kitamura S, Ohta S (2006) Identification of prostatic-secreted proteins in mice by mass spectrometric analysis and evaluation of lobe-specific and androgen-dependent mRNA expression. *J Endocrinol* 190:793–803. doi: 10.1677/joe.1.06733
28. Genova T, Grolez GP, Camillo C, Bernardini M, Bokhobza A, Richard E, Scianna M, Lemonnier L, Valdembri D, Munaron L, Philips MR, Mattot V, Serini G, Prevarskaya N, Gkika D, Pla AF (2017) TRPM8 inhibits endothelial cell migration via a non-channel function by trapping the small GTPase Rap1. *J Cell Biol.* 216(7):2107-2130. doi: 10.1083/jcb.201506024.
29. Geretti E, Leonard SC, Dumont N, Lee H, Zheng J, De Souza R, Gaddy DF, Espelin CW, Jaffray DA, Moyo V, Nielsen UB, Wickham TJ, Hendriks BS (2015) Cyclophosphamide-Mediated Tumor Priming for Enhanced Delivery and Antitumor Activity of HER2-Targeted Liposomal Doxorubicin (MM-302). *Mol Cancer Ther* 14:2060–2071. doi: 10.1158/1535-7163.MCT-15-0314
30. Gkika D, Flourakis M, Lemonnier L, Prevarskaya N (2010) PSA reduces prostate cancer cell motility by stimulating TRPM8 activity and plasma membrane expression. *Oncogene* 29:4611–4616. doi: 10.1038/onc.2010.210
31. Gkika D, Lemonnier L, Shapovalov G, Gordienko D, Poux C, Bernardini M, Bokhobza A, Bidaux G, Degerny C, Verreman K, Guarmit B, Benahmed M, de Launoit Y, Bindels RJM, Fiorio Pla A, Prevarskaya N (2015) TRP channel-associated factors are a novel protein family that regulates TRPM8 trafficking and activity. *J Cell Biol* 208:89–107. doi: 10.1083/jcb.201402076

32. Gkika D, Mahieu F, Nilius B, Hoenderop JGJ, Bindels RJM (2004) 80K-H as a new Ca²⁺ sensor regulating the activity of the epithelial Ca²⁺ channel transient receptor potential cation channel V5 (TRPV5). *J Biol Chem* 279:26351–26357. doi: 10.1074/jbc.M403801200
33. Gkika D, Prevarskaya N (2011) TRP channels in prostate cancer: the good, the bad and the ugly? *Asian J Androl* 13:673–676. doi: 10.1038/aja.2011.18
34. Gkika D, Topala CN, Chang Q, Picard N, Thebault S, Houillier P, Hoenderop JGJ, Bindels RJM (2006) Tissue kallikrein stimulates Ca(2+) reabsorption via PKC-dependent plasma membrane accumulation of TRPV5. *EMBO J* 25:4707–4716. doi: 10.1038/sj.emboj.7601357
35. Grolez GP, Gkika D (2016) TRPM8 Puts the Chill on Prostate Cancer. *Pharm Basel Switz* 9. doi: 10.3390/ph9030044
36. Harteneck C, Gollasch M (2011) Pharmacological modulation of diacylglycerol-sensitive TRPC3/6/7 channels. *Curr Pharm Biotechnol* 12:35–41
37. Henshall SM, Afar DEH, Hiller J, Horvath LG, Quinn DI, Rasiah KK, Gish K, Willhite D, Kench JG, Gardiner-Garden M, Stricker PD, Scher HI, Grygiel JJ, Agus DB, Mack DH, Sutherland RL (2003) Survival analysis of genome-wide gene expression profiles of prostate cancers identifies new prognostic targets of disease relapse. *Cancer Res* 63:4196–4203
38. Karashima Y, Damann N, Prenen J, Talavera K, Segal A, Voets T, Nilius B (2007) Bimodal action of menthol on the transient receptor potential channel TRPA1. *J Neurosci Off J Soc Neurosci* 27:9874–9884. doi: 10.1523/JNEUROSCI.2221-07.2007
39. Kuhn FJP, Kuhn C, Luckhoff A (2009) Inhibition of TRPM8 by icilin distinct from desensitization induced by menthol and menthol derivatives. *J Biol Chem* 284:4102–4111. doi: 10.1074/jbc.M806651200
40. Lafuente EM, van Puijenbroek AAFL, Krause M, Carman CV, Freeman GJ, Berezovskaya A, Constantine E, Springer TA, Gertler FB, Boussiotis VA (2004) RIAM, an Ena/VASP and Profilin ligand, interacts with Rap1-GTP and mediates Rap1-induced adhesion. *Dev Cell* 7:585–595. doi: 10.1016/j.devcel.2004.07.021
41. Lashinger ESR, Steingra MS, Hieble JP, Leon LA, Gardner SD, Nagilla R, Davenport EA, Hoffman BE, Laping NJ, Su X (2008) AMTB, a TRPM8 channel blocker: evidence in rats for activity in overactive bladder and painful bladder syndrome. *Am J Physiol Renal Physiol* 295:F803–810. doi: 10.1152/ajprenal.90269.2008
42. Liu B, Qin F (2005) Functional control of cold- and menthol-sensitive TRPM8 ion channels by phosphatidylinositol 4,5-bisphosphate. *J Neurosci Off J Soc Neurosci* 25:1674–1681. doi: 10.1523/JNEUROSCI.3632-04.2005
43. Macpherson LJ, Hwang SW, Miyamoto T, Dubin AE, Patapoutian A, Story GM (2006) More than cool: promiscuous relationships of menthol and other sensory compounds. *Mol Cell Neurosci* 32:335–343. doi: 10.1016/j.mcn.2006.05.005

44. Mahieu F, Owsianik G, Verbert L, Janssens A, De Smedt H, Nilius B, Voets T (2007) TRPM8-independent menthol-induced Ca²⁺ release from endoplasmic reticulum and Golgi. *J Biol Chem* 282:3325–3336. doi: 10.1074/jbc.M605213200
45. Maingret F, Patel AJ, Lesage F, Lazdunski M, Honore E (2000) Lysophospholipids open the twopore domain mechano-gated K(+) channels TREK-1 and TRAAK. *J Biol Chem* 275:10128–10133
46. Malkia A, Madrid R, Meseguer V, de la Pena E, Valero M, Belmonte C, Viana F (2007) Bidirectional shifts of TRPM8 channel gating by temperature and chemical agents modulate the cold sensitivity of mammalian thermoreceptors. *J Physiol* 581:155–174. doi: 10.1113/jphysiol.2006.123059
47. Malkia A, Morenilla-Palao C, Viana F (2011) The emerging pharmacology of TRPM8 channels: hidden therapeutic potential underneath a cold surface. *Curr Pharm Biotechnol* 12:54–67
48. Malkia A, Pertusa M, Fernandez-Ballester G, Ferrer-Montiel A, Viana F (2009) Differential role of the menthol-binding residue Y745 in the antagonism of thermally gated TRPM8 channels. *Mol Pain* 5:62. doi: 10.1186/1744-8069-5-62
49. McKemy DD, Neuhausser WM, Julius D (2002) Identification of a cold receptor reveals a general role for TRP channels in thermosensation. *Nature* 416:52–58. doi: 10.1038/nature719
50. Miller S, Rao S, Wang W, Liu H, Wang J, Gavva NR (2014) Antibodies to the extracellular pore loop of TRPM8 act as antagonists of channel activation. *PLoS One* 9:e107151. doi: 10.1371/journal.pone.0107151
51. Morgan K, Sadofsky LR, Crow C, Morice AH (2014) Human TRPM8 and TRPA1 pain channels, including a gene variant with increased sensitivity to agonists (TRPA1 R797T), exhibit differential regulation by. *Biosci Rep* 34. doi: 10.1042/BSR20140061
52. Mukerji G, Yiangou Y, Corcoran SL, Selmer IS, Smith GD, Benham CD, Bountra C, Agarwal SK, Anand P (2006) Cool and menthol receptor TRPM8 in human urinary bladder disorders and clinical correlations. *BMC Urol* 6:6. doi: 10.1186/1471-2490-6-6
53. Patel R, Goncalves L, Newman R, Jiang FL, Goldby A, Reeve J, Hendrick A, Teall M, Hannah D, Almond S, Brice N, Dickenson AH (2014) Novel TRPM8 antagonist attenuates cold hypersensitivity after peripheral nerve injury in rats. *J Pharmacol Exp Ther* 349:47–55. doi: 10.1124/jpet.113.211243
54. Peier AM, Moqrich A, Hergarden AC, Reeve AJ, Andersson DA, Story GM, Earley TJ, Dragoni I, McIntyre P, Bevan S, Patapoutian A (2002) A TRP channel that senses cold stimuli and menthol. *Cell* 108:705–715
55. Peng M, Wang Z, Yang Z, Tao L, Liu Q, Yi LU, Wang X (2015) Overexpression of short TRPM8 variant alpha promotes cell migration and invasion, and decreases starvation-induced apoptosis in prostate cancer LNCaP cells. *Oncol Lett* 10:1378–1384. doi: 10.3892/ol.2015.3373
56. Prevarskaya N, Skryma R, Shuba Y (2018) Ion Channels in Cancer: Are Cancer Hallmarks Oncochannelopathies? *Physiol Rev* 98:559–621. doi: 10.1152/physrev.00044.2016

57. Redondo PC, Rosado JA (2015) Store-operated calcium entry: unveiling the calcium handling signalplex. *Int Rev Cell Mol Biol* 316:183–226. doi: 10.1016/bs.ircmb.2015.01.007
58. Reedquist KA, Ross E, Koop EA, Wolthuis RM, Zwartkruis FJ, van Kooyk Y, Salmon M, Buckley CD, Bos JL (2000) The small GTPase, Rap1, mediates CD31-induced integrin adhesion. *J Cell Biol* 148:1151–1158
59. Reid RC, Yau M-K, Singh R, Hamidon JK, Reed AN, Chu P, Suen JY, Stoermer MJ, Blakeney JS, Lim J, Faber JM, Fairlie DP (2013) Downsizing a human inflammatory protein to a small molecule with equal potency and functionality. *Nat Commun* 4:2802. doi: 10.1038/ncomms3802
60. Rohacs T, Lopes CMB, Michailidis I, Logothetis DE (2005) PI(4,5)P₂ regulates the activation and desensitization of TRPM8 channels through the TRP domain. *Nat Neurosci* 8:626–634. doi: 10.1038/nn1451
61. Stein RJ, Santos S, Nagatomi J, Hayashi Y, Minnery BS, Xavier M, Patel AS, Nelson JB, Futrell WJ, Yoshimura N, Chancellor MB, De Miguel F (2004) Cool (TRPM8) and hot (TRPV1) receptors in the bladder and male genital tract. *J Urol* 172:1175–1178. doi: 10.1097/01.ju.0000134880.55119.cf
62. Story GM, Peier AM, Reeve AJ, Eid SR, Mosbacher J, Hricik TR, Earley TJ, Hergarden AC, Andersson DA, Hwang SW, McIntyre P, Jegla T, Bevan S, Patapoutian A (2003) ANKTM1, a TRP-like channel expressed in nociceptive neurons, is activated by cold temperatures. *Cell* 112:819–829
63. Sweeney ZK, Minatti A, Button DC, Patrick S (2009) Small-molecule inhibitors of store-operated calcium entry. *ChemMedChem* 4:706–718. doi: 10.1002/cmdc.200800452
64. Thebault S, Lemonnier L, Bidaux G, Flourakis M, Bavencoffe A, Gordienko D, Roudbaraki M, Delcourt P, Panchin Y, Shuba Y, Skryma R, Prevarskaya N (2005) Novel role of cold/mentholsensitive transient receptor potential melastatine family member 8 (TRPM8) in the activation of store-operated channels in LNCaP human prostate cancer epithelial cells. *J Biol Chem* 280:39423–39435. doi: 10.1074/jbc.M503544200
65. Tsavaler L, Shapero MH, Morkowski S, Laus R (2001) Trp-p8, a novel prostate-specific gene, is up-regulated in prostate cancer and other malignancies and shares high homology with transient receptor potential calcium channel proteins. *Cancer Res* 61:3760–3769
66. Vanden Abeele F, Zholos A, Bidaux G, Shuba Y, Thebault S, Beck B, Flourakis M, Panchin Y, Skryma R, Prevarskaya N (2006) Ca²⁺-independent phospholipase A₂-dependent gating of TRPM8 by lysophospholipids. *J Biol Chem* 281:40174–40182. doi: 10.1074/jbc.M605779200
67. Vincent F, Acevedo A, Nguyen MT, Dourado M, DeFalco J, Gustafson A, Spiro P, Emerling DE, Kelly MG, Duncton MAJ (2009) Identification and characterization of novel TRPV4 modulators. *Biochem Biophys Res Commun* 389:490–494. doi: 10.1016/j.bbrc.2009.09.007
68. Voets T, Droogmans G, Wissenbach U, Janssens A, Flockerzi V, Nilius B (2004) The principle of temperature-dependent gating in cold- and heat-sensitive TRP channels. *Nature* 430:748–754. doi: 10.1038/nature02732

69. Voets T, Owsianik G, Janssens A, Talavera K, Nilius B (2007) TRPM8 voltage sensor mutants reveal a mechanism for integrating thermal and chemical stimuli. *Nat Chem Biol* 3:174–182. doi: 10.1038/nchembio862
70. Weil A, Moore SE, Waite NJ, Randall A, Gunthorpe MJ (2005) Conservation of functional and pharmacological properties in the distantly related temperature sensors TRVP1 and TRPM8. *Mol Pharmacol* 68:518–527. doi: 10.1124/mol.105.012146
71. Xiao B, Dubin AE, Bursulaya B, Viswanath V, Jegla TJ, Patapoutian A (2008) Identification of transmembrane domain 5 as a critical molecular determinant of menthol sensitivity in mammalian TRPA1 channels. *J Neurosci Off J Soc Neurosci* 28:9640–9651. doi: 10.1523/JNEUROSCI.2772-08.2008
72. Xu XZ, Moebius F, Gill DL, Montell C (2001) Regulation of melastatin, a TRP-related protein, through interaction with a cytoplasmic isoform. *Proc Natl Acad Sci U S A* 98:10692–10697. doi: 10.1073/pnas.191360198
73. Yallapu MM, Khan S, Maher DM, Ebeling MC, Sundram V, Chauhan N, Ganju A, Balakrishna S, Gupta BK, Zafar N, Jaggi M, Chauhan SC (2014) Anti-cancer activity of curcumin loaded nanoparticles in prostate cancer. *Biomaterials* 35:8635–8648. doi: 10.1016/j.biomaterials.2014.06.040
74. Yang Z-H, Wang X-H, Wang H-P, Hu L-Q (2009) Effects of TRPM8 on the proliferation and motility of prostate cancer PC-3 cells. *Asian J Androl* 11:157–165. doi: 10.1038/aja.2009.1
75. Yee NS, Zhou W, Lee M (2010) Transient receptor potential channel TRPM8 is over-expressed and required for cellular proliferation in pancreatic adenocarcinoma. *Cancer Lett* 297:49–55. doi: 10.1016/j.canlet.2010.04.023
76. Yin Y, Wu M, Zubcevic L, Borschel WF, Lander GC, Lee S-Y (2018) Structure of the cold- and menthol-sensing ion channel TRPM8. *Science* 359:237–241. doi: 10.1126/science.aan4325
77. Yu B, Tai HC, Xue W, Lee LJ, Lee RJ (2010) Receptor-targeted nanocarriers for therapeutic delivery to cancer. *Mol Membr Biol* 27:286–298. doi: 10.3109/09687688.2010.521200
78. Yudin Y, Lutz B, Tao Y-X, Rohacs T (2016) Phospholipase C delta4 regulates cold sensitivity in mice. *J Physiol* 594:3609–3628. doi: 10.1113/JP272321
79. Yudin Y, Rohacs T (2012) Regulation of TRPM8 channel activity. *Mol Cell Endocrinol* 353:68–74. doi: 10.1016/j.mce.2011.10.023
80. Zhang L, Barritt GJ (2004) Evidence that TRPM8 is an androgen-dependent Ca²⁺ channel required for the survival of prostate cancer cells. *Cancer Res* 64:8365–8373. doi: 10.1158/0008-5472.CAN-04-2146
81. Zhang L, Barritt GJ (2006) TRPM8 in prostate cancer cells: a potential diagnostic and prognostic marker with a secretory function? *Endocr Relat Cancer* 13:27–38. doi: 10.1677/erc.1.01093

82. Zhang L, Jones S, Brody K, Costa M, Brookes SJH (2004) Thermosensitive transient receptor potential channels in vagal afferent neurons of the mouse. *Am J Physiol Gastrointest Liver Physiol* 286:G983–991. doi: 10.1152/ajpgi.00441.2003
83. Zhu G, Wang X, Yang Z, Cao H, Meng Z, Wang Y, Chen D (2011) Effects of TRPM8 on the proliferation and angiogenesis of prostate cancer PC-3 cells in vivo. *Oncol Lett* 2:1213–1217. doi: 10.3892/ol.2011.410
84. Zhu G, Wang X, Yang Z, Cao H, Meng Z, Wang Y, Chen D (2011) Effects of TRPM8 on the proliferation and angiogenesis of prostate cancer PC-3 cells in vivo. *Oncol Lett* 2:1213–1217. doi: 10.3892/ol.2011.410

3. TRPV1 variants impair intracellular Ca²⁺ signaling and may confer susceptibility to malignant hyperthermia

Fabien Vanden Abeele^{1}, Sabine Lotteau^{2,3,4*}, Sylvie Ducreux^{2,3}, Charlotte Dubois¹, Nicole Monnier⁵, Amy Hanna⁶, Dimitra Gkika¹, Caroline Romestaing⁷, Lucile Noyer¹, Matthieu Flourakis¹, Nolwenn Tessier^{2,3}, Ribal Al-Mawla^{2,3}, Christophe Chouabe^{2,3}, Etienne Lefai^{2,3}, Joël Lunardi⁵, Susan Hamilton⁶, Julien Fauré^{5,8,9}, Fabien Van Coppenolle^{2,3*}, Natalia Prevarskaya^{1*}*

1: Inserm U1003, Laboratory of Excellence, Ion Channels Science and Therapeutics, Equipe Labélisée par la Ligue Nationale Contre le Cancer, SIRIC ONCOLille, Université des Sciences et Technologies de Lille, Villeneuve d'Ascq, 59656, France.

2: Université de Lyon, Lyon, Cedex 07, France.

3: Univ-Lyon, CarMeN laboratory, Inserm U1060, INRA U1397, Université Claude Bernard Lyon1, INSA Lyon, Hospital Cardiology, IHU OPERA Cardioprotection, B13 Building, Lyon East, 59 Boulevard Pinel, Fr-69500, Bron, France.

4: School of Biomedical Sciences, University of Leeds, Leeds, LS2 9JT, UK.

5: Laboratoire de Biochimie Génétique et Moléculaire, IBP, CHU Grenoble Alpes, F-38000, Grenoble, France.

6: Department of Molecular Physiology and Biophysics, Baylor College of Medicine, Houston, Texas, 77030, USA.

7: Université de Lyon, UMR 5023 Ecologie des Hydrosystèmes Naturels et Anthropisés, Université Lyon 1, ENTPE, CNRS, 6 rue Raphaël Dubois, 69622, Villeurbanne, France.

8: INSERM U1216, F-38000, Grenoble, France.

9: Univ. Grenoble Alpes, Grenoble Institut des Neurosciences, GIN, F-38000, Grenoble, France.

**: Equal contribution*

Genet Med. 2018 Jun 21.

doi: 10.1038/s41436-018-0066-9.

Purpose

Malignant hyperthermia (MH) is a pharmacogenetic disorder arising from uncontrolled muscle calcium release due to an abnormality in the sarcoplasmic reticulum (SR) calcium-release mechanism triggered by halogenated inhalational anesthetics. However, the molecular mechanisms involved are still incomplete.

Methods

We aimed to identify transient receptor potential vanilloid 1 (TRPV1) variants within the entire coding sequence in patients who developed sensitivity to MH of unknown etiology. In vitro and in vivo functional studies were performed in heterologous expression system, *trpv1*^{-/-} mice, and a murine model of human MH.

Results

We identified TRPV1 variants in two patients and their heterologous expression in muscles of *trpv1*^{-/-} mice strongly enhanced calcium release from SR upon halogenated anesthetic stimulation, suggesting they could be responsible for the MH phenotype. We confirmed the in vivo significance by using mice with a knock-in mutation (Y524S) in the type I ryanodine receptor (*Ryr1*), a mutation analogous to the Y522S mutation associated with MH in humans. We showed that the TRPV1 antagonist capsazepine slows the heat-induced hypermetabolic response in this model.

Conclusion

We propose that TRPV1 contributes to MH and could represent an actionable therapeutic target for prevention of the pathology and also be responsible for MH sensitivity when mutated.

Full text available at: <https://www.nature.com/articles/s41436-018-0066-9>

4. Activation of mutated TRPA1 ion channel by resveratrol in human prostate cancer associated fibroblasts (CAF)

Eric Vancauwenberghe^{1,2}, Lucile Noyer^{1,2}, Sandra Derouiche^{1,2}, Loïc Lemonnier^{1,2}, Pierre Gosset³, Laura R. Sadofsky⁴, Pascal Mariot^{1,2}, Marine Warnier^{1,2}, Alexandre Bokhobza^{1,2}, Christian Slomianny^{1,2}, Brigitte Mauroy^{1,5}, Jean-Louis Bonnal^{1,5}, Etienne Dewailly^{1,2}, Philippe Delcourt^{1,2}, Laurent Allart^{1,2}, Emilie Desruelles^{1,2}, Natalia Prevarskaya^{1,2}, Morad Roudbaraki^{1,2}

1: Univ. Lille, Inserm, U1003-PHYCEL-Physiologie Cellulaire, Equipe labellisée par la Ligue Nationale contre le cancer, Villeneuve d'Ascq, Lille, France.

2: Laboratory of Excellence, Ion Channels Science and Therapeutics, Université Lille I Sciences et Technologies, Villeneuve d'Ascq, France.

3: Faculté Libre de Médecine, Laboratoire d'Anatomie et de Cytologie Pathologique du groupement hospitalier de l'Institut Catholique de Lille, Lille, France.

4: Cardiovascular and Respiratory Studies, The University of Hull, Castle Hill Hospital, Cottingham, United Kingdom.

5: Service d'Urologie de l'hôpital St-Philibert, Lille, France. 1: Inserm, U1003, Laboratory of Cell Physiology, University Lille Nord de France, 59655 Cedex, Villeneuve d'Ascq, France.

Mol Carcinog. 2017 Aug;56(8):1851-1867.

doi: 10.1002/mc.22642.

Epub 2017 May 22.

Previous studies showed the effects of resveratrol (RES) on several cancer cells, including prostate cancer (PCa) cell apoptosis without taking into consideration the impact of the tumor microenvironment (TME). The TME is composed of cancer cells, endothelial cells, blood cells, and cancer-associated fibroblasts (CAF), the main source of growth factors. The latter cells might modify in the TME the impact of RES on tumor cells via secreted factors. Recent data clearly show the impact of CAF on cancer cells apoptosis resistance via secreted factors. However, the effects of RES on PCa CAF have not been studied so far. We have investigated here for the first time the effects of RES on the physiology of PCa CAF in the context of TME. Using a prostate cancer CAF cell line and primary cultures of CAF from prostate cancers, we show that RES activates the N-terminal mutated Transient Receptor Potential Ankyrin 1 (TRPA1) channel leading to an increase in intracellular calcium concentration and the expression and secretion of growth factors (HGF and VEGF) without inducing apoptosis in these cells. Interestingly, in the present work, we also show that when the prostate cancer cells were co-cultured with CAF, the RES-induced cancer cell apoptosis was reduced by 40%, an apoptosis reduction canceled in the presence of the TRPA1 channel inhibitors. The present work highlights CAF TRPA1 ion channels as a target for RES and the importance of the channel in the epithelial-stromal crosstalk in the TME leading to resistance to the RES-induced apoptosis.

Full text available at: <https://onlinelibrary.wiley.com/doi/full/10.1002/mc.22642>

5. Functional and Modeling Studies of the Transmembrane Region of the TRPM8 Channel

Gabriel Bidaux¹, Miriam Sgobba², Loic Lemonnier³, Anne-Sophie Borowiec³, Lucile Noyer³, Srdan Jovanovic⁴, Alexander V. Zholos⁵, Shozeb Haider⁴

1: Inserm, U1003, Laboratoire de Physiologie Cellulaire, Equipe labellisée par la Ligue contre le Cancer, Villeneuve d'Ascq, France; Laboratory of Excellence, Ion Channels Science and Therapeutics, Université de Lille 1, Villeneuve d'Ascq, France; Laboratoire Biophotonique Cellulaire Fonctionnelle. Institut de Recherche Interdisciplinaire, Villeneuve d'Ascq, France.

2: Centre for Cancer Research and Cell Biology, Queen's University of Belfast, Belfast, United Kingdom.

3: Inserm, U1003, Laboratoire de Physiologie Cellulaire, Equipe labellisée par la Ligue contre le Cancer, Villeneuve d'Ascq, France; Laboratory of Excellence, Ion Channels Science and Therapeutics, Université de Lille 1, Villeneuve d'Ascq, France.

4: UCL School of Pharmacy, London, United Kingdom.

5: Department of Biophysics, Educational and Scientific Centre, "Institute of Biology" Taras Shevchenko, Kiev National University, Kiev, Ukraine.

Biophys J. 2015 Nov 3;109(9):1840-51.

doi: 10.1016/j.bpj.2015.09.027.

Members of the transient receptor potential (TRP) ion channel family act as polymodal cellular sensors, which aid in regulating Ca(2+) homeostasis. Within the TRP family, TRPM8 is the cold receptor that forms a nonselective homotetrameric cation channel. In the absence of TRPM8 crystal structure, little is known about the relationship between structure and function. Inferences of TRPM8 structure have come from mutagenesis experiments coupled to electrophysiology, mainly regarding the fourth transmembrane helix (S4), which constitutes a moderate voltage-sensing domain, and about cold sensor and phosphatidylinositol 4,5-bisphosphate binding sites, which are both located in the C-terminus of TRPM8. In this study, we use a combination of molecular modeling and experimental techniques to examine the structure of the TRPM8 transmembrane and pore helix region including the conducting conformation of the selectivity filter. The model is consistent with a large amount of functional data and was further tested by mutagenesis. We present structural insight into the role of residues involved in intra- and intersubunit interactions and their link with the channel activity, sensitivity to icilin, menthol and cold, and impact on channel oligomerization.

Full text available at: [https://www.cell.com/biophysj/fulltext/S0006-3495\(15\)00998-4](https://www.cell.com/biophysj/fulltext/S0006-3495(15)00998-4)

Résumé substantiel

Rôle d'Orai1 dans la prolifération des cellules cancéreuses prostatiques et la transition quiescence/activation des cellules souches cancéreuses

Introduction

I. *Physiologie et pathologies de la prostate*

1. *Physiologie*

a. *Anatomie et fonction*

La prostate est une glande accessoire de l'appareil reproducteur masculin. Cette glande fibromusculaire est divisée en quatre parties anatomiquement et fonctionnellement distinctes : zone centrale, zone périphérique, zone de transition et stroma fibromusculaire antérieur.

Cette glande fibromusculaire remplit deux fonctions :

- Les cellules exocrines de la prostate produisent le liquide prostatique, composant un tiers du liquide spermatique.
- La composante musculaire de la prostate aide à l'expulsion des liquides par l'urètre.

b. *Histologie*

D'un point de vue histologique, le tissu prostatique est composé d'un stroma fibromusculaire et de glandes épithéliales. Chaque acinus est formé d'une couche de cellules épithéliales luminales exocrines et d'une couche de cellules basales.

c. *Régulation par les androgènes*

L'épithélium prostatique a la particularité s'être sous dépendance hormonale. En effet, les androgènes régulent la survie, la prolifération, la sécrétion et la différenciation des cellules épithéliales prostatiques. La perturbation des signaux androgéniques peut conduire à des processus pathologiques tels que le cancer de la prostate (CaP) via la dérégulation de l'équilibre entre la prolifération et la mort cellulaire. Les androgènes sont principalement produits dans les testicules, sous régulation hypothalamique. Ces hormones agissent au niveau des cellules prostatiques via les récepteurs aux androgènes (RA).

2. *Le cancer de la prostate*

a. *Chiffres*

Le CaP est le cancer le plus fréquemment diagnostiqué chez l'homme en Europe, et il représente actuellement la troisième cause de mortalité par cancer. Le développement de cette pathologie étant fortement lié à l'âge, sa prévalence ne cesse d'augmenter avec le vieillissement de la population.

b. *Développement*

Le CaP se développe à partir de lésions précancéreuses épithéliales (preneoplastic intraepithelial neoplasia, PIN) accompagnées d'une instabilité génomique. Ce cancer se développe d'abord localement au sein de la glande. Lorsque le CaP devient invasif au-delà de la capsule prostatique,

il atteint d'abord les vésicules séminales et la vessie, puis les ganglions lymphatiques, et enfin des organes distants tels que les os via la circulation sanguine.

c. Diagnostic et pronostic

Le diagnostic précoce du CaP permet d'augmenter considérablement les chances de survie du patient. En effet, les taux de survie à cinq ans sont de 100% pour les patients atteints d'un cancer localisé au moment du diagnostic, mais chutent à 30% pour un cancer détecté à un stade avancé métastatique. Le diagnostic de cette pathologie repose actuellement sur trois éléments :

- Le toucher rectal : permet de détecter une masse anormale au niveau de la zone périphérique postérieure.
- Le taux de PSA : la PSA (prostate specific antigen) est une protéine spécifiquement sécrétée par l'épithélium prostatique sous le contrôle des androgènes. La concentration sanguine de PSA augmente lors du CaP. Néanmoins, sa concentration peut aussi augmenter lors de pathologies bénignes telles que l'hyperplasie bénigne de la prostate (HBP), ce qui en fait un marqueur contesté.
- Biopsie et analyse histopathologique : étape essentielle afin de poser le diagnostic d'un CaP.

d. Grade histologique

La détermination du grade histologique permet de poser le diagnostic et de déterminer l'agressivité du cancer. Pour cela, la méthode de Gleason est appliquée. Cette technique évalue l'état de différenciation du tissu, une note élevée représentant un cancer agressif peu différencié.

e. Classification de la tumeur

La tumeur est ensuite classée selon la méthode TNM (tumor, node, metastasis) afin d'évaluer son agressivité et d'adapter l'approche thérapeutique. Cette classification prend en compte la nature de la tumeur (T ; taille, envahissement), l'invasion des ganglions lymphatiques locaux (N) et la présence de métastases (M).

f. Traitements

Le CaP peut avoir un développement très lent. Ainsi, pour les tumeurs à faible risque, la surveillance active peut être la meilleure option. Pour une tumeur localisée à risque, la première ligne de traitement est la chirurgie. Lorsque cette option n'est pas possible, plusieurs approches thérapeutiques sont possibles, en fonction de l'avancement de la pathologie :

- Radiothérapie : employée pour le traitement de tumeur à invasion locale. On retrouve deux approches, la curiethérapie et la radiothérapie externe.
- Castration chimique : la suppression des signaux androgénique permet de stopper la croissance tumorale. Malheureusement, ce traitement conduit inévitablement à un échappement thérapeutique et au développement de tumeurs agressives résistantes à la castration pour lesquelles il n'y a pas de traitement curatif à l'heure actuelle.
- Chimiothérapie : utilisée pour les cancers avancés métastatiques.

g. Mécanismes de résistance

Lors de la suppression androgénique, les cellules cancéreuses prostatiques peuvent mettre en place plusieurs stratégies pour résister au traitement. Parmi celles-ci on retrouve de nombreux mécanismes impliquant le RA. En effet, par mutation, épissage alternatif ou surexpression, les cellules cancéreuses prostatiques résistantes sont capables de proliférer en l'absence des androgènes.

Un autre mécanisme proposé est l'existence de cellules souches cancéreuses.

II. Les cellules souches cancéreuses

Les cellules souches cancéreuses (CSCs) représentent une sous-population de cellules cancéreuses indifférenciées ayant la capacité de se diviser de façon asymétrique, permettant le maintien de leur population et le développement de la tumeur. De plus, ces cellules sont résistantes aux thérapies conventionnelles et peuvent entrer en quiescence en cas de stress. Ce phénomène permettrait notamment d'expliquer les récurrences suite à l'activation des CSCs quiescentes après une phase de dormance plus ou moins longue, ainsi que la résistance de certains cancers, dont celui de la prostate, aux chimiothérapies. Les mécanismes mis en jeu dans la transition entre la quiescence et la prolifération constituent une question centrale de l'étude des CSCs aujourd'hui. Il a ainsi été montré que des mécanismes touchant l'homéostasie calcique peuvent être impliqués dans le contrôle de la transition entre prolifération et quiescence dans plusieurs modèles de CSCs.

La caractérisation des mécanismes calciques présidant à l'orientation des CSCs vers la quiescence ou la prolifération représente donc une étape indispensable qui pourrait permettre, sur le long terme, de les cibler spécifiquement afin de développer des approches thérapeutiques efficaces, notamment pour les stades tardifs androgéno-résistants du cancer de la prostate.

III. Les canaux calciques

Le calcium est un second messager intervenant dans de nombreux phénomènes cellulaires tels que la prolifération, la migration, la sécrétion... Par conséquent, des altérations de l'homéostasie calcique, résultant notamment de variations d'expression et/ou d'activité de canaux calciques, ont été impliquées dans différentes pathologies comme le cancer.

La signalisation calcique résulte de l'action coordonnée de canaux calciques membranaires présents au niveau de la membrane plasmique ou d'organites tels que le réticulum endoplasmique (RE) et de protéines sensibles au calcium. Dans les cellules non-excitables, on retrouve deux grandes familles de canaux calciques : les canaux de la grande famille des TRP (transient receptor potential) et les canaux SOC (store-operated channels). Contenant la majorité

du calcium intracellulaire, le RE joue un rôle clé dans la signalisation calcique. La signalisation du RE est gouvernée par les récepteurs à l'IP₃ (inositol 1,4,5-trisphosphate ; RIP₃), les canaux de fuite et les pompes SERCA (sarcoplasmic/endoplasmic reticulum calcium ATP-ase).

IV. Les canaux SOC (store-operated channels)

Situés au niveau de la membrane plasmique, ces canaux sont responsables de l'entrée capacitive de calcium (ECC, ou SOCE pour Store-Operated Calcium Entry). Ces canaux sont activés suite à la vidange des stocks calciques du RE, la réserve majeure de calcium cellulaire. Cette activation se fait via la protéine STIM1 (Stromal Interaction Molecule 1, 74 kDa) ancrée dans le RE qui, grâce à son motif EF-hand, fixe le calcium présent à l'intérieur de l'organite. Lorsque STIM1 ne fixe plus de calcium, il s'oligomérisse et se relocalise dans les régions du RE proches de la membrane plasmique afin de lier et d'activer les protéines canal Orai1 (33 kDa), responsables du courant SOC. Les protéines Orai1, chacune constituée de quatre segments transmembranaires, s'oligomérisent en homohexamère pour former le canal calcique SOC, ce qui provoque une entrée dite capacitive de calcium permettant de reconstituer les stocks calciques réticulaires.

Les canaux SOC ont été impliqués dans de nombreux phénomènes cellulaires tels que la prolifération. En effet, après fixation de facteurs de croissance, les récepteurs de type tyrosine kinase (TKR) ou couplés aux protéines G (RCPG) peuvent, entre autres, activer la phospholipase C (PLC) qui va transformer le PIP₂ (phosphatidyl inositol 4,5-bisphosphate) en diacylglycérol (DAG) et IP₃. L'IP₃ provoquera une sortie du calcium réticulaire via l'activation des RIP₃, induisant l'ECC. Le DAG, quant à lui, va stimuler la protéine kinase C (PKC) activant, là aussi, les canaux SOC. Le calcium entré dans le cytoplasme suite à l'activation des canaux SOC va se fixer à la calmoduline, puis le complexe calcium-calmoduline va activer la phosphatase calcineurine. La calcineurine pourra alors déphosphoryler le facteur de transcription NFAT (Nuclear Factor of Activated T-cells), permettant le démasquage de ses séquences de localisation nucléaire et donc sa translocation dans le noyau. NFAT pourra alors induire la transcription de gènes impliqués, entre autres, dans la prolifération. En plus de ces effets au long terme sur l'expression génique, les canaux SOC peuvent également avoir des effets à court terme en modulant d'autres voies de signalisation.

Par ses effets à long et court terme, les canaux SOC ont été impliqués dans différents cancers. Par exemple, les canaux SOC modulent la migration des cellules cancéreuses mammaires par la régulation des adhésions focales. Les canaux SOC ont également été impliqués dans le contrôle de la prolifération et de l'apoptose dans différents cancers, par des actions à long ou court terme. De précédents travaux ont montré que les canaux SOC jouent un rôle clé dans le déclenchement de l'apoptose des cellules cancéreuses prostatiques. D'autres travaux ont mis en évidence

l'implication d'Orai1 et de son isoforme Orai3 dans la prolifération des cellules cancéreuses prostatiques via la formation de canaux ARC (arachidonic acid-regulated channels) et l'activation de la voie NFAT. Cependant, le rôle des canaux SOC dans la prolifération des cellules cancéreuses prostatiques n'a pas été étudié.

Enfin, bien qu'il existe de nombreux modulateurs pharmacologiques des canaux SOC, seul leur inhibition est actuellement possible. De nombreuses études ont montré l'importance des protéines partenaires dans la régulation des canaux ioniques. Une alternative serait donc de cibler les canaux SOC indirectement via une protéine partenaire.

V. *Le récepteur Sigma 1 (S1R)*

Initialement identifié comme un récepteur aux opioïdes, le récepteur Sigma 1 (S1R) répond en réalité à de nombreuses molécules. Cette protéine de 25 kDa ne possède d'homologie avec aucune autre protéine présente chez les Mammifères. Le S1R est constitué d'au moins un segment transmembranaire permettant son insertion au niveau de la membrane plasmique, et du RE. Contrairement à ce que son nom indique, le S1R n'agit pas comme un récepteur. En effet, cette protéine a un rôle de chaperonne et va ainsi lier et moduler de nombreuses protéines. De plus, la liaison au ligand va avoir des effets complexes influençant les interactions protéiques du S1R ou encore sa localisation cellulaire.

Le S1R a été impliqué dans différentes pathologies pour la plupart neurologiques, mais de nombreuses études ont également associé ce récepteur au cancer. En effet, il voit son expression augmenter dans de nombreux cancers, notamment celui de la prostate, et ce proportionnellement à l'agressivité tumorale. La modulation de l'activité du S1R pourrait donc être prometteuse pour le traitement du cancer, mais le rôle du S1R dans ce contexte reste pour le moment assez flou. Récemment, de plus en plus d'études lui montrent un rôle de protéine partenaire permettant la régulation de canaux ioniques, notamment dans le cancer.

Problématique et but du travail

Ces travaux sont divisés en deux parties, la première portant sur le rôle des canaux SOC dans la physiologie des cellules souches cancéreuses. Le deuxième versant de ce projet a porté sur l'étude du S1R en tant que protéine partenaire des canaux SOC dans le cancer de la prostate. Les canaux SOC semblent en effet jouer un rôle central dans le contrôle de la prolifération des cellules cancéreuses, et leur ciblage directement ou indirectement via le S1R pourrait permettre de développer des nouvelles approches thérapeutiques.

Pour se faire, ce projet est divisé en plusieurs points :

- I. Le rôle des canaux SOC dans les cellules souches cancéreuses
 1. L'isolation des CSCs
 2. L'expression et l'activité des canaux SOC dans les CSCs
 3. Le rôle des canaux SOC dans les CSCs

- II. L'étude du S1R, une protéine partenaire d'Orai1 dans le cancer de la prostate
 1. L'expression du S1R dans le cancer de la prostate
 2. La modulation de l'activité d'Orai1 par le S1R
 3. Les impacts physiopathologiques des modulations par le S1R

Résultats

1. La voie Orai1/NFAT régule la transition quiescence/prolifération des cellules cancéreuses

Cette première partie porte sur l'étude des canaux SOC dans les cellules souches cancéreuses de deux modèles différents : le cancer de la prostate et le mélanome.

1. L'expression et la fonction d'Orai1 sont diminués dans les CSC prostatiques

Les CSC ont la caractéristique d'être majoritairement quiescentes et de ne se diviser que rarement. Ceci nous permet d'isoler les CSC par le principe de rétention de marqueur (LCR, pour label retaining cells).

Nous avons tout d'abord utilisé la lignée cancéreuse prostatique PC3. Cette lignée agressive résistante aux androgènes et fortement différenciée est souvent utilisée dans l'étude des CSC prostatiques. Les LRC de PC3 ont été isolées grâce à un marquage membranaire au Dil couplé à la reconnaissance du CD44, un marqueur spécifique des CSC prostatiques. Nous avons ainsi placé les cellules en culture en suspension afin d'augmenter les proportions de CSC, et nous avons isolé deux populations : les Dil^{hi}CD44^{hi} et les Dil^{lo}CD44^{lo}. La caractérisation de ces populations montre que les cellules Dil^{hi} possèdent des caractéristiques de CSC telles que la perte de marqueurs de différenciation et une agressivité accrue.

Nous avons mis en évidence la chute d'expression d'Orai1 dans les CSC prostatiques par rapport aux cellules cancéreuses non souches (RT-qPCR et immunofluorescence). Orai1 est un composant majeur des canaux SOC dans notre modèle PC3, sa diminution d'expression se traduit ainsi par une ECC diminuée dans les cellules Dil^{hi} par rapport aux cellules Dil^{lo} (imagerie calcique).

2. L'expression et la fonction d'Orai1 sont diminuées dans les CSC de mélanome

Nous avons ensuite cherché à voir si la diminution d'Orai1 était limitée au cancer de la prostate. Pour cela, nous avons utilisé un deuxième modèle de CSC, développé par l'équipe du Dr Polakowska : un clone de la lignée HBL qui exprime de façon stable une construction Histone-2B fusionnée à la GFP inducible par tétracycline (Ostyn et al. 2014). Ce clone nous a ainsi permis d'isoler des CSC de mélanome (sous-population GFP^{hi}) qui perdent l'expression de marqueurs de différenciation et qui présentent une agressivité accrue.

Comme dans le cancer de la prostate, les CSC HBL GFP^{hi} expriment significativement moins Orai1. Nous avons mis en évidence l'importance d'Orai1 dans l'ECC des HBL souches et non souches par siARN. La chute d'expression d'Orai1 dans les cellules GFP^{hi} conduit ainsi à la diminution basale et induite de l'ECC par rapport aux cellules de mélanome non souches HBL GFP^{lo}.

3. L'inhibition d'Orai1 augmente la population de cellules cancéreuses avec des propriétés de cellules souches

Afin de mieux comprendre le rôle de la diminution d'expression et d'activité des canaux SOC dans les CSCs, nous avons réalisé des expériences visant à déterminer l'impact de la modulation de ces canaux sur nos modèles cellulaires. Ainsi, après marquage des cellules, l'inhibition pharmacologique (BTP2, 1 μ M) des canaux SOC pendant les sept jours de culture en suspension induit une augmentation du nombre de cellules quiescentes positives aux marqueurs (GFP ou Dil) ainsi qu'une augmentation du nombre de sphères formées (SFU, pour sphere forming unit), un indicateur du potentiel souche. L'inhibition des canaux SOC permet donc d'augmenter la population de CSCs, ce qui montre l'importance de ces canaux dans la transition entre la quiescence et la prolifération.

4. Orai1 régule la quiescence via la voie NFAT

Les canaux SOC dans lesquels Orai1 est impliqué peuvent réguler la prolifération via la voie calcium-dépendante NFAT. Nous avons montré que l'activation de NFAT est fortement diminuée dans nos deux modèles de CSC. De plus, l'inhibition pharmacologique de cette voie (FK506, 10 μ M) permet d'augmenter la sous-population de CSC, avec des résultats comparables à l'inhibition pharmacologique du SOC indiquée précédemment.

5. La quiescence induite par la chimiothérapie est associée à une chute d'expression d'Orai1

Les CSC sont particulièrement résistantes à la chimiothérapie grâce à leur capacité à entrer en quiescence face au stress (Borst 2012; Ehninger et al. 2014; Touil et al. 2014). Nous montrons ici que dans notre modèle de mélanome, un traitement avec le 5-fluorouracile (100 μ M) ou l'oxaliplatine (40 μ M) conduit à une forte augmentation de la proportion de cellules quiescentes. Cette quiescence est associée à une augmentation de la sous-population cellulaire qui exprime faiblement Orai1. De plus, ces cellules exprimant faiblement Orai1 sont majoritairement en phase G0 du cycle cellulaire.

Ainsi, dans ces deux modèles de CSCs, les canaux SOC et la voie NFAT semblent jouer un rôle clé dans la transition entre la quiescence et la prolifération, ainsi que dans l'acquisition de la chimiorésistance. Cependant, les possibilités de ciblage sont actuellement limitées pour les canaux SOC, seule leur inhibition étant possible à l'heure actuelle. C'est pour répondre à cette limite, et mieux comprendre le fonctionnement de ces canaux, que nous avons cherché à identifier une protéine partenaire capable de réguler l'activité de ces canaux.

II. Le S1R : protéine partenaire d'Orai1 dans le cancer de la prostate

Dans cette deuxième partie, nous nous sommes intéressés à la protéine chaperonne S1R en tant que potentiel régulateur des canaux SOC dans le cancer de la prostate.

1. L'expression du S1R dans le cancer de la prostate

De précédentes études ont montré que l'expression du S1R est augmentée dans de nombreux cancer, donc celui de la prostate.

Afin de confirmer ces résultats, nous avons étudié l'expression du S1R dans des prélèvements de prostates saines et cancéreuses dans deux séries de prélèvements humains. Grâce à des expériences de RT-qPCR, nous avons ainsi pu mettre en évidence l'augmentation de l'expression du S1R dans le cancer de la prostate (en collaboration avec le Pr Fromont (INSERM UMR1069 Tours) et Dr Gkika). Cette augmentation a été confirmée au niveau protéique sur une deuxième série de prélèvements par immunohistochimie sur des coupes de tissus humains sains et cancéreux (en collaboration avec les Pr Gosset et Dr Mihalache, Hôpital St Philibert, Lille).

Parallèlement, nous avons réalisé des RT-qPCR et des western blots afin de quantifier l'expression du S1R dans différentes lignées cellulaires. Nous montrons ainsi que les cellules cancéreuses prostatiques LNCaP expriment fortement le S1R. Cependant, l'expression du S1R est très fortement diminuée dans la lignée PC3. La différence principale entre ces deux lignées est leur sensibilité aux androgènes : les LNCaP sont sensibles aux androgènes tandis que les PC3 sont androgéno-résistantes car dépourvues du récepteur aux androgènes (RA). Ces résultats laissent donc à penser que l'expression du S1R pourrait être régulée par les androgènes. Pour vérifier si c'est le cas, nous avons cultivé la lignée androgéno-dépendante LNCaP en absence de stéroïdes. Après trois jours de traitement, nous avons pu observer une forte diminution de l'expression du S1R. L'ajout de la forme active de la testostérone (dihydrotestostérone, DHT, 100nM) en milieu dépourvu de stéroïdes permet de ré-augmenter l'expression du S1R de façon significative. D'autre part, l'inhibition pharmacologique du RA par le Casodex® (10µM) dans ces mêmes cellules induit une diminution significative d'environ 50% de l'expression du S1R par rapport au contrôle. Nous avons obtenu des résultats similaires par une inhibition du AR via siARN. Enfin, nous avons confirmé ces résultats dans un autre modèle cellulaire en ré-exprimant le RA dans les cellules PC3, ce qui permet d'augmenter significativement l'expression du S1R.

L'ensemble de ces résultats, confirmés au niveau protéique (western blot) et ARNm (RT-qPCR), montrent que l'expression du S1R est androgéno-dépendante dans les cellules cancéreuses prostatiques.

2. L'expression d'Orai et STIM dans le cancer de la prostate

Des études précédentes se sont penchées sur l'expression d'Orai et STIM dans le cancer de la prostate. Il a été ainsi montré que l'expression d'Orai1 et STIM1, les constituants majeurs du SOC dans nos modèles, est inchangée dans le CaP. Cependant, de manière intéressante, une étude a suggéré que l'expression d'Orai1 pouvait être régulée par les androgènes dans les cellules cancéreuses prostatiques. Grâce à nos modèles, nous avons pu confirmer ces résultats et montrer que l'expression d'Orai1 est sensible aux androgènes, comme c'est le cas pour le S1R. Nous montrons également que l'expression de STIM1 est insensible aux stéroïdes, contrairement à Orai3 dont l'expression augmente en l'absence de stéroïdes. Il est à noter que d'après nos résultats, les androgènes ne semblent avoir aucun effet sur Orai3.

3. Le S1R module positivement les canaux SOC dans le cancer de la prostate

Malgré le fait que la surexpression du S1R dans le cancer est bien connu, son rôle reste à ce jour peu compris. Il faut savoir que malgré ce que son nom indique, le S1R n'agit pas comme un récepteur, mais comme une protéine chaperonne. Parmi ses cibles, on retrouve les canaux ioniques. Au vu du rôle du S1R et de l'importance des canaux SOC dans le cancer, nous avons voulu savoir si le S1R était capable de moduler ces canaux dans le cancer de la prostate. Pour cela, nous avons mesuré l'activité des canaux SOC par les techniques de patch-clamp et d'imagerie calcique, tout en modulant le S1R. Nous avons ainsi eu recours à la surexpression du S1R, à son inhibition par siARN et à sa modulation pharmacologique (Igmésine, SKF 10047). Ces expériences nous ont permis de montrer que le S1R augmente l'activité des canaux SOC dans les cellules cancéreuses prostatiques.

4. Le S1R se déplace vers la membrane plasmique lors de l'activation des SOC

Les canaux SOC sont constitués de deux éléments : la protéine canal Orai1 située au niveau de la membrane plasmique et son activateur STIM1 inséré dans la membrane du RE. Afin de mieux comprendre la modulation des canaux SOC par le S1R, nous avons étudié sa localisation cellulaire. En effet, le S1R est majoritairement localisé au niveau du RE, mais il a également été retrouvé au niveau de la membrane plasmique. Le S1R pourrait donc agir à deux niveaux sur les canaux SOC : via STIM1 au niveau du RE et via Orai1 au niveau de la membrane plasmique.

Nous avons commencé par une étude par microscopie confocale de cellules LNCaP transfectées avec une construction S1R-eGFP et un plasmide permettant de marquer le RE (ER-DsRed), dont la membrane plasmique est mise en évidence par l'utilisation d'un marquage lipophile (CellMask Deep Red). Ces outils nous ont permis d'avoir un suivi dynamique de la localisation cellulaire du S1R lors de l'activation des canaux SOC. Pour ces expériences, les canaux ont été activés par la vidange des stocks calciques réticulaires provoquée par de l'acide cyclopiazonique (CPA, 50 μ M),

un inhibiteur des pompes SERCA. Nous avons ainsi pu mettre en évidence la présence majoritairement réticulaire du S1R dans les conditions basales, puis, sa translocation au niveau de la membrane plasmique lors de l'activation des canaux SOC suite à la vidange des stocks calciques réticulaires.

Ces résultats ont ensuite été confirmés au niveau endogène par immunofluorescence et biotinylation sur les cellules LNCaP.

Ainsi, ces différentes expériences montrent que lors de l'activation des canaux SOC, le S1R, majoritairement localisé au niveau du RE, est transloqué au niveau de la membrane plasmique où il exerce une modulation positive sur les canaux SOC.

5. Le S1R interagit avec les canaux SOC

Au vu de la translocation du S1R vers la membrane plasmique lors de l'activation des canaux SOC, et de son effet sur ces canaux, nous avons voulu étudier l'éventuelle interaction entre le S1R et Orai1. Pour cela, nous avons réalisé des co-immunoprécipitations en ciblant le S1R et Orai1 dans les cellules LNCaP. Lors de la précipitation de la protéine S1R grâce à un anticorps spécifique, Orai1 est également précipité, et inversement. Ces premiers résultats montrent ainsi que le S1R serait capable de former un complexe protéique avec les canaux SOC. Afin de savoir si le S1R interagit directement avec Orai1, nous avons réalisé des expériences de FRET (Förster resonance energy transfer) avec la technique de TD-FLIM (time domain-fluorescence lifetime imaging microscopy) en collaboration avec le Dr Heliot et le Dr Furlan (PhLAM, Lille). Grâce à l'utilisation de constructions fluorescentes de nos protéines d'intérêt, nous avons pu montrer que dans les conditions basales, le S1R, majoritairement localisé au niveau du RE, interagit avec STIM1, ce qui se traduit par une diminution du temps de demi-vie du donneur de fluorescence. Puis, lors de l'activation des canaux SOC (CPA, 50 μ M), le S1R se sépare de STIM1 pour aller interagir avec Orai1 au niveau de la membrane plasmique. Enfin, nous avons également pu montrer que le S1R contribue à diminuer l'interaction entre Orai1 et Orai3, cet effet étant d'autant plus marqué lors de l'activation des canaux SOC par le CPA.

Ainsi, l'ensemble des résultats obtenus sur cette partie du projet montrent que le S1R est capable de se déplacer du RE vers la membrane plasmique afin d'interagir avec Orai1. Par cette interaction directe, le S1R contribuerait au recrutement d'Orai1 et à l'activation du courant SOC. De plus, nos résultats suggèrent que l'augmentation de l'activité des canaux SOC par le S1R se ferait au détriment des canaux ARC en prévenant l'association entre Orai1 et Orai3.

6. L'inhibition du S1R ralentit la prolifération et la croissance tumorale

Les canaux SOC ayant été impliqués dans la prolifération de différents modèles cellulaires via la voie calcineurine-NFAT (Parekh, 2010), nous nous sommes intéressés aux impacts des activités modulatrices du S1R sur la prolifération des cellules cancéreuses prostatiques.

Nous avons donc suivi la prolifération des cellules LNCaP et PC3 sur sept jours avec le kit de viabilité MTS (sel de tétrazolium) associé à un comptage cellulaire au bleu Trypan, tout en modulant l'expression du S1R. Nous avons ainsi pu mettre en évidence une diminution significative de la prolifération cellulaire après inhibition du S1R par siARN. Ces résultats ont été confirmés *in vitro* par la diminution de l'expression du marqueur de prolifération PCNA (proliferating cell nuclear antigen, 4 jours) et la diminution du nombre de cellules en phase S (EdU, 4 jours). Enfin, l'effet du siS1R sur la prolifération des cellules cancéreuses prostatiques a été confirmé *in vivo*. L'injection sous-cutanée de LNCaP (3 millions, 1:2 PBS/Matrigel, souris mâles NMRI Nude) préalablement transfectées avec un siS1R (16h) conduit à une diminution de la croissance tumorale par rapport au contrôle (siLuc). Nous avons obtenu des résultats similaires avec les cellules PC3, confirmant l'importance du S1R dans la prolifération des cellules cancéreuses prostatiques.

7. Le S1R régule la prolifération via Orai1 et la voie NFAT

Nos résultats précédents montrent l'importance d'Orai1 dans la régulation de la prolifération des cellules cancéreuses prostatiques. Nous avons donc cherché à savoir si l'impact du S1R sur la prolifération des cellules cancéreuses passait par la modulation du SOC. Nos premiers résultats de MTS indiquent que l'inhibition conjointe d'Orai1 et du S1R (siARN) a autant d'effet que l'inhibition d'Orai1 seule. L'absence d'effet cumulatif entre l'inhibition d'Orai1 seule ou couplée avec l'inhibition du S1R laisse à penser qu'il s'agit d'une seule et même voie.

Comme nous l'avons vu précédemment, les canaux SOC sont en amont d'une voie de signalisation conduisant à la prolifération cellulaire grâce à l'activation du facteur de transcription NFAT. Nous donc regardé si l'inhibition du S1R avait un impact sur cette voie de signalisation. Pour cela nous avons utilisé un rapporteur d'activité de ce facteur de transcription constitué du gène permettant l'expression de la luciférase sous le contrôle d'un promoteur cible de NFAT. Cette construction nous a permis de mettre en évidence que l'inhibition du S1R dans les cellules cancéreuses prostatiques conduit à une diminution de l'activité de NFAT, confirmant l'implication de ce dernier. Ces résultats ont été confirmés par le suivi dynamique de la translocation de NFAT dans nos cellules par microscopie confocale.

8. Le S1R permet de réguler la quiescence des CSC prostatiques via Orai1

Nous avons obtenu des résultats préliminaires indiquant que le S1R pourrait également réguler l'entrée en quiescence des CSC prostatiques via Orai1 et la voie NFAT, un résultat en accord avec nos données concernant le rôle du SOC dans le contrôle de la balance quiescence/prolifération.

9. Le S1R participe à l'apoptose

De précédents travaux ont montré que les canaux SOC régulent l'entrée en apoptose des cellules cancéreuses prostatiques. Ainsi, la diminution de l'expression d'Orai1 dans les stades androgéno-dépendants conduirait à une résistance à l'apoptose due à la forte diminution de l'ECC. Nous avons donc cherché à savoir si la modulation du SOC par le S1R pouvait également impacter la sensibilité de nos cellules à l'apoptose. Nos résultats préliminaires montrent que l'inhibition de l'expression du S1R (siARN) n'impacte pas la viabilité des cellules cancéreuses prostatiques, mais les rends plus résistantes à la mort induite par la thapsigargine (2 μ M, 24h) ou la chimiothérapie (docetaxel, 10nM, 24h).

10. Le S1R est capable de moduler l'activité de TRPV6

Le canal calcique TRPV6 (transient receptor potential vanilloid 6) est capable de moduler la prolifération et l'apoptose des cellules cancéreuses prostatiques via sa participation tardive dans l'ECC. Nous montrons ici des résultats préliminaires indiquant que le S1R est capable d'inhiber l'activité de ce canal dans les cellules HEK-293. Il serait intéressant de voir si c'est également le cas dans les cellules cancéreuses prostatiques, et d'étudier comment cette régulation s'inscrit dans la modulation d'Orai1 que nous avons mis en évidence ici.

11. Le S1R est également capable de moduler l'activité de TRPM8 et la migration

Le canal calcique TRPM8 (transient receptor potential melastatin 8) a été initialement identifié dans la prostate où il joue un rôle clé d'inhibiteur de la migration. De plus, l'expression de ce canal est sous la dépendance des androgènes.

Nos résultats montrent, tout d'abord dans les HEK-293, que le S1R est capable d'augmenter l'activité de TRPM8 (patch-clamp). Nous avons confirmé ces résultats dans les cellules cancéreuses prostatiques PC3-TRPM8. Dans ce même modèle, nous montrons que l'inhibition du S1R (siARN) diminue l'entrée calcique par TRPM8 (imagerie calcique) et augmente la vitesse de migration. A l'inverse, la surexpression du S1R dans ces cellules réduit la vitesse de migration. Ces résultats indiquent que le S1R pourrait jouer un rôle dans la régulation de la migration des cellules cancéreuses prostatiques via la potentialisation de l'effet inhibiteur de TRPM8.

Discussion

I. La voie Orai1/NFAT joue un rôle clé dans la transition quiescence/prolifération des CSC

Nos résultats renforcent l'hypothèse de l'importance du calcium pour déterminer le devenir des CSC. En effet, nous mettons en évidence l'importance de la voie SOC/NFAT dans le contrôle de la quiescence dans deux modèles différents, le mélanome et le CaP. Nous proposons ainsi un nouveau phénotype pour détecter les cellules quiescentes avec des propriétés de cellules souches dans ces deux cancers : $CBP^{hi}/Orai^{lo}/NFAT^{inactif}$.

L'ECC joue un rôle clé dans l'activation du facteur de transcription NFAT via l'augmentation locale de calcium dans des microdomaines spécifiques réunissant les canaux SOC, la calmoduline, la calcineurine et NFAT. Nos résultats montrent que la diminution d'expression d'Orai1 va diminuer l'ECC et donc la translocation nucléaire de NFAT. L'inhibition de cette voie à différents niveaux (BTP2, FK506) diminue l'activité de NFAT et augmente le compartiment des cellules cancéreuses quiescentes possédant des propriétés de cellules souches.

Enfin, nous montrons que la chimiothérapie, connue pour induire la quiescence, va également diminuer l'expression d'Orai1. Une étude précédente dans le CaP a montré que la diminution de l'ECC induit une résistance à l'apoptose dans les cellules cancéreuses. Ainsi, la chimiothérapie va augmenter la population de cellules cancéreuses quiescentes possédant des propriétés de cellules souches et une résistance accrue aux traitements.

De précédentes études ont montré que l'inhibition d'Orai1 permet de diminuer la prolifération cellulaire. Or, nos résultats suggèrent que cette inhibition conduirait plutôt à une induction de la quiescence.

Enfin, nos travaux mettent en évidence un mécanisme commun pour deux cancers différents, le mélanome et le cancer de la prostate. Il serait donc intéressant d'étudier d'autres cancers pour voir si ce phénomène peut être généralisé.

II. Le S1R est un nouveau partenaire des canaux SOC dans le cancer de la prostate

1. L'expression du S1R est régulée par les androgènes dans le CaP

Avec ces travaux, nous montrons pour la première fois que l'expression du S1R est sous le contrôle des androgènes dans les cellules cancéreuses prostatiques. Nous avons tout d'abord confirmé la surexpression du S1R dans le CaP androgéno-dépendant. Nos résultats montrent également que la suppression des androgènes ou de leur récepteur diminue fortement l'expression du S1R dans les cellules cancéreuses prostatiques. Des expériences complémentaires seront cependant nécessaires afin d'identifier les modalités de cette régulation. De manière intéressante, une récente étude a montré que le S1R est capable de stabiliser le RA dans le CaP, montrant l'existence d'une boucle de rétrocontrôle positif permettant de maintenir une forte expression du RA et du S1R dans le CaP androgéno-dépendant.

Ainsi l'expression du S1R est fortement augmentée dans le CaP androgéno-dépendant, en corrélation avec l'agressivité. Puis, lors de la castration chimique, l'expression du S1R va chuter. Le devenir de l'expression du S1R reste à déterminer par l'étude d'échantillons humains. Cependant, nous savons que les cellules cancéreuses prostatiques peuvent avoir recours à différents mécanismes pour aboutir à l'échappement thérapeutique, dépendant ou non du RA. Le devenir de l'expression du S1R dans ces stades tardifs serait ainsi dépendant des mécanismes mis en place.

2. L'expression d'Orai1 est régulée par les androgènes dans le CaP

Une étude précédente a montré que l'expression d'Orai1 pourrait également être régulée par les androgènes dans le CaP. Nos résultats mettent en évidence une diminution de l'expression du canal lors de la suppression de la signalisation androgénique, confirmant ces données. Il est reconnu que les CSC prostatiques sont fortement dédifférenciées, principalement quiescentes et expriment peu ou pas de RA. Une équipe a récemment identifié les mécanismes permettant de limiter l'expression du RA dans les CSC prostatiques et a montré que, par l'inhibition de la signalisation du RA, ce mécanisme permettait le maintien de l'état souche de ces cellules. Ce même mécanisme permet d'expliquer la diminution d'expression d'Orai1 que nous avons mise en évidence dans les CSC prostatiques.

Nous nous sommes également penchés sur la possibilité d'une même régulation pour les protéines Orai3 et STIM1. De précédents travaux ont montré que l'expression de STIM1 reste inchangée dans le CaP. Nos résultats montrent que l'expression de cette protéine est insensible aux androgènes. Orai3, par contre, est surexprimé dans le CaP. De plus, il a été montré que son expression est positivement régulée par les estrogènes dans les cellules cancéreuses mammaires. De manière surprenante, nos résultats montrent dans le CaP que les androgènes n'ont pas d'effet sur l'expression d'Orai3, mais que ce canal est surexprimé en réponse à la

suppression des stéroïdes du milieu de culture. Il serait intéressant d'étudier ce phénomène plus en détail afin de mieux comprendre la régulation d'Orai3 par les stéroïdes.

L'ensemble de ces résultats nous a permis de déduire les profils d'expression du S1R, STIM1, Orai1 et Orai3 dans la progression du CaP. Cependant, la difficulté d'obtenir des échantillons de patients en échappement thérapeutique ne nous a pas permis d'étudier les stades les plus avancés de la maladie.

3. Le S1R augmente l'activité des canaux SOC dans le CaP

Nos résultats montrent que dans les conditions basales, le S1R, résident du RE, interagit directement avec STIM1. Puis, lors de l'activation des canaux SOC, le S1R migre vers la membrane plasmique pour interagir directement avec Orai1. Bien que nos résultats actuels indiquent une dissociation entre le S1R et STIM1 pendant l'activation des canaux SOC, des expériences complémentaires seront nécessaires afin de conclure sur ce point.

Par son interaction avec Orai1, le S1R est capable d'augmenter l'activité des canaux SOC dans les cellules cancéreuses prostatiques. Nous montrons que ces effets sont très rapides grâce à des traitements pharmacologiques aigus, mais des traitements chroniques indiquent que des mécanismes à long terme pourraient également se mettre en place. Nous sommes en train de réaliser des expériences complémentaires afin de mieux comprendre ces mécanismes.

Nos résultats présentés ici vont cependant à l'encontre d'une précédente étude qui a mis en évidence un rôle inhibiteur du S1R sur les canaux SOC. Cette étude menée dans les cellules HEK-293 a été réalisée avec la surexpression du rS1R. Nous avons donc testé ce plasmide, et nous montrons que dans nos cellules, le rS1R conduit également à une inhibition des canaux SOC, contrairement au hS1R. Cependant, le S1R est fortement conservé entre les espèces, ce qui ne nous permet pas pour le moment d'expliquer ces effets opposés.

Enfin, nos résultats montrent que le S1R va diminuer l'interaction entre Orai1 et Orai3 dans nos cellules, indiquant qu'il pourrait diminuer l'activité des canaux ARC dans nos cellules.

L'ensemble de ces données nous permet de déduire le profil d'activité des canaux SOC dans la progression du CaP. En effet, dans les stades androgéno-dépendants, suite à la forte expression d'Orai1 et à la surexpression du S1R, les canaux SOC sont fortement actifs. Puis, lors de la castration chimique, la chute d'expression d'Orai1 et du S1R va fortement diminuer l'activité des canaux SOC, et les canaux ARC prendraient alors le relais.

4. Le S1R augmente la prolifération des cellules du CaP via la voie SOC/NFAT

Nos résultats montrent que, via son effet sur l'ECC, le S1R module positivement la prolifération des cellules du CaP.

Ainsi, l'inhibition du S1R dans les cellules cancéreuses prostatiques diminue la prolifération cellulaire et la croissance tumorale. L'inhibition d'Orai1 diminue d'avantage la prolifération, mais

l'inhibition combinée du S1R et d'Orai1 ne donne pas d'effet additif, indiquant qu'il s'agit très probablement d'une seule et même voie de signalisation.

Nous montrons également que le S1R impacte fortement la localisation du facteur de transcription NFAT activé par les canaux SOC. En effet, l'inhibition du S1R va empêcher NFAT de rester activé dans le noyau, ne permettant que sa translocation transitoire. Il est connu que le temps que NFAT passe dans le noyau détermine les gènes qu'il pourra activer, la diminution de ce temps impactant donc directement le devenir cellulaire. Une étude a montré que l'activation de NFATc3, l'isoforme majoritaire dans nos cellules, nécessite l'action conjointe des canaux SOC à la membrane plasmique et des RIP_3 du RE. Nos expériences montrent que, dans nos cellules, l'inhibition des RIP_3 n'impacte pas la translocation de NFATc3, confirmant que l'effet du S1R passe par les canaux SOC.

D'autre part, des travaux ont montré que le S1R serait également capable de contrôler la prolifération des cellules cancéreuses prostatiques via son rôle de stabilisateur du RA.

Une étude précédente a montré que l'inhibition des canaux SOC diminue la sensibilité à l'apoptose des cellules cancéreuses prostatiques. L'inhibition du S1R va conduire au même phénomène via son action sur l'ECC, protégeant les cellules de la mort cellulaire.

Nous montrons également des données préliminaires indiquant que le S1R peut également impacter la quiescence des CSC prostatiques via la voie Orai1/NFAT que nous avons mise en évidence.

Enfin, les canaux ARC peuvent, eux aussi, augmenter la prolifération via la voie NFAT. Nos résultats montrent que l'inhibition d'Orai3 diminue fortement la prolifération cellulaire, cependant l'inhibition combinée d'Orai3 et du S1R réaugmente de façon significative la prolifération, ce qui va dans le sens d'une potentielle inhibition des canaux ARC par le S1R.

Pour comprendre ce qu'il se passe dans le CaP, il est essentiel de remettre ces résultats dans le contexte pathologique avec les profils d'expression que nous avons mis en évidence.

Ainsi, dans les stades androgéno-dépendants, la surexpression du S1R et la forte activité des canaux SOC va conduire à une prolifération accrue associée à une forte sensibilité à l'apoptose. Par contre, lors de la castration chimique, la chute d'expression d'Orai1 et du S1R va conduire à une forte prolifération contrôlée par les canaux ARC, et à une résistance accrue à l'apoptose due à la forte diminution de l'activité des canaux SOC. Ce profil plus agressif pourrait également être renforcé par l'augmentation de la population de CSC due à la diminution d'expression d'Orai1.

5. Le S1R est capable de réguler d'autres canaux calciques dans le CaP

Tout d'abord, le S1R est connu pour réguler l'activité des RIP_3 , des canaux clé dans la régulation de l'homéostasie calcique au niveau du RE. Cette régulation ayant été principalement étudiée dans les neurones, il serait intéressant de voir si elle intervient également dans le CaP.

D'autre part, nos travaux montrent que le S1R serait également capable d'inhiber l'activité des canaux de type TRPV6, des canaux impliqués dans la régulation de la prolifération et de l'apoptose des cellules cancéreuses prostatiques via leur participation tardive dans l'ECC. Ces résultats montrent que, lors de la chute d'expression d'Orai1 et du S1R pendant la castration chimique, TRPV6 pourrait prendre le relais pour maintenir l'ECC.

De plus, nous montrons également que le S1R est capable d'activer les canaux TRPM8 dans les cellules cancéreuses prostatiques. Cette modulation va permettre de potentialiser l'effet inhibiteur de TRPM8 sur la migration des cellules cancéreuses prostatiques. De manière intéressante, TRPM8 est positivement régulé par les androgènes et présente un profil d'expression similaire à celui du S1R dans le CaP.

Le S1R est ainsi capable de réguler d'autres canaux que le SOC dans le CaP. Ainsi, le ciblage du S1R pourrait permettre la modulation simultanée de plusieurs canaux ioniques impliqués dans différents processus du PCa à différents stades de la pathologie. Des études complémentaires seront nécessaires afin d'évaluer le potentiel d'une telle régulation.

6. Le S1R : une nouvelle cible pharmacologique dans le traitement du CaP ?

L'ensemble de ces données montre que le S1R est une nouvelle cible thérapeutique intéressante pour le CaP. Cette protéine est capable de lier de nombreuses molécules, certaines déjà utilisées dans d'autres contextes cliniques. Nos résultats montrent que des agonistes du S1R sont capables d'augmenter l'activité des canaux SOC suite à un traitement aigu ou chronique. Il serait intéressant de tester ces molécules sur les effets physiologiques que nous avons identifiés, ainsi que sur les autres canaux modulés par le S1R. D'autres équipes se sont déjà penchées sur le potentiel thérapeutique du ciblage du S1R grâce à son activité stabilisatrice du RA. Les auteurs ont ainsi montré que des inhibiteurs du S1R étaient capables de diminuer la prolifération des cellules cancéreuses prostatiques *in vitro* et *in vivo*.

D'autre part, aucun ligand endogène n'a été clairement identifié pour le S1R. Parmi les candidats, nous retrouvons le DMT (diméthyl tryptamine). De manière intéressante, une étude a montré la surexpression de l'enzyme productrice de DMT dans le CaP (INMT, indoléthylamine-N-méthyltransférase). Il serait donc intéressant d'étudier l'impact de ce ligand sur le S1R afin de mieux comprendre le rôle de cette protéine dans le CaP.

III. Conclusion générale et perspectives

Nos résultats montrent le rôle clé de la voie Orai1/NFAT dans le contrôle de la prolifération et de la quiescence des CSC, mais aussi dans la prolifération des cellules cancéreuses prostatiques. De plus, nous mettons en évidence que cette voie peut être régulée par le S1R, ouvrant de nouvelles perspectives thérapeutiques. De plus, nous présentons des données préliminaires identifiant d'autres cibles du S1R dans le CaP, telles que les canaux TRPM8 et TRPV6.

L'ensemble de nos résultats montrent que le ciblage du S1R permettrait de réguler simultanément l'activité de différentes protéines jouant un rôle crucial dans le CaP. Ainsi, l'activation du S1R conduirait à une augmentation de la prolifération cellulaire via les canaux SOC et la voie NFAT. Cette activation permettrait aussi de sensibiliser les cellules à l'apoptose via l'ECC, augmentant ainsi l'efficacité de la chimiothérapie. Nos données préliminaires indiquent que l'activation du S1R permettrait également d'inhiber la migration cellulaire via les canaux TRPM8. Enfin, l'activation du S1R pourrait également permettre d'activer les CSC prostatiques, en les forçant vers un programme de prolifération, permettant leur ciblage par chimiothérapie. De plus, ces effets seraient renforcés par une stabilisation accrue du RA et l'augmentation de sa signalisation induisant la prolifération et la différenciation cellulaire.

Abstract

Prostate cancer (PCa) is the most frequent and the third deadliest cancer in men in Europe. Cancer stem cells (CSC) are a rare subset of cancer cells possessing stem cell properties leading to a high resistance to therapy and an enhanced tumorigenicity. As a result, CSCs have been linked to tumor dormancy and relapse upon reactivation. Thus, the mechanisms regulating CSC dormancy/activation transition are of critical importance in PCa.

Previous studies showed the importance of Orai proteins in PCa, through their roles in SOC (store-operated channel) and ARC (arachidonic acid-regulated calcium channel) channels. But the role of Orai1 in PCa proliferation and CSC physiology remained to be studied. Moreover, in order to bypass current targeting limitations for Orai1, we aimed to identify a partner protein able to regulate Orai1 in PCa. For this purpose, we focused on the Sigma 1 receptor (S1R), a chaperone protein capable of ion channel regulation. Interestingly, S1R expression is increased in PCa and this protein can bind many pharmacological compounds currently used for other clinical applications. This work thus aimed to first study the role of Orai1 in PCa and CSC physiology, and then characterize the role of S1R as a new regulator of Orai1 in PCa.

Our results first show that Orai1 is a key regulator of CSC transition between quiescence and proliferation via the NFAT pathway. Moreover, this role is not limited to PCa, since these results were also confirmed in melanoma CSCs. We also show here that the S1R directly interacts with Orai1 and increases its activity, thus modulating PCa cell proliferation. Finally, we characterized the regulation of Orai1 and S1R expression by androgens, which is highly significant during PCa development.

Our results therefore allowed the identification of a key regulator of PCa proliferation (Orai1), and propose an alternative method for its targeting via the identification of its partner protein (S1R). These results could lead to the development of new markers and innovative therapeutic strategies.

Résumé

Le cancer de la prostate (CaP) est le cancer le plus fréquent et le troisième plus mortel chez l'homme en Europe. Les cellules souches cancéreuses (CSC) représentent une sous population de cellules cancéreuses possédant des propriétés de cellules souches qui les rendent résistantes aux thérapies et hautement tumorigènes. Les CSCs sont ainsi associées aux phénomènes de dormance tumorale, puis de rechute suite à leur réactivation. Les mécanismes régulant la transition dormance/prolifération constituent donc une question centrale dans la prise en charge du cancer.

L'importance des protéines Orai dans le CaP a déjà été montrée dans de précédentes études, via leur implication dans les canaux de type SOC (store-operated calcium channel) et ARC (arachidonic acid-regulated channel). Cependant, le rôle du canal Orai1 dans la prolifération du CaP, ou son éventuelle implication dans la physiologie des CSC, restaient inconnus. Parallèlement, pour répondre aux limitations de son ciblage direct, nous avons cherché à identifier ses protéines partenaires. Nous nous sommes ainsi intéressés au récepteur Sigma 1 (S1R), une protéine chaperonne dont l'expression augmente dans le CaP, et qui possède de nombreux modulateurs pharmacologiques utilisés en clinique. Ce travail avait donc un double objectif : étudier le rôle d'Orai1 dans le CaP et les CSC prostatiques, et caractériser fonctionnellement le rôle du S1R en tant que nouveau partenaire du canal Orai1.

Ces travaux ont tout d'abord permis de mettre en évidence l'importance d'Orai1 dans le contrôle de la transition entre la quiescence et la prolifération des CSCs prostatiques via la voie NFAT. De plus, ces résultats ont été confirmés dans les CSCs de mélanome, montrant que le rôle d'Orai1 serait généralisable au-delà du modèle prostatique. Nous avons également montré que le S1R interagit directement avec Orai1 et module positivement son activité, impactant ainsi la prolifération des cellules cancéreuses prostatiques. Enfin, nous avons mis en évidence la régulation de l'expression de ces protéines par les androgènes, ce qui est d'importance cruciale dans l'évolution du CaP.

Nos résultats ont donc permis l'identification d'un acteur central du contrôle de la prolifération du CaP (Orai1), et la caractérisation d'une nouvelle protéine partenaire du canal Orai1 dans le CaP : le S1R. Ces travaux montrent que le S1R et Orai1 pourraient constituer de nouveaux marqueurs intéressants, ainsi que de potentielles nouvelles cibles thérapeutiques.